3-30-2015

Investigation of Factors Affecting Opalescence and Phase Separation in Protein Solutions

Ashlesha S. Raut
University of Connecticut - Storrs, ashlesha0105@gmail.com

Investigation of Factors Affecting Opalescence and Phase Separation in Protein Solutions

Ashlesha Shirish Raut

University of Connecticut, 2015

Abstract

Opalescence and liquid-liquid phase separation reduce physical stability of a therapeutic protein formulation and have been recently reported for high concentration monoclonal antibody solutions. Liquid-liquid phase separation resulting in opalescence can be attributed to attractive intermolecular interactions; formulation factors that mitigate these interactions reduce solution opalescence and tendency to phase separate. Protein-protein interactions in solution have also been reported to enhance reversible/irreversible aggregation and viscosity of the solution. These formulation challenges are further enhanced for the second generation of antibodies due to the increased complexity of the molecules. Current work focuses on understanding the formulation factors and nature of intermolecular interactions that result in opalescence and liquid-liquid phase separation for monoclonal antibody (mAb) and Dual variable domain immunoglobulin antibody (DVD-Ig^{TM}) protein solutions. Opalescence for protein solution was measured as a function of formulation factors and correlated to interactions in dilute and concentrated solutions. Results show that presence of attractive interactions (enthalpy effect) and strong temperature dependence (entropy effect) result in liquid-liquid phase separation in solution. On undergoing phase separation, solutions attain thermodynamic equilibrium, and protein does not exhibit structural changes. Other than the traditional non-specific interactions, the presence of

specific protein interactions also affects phase separation and was investigated for DVD-Ig™ protein. Determining the nature of these attractive protein-protein interactions is of utmost significance so as to facilitate the selection of appropriate excipients. The effect of different excipients to suppress phase separation and irreversible aggregation in solution was also studied. The mechanism by which these excipients affect aggregation and liquid-liquid phase separation in solution is different, as both these phenomena show a strong and opposite temperature dependence. The effect of size of the molecule with respect to intrinsic viscosity and excluded volume effect, electroviscous effect and interactions, on the viscous behavior of DVD-Ig™ protein was investigated. Interplay of more than one factor contributes to significantly high viscosity of DVD-Ig™ protein compared to mAb solutions.

The overall results demonstrated that opalescence and liquid-liquid phase separation are a concern in formulation development of therapeutic protein solutions. Excipients and solution conditions (pH, ionic strength, concentration and temperature) that reduce non-covalent interactions in solution provide physically stable products.

Investigation of Factors Affecting Opalescence and Phase Separation in Protein Solutions

Ashlesha Shirish Raut

M.Pharm. (Pharmaceutics), Institute of Chemical Technology, 2008

B. Pharm., Mumbai University, 2006

A Dissertation

Submitted in Partial Fulfillment of the

Requirements for the Degree of

Doctor of Philosophy

at the

University of Connecticut

2015

APPROVAL PAGE

Doctor of Philosophy Dissertation

Investigation of Factors Affecting Opalescence and Phase Separation in Protein Solutions

Presented by

Ashlesha Shirish Raut

Major Advisor _____

Devendra S. Kalonia

Associate Advisor _____

Robin H. Bogner

Associate Advisor _____

Tai-Hsi Fan

University of Connecticut

2015

Dedication

Dedicated to my wonderful Family for all their love and support

Acknowledgements

I take this opportunity to thank my advisor, Dr. Devendra S. Kalonia, “Boss”, for his invaluable guidance and support throughout my PhD. I am grateful to him for providing me with the opportunity to work in his lab and gain experience in this interesting and challenging area of research. I sincerely appreciate his encouragement and advice that helped me grow, both professionally and personally. I am thankful for the intense group meetings and his insightful questions that helped me in gaining a better understanding of the basic concepts. Numerous scientific discussions driven by his impressive experience and knowledge inspired me to work independently and think critically. I feel incredibly fortunate to have him as my major advisor.

I would also like to express my deepest gratitude to my associate advisors, Dr. Robin Bogner and Dr. Tai-Hsi Fan for their constant guidance and support during my graduate research. Their encouragement, insightful comments and critical questions helped me gain a deeper understanding of the subject and a different perspective on my research.

I am grateful to our industrial collaborators from AbbVie Bioresearch Center, Vineet Kumar (now J&J), Ravi Chari and Michael Siedler for providing me an opportunity to work as a summer intern and pursue research project relevant to the industry. My special thanks to Vineet for his insightful scientific comments and suggestions which have helped me to improve my work and develop scientific acumen.

I am grateful to the Pharmaceutics faculty and the Department of Pharmaceutical Sciences for offering intensive coursework and seminar series that were very useful in my graduate research.

My sincere gratitude to the administrative staff at the School of Pharmacy, Leslie Lebel, Mark Armati, Kathy Koji, Sharon Giovenale, Jackie Patry, Deb Milvae, Laura Burnett and Elizabeth Anderson, for all of their help in creating a smooth graduate life.

I would also like to thank Dr. Laura Pinnati, graduate students in Dr. Challa Kumar's lab and Dr. Fan's lab, especially Mehdi and Carl, for training me and allowing me to use facilities in their lab.

I would like to acknowledge the AAPS Student Chapter at The University of Connecticut, along with its past and present members, for their support and cooperation during my tenure on the executive committee, and for conducting academic and non-academic activities.

Thank you to AbbVie Bioresearch Center, the Department of Pharmaceutical Sciences, the Graduate School at the University of Connecticut, and the American Association of Pharmaceutical Scientist for providing financial support and travel awards during different stages of my graduate studies.

My heartfelt thanks to my past and present labmates, Shermeen, Nitin, Shubhadra, Rajni, Sandeep, Masha, Liz, Japneet and Lauren, for being great labmates and amazing friends.

I would also like to thank my past and present colleagues and friends in the Pharmaceutics department Pooja, Rui, Pawel, Saurabh, Ekneet, Mary, Shilpa, Vamsi, Mike, Bing and Jie.

I would like to express sincere thanks to my friends Amey, Atul, Abhijeet, Shrirang, Tejal, Geetanjali, Dhanashree and Shreehan for being my family in the US, for all their support and encouragement and always being by my side.

PhD is full of ups and downs, and the only thing that keeps you going is the love and support of your family. I would like to thank my in-laws for being supportive throughout my graduate studies. I am indebted to my husband, Haresh for his unconditional love, moral support and constant encouragement throughout these last five years. His positive outlook for life has helped me get through some tough times. His constant inputs in my research have also helped me tremendously improve myself and be better at whatever task is at hand. Thank you for everything. Special thanks to my younger sister, Nimisha, for being supportive and for always cheering me up. I thank her for always believing in me. Words cannot truly express my gratitude towards my parents. I would like to thank my mom, Nisha for her love, support encouragement and trust, without which I could not have made it till here. I thank my dad, Shirish, for his infinite blessings. I owe them all of my accomplishments and success and thank them profusely for making me the person that I am today. I love you all, thank you for being there for me always.

Table of Contents

Chapter 1

Introduction, Aims and Organization of the Thesis

1. Introduction

Since their first approval over 25 years ago, monoclonal antibodies (mAbs) have emerged as the fastest growing and most successful biotherapeutics in the treatment of several terminal diseases including cancer and auto-immune disorders.[1] Second generation of antibody-based therapeutics such as ADCs, bispecific antibodies, engineered antibodies and antibody fragments or domains have generated quite an interest over last few years. These newer molecules have further enhanced the therapeutic efficacy of the first generation of antibodies and have vastly improved their safety profiles.[2,3] Dual Variable Domain immunoglobulin (DVD-Ig^{TM}) protein is a bispecific antibody and is engineered from two mAbs by adding an additional binding domain to variable domain of the parent mAb molecule. This structural design enables DVD-Ig^{TM} protein to achieve dual-targeting resulting in the improved overall efficacy.[4,5] Therapeutic proteins are generally formulated at high concentrations (>100 mg/mL) because of their low potency and low volume restriction (<1.5 mL) imposed by the subcutaneous route of administration. At high concentrations, inter-separation distance between the molecules decreases, thereby increasing their tendency to interact with each other resulting in several formulation challenges including high viscosity, formation of reversible and/or irreversible aggregates, solubility, opalescence and phase transitions.[6-10] These challenges become more exaggerated in DVD-Ig^{TM} protein solutions since these molecules are larger and more complex.

Opalescence at high concentrations reduces aesthetic appeal of the formulation and can be a precursor to phase separation or indicator of the presence of aggregates in solution signifying reduced product stability.[11] Solution conditions where proteins exhibit solid-liquid phase separation (crystallization or amorphous precipitation) or liquid-liquid phase

separation (formation of protein-rich and protein-poor phase) is related to reduced solubility of the proteins.[12] From a pharmaceutical point of view, liquid-liquid phase separation (LLPS) is a concern for formulation development since various protein solutions are stored at refrigerated condition (2-8˚C) where proteins show a higher tendency to phase separate. Protein-rich phase (high concentration) formed on phase separation can promote formation of reversible or irreversible aggregates in solution which compromises physical stability of the formulation, and can reduce safety and efficacy of the product.

Depending on the solution conditions and molecular properties, attractive and repulsive protein-protein interactions (PPI) are present in solution. Opalescence and LLPS in solution can be attributed to attractive interactions which may be specific or non-specific in nature. These interactions depend on the electrostatic charge, dipole moments in macromolecules (charge-dipole, charge–induced dipole, and van der Waals forces), surface amino acids and/or the hydrophobic patches on the surface of the protein (hydrophobic interactions).[13,14] Repulsive interactions in solution result in increased viscosity due to electroviscous effect and excluded volume interactions. Determination of the nature of these interactions in protein solution is of utmost significance so as to select appropriate solution conditions and excipients that reduce these PPI and develop an optimal formulation.

Development of a stable and efficacious therapeutic protein formulation requires a thorough understanding of the problems associated with high concentrations, especially for newer molecules such as DVD-Ig™ protein, which are larger than the naturally occurring IgG molecules. Literature review shows that, extrinsic factors such as pH, ionic strength, excipients, protein concentration and temperature affect opalescence and phase separation in solution. However, there is a lack of clear understanding on how these factors affect the

nature of protein-protein interactions resulting in opalescence and phase separation. Similar factors also play a role in increased viscosity and potential aggregation in protein solutions and needs to be thoroughly investigated. In the view of the available literature, following problems need to be further investigated:

1. Is opalescence in solution due to liquid-liquid phase separation or increased Rayleigh scattering?
2. How do the extrinsic factors affect protein-protein interactions resulting in opalescence and liquid-liquid phase separation?
3. Do DVD-Ig^{TM} protein molecules have a greater propensity to show concentration based effects (phase separation and increased viscosity) at much lower concentrations as compared to mAbs?
4. Does liquid-liquid phase separation in solution result in increased tendency to form aggregates?

2. Objective

The overall objective of the work is to investigate the factors and the nature of intermolecular interactions resulting in opalescence and phase separation for mAb and DVD-Ig^{TM} protein molecules, and understand their relation with increased viscosity and aggregation in solution.

Specific aims of the project are:

1. To study the effect of solution conditions on opalescence in mAb solutions and correlating opalescence with the nature of protein-protein interactions in dilute and concentrated solutions

2. To determine the formulation factors affecting liquid-liquid phase separation in DVD-Ig^{TM} protein solutions
3. To investigate the effect of excipients on liquid-liquid phase separation and aggregation in DVD-Ig^{TM} protein solutions
4. To characterize viscous behavior of DVD-Ig^{TM} protein solutions and understand the role of size, charges and interactions in solution resulting in the increased viscosity

3. Chapter Organization and Outline

A detailed review with the theoretical basis and literature examples of opalescence and liquid-liquid phase separation in protein solutions is presented in **Chapter 2**. Review briefly highlights the theory of opalescence and liquid-liquid phase separation with focus on thermodynamic, kinetic, and light scattering aspects. Overview of intermolecular interactions resulting in physical instability and the relevant parameters (B_2 and T_{cloud}) to measure these interactions in solution is presented in the review. Formulation factors affecting opalescence and phase separation resulting in protein instability are discussed with relevant examples from the literature.

Opalescence in protein solutions can be due to the presence of aggregates in solution or liquid-liquid phase separation (LLPS). **Chapter 3** discusses the solution factors affecting opalescence of a monoclonal antibody (mAb) solution; temperature dependence indicates that LLPS results in opalescent appearance. From literature studies, opalescence is attributed to attractive interactions in solution, however, protein-protein interactions are routinely measured in dilute solutions using techniques including light scattering, while opalescence is observed at relatively higher concentrations. Opalescence was correlated to protein-protein

interactions measured in dilute and concentrated monoclonal antibody solutions. Results indicate that high opalescence and liquid-liquid phase separation are due to the attractive interactions in solution, however, the presence of attractive interactions do not always imply phase separation.

Chapter 4 presents factors influencing liquid-liquid phase separation resulting in opalescence for a DVD-Ig^{TM} protein solution. Larger size and increased asymmetry of the molecule (with respect to shape and surface charge distribution) results in many fold increase in formulation challenges for DVD-Ig^{TM} protein. We first established the thermodynamic basis for phase separation and then studied the effect of different formulation factors on LLPS. No structural changes were observed in the protein before and after phase separation. Interaction parameter, k_D, and T_{cloud} (temperature that marks onset of LLPS in solution) were measured to assess specific and non-specific attractive interactions in solution. A good correlation exists between k_D measured in dilute solution with T_{cloud} measured in the critical concentration range.

Investigation of the effect of different excipients (PEG, Sucrose and Tween) on liquid-liquid phase separation and aggregation in a DVD-Ig^{TM} protein solution is presented in **Chapter 5**. PEG is a precipitant, while other excipients are reported to reduce aggregation in protein solutions; however their effect on LLPS is not known. Results indicate that the mechanism by which different excipients exert their stabilizing/destabilizing effect varies for LLPS and aggregation. Stability studies were performed as a function of temperature to investigate if the systems that undergo phase separation promote aggregate formation in the protein-rich (high concentration) phase. LLPS may promote aggregation in protein solution; however, both show phenomenon strong temperature dependence.

Increased viscosity of solution is observed at high concentration that causes challenges in successful manufacturing and delivery of the therapeutic proteins. Role of the size of the molecule, electroviscous effect and protein-protein interactions on viscosity of DVD-Ig™ protein is discussed in **Chapter 6**. We first established that increased size and asymmetry of the molecule for DVD-Ig™ protein compared to mAb by itself is a significant contributor to the increased viscosity in the form of intrinsic viscosity and excluded volume effects; however, these size effects are significant at higher concentrations. Significant increase in viscosity due to electroviscous effect was observed in the absence of ions in solution, while the presence of ions show minimal electroviscous effect. Intermolecular interactions were studied by changing pH and ionic strength of the solution. Interplay of more than one factor modulates viscosity behavior at high concentration; hence, rank-ordering these factors can provide valuable information on how to approach the high viscosity problem for protein formulations.

Chapter 7 presents a summary of the entire work.

4. References

1. Elbakri A, Nelson PN, Abu Odeh RO. 2010. The state of antibody therapy. Hum Immunol 71(12):1243-1250.
2. Reichert JM, Beck A, Lugovskoy AA, Wurch T, Coats S, Brezski RJ. 2014. 9th annual European Antibody Congress, November 11-13, 2013, Geneva, Switzerland. MAbs 6(2):309-326.
3. Evans JB, Syed BA. 2014. From the analyst's couch: Next-generation antibodies. Nat Rev Drug Discov 13(6):413-414.
4. Gu J, Ghayur T. 2012. Generation of dual-variable-domain immunoglobulin molecules for dual-specific targeting. Methods Enzymol 502:25-41.
5. Kontermann RE. 2012. Dual targeting strategies with bispecific antibodies. MAbs 4(2):182-197.
6. Harris RJ SS, Winter C. . 2004. Commercial Manufacturing Scale Formulation and Analytical Characterization of Therapeutic Recombinant Antibodies. Drug Dev Res 61:137–154.
7. Manning MC, Chou DK, Murphy BM, Payne RW, Katayama DS. 2010. Stability of protein pharmaceuticals: an update. Pharm Res 27(4):544-575.
8. Saluja A, Kalonia DS. 2008. Nature and consequences of protein-protein interactions in high protein concentration solutions. Int J Pharm 358(1-2):1-15.
9. Goswami S, Wang W, Arakawa T, Ohtake S. 2013. Developments and Challenges for mAb-Based Therapeutics. Antibodies 2(3):452-500.
10. Vekilov PG. 2010. Phase transitions of folded proteins. Soft Matter 6(21):5254-5272.
11. Mahler HC, Friess W, Grauschopf U, Kiese S 2009. Protein aggregation: pathways, induction factors and analysis. Journal of pharmaceutical sciences 98(9):2909-2934.
12. Rosenbaum DF, Zukoski CF 1996. Protein interactions and crystallization. Journal of Crystal Growth 169(4):752-758.
13. Laue T. 2012. Proximity energies: a framework for understanding concentrated solutions. J Mol Recognit 25(3):165-173.
14. Israelachvili JN. 2011. Intermolecular and Surface Forces Third ed., San Diego: Academic Press.

Chapter 2

Pharmaceutical Perspective on Opalescence and Liquid-Liquid Phase Separation in Protein Solutions

Contents

Chapter 2

1. Abstract

Opalescence in protein solutions reduces aesthetic appeal of a formulation and can be an indicator of the presence of aggregates or precursor to phase separation in solution signifying reduced product stability. Liquid-liquid phase separation of a protein solution into a protein-rich and a protein-poor phase has been well documented for globular proteins and recently observed for monoclonal antibody solutions, resulting in physical instability of the formulation. The present review discusses opalescence and liquid-liquid phase separation (LLPS) for therapeutic protein formulations. A brief discussion on the theoretical concepts based on thermodynamics, kinetics and light scattering is presented. Review also discusses theoretical concepts behind intense light scattering in the vicinity of the critical point termed as 'critical opalescence'. Both opalescence and LLPS are affected by the formulation factors including pH, ionic strength, protein concentration, temperature and excipients. Literature reports for the effect of these formulation factors on attractive protein-protein interactions in solution as assessed by B_2 and T_{cloud} measurements are also presented. The review also highlights some physiological and mainly pharmaceutical implications of LLPS in protein solutions.

Keyword: opalescence, liquid-liquid phase separation, aggregation, light scattering, thermodynamics, phase diagram, formulation, stability, protein-protein interactions, crystallization, B_2, T_{cloud}

2. Introduction

Monoclonal antibodies (mAbs) have emerged as successful bio-therapeutics in the treatment of several terminal diseases.[1] Continual efforts to enhance the safety and efficacy of these molecules against numerous indications have led to a growing interest in the second generation of antibody-based therapeutics such as ADCs, bispecific antibodies, engineered antibodies and antibody fragments or domains.[2,3] Therapeutic proteins are generally formulated at high concentrations (>100 mg/mL) because of their low potency and low volume restriction (<1.5 mL) imposed by the subcutaneous route of administration. Such formulations present many challenges in the analytical characterization, manufacturing, delivery to the patient, and maintaining stability across the shelf-life.[4] At high concentrations, interactions between the molecules increases,[5,6] resulting in increased opalescence, significantly higher solution viscosity and increased tendency of proteins to undergo phase separation and aggregation, which pose major challenges in the formulation development.[7,8]

Opalescent/turbid appearance of the solution compromises aesthetic appeal of the protein formulation. Opalescence also indicates the presence of aggregates in solution or that the system shows a tendency to undergo phase separation (solid-liquid or liquid-liquid phase separation), both, signifying reduced product stability.[9-15] Presence of higher order reversible (native) or irreversible (non-native) aggregates can compromise protein activity, physical stability of the product and cause immunogenicity concerns.[16-18] Solid-liquid phase separation results in formation of protein crystals or amorphous precipitate indicating reduced solubility of the protein in solution. Liquid-liquid phase separation into a protein-rich and protein-poor phase is a concern from pharmaceutical point of view as most

therapeutic proteins are stored at refrigerated conditions, where tendency to phase separate is much higher.

Dictionary definition of opalescence is "reflection of iridescent light (dichroism) similar to opal". The solution exhibits different colors depending on the angle between incident light and transmitted light. However, in the pharmaceutical literature, turbidity or opacity of the solution i.e. cloudy-whitish appearance is also termed as opalescence. Solution opalescence/turbidity can be attributed to the increased scattering from the solution due to presence of particles (termed as aggregates) or it may also be due to fluctuations of density and concentration (liquid-liquid phase separation). Figure 1 shows opalescence in a protein solution due to liquid-liquid phase separation after the solution was stored at refrigerated condition. For a system exhibiting liquid-liquid phase separation, fluctuations of the thermodynamic quantities increase enormously in the vicinity of the critical point which results in intense scattering from the solutions and is termed as critical opalescence.[19]

Increased opalescence in solution due to insoluble aggregates has been reported for globular proteins[20-24] as well as monoclonal antibodies.[25-28] Examples for opalescence in mAb solution due to liquid-liquid phase separation, which may or may not be associated with critical opalescence, are also present in the literature.[12,13,15] Opalescence has been observed for monoclonal antibody formulation without any aggregate formation or phase separation in solution.[9-11,29] In another case, soluble aggregates of monoclonal antibody resulted in increased turbidity at lower temperatures, which reversed on increasing the temperature. The authors confirmed that the turbidity in solution was indeed due to soluble aggregates (and not phase separation) by performing SEC and DSC studies.[14] Liquid-liquid phase separation (LLPS) in solution is characterized by a temperature-concentration phase diagram (also

termed as coexistence curve) and the presence of aggregates in solution can change the apparent position of the liquid–liquid coexistence curve, affecting the accurate determination of the temperature at which phase separation occurs.[30,31] Opalescence, LLPS and irreversible aggregation for therapeutic protein solutions are well documented in literature, especially for globular proteins; however there is no clear understanding of the inter-relationships between these phenomena.

Aggregation and phase separation result in physical instabilities in solution; however, the underlying thermodynamic and kinetic principles are different for these two phenomena. While on phase separation, protein retains its native structure; aggregation may be associated with formation of native or non-native species in solution. Phase separation is reversible, while aggregation can either be reversible and/or irreversible in nature.[32] Schematic in Figure 2 highlights the difference between these two aspects in protein solution based on protein-protein interactions and temperature. Both aggregation and LLPS in solution result in opalescent appearance of the formulation; however the theoretical basis for light scattering is different for the two i.e, particles in solution and fluctuation of thermodynamic quantities, respectively. Aggregation in protein solutions has been extensively studied and reported in the literature[33-38] and hence in this review, the focus will be on LLPS and its relation to solution opalescence. The review discusses following aspects of opalescence and LLPS:

i. Theoretical aspects
ii. Characterizing opalescence and phase separation
iii. Protein-protein interactions
iv. Factors affecting opalescence and LLPS
v. Implications

3. Theoretical Aspects of Opalescence and Liquid-Liquid Phase Separation

Opalescence and phase separation in solution are thoroughly studied in binary liquid systems and in polymer (colloidal) solutions,[19,39-41] and the knowledge gained has been of immense help in understanding the physical instabilities in protein solutions. In this section, we briefly discuss the thermodynamics defined in terms of free energy and the kinetic mechanism resulting in phase separation for protein solutions. The theoretical concepts of opalescence or light scattering due to particles in solution (aggregates), fluctuation in solution and in the vicinity of the critical point resulting in critical opalescence are also discussed.[40,42]

3.1. Thermodynamics

3.1.1. Phase Diagram

The thermodynamic quantity that undergoes continuous change resulting in phase transitions is termed as the order parameter- Φ (as defined by Landau).[43] For pure liquids (one-component system), the change in density or density fluctuations is the order parameter, while for the binary systems (protein-water system), concentration fluctuation is the order parameter. Phase separation in pure liquid and binary system are commonly described by a pressure-volume and temperature-concentration phase diagram, respectively.[41,43-47] Phase diagram for a binary system (Figure 3) has a liquidus or solubility line, corresponding to the solid-liquid phase transition in one-component system, and a liquid–liquid coexistence line (binodal curve/miscibility curve), corresponding to the gas-liquid phase transition in one-component system. Liquid-liquid phase separation curve lies below the solid-liquid curve and is metastable with respect to crystallization and amorphous precipitate formation.[48,49] Binodal

or coexistence curve is the phase boundary, above which the solution exists as stable one phase system over the entire concentration range. In the area between the binodal and the spinodal curve the system exists in the metastable phase (formation of two phases is kinetically hindered). Inside the spinodal curve, system is thermodynamically unstable and separates into two phases at all conditions of temperature and concentration. The cross-over point of binodal and spinodal is termed as the Critical point defined by a Critical temperature (T_c) and Critical concentration (C_c). Solid-liquid curve do not exhibit a critical point.[50]

Most of the globular proteins[51-56] and monoclonal antibodies[10,12,13,15] studied, exhibit an upper critical solution temperature (UCST) type of phase behavior as illustrated in Figure 3, i.e, phase separation occurs at lower temperatures and system is homogeneous at higher temperatures. Hemoglobin exhibits lower critical solution temperature (LCST) type of phase behavior, where phase separation occurs at higher temperature and system is homogenous at lower temperatures (also termed as retrograde solubility).[57,58]

3.1.2. Fluctuation of Thermodynamic Quantities

A system is said to be thermodynamically stable when the free energy of the system is minimum. Fluctuations of the order parameter (density and concentration fluctuations) results in a change in the free energy of the system.[43,59] Landau, defined the Helmholz free energy of the system (F) in the form of power expansion with respect to order parameter (Φ) and temperature (T). At equilibrium, free energy of the system is minimum ($\partial F / \partial \Phi = 0$) and the equation is given as,

$$\Phi^{\pm} = \pm \left(\frac{a}{b}\right)^{1/2} (T_c - T)^{1/2} \qquad (1)$$

where, T_c is the critical temperature, and T is the temperature above or below the critical temperature, a and b are constants. At $T>>T_c$ there is only one solution to equation 1 and hence one phase exists, while at $T \leq T_c$ two solutions exist for the order parameter (positive and negative), forming two points of the coexistence curve. For a binary system, where concentration fluctuation is the order parameter, Equation 1 can be rearranged to define the coexistence curve in terms of distance from the critical point as,

$$\frac{C - C_C}{C_C} = A\left(\frac{T - T_c}{T_c}\right)^{-\beta} \tag{2}$$

where, C_c is the critical concentration, C is any concentration on the coexistence curve, T_c and T are as defined in Equation 1, A is a constant that defines the width of the coexistence curve and β is the critical exponent that describes the critical behavior close to the critical point. Scaling laws relate all these critical exponents of various thermodynamic quantities.[43]

For binary systems, concentration fluctuations result in liquid-liquid phase separation of the system into two phases of different concentrations. Concentration of the solute in solution is related to its chemical potential, which is defined as partial molar Gibbs free energy and expressed as,

$$\mu_p = \left(\frac{\partial \Delta G}{\partial n_p}\right) \tag{3}$$

where, μ_p is the chemical potential of the protein (solute) in solution and n_p is the total number of protein (solute) molecules in solution (related to protein concentration by mole fraction). Change in free energy of the system for transfer of ∂n_p amount of substance from phase 1 to phase 2 is given by;

$$\partial G = (\mu_p^1 - \mu_p^2)\partial n_p \tag{4}$$

At Equilibrium, $\partial G/\partial n_p$=0 and hence, chemical potential of the solute is same throughout the system ($\mu_p^1 = \mu_p^2$), regardless of the number of phases present.[41] Therefore, on phase separation, the chemical potential for protein is same in both the phases. Figure 4 illustrates the phase diagram for a binary system in terms of free energy (upper part). At any temperature T_1 above T_c, ΔG is negative with one minimum indicating that the solution exists as homogenous one phase system over the entire concentration range. At T_2, which is below T_c, the system has a tendency to phase separate and hence, even though ΔG of the entire system is negative, it has two local minima indicating that the system will separate into two thermodynamically stable phases. Concentrations of these phases are determined by the tangent point on ΔG curve, and are called as binodal points which define the binodal curve. At inflexion point, second derivative of free energy is zero ($\partial^2 \Delta G/\partial c^2 = 0$) and these points are the spinodal points which define the spinodal curve. Critical point is defined as the point where binodal and spinodal curves cross and second as well as third derivative of free energy is zero,

$$\frac{\partial^2 \Delta G}{\partial c^2} = \frac{\partial^3 \Delta G}{\partial c^3} = 0 \qquad (5)$$

At extremely low temperature T_3, within the spinodal curve, there is no energy barrier (free energy of mixing is positive) and system spontaneously phase separates in two thermodynamically stable phases.[41,45]

3.1.3. Free Energy of Mixing: Enthalpic and Entropic Effect

Phase separation ideally means lower solubility of the system or that the system is immiscible.[60-63] Miscibility/immiscibility of the system taking into account enthalpic and

entropic contributions to the free energy of the mixing can be represented as,

$$\Delta G_{mix} = \Delta H_{mix} - T\Delta S_{mix} \quad (6)$$

For a dilute/ideal system, where energy of solute-solvent interactions is greater than the solute-solute interactions, enthalpy of the system is negative ($\Delta H_{mix} < 0$). ΔG_{mix} depends on the entropy of the system; mixing of a solute in solvent increases the disorder of the system and hence promotes mixing by decreasing the free energy. For a system, where enthalpy is positive ($\Delta H_{mix} > 0$), i.e., the energy of interactions between solute-solute and solvent-solvent is greater than the solute-solvent interactions, ΔG_{mix} shows a strong temperature dependence. As observed in Figure 4, at some temperature $T_1 >>> T_c$, entropic contribution ($-T\Delta S$) balances the positive enthalpic contributions resulting in negative ΔG_{mix}, hence promotes mixing. As temperature T_2 approaches and decreases below the critical temperature ($T \rightarrow T_c$), entropic contribution decreases and does not compensate for the positive mixing enthalpy resulting in phase separation. At an extremely low temperature, $T_3 <<< T_c$, ΔG_{mix} is positive and system spontaneously phase separates. On undergoing LLPS, protein separates into a protein rich phase with higher enthalpy (attractive protein-protein interactions) and lower entropy, while protein-poor phase has lower enthalpy and higher entropy. This enthalpy-entropy effect, balances the free energy of the system, hence stabilizing the two phases.[15,64]

3.2. Kinetics of Phase Separation

Attaining thermodynamic equilibrium forms the basis of separation of a binary mixture; however, kinetics controls the ultimate phase separation process. This section discusses the basic kinetic mechanism by which binary system undergoes phase separation as

solution conditions change and a system transitions from stable region to metastable or unstable region. Phase separation of a binary mixture into a protein-rich and protein-poor phase occurs in the metastable region by Nucleation and Growth process while the kinetics of phase separation in spinodal or unstable region is by Spinodal Decomposition.[47] Table 1, outlines the fundamental difference between the two kinetic mechanisms for phase separation.

3.2.1. Nucleation and Growth Process

As the system transitions in the metastable region, formation of a protein-rich phase is initiated, either by homogeneous or heterogeneous nucleation. Phase separation occurs down the concentration gradient as the fluctuation of thermodynamic quantities in the solution increases and diffusion coefficient is positive. Protein-rich phase is surrounded by the protein-poor phase, which is different from the bulk phase and hence results in the formation of an interface, and increases the interfacial free energy ($4\pi r^2\sigma$) of the system, which is proportional to the surface area. Formation of two phases reduces the bulk energy ($4/3\pi r^3\varepsilon$) of the system and is proportional to the volume associated with the formation of a new phase. Free energy term is always negative while interfacial energy term is always positive and hence there are variations in the energy. Total energy of the system is the sum of the two energies and is presented as,[43]

$$\Delta F = 4\pi r^2\sigma + \frac{4}{3}\pi r^3\varepsilon \qquad (7)$$

where, ΔF is a function of size of the nucleus of the new phase. Smaller sized clusters formed on smaller fluctuations, revert back to one-phase; however as the size of the nucleus

reaches a critical size called as critical radius represented by equation 8, these clusters become stable and grow further resulting in the formation of new phase droplets.[65]

$$R = \frac{2\sigma}{\varepsilon} \tag{8}$$

The growth of the nucleus or the nucleation rate is as follows,[66]

$$J = Ae^{-\frac{\omega}{kT}} \tag{9}$$

where, '*A*' is a factor that depends on many parameters such as the size, surface area and total number of droplets.[67] Nucleation rate increases as the system goes further down the coexistence curve i.e, as the temperature of the system is lowered. Due to the formation of spherical droplets on nucleation, the two phases so formed have a sharp interface between them.[67]

3.2.2. Spinodal Decomposition

The phase separation process inside the unstable region occurs by spinodal decomposition mechanism. Since, there is no kinetic barrier, small fluctuations in density or concentration grow in time and space and follow an uphill diffusion (against the concentration gradient). Diffusion coefficient obtained by the Cahn Hilliard approximation is negative.[67] While, nucleation and growth is a local phenomenon, systems exhibiting spinodal decomposition have long-range order. Hence, instead of the formation of droplets there is formation of domains in the unstable region and initially there is no sharp interface between the two phases so formed.[43,63,67]

3.3. Light Scattering from Solution

Opalescence in solution is due to scattering of light, which can either be due to presence of particles or fluctuations in the solution. Theoretical concepts behind both are briefly discussed below, and readers are directed to general references on the topics focusing on light scattering from protein/colloid solutions for further details.[68-74]

3.3.1. Scattering due to Particles in Solution

Intensity of scattering from solution increases with increasing size of the particles. Scattering in the presence of small, isotropic particles (size < λ/10) is described by Rayleigh theory as,

$$I_s = I_0 \frac{2\pi^2}{r^2\lambda^4} \frac{n_p N_A \alpha^2}{V} (1 + cos^2\theta) \quad (10)$$

where, I_s is the intensity of scattered light, I_0 is the intensity of incident light, r is the distance from the scattering center, λ is the wavelength of the light, n_p is the number of particles, α is the polarizability of molecule, V is the molar volume and θ is the scattering angle. Scattering intensity can also be expressed in terms of Turbidity (τ) defined as the total relative amount of light scattered by unit volume in all directions. Particles scattering light in accordance with the Rayleigh theory exhibit an angular symmetry, intensity of light scattered in forward directions is equal to light scattered in backward direction. Maximum scattering intensity is at θ = 0° and 180°, while minimum scattering intensity is at θ= 90°.[74]As the size of the particles increases, more than one site acts as scattering center. Larger particles exhibit an angular asymmetry, the scattering intensity in the forward direction is greater than the intensity for back scattering. At θ = 0°, path lengths are identical, absence of destructive interference results in maximum scattering intensity; while, as scattering angle increases, the

scattering intensity decreases due to destructive interference. Several theories including Mie, Rayleigh-Gans, Debye provide a general correction for scattering intensity in solution for larger particles by considering a form factor.[71]

Table 2 briefly summarizes the size and wavelength dependence of scattering from the solution.[70] According to Rayleigh theory, intensity of scattered light is inversely proportional to the fourth power of wavelength ($I_S \propto \lambda^{-4}$) and hence, shorter wavelengths scatter more light, resulting in bluish appearance of the solution. As the size of the particles increases above that defined by the Rayleigh theory, but smaller than the wavelength of light, scattering intensity exhibits an inverse dependence on second power ($I_S \propto \lambda^{-2}$) of the wavelength of the incident light. As the size of the particles increases and becomes larger than the wavelength of the light, intensity is independent of the wavelength; hence, solution appears whitish instead of bluish as seen in Rayleigh scattering.

3.3.2. Scattering due to Fluctuations in Solution

There are constant density and concentration fluctuations in solution due to thermal (Brownian) motions. Scattering of light in solution occurs due to fluctuations of refractive index $\langle\overline{\Delta\eta}\rangle^2$ in the volume element, ΔV, which in turn depends on fluctuations of density ($\Delta\rho$) and concentrations (Δc) in solution and are represented as,[70]

$$\langle\overline{\Delta\eta}\rangle^2 = \left(\overline{\frac{\partial\eta}{\partial\rho}\Delta\rho + \frac{\partial\eta}{\partial c}\Delta c}\right)^2 = \left(\frac{\partial\eta}{\partial\rho}\right)^2 \langle\overline{\Delta\rho}\rangle^2 + \left(\frac{\partial\eta}{\partial c}\right)^2 \langle\overline{\Delta c}\rangle^2 \qquad (11)$$

The scattering intensity as obtained from Rayleigh theory (equation 10) is modified to accommodate the fluctuations term as,

$$I_s = I_0 \frac{4\pi^2 \Delta V\, \eta^2 \langle\overline{\Delta\eta}\rangle^2}{r^2\lambda^4}(1 + cos^2\theta) \qquad (12)$$

where, η is the refractive index of the medium and is related to polarizability (α) by Clausius Mosotti relation. Eq. 11 can also be expressed in terms of turbidity (τ) of the solution as,

$$\tau = \frac{32\pi^2\eta^2\langle\overline{\Delta\eta}\rangle^2\Delta V}{3\lambda^4} \tag{13}$$

Density fluctuations in pure liquid and concentration fluctuations in binary mixtures are related to the turbidity of the solution and given by Einstein-Smoluchowski Equation;

$$\tau = \frac{4\pi^2}{\lambda^4}\left\{(\rho\frac{dn}{d\rho})^2 kT\chi + (n\frac{dn}{dc})^2 kTV\frac{c}{(\frac{-d\pi_{osm}}{dc})}\right\} \tag{14}$$

τ is the turbidity, λ is the wavelength of the light, ρ is the solvent density, χ is the isothermal compressibility, η is the refractive index, π_{osm} is the osmotic pressure, V is the molar volume, c is the concentration. Isothermal compressibility (χ) is related to the density fluctuations in pure liquids and is defined as the change in volume as a response to change in pressure of the system.[19] Osmotic pressure is related to the concentration fluctuations and as solute-solute interactions increases, osmotic pressure decreases. Increase in fluctuations from solutions due to liquid-liquid phase separation in binary systems results in increased scattering from the solution.

3.3.3. Critical Opalescence

Infinite increase in fluctuations close to the critical point results in increased scattering from the solution termed as critical opalescence.[19,39,75-77] Scattering of light due to fluctuations in solution is given by Einstein equation (equation 14); however, Einstein assumed that the fluctuations in solution were independent or there are no correlations between these fluctuations. In that case, in the vicinity of critical point, fluctuations would be infinite ($1/\chi$ and $d\pi_{osm}/dc$ are zero from pressure-volume and temperature-concentrations

phase diagram, respectively) and hence the intensity of scattered light would be infinite; but in real solutions, intensity of scattering is finite. Ornstein-Zernike accounted for finite correlation between the fluctuations in the volume element ΔV characterized by a correlation length (ξ). [43] By definition, Correlation length is the spatial extent of correlations between the fluctuations and is given by;

$$\xi \propto \left(\frac{T - T_c}{T_c}\right)^{-\nu} \tag{15}$$

where, T is any temperature, T_c is the Critical temperature and ν is the critical exponent. Figure 5 represents schematic for correlation length of fluctuations in solution as temperature approaches critical temperature. At some temperature $T >> T_c$, fluctuations are correlated in small volume element as observed in Figure 5a. As T approaches T_c, correlation between fluctuations increases (Figure 5b) and at T_c, ξ diverges i.e.; fluctuations become correlated over the entire volume element (Figure 5c). This correlation length is related to the intensity of scattered light by a correlation factor and equation 11 is modified as;

$$\frac{I_s}{I_0} = \frac{4\pi^2}{\lambda^4 r^2}\left(\eta \frac{dn}{dc}\right)^2 \left(\frac{kTc}{\left(\frac{-d\pi_{osm}}{dc}\right)}\right) \frac{1}{1 + \left(\xi \frac{4\pi}{\lambda} sin\frac{\theta}{2}\right)^2} (1 + cos^2\theta) \tag{16}$$

Near critical point, scattering intensity due to concentration fluctuations is much larger than density fluctuations.[78] As $T \rightarrow T_c$, scattering intensity depends on $\boldsymbol{\lambda^{-2}}$ as compared to $\boldsymbol{\lambda^{-4}}$, in simple/regular solutions; hence solution appears opalescent in the vicinity of the critical point.[77]

4. Characterizing Opalescence and Phase Separation in Protein Solutions

4.1. Opalescence Measurements

Opalescence in solution is routinely measured using turbidity meter, nephelometer or spectrophotometer and depends on the size and concentration of the particles. Nephelometric turbidity units (NTUs), Formazin turbidity units (FTUs), absorbance (optical density) or percent transmittance are the commonly used units representing opalescence in solution. Opalescence measured in different units can be expressed in standard NTU's by using appropriate calibration standards.[10,13] Opalescence or turbidity of the solution is measured at a fixed wavelength, usually between 450-650 nm, were protein is non-absorbing.[33] Opalescence in solution can also be measured using phase contrast or polarized light microscope.[13,53,79] LLPS and critical opalescence are further characterized by measuring opalescence as a function of temperature and determining correlation length between the fluctuations.

4.2. Phase Separation- Constructing a Phase diagram

Two techniques are generally employed to study phase separation in solution: 1) Temperature quenching and centrifugation method and 2) Cloud-point measurement.[52,80] In temperature quenching method, samples are placed in tubes and then centrifuged at certain speed and time. If there is a phase separation in the sample, concentration is determined in the protein-rich and protein-poor phase by UV-spectrophotometer. Samples are then gently inverted and centrifuged again at lower temperatures. Phase diagram is then constructed by plotting temperature against the concentrations measured in two phases. T_c and C_c are then determined from the phase diagram using equation 2.

In Cloud-point measurement, sample is placed in temperature controlled water bath/chamber and turbidity of the sample is measured as temperature is lowered. Onset of the liquid-liquid phase separation is characterized by a dramatic increase in solution turbidity; this temperature is marked as $T_{opacity}$. Temperature is then increased step wise till solution becomes clear, and this temperature is marked as T_{clear}. Average temperature between $T_{opacity}$ and T_{clear} is the T_{cloud} temperature.[81] Cloud point measurements can also be performed using microscope fitted with a temperature control. On lowering the temperature, onset of phase separation can be visually assessed by darkening of the field.[79] The spinodal temperatures are determined by extrapolating inverse of the intensity measured at 90° angle to zero at varying concentrations.[80,81] The coexistence curve and spinodal curve are then fitted to equation 2 to determine the Critical point.

4.3. Characterizing Critical Opalescence

Several studies are reported in the literature where LLPS for globular proteins was related to critical opalescence in solution.[80-82] Though there are speculations for increased solution opalescence for mAb as critical opalescence,[10] there are very few studies were divergence of thermodynamic properties close to the critical point are actually quantified.[83] Earliest studies on liquid-liquid phase separation in lysozyme-salt solution using light scattering methods were performed by Ishimoto and Tanaka, were they demonstrated existence of critical point for protein in binary solutions. They characterized the asymptomatic behavior of fluctuations close to the critical point, confirming critical opalescence for lysozyme solution. Authors also determined correlation length (ξ) of the fluctuations using mean-field approximation.[81] In the vicinity of the critical point, scattering

at coexistence temperatures and spinodal temperatures are reported to be similar (and converge) for γ-crystallins.[80] Detailed experimentation and relationships to determine osmotic isothermal compressibility (χ) and correlation length is described in the literature.[82]

5. Protein-Protein Interactions and LLPS

Liquid-liquid phase separation in a binary system occurs when solute-solute interactions are greater than solute-solvent interactions (enthalpy effect) and when temperature of the system is lowered (entropy effect). For a protein solution, attractive protein-protein interactions determine if a system will undergo liquid-liquid phase separation. Crystallization and its relation to protein-protein interactions in solution has been thoroughly studied and reported in the literature.[84] LLPS is metastable with respect to crystal formation and hence, similar to solid-liquid phase transition, attractive interactions result in liquid-liquid phase separation in solution. In this section, we briefly discuss different types of attractive interactions determined for protein solutions, followed by parameters that indicate attractions in solution, B_2 (second virial coefficient) and T_{cloud}/T_c (cloud temperature/ critical temperature).

5.1. Nature of Attractive PPI in Protein Solution

Protein-protein interactions play a significant role in opalescence and phase separation in solutions and determining the nature of these interactions holds the key for the selection of appropriate solution conditions (pH, ionic strength, salt type, etc.) and excipients to formulate a physically stable product. Interactions in protein/colloidal solutions are a well-researched area, and details for the same are extensively available in the literature.[5,74,85-87]

Molecular properties and solution conditions that strongly influence protein-protein interactions are discussed below.

Charges

Though the presence of charges on proteins results in repulsive interactions between them, as the inter-separation distance decreases and protein molecules approach each-other, charges on the protein molecule may interact with oppositely charge dipole/induced-dipole resulting in attractive interactions in solution.

Dipolar interactions

At high protein concentration, van der Waals interaction including dipole-dipole, dipole-induced dipole and induced dipole-induced dipole, are the dominant forces in solution. Dipole-mediated interactions in proteins are further enhanced for asymmetrical and larger molecules like mAb (and DVD-Ig™) due to their geometry and orientation/asymmetric charge distribution on the protein surface.[88] Dipolar interactions are dominant close to the pI of the molecule, while charge-dipole interactions dominate at pH away from the pI (where protein carries net charge). The mean potential force due to the charge and dipole interactions decreases on increasing the ionic strength of the solution.[89,90]

Hydrophobic interactions

Presence of hydrophobic amino acids/patches on protein surface results in attractive hydrophobic interactions in solution which are short-ranged in nature (i.e, proximity energy increases as protein molecules approach each other at high concentrations). Low ionic strengths have no effect on these interactions, however, high ionic strength, increases hydrophobic interactions. Any excipient that interacts with the surface hydrophobic amino acids reduces these attractive interactions in solution.[91-93 94]

Specific interactions

The presence of certain specific amino acids on protein surface results in specific-interactions between the protein molecules; these interactions include cation-π, π-π aromatic interactions,[95] etc. These attractive interactions decrease on addition of amino acids and its derivatives that bind specifically with amino acids on protein surface.[94,96-98]

5.2. Second Virial Coefficient (B_2)

Second virial coefficient (B_2) is routinely used to characterize protein-protein interactions in formulation development. B_2 can be measured using various techniques including Membrane osmometry, Static Light scattering, Self-interaction chromatography, etc. Virial expansion for osmotic pressure in protein solution is presented as,

$$\pi = RTc\left(\frac{1}{M_w} + 2B_2c + 3B_3c^{\,2} + 4B_4c^{\,3} + \cdots\right) \qquad (17)$$

where, π isosmotic pressure, R is the universal gas constant, T is the absolute temperature, c is the solute concentration, M_w is the average molecular weight. At infinite dilutions, higher order terms are neglected and equation 17 reduces to van't Hoff equation for ideal solution. B_2 is the first measure of deviation from ideality in solution and characterizes interactions in solutions. The value of B_2 reflects the magnitude of the deviation from the ideality, while its sign reflects the nature of this deviation. A positive value corresponds to net repulsive interactions between the solute molecules wherein the osmotic pressure increases above that for an ideal solution whereas a negative value corresponds to net attractive interactions between the solute molecules with a consequent decrease in solution osmotic pressure below that for an ideal solution.[99] Good correlation has been established between B_2 and protein

solubility, [100,101] crystallization,[48,102,103] and protein precipitation;[104] all of which characterize phase separation in solution.[101,105]

Several studies in the literature refer to a 'crystallization slot' i.e a range of B_2 values which allows for the formation and growth of crystals in solution. Crystallization occurs only when B_2 values are between -1 and $-8*10^{-4}$ mol. mL/gm^2; high B_2 indicating strong attractive interactions would result in the formation of amorphous precipitate, while low B_2 indicating weak interactions would prevent crystal formation.[106] These B_2 values are in good agreement with crystal formation for globular proteins; however as the complexity of the molecule increases as observed for mAb, crystallization slot may not be an ideal predictor of crystallization or LLPS in solution. There are several examples in the literature, where crystallization occurs in solution with B_2 values outside the crystallization slot.[107,108]

5.3. Critical Temperature T_c, T_{cloud}

Critical temperature is the temperature at the critical concentrations, i.e., concentration indicating maximum opalescence and below which system is unstable, while T_{cloud} marks the onset of liquid-liquid phase separation in solution at any concentration on the coexistence curve. For a system exhibiting attractive interactions (positive enthalpy), the change in temperature modulates the entropy and hence the free energy of the system. On similar lines, the change in temperature of onset of LLPS indicates increased or decreased attractive interactions in solution. B_2 is measured under dilute solution conditions, however LLPS occurs at relatively higher concentrations and hence T_{cloud} or T_c, which can be measured at high concentrations can be a better indicator of attractions at higher

concentrations. T_{cloud} can be determined by any of the opalescence measurement techniques mentioned earlier (Section 4).

Taratuta and coworkers established the coexistence curve for lysozyme solution at various pHs and determined that the coexistence curve shifts parallel with temperature as a function of solution conditions. Shape and width of the coexistence curve as well as Critical concentration C_c (230±10 mg/mL) remains fairly constant. As a result, they optimized T_{cloud} as a parameter to asses LLPS in lysozyme solution with change in pH, ionic strength and salt type details of which are provided in the next section (Section 6). Shifts in T_{cloud} with solution conditions were modeled to thermodynamic Gibbs free energy with contribution from attractive interactions between the hard spheres. Authors suggested that C_c is similar for similar sized molecules while T_c is a physical property that changes with the solution conditions.[52] Similar observations were reported by Broide et al., where Critical concentration (C_c ~289±20 mg/mL) and width of the coexistence curve (A ~2.6±0.1) remains same for different γ-crystallins, while T_c changes.[53] In another study, authors investigated T_{cloud} for lysozyme as a function of different salt ions and correlated it to the strength of protein interactions using DLVO theory model for colloids.[109] Similar studies are reported in the literature for globular proteins and monoclonal antibodies, where, critical temperature or T_{cloud} is measured as a function of solution conditions to assess attractive interactions in solution and are elaborated in the next section.

6. Factors Affecting Opalescence and LLPS

In this section, we briefly discuss the effect of formulation factors including pH, ionic strength, salt types and other excipients on LLPS in protein solutions with relevant examples.

These factors modulate the PPI in solution, thereby, increasing or decreasing opalescence and tendency to undergo LLPS.

6.1. Effect of Excipients on Opalescence in mAb Solutions

Formation of irreversible aggregates and LLPS in solution results in increased opalescence; however there are few studies, where mAb solution is opalescent and neither aggregation nor LLPS is observed in the solution. Salinas et al., reported increased opalescence at high ionic strength (due to attractive interactions as determined from B_2) which decreased on reducing the ionic strength of the solution.[10] Similar observations were reported by Wang et al., where solution was clear at low ionic strength and opalescence increased on addition of salt. They attributed increased opalescence to hydrophobic interactions, which become dominant on charge shielding; consequently, Tween 80 reduces opalescence by disrupting hydrophobic interactions between the protein molecules. They also concluded from their studies that ionic strength rather than specific ions from Hofmeister series influences opalescence in solution.[11] On the contrary, Woods et al., concluded that at low salt concentration different salts affect opalescence differently; citrate and succinate buffers reduce opalescence, while, acetate increases opalescence. They rank ordered different buffer species on reducing opalescence by their ability to interact with hydrophobic regions and preventing mAb self-association.[29] Though, LLPS was not observed in any of the above studies, opalescence in solution increased on lowering the temperature (Wang and coworkers did not study the temperature effect), and was reversible with changing solution conditions.

6.2. Effect of Excipients on LLPS in Protein Solution

6.2.1. pH and Ionic Strength

Maintaining a constant pH and ionic strength is necessary not only from physiological point of view, but for proper storage of the formulation and maintaining its stability and solubility throughout the shelf life. Most studies reported in the literature indicate increased tendency of a protein to undergo LLPS close to the pI of the molecule. Taratuta and coworkers observed T_{cloud} shifts to higher temperature for lysozyme solution as pH was adjusted close to the pI (~11.2) of the protein.[52] Similar observation was reported for a certain mAb (IgG2), where solution opalescence was maximum close to the pI (pH ~7.1) and decreased on increasing the ionic strength, while at pH away from pI, opalescence increased at high ionic strength.[13] This change in opalescence with changing pH and ionic strength correlated well with change in critical temperature at a constant critical concentration (C_c ~ 90 mg/mL).[110] Nishi et al., reported increased opalescence, due to LLPS, close to the pI (pH~6.5) of the molecule for another mAb (IgG1) at low ionic strength conditions, which reversed on increasing the ionic strength of the solution.

This pH dependence of opalescence and phase separation is similar to the solubility of the protein, where, solubility increases at pH conditions away from pI and is minimal at the pI. At low ionic strength, strong attractive interactions are present close to the pI of the molecule and can be attributed to dipoles and multipoles on the molecule, which are shielded on increasing the ionic strength of the solution. At pH conditions away from the pI, molecules carry a net charge and hence repel each other resulting in increased solubility (salting-in) and lower tendency to phase separate. However, as ionic strength is increased, charges on the molecules are shielded and there may be attractions between the protein

molecules due to preferential exclusion of salts resulting in reduced solubility (salting-out). Broide et al., correlated the solubility of lysozyme with T_{cloud} measurements as a function of ionic strength and observed that point of minimal solubility correlated to the maximum T_{cloud} in the solution.[109]

Though, pH and ionic strength result in increased or decreased tendency of protein to undergo LLPS, this behavior cannot be generalized as it also depends on the nature/identity of the salt-ion. For lysozyme protein, Taratuta and coworkers observed that the effect of anionic species is more prominent than cationic species as protein carries a net positive charge at the conditions studied.[52] While in another study, it was determined that both cationic and anionic salt species have varying effect on T_{cloud} of lysozyme depending on the pH and ionic strength.[111] Broide et al., reported the effect of two anions, Cl^- and Br^-, on T_{cloud}, which reversed with ionic strength; below 1 M ionic strength, T_{cloud} value for Br^- is larger than T_{cloud} for Cl^-, while between 1 and 2 M ionic strength, T_{cloud} for Cl^- is larger than that for Br^-.[109] Mason and coworkers performed extensive studies on the effect of different salts from Hofmeister series on LLPS in mAb solution. T_c decreases with increasing ionic strength and anions have a non-monotonic (no particular trend observed) influence on LLPS in solution at pH conditions away from the pI.[110] Salts and buffer species exert their effects mostly by electrostatic interactions which can be explained by DLVO theory. This is supported by several studies in the literature that discuss the differential hydration of the protein molecules in the presence of different salt ions as the cause for change in T_{cloud}.[109,111-113] The exact mechanism by which salt-species affect salting-in vs. salting-out behavior is still under investigation and the discussion is beyond the scope of this review.

6.2.2. Polyethylene Glycol (PEG)

Polyethylene glycol (PEG) is a known macromolecular crowder and a precipitating agent for proteins.[114,115] It is frequently used in purification of proteins and production of protein crystals in the solution. PEG precipitation has also been reported as a method for solubility screening of proteins in solution.[116-118] PEG exerts its effect by depletion force, thereby increasing protein-protein interactions in solution. This results in the increased tendency of proteins to precipitate out of the solution either as solid phase or liquid phase. Liquid-liquid coexistence curve shifts to higher or lower temperatures with change in pH or ionic strength of the solution; similarly, increasing concentration as well as molecular weight of PEG raises T_c to higher temperatures. Extensive work has been carried out for the determination of colloidal stability by assessing shifts in the coexistence curve of protein solutions using PEG-induced LLPS.[119-123] Every proteins undergoes phase separation at some temperature, which depends on both, the intrinsic nature of the protein and solution conditions; for a few proteins phase separation temperatures is above freezing, while others do not exhibit phase separation at temperatures as low as 0 °C. PEG raises the phase separation temperature of the protein and hence is extensively used to study the solubility of proteins as a function of solution conditions. However, PEG is also known to bind with proteins resulting in uncertainties in LLPS determination. Also, screening of the excipients that have a mechanism similar to PEGs may increase the challenge to determine T_c as PEG may also interact with other added excipients.[124]

6.2.3. Other Proteins

Wang et al., studied LLPS for a monoclonal antibody in the presence of Human Serum Albumin (HSA) at physiological pH (7.4) to mimic blood serum conditions where HSA forms a major component. At pH 7.4, the two molecules carry opposite charge resulting in interaction of HSA (pI ~5.7) with mAb (pI ~8.8) and hence partitioning into protein-rich phase. Favorable interactions of mAb with HSA reduce attractive interactions/self-association between the mAb molecules and shift the coexistence curve to lower temperatures. [125]

6.2.4. Polyols

Though, polyols are commonly used for reducing thermal aggregation in solution, its effect on phase separation are not well understood. There is only one study in the literature, where increasing concentration of glycerol has been reported to decrease the phase separation temperature for lysozyme, which was hypothesized to be due to specific binding of glycerol with protein.[79]

6.3. Effect of Molecular Properties on LLPS

Proteins that have a higher proximity energy of attractions will show an increased tendency to phase separate. Other than formulation factors, the inherent nature of the protein molecule including, its size, shape, surface charge heterogeneity, amino acid sequence, hydrophobicity etc., may result in increased interactions between them. Broide et al., compared LLPS for four different γ-crystallins which differed in their amino acid sequence. They observed that the coexistence curve for different γ-crystallins can be divided into low

T_c (5 °C) and high T_c (38 °C) group; γ-crystallins with high T_c resulted in cataract at body temperature.[53]

Wang et al., plotted a scaled coexistence curve (binodal curve of phase diagram) for three different proteins and hard-spheres.[125] Globular proteins, crystallins (MW ~ 20 kDa) and lysozyme (MW ~ 14 kDa) have narrow and symmetrical coexistence curves, similar to that for a hard sphere, while monoclonal antibody (MW ~ 150 kDa) exhibits a wider and asymmetrical coexistence curve due to its non-spherical shape and increased flexibility. Critical concentration for crystallins and lysozyme are 240 ± 10 mg/mL and 230 ± 10 mg/mL,[52] respectively, while for the mAb the critical concentration is a range of 50- 100 mg/mL.[10,13,15,125] Our unpublished studies on a LLPS in bispecific antibody solution (Chapter 4) indicates that as the size and the complexity of the protein molecules increases, it shows a higher tendency to phase separate even at lower protein concentrations.

7. Implications of Liquid-Liquid Phase Separation

Liquid-liquid phase separation of globular proteins under physiological conditions results in certain diseases and has been studied and reported in the literature from physiological point of view. However, recently, implications of liquid-liquid phase separation from pharmaceutical perspective are also accounted for and will be briefly discussed in this section.

7.1. Physiological Consequences

Phase separation of biological fluids has been reported to result in condensation diseases. Some examples include cold cataract [31,126], sickle-cell disease,[127-129]

neurodegenerative and amyloidogenic diseases[130] and cryoimmunoglobinemia.[131] Hence, investigation of a protein formulation for LLPS under solution conditions mimicking physiological conditions can provide a better picture and help in prevention of physiological disorders.

7.2. Aesthetic Appeal

Marketed protein formulations are generally stored at refrigerated conditions where they may exhibit slight turbidity or cloudiness in the solution. Though this cloudiness/haziness is reversible as the formulation is brought to the room temperature and may not be serious from a physical stability point of view, opalescent appearance of the solution reduces its aesthetic appeal. It can also raise concerns about the quality of the product leading to patient incompliance. Mahler et al., have compiled the description/definition of opalescence in solution as per European Pharmacopeia limits.[33] Any solution above 3 FTUs is termed as opalescent and from formulation point of view should be investigated for possibility of presence of aggregates or phase separation.

7.3. Physical Instability

Phase separation, both solid-liquid and liquid-liquid, indicate reduced physical stability of a protein solution. Though, native structure of the protein is retained on phase separation, the overall integrity of the product is compromised. Also, formation of solid phase or solid-liquid phase separation in solutions is associated with reduced solubility of proteins. High concentration phase formed on LLPS can also promote formation of irreversible aggregate in solution which is of serious concern in formulation development.

On phase separation, the chemical potential of the protein is same in both phases even though their concentrations are different.[132,133] To account for the Donnan effect, salts in the solution would also partition in two phases according to the concentration gradient and maintain the chemical potential across the solution.[134,135] This can result in pH shift/ionic strength difference in two phases and may further enhance physical instability.[136]

7.4. Concentrating Proteins in Solution

Phase separation is a concern for formulation development and results in physical instability, however, under controlled conditions LLPS can be used to concentrate proteins as the formation of a protein-rich phase in the solution is spontaneous.[56,137,138] High concentrations of protein formulation can be easily achieved on a large scale compared to other such techniques as ultrafiltration, drying, chromatography and dialysis,[4] which are time consuming and increase production cost. Nishi and coworkers studied the properties of concentrated phase obtained on phase separation and reported no change in physical or chemical properties and binding ability of the antibody before phase separation.[12]

7.5. Crystallization in Solution

Obtaining high quality crystals of proteins is one of the major challenges for crystallographers, as crystal formation occurs in very narrow range of conditions.[139] Also, crystallization is a tedious process and nucleation and crystal growth may normally take weeks to occur and grow. LLPS is metastable with respect to protein crystallization and hence for systems that exhibit LLPS, crystallization follows a two-step nucleation mechanism where formation of dense phase is followed by nucleation within the phase.[138,140]

Process of nucleation can be hastened in the dense phase reducing the time and energy for crystal growth. For any protein solutions, formulation conditions where crystal growth can occur can be easily optimized by studying LLPS for that system.[141,142] Measuring B_2 and T_{cloud}, that exhibits a good correlation with LLPS, can also be easily optimized for high throughput techniques resulting in better and efficient formulation development process.

8. Summary

A thorough understanding of the opalescence and liquid-liquid phase separation in solution is important for formulation development of therapeutic proteins. This review addresses the basic theoretical difference between scattering of light due to aggregates in solution and due to liquid-liquid phase separation; understanding of which may help in better optimization of solution conditions to reduce physical instabilities. The thermodynamic and kinetic basis for phase separation is different from that of aggregation and is briefly discussed in this review. Nature of protein-protein interactions and parameters to measure the same, effect of formulation factors and molecular properties affecting opalescence and liquid-liquid phase separation in solutions is also discussed with relevant literature examples. Finally the review discusses the implications of these physical instabilities both from physiological and pharmaceutical point of view.

9. References

1. Elbakri A, Nelson PN, Abu Odeh RO. 2010. The state of antibody therapy. Hum Immunol 71(12):1243-1250.
2. Reichert JM, Beck A, Lugovskoy AA, Wurch T, Coats S, Brezski RJ. 2014. 9th annual European Antibody Congress, November 11-13, 2013, Geneva, Switzerland. MAbs 6(2):309-326.
3. Evans JB, Syed BA. 2014. From the analyst's couch: Next-generation antibodies. Nat Rev Drug Discov 13(6):413-414.
4. Shire SJ, Shahrokh Z, Liu J. 2004. Challenges in the development of high protein concentration formulations. J Pharm Sci 93(6):1390-1402.
5. Saluja A, Kalonia DS. 2008. Nature and consequences of protein-protein interactions in high protein concentration solutions. Int J Pharm 358(1-2):1-15.
6. Hall D, Minton AP. 2003. Macromolecular crowding: qualitative and semiquantitative successes, quantitative challenges. Biochim Biophys Acta 1649(2):127-139.
7. Daugherty AL, Mrsny RJ. 2006. Formulation and delivery issues for monoclonal antibody therapeutics. Adv Drug Deliv Rev 58(5-6):686-706.
8. Harris RJ SS, Winter C. . 2004. Commercial Manufacturing Scale Formulation and Analytical Characterization of Therapeutic Recombinant Antibodies. Drug Dev Res 61:137–154.
9. Sukumar M, Doyle BL, Combs JL, Pekar AH. 2004. Opalescent appearance of an IgG1 antibody at high concentrations and its relationship to noncovalent association. Pharm Res 21(7):1087-1093.
10. Salinas BA, Sathish HA, Bishop SM, Harn N, Carpenter JF, Randolph TW. 2010. Understanding and modulating opalescence and viscosity in a monoclonal antibody formulation. J Pharm Sci 99(1):82-93.
11. Wang N HB, Ionescu R, Mach H, Sweeney J, Hamm C, Kirchmeier MJ, Meyer BK. 2009. Opalescence of an IgG1 monoclonal antibody formulation is mediated by ionic strength and excipients. BioPharm Int 22(4):36-47.
12. Nishi H, Miyajima M, Nakagami H, Noda M, Uchiyama S, Fukui K. 2010. Phase separation of an IgG1 antibody solution under a low ionic strength condition. Pharm Res 27(7):1348-1360.
13. Mason BD, Zhang L, Remmele RL, Jr., Zhang J. 2011. Opalescence of an IgG2 monoclonal antibody solution as it relates to liquid-liquid phase separation. J Pharm Sci 100(11):4587-4596.
14. Sahin E, Weiss WFt, Kroetsch AM, King KR, Kessler RK, Das TK, Roberts CJ. 2012. Aggregation and pH-temperature phase behavior for aggregates of an IgG2 antibody. J Pharm Sci 101(5):1678-1687.
15. Raut AS, Kalonia DS. 2015. Opalescence in a Monoclonal Antibody Solution and its Correlation with Intermolecular Interactions in Dilute and Concentrated Solutions. Journal of Pharmaceutical Sciences (accepted).
16. Wang W, Singh S, Zeng DL, King K, Nema S. 2007. Antibody structure, instability, and formulation. J Pharm Sci 96(1):1-26.
17. Liu J, Nguyen MD, Andya JD, Shire SJ. 2005. Reversible self-association increases the viscosity of a concentrated monoclonal antibody in aqueous solution. J Pharm Sci 94(9):1928-1940.

18. Saluja A, Badkar AV, Zeng DL, Nema S, Kalonia DS. 2006. Application of high-frequency rheology measurements for analyzing protein-protein interactions in high protein concentration solutions using a model monoclonal antibody (IgG2). J Pharm Sci 95(9):1967-1983.
19. Gopal ESR. 2000. Critical opalescence. Resonance 5(4):37-45.
20. Pearlman R, Bewley T. 1993. Stability and Characterization of Human Growth Hormone. In Wang YJ, Pearlman R, editors. Stability and Characterization of Protein and Peptide Drugs, ed.: Springer US. p 1-58.
21. Eckhardt BM, Oeswein JQ, Yeung DA, Milby TD, Bewley TA. 1994. A turbidimetric method to determine visual appearance of protein solutions. J Pharm Sci Technol 48(2):64-70.
22. Hsu CC, Nguyen HM, Yeung DA, Brooks DA, Koe GS, Bewley TA, Pearlman R. 1995. Surface denaturation at solid-void interface--a possible pathway by which opalescent particulates form during the storage of lyophilized tissue-type plasminogen activator at high temperatures. Pharm Res 12(1):69-77.
23. Eberlein GA, Stratton PR, Wang YJ. 1994. Stability of rhbFGF as determined by UV spectroscopic measurements of turbidity. PDA J Pharm Sci Technol 48(5):224-230.
24. Yu CM, Chin CY, Franses EI, Wang NH. 2006. In situ probing of insulin aggregation in chromatography effluents with spectroturbidimetry. J Colloid Interface Sci 299(2):733-739.
25. Mahler HC, Muller R, Friess W, Delille A, Matheus S. 2005. Induction and analysis of aggregates in a liquid IgG1-antibody formulation. Eur J Pharm Biopharm 59(3):407-417.
26. Kiese S, Papppenberger A, Friess W, Mahler HC. 2008. Shaken, not stirred: mechanical stress testing of an IgG1 antibody. J Pharm Sci 97(10):4347-4366.
27. Sharma DK, Oma P, Pollo MJ, Sukumar M. 2010. Quantification and characterization of subvisible proteinaceous particles in opalescent mAb formulations using micro-flow imaging. J Pharm Sci 99(6):2628-2642.
28. Kiese S, Pappenberger A, Friess W, Mahler H-C. 2010. Equilibrium studies of protein aggregates and homogeneous nucleation in protein formulation. Journal of Pharmaceutical Sciences 99(2):632-644.
29. J. Woods DN. 2010. Formulation effects on opalescence of a high-concentration MAb. BioProcess Int 8(48-59).
30. Asherie N. 2004. Protein crystallization and phase diagrams. Methods 34(3):266-272.
31. Pande A, Pande J, Asherie N, Lomakin A, Ogun O, King J, Benedek GB. 2001. Crystal cataracts: human genetic cataract caused by protein crystallization. Proc Natl Acad Sci U S A 98(11):6116-6120.
32. Roberts CJ. 2014. Protein aggregation and its impact on product quality. Current Opinion in Biotechnology 30(0):211-217.
33. Mahler HC, Friess W, Grauschopf U, Kiese S. 2009. Protein aggregation: pathways, induction factors and analysis. J Pharm Sci 98(9):2909-2934.
34. Weiss WF, Young TM, Roberts CJ. 2009. Principles, approaches, and challenges for predicting protein aggregation rates and shelf life. Journal of Pharmaceutical Sciences 98(4):1246-1277.
35. Li Y, Roberts CJ. 2010. Protein Aggregation Pathways, Kinetics, and Thermodynamics. Aggregation of Therapeutic Proteins, ed.: John Wiley & Sons, Inc. p 63-102.

36. Sharma VK, Kalonia DS. 2010. Experimental Detection and Characterization of Protein Aggregates. Aggregation of Therapeutic Proteins, ed.: John Wiley & Sons, Inc. p 205-256.
37. Sanchez-Ruiz JM. 2010. Protein kinetic stability. Biophys Chem 148(1-3):1-15.
38. den Engelsman J, Garidel P, Smulders R, Koll H, Smith B, Bassarab S, Seidl A, Hainzl O, Jiskoot W. 2011. Strategies for the assessment of protein aggregates in pharmaceutical biotech product development. Pharm Res 28(4):920-933.
39. Furth R, Williams CL. 1954. Opalescence and Concentration Fluctuations in Binary Liquid Mixtures Near the Critical Mixing Point. II. Theoretical. ed. p 104-119.
40. Rowlinson J. 1969. Liquids and liquid mixtures.
41. Van Dijk MA, Wakker A. 1998. Concepts in Polymer Thermodynamics. ed.: CRC Press.
42. Fisher M. 1971. Critical Phenomena, Proceedings of the International School of Physics" Enrico Fermi," Course LI.
43. D. Beysens JS, and D.J. Turner,. 1987. Phase Transition and Near Critical Phenomena,. ed., Berlin: Springer,.
44. Atkins P, De Paula J. 2014. Atkins' physical chemistry. ed.: Oxford University Press.
45. Utracki LA. 1994. Thermodynamics and Kinetics of Phase Separation. Interpenetrating Polymer Networks, ed.: American Chemical Society. p 77-123.
46. Zhang W. 2005. Phase behavior and phase separation kinetics in polymer solutions under high pressure. ed.: Virginia Polytechnic Institute and State University.
47. Lipatov IS. 1988. Colloid chemistry of polymers. ed.: Elsevier.
48. Rosenbaum DF, Zukoski CF. 1996. Protein interactions and crystallization. Journal of Crystal Growth 169(4):752-758.
49. Piazza R. 2000. Interactions and phase transitions in protein solutions. Current Opinion in Colloid & Interface Science 5(1–2):38-43.
50. Tisza L. 1950. The The Theory of Critical Points. The Journal of Physical Chemistry 54(9):1317-1323.
51. Thomson JA, Schurtenberger P, Thurston GM, Benedek GB. 1987. Binary liquid phase separation and critical phenomena in a protein/water solution. Proc Natl Acad Sci U S A 84(20):7079-7083.
52. Taratuta VG HA, Thurston GM, Blankschtein D, Benedek GB. 1990. Liquid–liquid phase separation of aqueou lysozyme solutions: Effects of pH and salt identity. J Phys Chem 94:2140-2144.
53. Broide ML, Berland CR, Pande J, Ogun OO, Benedek GB. 1991. Binary-liquid phase separation of lens protein solutions. Proc Natl Acad Sci U S A 88(13):5660-5664.
54. Manno M, Xiao C, Bulone D, Martorana V, San Biagio PL. 2003. Thermodynamic instability in supersaturated lysozyme solutions: effect of salt and role of concentration fluctuations. Phys Rev E Stat Nonlin Soft Matter Phys 68(1 Pt 1):011904.
55. Wentzel N, Gunton JD. 2007. Liquid-liquid coexistence surface for lysozyme: role of salt type and salt concentration. J Phys Chem B 111(6):1478-1481.
56. Dumetz AC, Chockla AM, Kaler EW, Lenhoff AM. 2008. Protein phase behavior in aqueous solutions: crystallization, liquid-liquid phase separation, gels, and aggregates. Biophys J 94(2):570-583.

57. Vekilov PG, Feeling-Taylor AR, Petsev DN, Galkin O, Nagel RL, Hirsch RE. 2002. Intermolecular interactions, nucleation, and thermodynamics of crystallization of hemoglobin C. Biophys J 83(2):1147-1156.
58. Galkin O, Chen K, Nagel RL, Hirsch RE, Vekilov PG. 2002. Liquid-liquid separation in solutions of normal and sickle cell hemoglobin. Proc Natl Acad Sci U S A 99(13):8479-8483.
59. Stanley HE. 1971. Introduction to Phase Transition and Critical Phenomena. ed., New York: Oxford University Press.
60. Young RJ, Lovell PA. 1991. Introduction to polymers. ed.: Chapman & Hall London.
61. Strobl GR, Strobl GR. 1997. The physics of polymers. ed.: Springer.
62. Holyst R. 1996. Solubility and mixing in fluids. arXiv preprint cond-mat/9603062.
63. Favvas E, Mitropoulos AC. 2008. What is spinodal decomposition. Journal of Engineering Science and Technology Review 1:25-27.
64. Drenth J. 2005. The Nucleation of Lysozyme from a Fluctuation Point of View. Crystal Growth & Design 5(3):1125-1127.
65. Wagner R, Kampmann R, Voorhees PW. 2005. Homogeneous Second-Phase Precipitation. Phase Transformations in Materials, ed.: Wiley-VCH Verlag GmbH & Co. KGaA. p 309-407.
66. J. J. De Yoreo PV. 2003. Principles of crystal nucleation and growth. ed., Washington, DC: Mineral Society of America.
67. Gunton JD. 1999. Homogeneous Nucleation. Journal of Statistical Physics 95(5-6):903-923.
68. Debye P. 1944. Light Scattering in Solutions. Journal of Applied Physics 15(4):338-342.
69. Morel A. 1974. Optical properties of pure water and pure sea water. Optical aspects of oceanography 1.
70. Oster G. 1948. The Scattering of Light and its Applications to Chemistry. Chemical Reviews 43(2):319-365.
71. Hiemenz P. C RR. 1997. Principles of Colloid and Surface Chemistry. 3 ed., New York: Marcel Dekker, Inc.
72. Berne BJ, Pecora R. 2000. Dynamic light scattering: with applications to chemistry, biology, and physics. ed.: Courier Dover Publications.
73. Brown W NT. 1993. Dynamic light scattering: The method and some applications. ed., New York: Oxford UniversityPress.
74. Hunter RJ. 2001. Foundations of Colloid Science Ch. ed.
75. Debye P, Chu B, Kaufmann H. 1962. Critical Opalescence of Binary Liquid Mixtures: Methanol—Cyclohexane; Aniline—Cyclohexane. The Journal of Chemical Physics 36(12):3378-3381.
76. Zimm BH. 1950. The Opalescence of a Two-Component Liquid System near the Critical Mixing Point. The Journal of Physical Chemistry 54(9):1306-1317.
77. Stenland C, Pettitt BM. 1995. Binary-solution critical opalescence: mole fraction versus temperature phase diagram. Journal of chemical education 72(6):560.
78. Chu B. 1964. Critical Opalescence of a Binary Liquid Mixture, n-Decane—β,β′-Dichloroethyl Ether. I. Light Scattering. The Journal of Chemical Physics 41(1):226-234.

79. Galkin O, Vekilov PG. 2000. Control of protein crystal nucleation around the metastable liquid–liquid phase boundary. Proceedings of the National Academy of Sciences 97(12):6277-6281.
80. Thomson JA, Schurtenberger P, Thurston GM, Benedek GB. 1987. Binary liquid phase separation and critical phenomena in a protein/water solution. Proceedings of the National Academy of Sciences 84(20):7079-7083.
81. Ishimoto C, Tanaka T. 1977. Critical Behavior of a Binary Mixture of Protein and Salt Water. Physical Review Letters 39(8):474-477.
82. Schurtenberger P, Chamberlin RA, Thurston GM, Thomson JA, Benedek GB. 1989. Observation of critical phenomena in a protein-water solution. Physical Review Letters 63:2064.
83. Manno M, Xiao C, Bulone D, Martorana V, San Biagio PL. 2003. Thermodynamic instability in supersaturated lysozyme solutions: Effect of salt and role of concentration fluctuations. Physical Review E 68(1):011904.
84. Wilson WW, DeLucas LJ. 2014. Applications of the second virial coefficient: protein crystallization and solubility. Acta Crystallographica Section F: Structural Biology Communications 70(5):543-554.
85. Laue T. 2012. Proximity energies: a framework for understanding concentrated solutions. J Mol Recognit 25(3):165-173.
86. Israelachvili JN. 2011. Intermolecular and Surface Forces Third ed., San Diego: Academic Press.
87. Hiemenz PC, Rajagopalan R. 1997. Principles of Colloid and Surface Chemistry, revised and expanded. ed.: CRC Press.
88. Yadav S, Liu J, Shire SJ, Kalonia DS. 2010. Specific interactions in high concentration antibody solutions resulting in high viscosity. J Pharm Sci 99(3):1152-1168.
89. Chari R, Jerath K, Badkar AV, Kalonia DS. 2009. Long- and short-range electrostatic interactions affect the rheology of highly concentrated antibody solutions. Pharm Res 26(12):2607-2618.
90. Lockhart DJ, Kim PS. 1993. Electrostatic screening of charge and dipole interactions with the helix backbone. Science 260(5105):198-202.
91. Du W, Klibanov AM. 2011. Hydrophobic salts markedly diminish viscosity of concentrated protein solutions. Biotechnol Bioeng 108(3):632-636.
92. Guo Z, Chen A, Nassar RA, Helk B, Mueller C, Tang Y, Gupta K, Klibanov AM. 2012. Structure-activity relationship for hydrophobic salts as viscosity-lowering excipients for concentrated solutions of monoclonal antibodies. Pharm Res 29(11):3102-3109.
93. Kamerzell TJ, Pace AL, Li M, Danilenko DM, McDowell M, Gokarn YR, Wang YJ. 2013. Polar solvents decrease the viscosity of high concentration IgG1 solutions through hydrophobic solvation and interaction: Formulation and biocompatibility considerations. Journal of Pharmaceutical Sciences 102(4):1182-1193.
94. He F, Woods CE, Trilisky E, Bower KM, Litowski JR, Kerwin BA, Becker GW, Narhi LO, Razinkov VI. 2011. Screening of monoclonal antibody formulations based on high-throughput thermostability and viscosity measurements: Design of experiment and statistical analysis. Journal of Pharmaceutical Sciences 100(4):1330-1340.
95. Mahadevi AS, Sastry GN. 2013. Cation-pi interaction: its role and relevance in chemistry, biology, and material science. Chem Rev 113(3):2100-2138.

96. Falconer RJ, Chan C, Hughes K, Munro TP. 2011. Stabilization of a monoclonal antibody during purification and formulation by addition of basic amino acid excipients. Journal of Chemical Technology & Biotechnology 86(7):942-948.
97. Bye J, Platts L, Falconer R. 2014. Biopharmaceutical liquid formulation: a review of the science of protein stability and solubility in aqueous environments. Biotechnology Letters 36(5):869-875.
98. Inoue N, Takai E, Arakawa T, Shiraki K. 2014. Specific Decrease in Solution Viscosity of Antibodies by Arginine for Therapeutic Formulations. Molecular Pharmaceutics 11(6):1889-1896.
99. Neal BL, D. Asthagiri, and A. M. Lenhoff. 1998. Molecular origins of osmotic second virial coefficients of proteins. Biophys. J. 75:2469-2477.
100. Demoruelle K, B. Guo, S. Kao, M. McDonald Heather, B. Nikic Dragan, C. Holman Steven, and W. W. Wilson. 2002. Correlation between the osmotic second virial coefficient and solubility for equine serum albumin and ovalbumin. . Acta Crystallogr. D Biol. Crystallogr. 58:1544-1548.
101. Valente JJ, R. W. Payne, M. C. Manning, W. W. Wilson, and C. S. Henry. 2005. Colloidal behavior of proteins: Effects of the second virial coefficient on solubility, crystallization and aggregation of proteins in aqueous solution. Curr. Pharm. Biotechnol. 6:427-436.
102. George A, Y. Chiang, B. Guo, A. Arabshahi, Z. Cai, and W. W. Wilson. 1997. Second virial coefficient as predictor in protein crystal growth. Methods Enzymol 276:100-110.
103. Neal BL, D. Asthagiri, O. D. Velev, A. M. Lenhoff, and E. W. Kaler. 1999. Why is the osmotic second virial coefficient related to protein crystallization? J. Cryst. Growth. 196:377-387.
104. Curtis RA, Prausnitz JM, Blanch HW. 1998. Protein-protein and protein-salt interactions in aqueous protein solutions containing concentrated electrolytes. Biotechnol Bioeng 57(1):11-21.
105. Dumetz AC. 2007. Protein interactions and phase behavior in aqueous solutions: Effects of salt, polymer, and organic additives. ed.: ProQuest.
106. George A, Wilson WW. 1994. Predicting protein crystallization from a dilute solution property. Acta Crystallogr D Biol Crystallogr 50(Pt 4):361-365.
107. Bonnete F, Vivares D. 2002. Interest of the normalized second virial coefficient and interaction potentials for crystallizing large macromolecules. Acta Crystallogr D Biol Crystallogr 58(Pt 10 Pt 1):1571-1575.
108. Lewus RA, Darcy PA, Lenhoff AM, Sandler SI. 2011. Interactions and phase behavior of a monoclonal antibody. Biotechnol Prog 27(1):280-289.
109. Broide M, Tominc T, Saxowsky M. 1996. Using phase transitions to investigate the effect of salts on protein interactions. Physical Review E 53(6):6325-6335.
110. Mason BD, Zhang-van Enk J, Zhang L, Remmele RL, Jr., Zhang J. 2010. Liquid-liquid phase separation of a monoclonal antibody and nonmonotonic influence of Hofmeister anions. Biophys J 99(11):3792-3800.
111. Grigsby JJ, Blanch HW, Prausnitz JM. 2001. Cloud-point temperatures for lysozyme in electrolyte solutions: effect of salt type, salt concentration and pH. Biophys Chem 91(3):231-243.
112. Zhang Y, Cremer PS. 2009. The inverse and direct Hofmeister series for lysozyme. Proceedings of the National Academy of Sciences 106(36):15249-15253.

113. Dumetz AC, Chockla AM, Kaler EW, Lenhoff AM. 2008. Effects of pH on protein–protein interactions and implications for protein phase behavior. Biochimica et Biophysica Acta (BBA) - Proteins and Proteomics 1784(4):600-610.
114. Ingham KC. 1990. [23] Precipitation of proteins with polyethylene glycol. In Murray PD, editor Methods in Enzymology, ed.: Academic Press. p 301-306.
115. Atha DH, Ingham KC. 1981. Mechanism of precipitation of proteins by polyethylene glycols. Analysis in terms of excluded volume. J Biol Chem 256(23):12108-12117.
116. Gibson TJ, McCarty K, McFadyen IJ, Cash E, Dalmonte P, Hinds KD, Dinerman AA, Alvarez JC, Volkin DB. 2011. Application of a high-throughput screening procedure with PEG-induced precipitation to compare relative protein solubility during formulation development with IgG1 monoclonal antibodies. J Pharm Sci 100(3):1009-1021.
117. Stevenson CL, Hageman MJ. 1995. Estimation of recombinant bovine somatotropin solubility by excluded-volume interaction with polyethylene glycols. Pharm Res 12(11):1671-1676.
118. Li L, Kantor A, Warne N. 2013. Application of a PEG precipitation method for solubility screening: a tool for developing high protein concentration formulations. Protein Sci 22(8):1118-1123.
119. Annunziata O, Asherie N, Lomakin A, Pande J, Ogun O, Benedek GB. 2002. Effect of polyethylene glycol on the liquid-liquid phase transition in aqueous protein solutions. Proc Natl Acad Sci U S A 99(22):14165-14170.
120. Wang Y, Annunziata O. 2007. Comparison between protein-polyethylene glycol (PEG) interactions and the effect of PEG on protein-protein interactions using the liquid-liquid phase transition. J Phys Chem B 111(5):1222-1230.
121. Wang Y, Lomakin A, Latypov RF, Laubach JP, Hideshima T, Richardson PG, Munshi NC, Anderson KC, Benedek GB. 2013. Phase transitions in human IgG solutions. J Chem Phys 139(12):121904.
122. Wang Y, Latypov RF, Lomakin A, Meyer JA, Kerwin BA, Vunnum S, Benedek GB. 2014. Quantitative evaluation of colloidal stability of antibody solutions using PEG-induced liquid-liquid phase separation. Mol Pharm 11(5):1391-1402.
123. Jion AI, Goh LT, Oh SK. 2006. Crystallization of IgG1 by mapping its liquid-liquid phase separation curves. Biotechnol Bioeng 95(5):911-918.
124. Bloustine J, Virmani T, Thurston GM, Fraden S. 2006. Light Scattering and Phase Behavior of Lysozyme-Poly(Ethylene Glycol) Mixtures. Physical Review Letters 96(8):087803.
125. Wang Y, Lomakin A, Latypov RF, Benedek GB. 2011. Phase separation in solutions of monoclonal antibodies and the effect of human serum albumin. Proc Natl Acad Sci U S A 108(40):16606-16611.
126. Siezen RJ, Fisch MR, Slingsby C, Benedek GB. 1985. Opacification of gamma-crystallin solutions from calf lens in relation to cold cataract formation. Proc Natl Acad Sci U S A 82(6):1701-1705.
127. Eaton WA, Hofrichter J. 1990. Sickle cell hemoglobin polymerization. Adv Protein Chem 40:63-279.
128. Chen Q, Vekilov PG, Nagel RL, Hirsch RE. 2004. Liquid-liquid phase separation in hemoglobins: distinct aggregation mechanisms of the beta6 mutants. Biophys J 86(3):1702-1712.

129. Galkin O, Chen K, Nagel RL, Hirsch RE, Vekilov PG. 2002. Liquid–liquid separation in solutions of normal and sickle cell hemoglobin. Proceedings of the National Academy of Sciences 99(13):8479-8483.
130. Koo EH, Lansbury PT, Jr., Kelly JW. 1999. Amyloid diseases: abnormal protein aggregation in neurodegeneration. Proc Natl Acad Sci U S A 96(18):9989-9990.
131. Yagi H, Takahashi N, Yamaguchi Y, Kato K. 2004. Temperature-dependent isologous Fab-Fab interaction that mediates cryocrystallization of a monoclonal immunoglobulin G. Mol Immunol 41(12):1211-1215.
132. Van Dijk M.A WA. 1997. Polymer Thermodynamics Library;. ed., Pennyslyvania: Technomic Publishing Company. p 205.
133. P. A. 2006. Atkin's Physical Chemistry. 8 ed.: Oxford University Press.
134. Vis M, Peters VF, Tromp RH, Erne BH. 2014. Donnan potentials in aqueous phase-separated polymer mixtures. Langmuir 30(20):5755-5762.
135. Mishra S, Schmit JD. 2013. Electrostatic interactions in concentrated protein solutions. arXiv preprint arXiv:1304.2481.
136. Bolton GR, Boesch AW, Basha J, Lacasse DP, Kelley BD, Acharya H. 2011. Effect of protein and solution properties on the Donnan effect during the ultrafiltration of proteins. Biotechnol Prog 27(1):140-152.
137. Johnson HR, Lenhoff AM. 2013. Characterization and suitability of therapeutic antibody dense phases for subcutaneous delivery. Mol Pharm 10(10):3582-3591.
138. Trilisky E, Gillespie R, Osslund TD, Vunnum S. 2011. Crystallization and liquid-liquid phase separation of monoclonal antibodies and fc-fusion proteins: screening results. Biotechnol Prog 27(4):1054-1067.
139. Navarro A, Wu H-S, Wang SS. 2009. Engineering problems in protein crystallization. Separation and Purification Technology 68(2):129-137.
140. Kuznetsov YG, Malkin AJ, McPherson A. 2001. The liquid protein phase in crystallization: a case study—intact immunoglobulins. Journal of Crystal Growth 232(1–4):30-39.
141. Tanaka S, Yamamoto M, Ito K, Hayakawa R, Ataka M. 1997. Relation between the phase separation and the crystallization in protein solutions. Physical Review E 56(1):R67-R69.
142. Astier J-P, Veesler S. 2008. Using Temperature To Crystallize Proteins: A Mini-Review†. Crystal Growth and Design 8(12):4215-4219.

10. List of symbols

C_c: Critical concentration
T_c: Critical temperature
T_{cloud}: Cloud-point temperature
Φ: order parameter
F: Helmholz free energy of the system
$*A$: width of the coexistence curve
($*A$ also represents factor that controls nucleation in solution as presented in in equation 9)
β, υ: Critical exponent
μ_p: Chemical potential of the protein
n_p: total number of protein
G_{mix}: Gibbs free energy of mixing
S_{mix}**:** Entropy of mixing
H_{mix} **:** Enthalpy of mixing
σ: Interfacial tension
ε: Bulk energy
R: Critical radius
J: Nucleation rate
I_s: Intensity of scattered light
I_0: Intensity of incident light,
λ: Wavelength of the light,
α: Polarizability of molecule,
V: Molar volume
θ: Scattering angle
η: Refractive index of the medium
τ: Turbidity of solution
ξ: Correlation length
χ: Isothermal compressibility,
π_{osm} : Osmotic pressure,
B_2: Second virial coefficient

11. Tables and Figures

Table 1: Compare and contrast for kinetics of phase separation by Nucleation and growth mechanism and by Spinodal decomposition

Nucleation and growth	Spinodal decomposition
Formation of a stable nucleus of a critical size is essential for growth of the phases	No thermodynamic barrier, results in formation of domains
Downhill diffusion down the concentration gradient	Uphill diffusion against concentration gradient
Sharp interface formation	No sharp boundaries between the phases due to long range fluctuations
Explained by Ostwald ripening	Explained by Cahn-Hillard approximation

Table 2: Effect of particle size and wavelength dependence for light scattering from solution

Size	**Diameter (d)**	**Turbidity (τ)**	**Wavelength (λ)**
Small (x<<1) (Rayleigh Theory)	$I_S \propto d^6$	Turbidity (τ) depends on d^3	λ^{-4}
Large x~1 (Mie Scattering, Rayleigh-Debye-Gans Theory)	$I_S \propto d^4$	τ increases linearly with d	λ^{-2}
Very large x>>1 (Fraunhofer Diffraction)	$I_S \propto d^2$	τ decreases with increase in d	Independent of λ

x: dimensionless optical size parameter, $x = \frac{\pi d}{\lambda}$

Figures

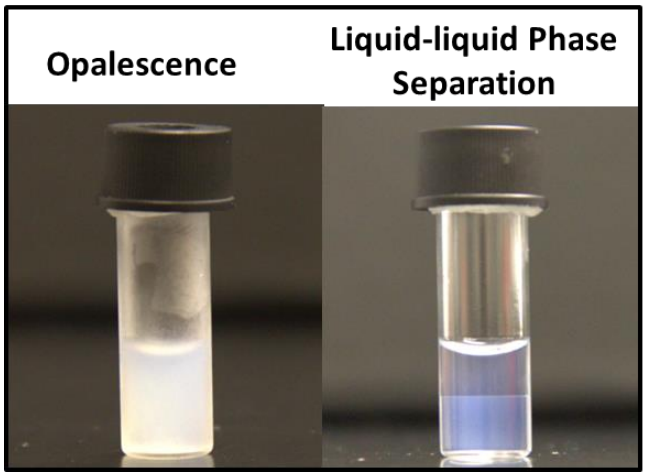

Figure 1: Images showing opalescence and liquid-liquid phase separation for protein solutions after solution was stored at 4 °C for 30 min and 12 hours, respectively. Reproduced from Chapter 3.[15]

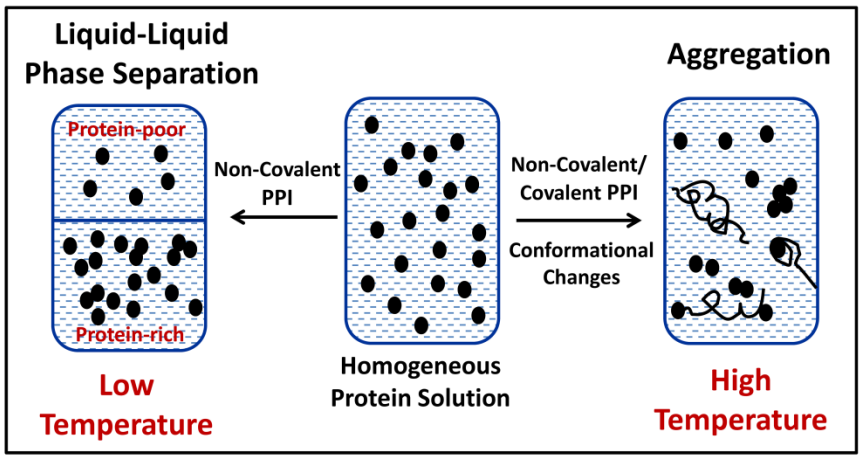

Figure 2: A schematic representation for Liquid-liquid phase separation and Aggregate formation in protein solution.

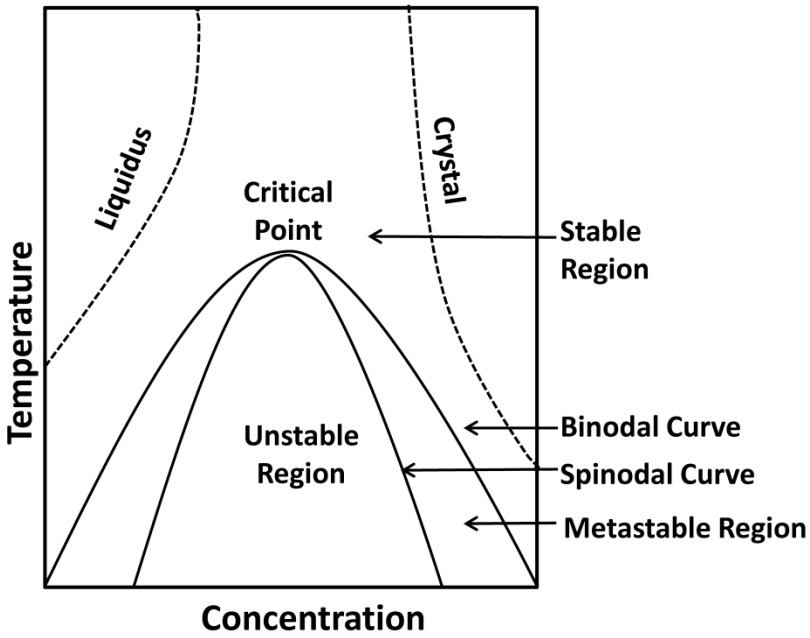

Figure 3: Temperature-concentration curve showing liquid-liquid phase separation (solid-line) and Solid-liquid phase separation curve (dotted line) for binary systems. Adapted from general references.[41,44]

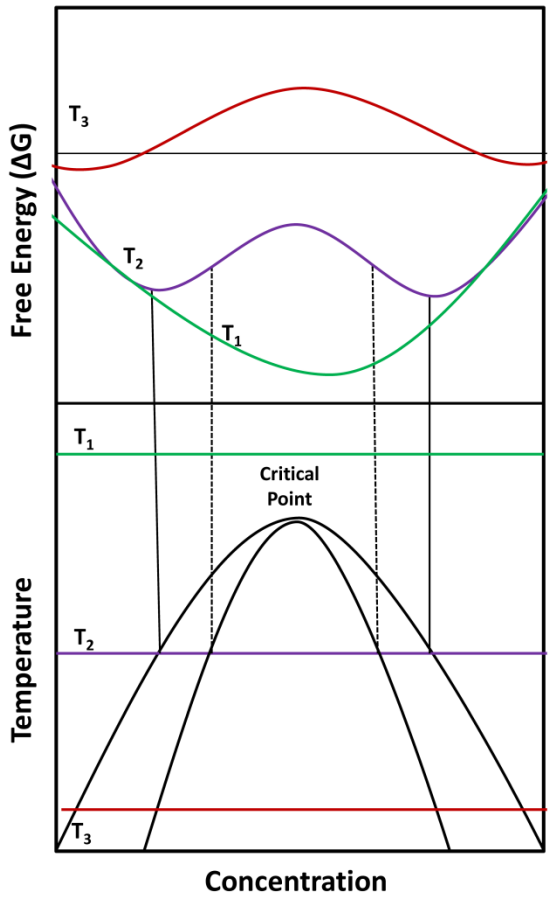

Figure 4: Schematic for Liquid-liquid phase separation in solution defined in terms of free energy (upper part) at temperatures above (T_1) and below (T_2 and T_3) the critical temperature (T_c). Adapted from general references. [41,43,63]

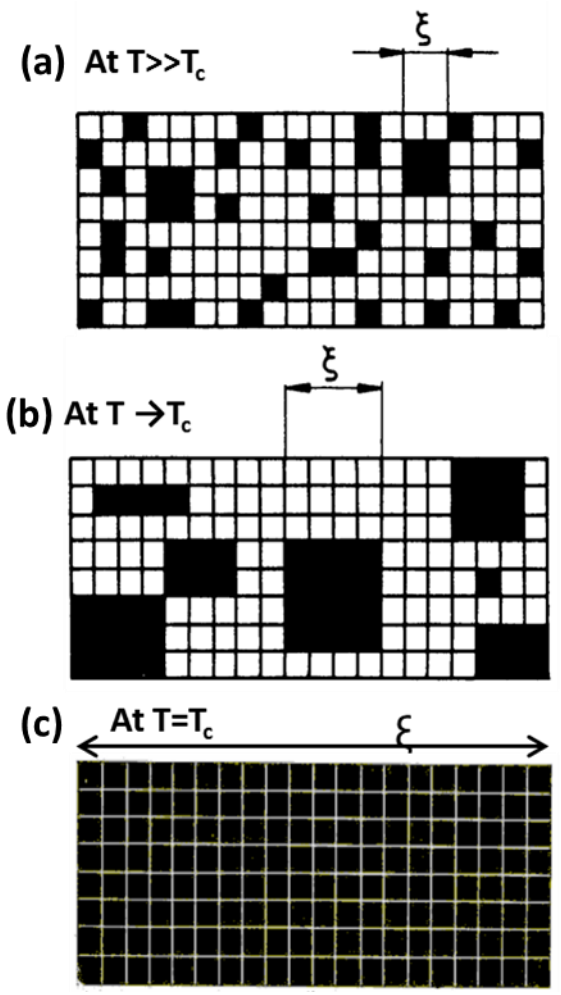

Figure 5: Correlations between fluctuations of thermodynamic quantity in a system (density fluctuations in pure liquids or concentration fluctuations in binary systems) in terms of correlation length ξ at (a) temperature above critical temperature, (b) temperature approaching critical temperature and (c) at critical temperature. Adapted from Beysens et al.[43]

Chapter 3

Opalescence in Monoclonal Antibody Solutions and its Correlation with Intermolecular Interactions in Dilute and Concentrated Solutions

Contents

Chapter 3

1. Abstract

Opalescence indicates physical instability of a formulation because of the presence of aggregates or liquid-liquid phase separation in solution and has been reported for monoclonal antibody formulations. Increased solution opalescence can be attributed to attractive protein-protein interactions. Techniques including light scattering, AUC or membrane osmometry are routinely employed to measure protein-protein interactions in dilute solutions, whereas opalescence is seen at relatively higher concentrations, where both long and short range forces contribute to overall protein-protein interactions. The monoclonal antibody molecule studied here shows a unique property of high opalescence due to liquid-liquid phase separation. In this study, opalescence measurements are correlated to protein-protein interactions measured in dilute and concentrated solutions using Light scattering (k_D) and High frequency rheology (G'), respectively. Charges on the molecules were calculated using zeta potential measurements. Results indicate that high opalescence and phase separation are due to the attractive interactions in solution as measured using light scattering and rheology, however, the presence of attractive interactions do not always imply phase separation. Temperature dependence of opalescence, suggests that thermodynamic contribution to opalescence is significant and T_{cloud} can be utilized as a potential tool to assess attractive interactions in solution.

Keywords: Protein, light scattering, stability, protein formulation, physical characterization, Opalescence, phase separation, rheology, protein-protein interactions, monoclonal antibody

2. Introduction

The use of therapeutic proteins, especially monoclonal antibodies (mAbs) is growing at an exponential rate because of their target specificity and efficiency in the treatment of diseases including cancer and autoimmune disorders. Antibodies are low potency drugs which require daily doses ranging from 100-200 mg.[1,2] Preferred route of administration for these drugs is subcutaneous route, as it provides convenience and ease of administration for the patient either as an out-patient at a clinic or self-administration at home. The major challenge of administration by this route is posed by the need of formulating these drugs at high concentrations, which is necessitated by low volume restriction of less than 1.5 mL and high drug dose.[3] Such formulations present many challenges in analytical characterization, manufacturing, delivery to the patient, and maintaining stability across the shelf-life.[3-5] At high concentrations, inter-separation distance between the protein molecules decreases, thereby increasing their tendency to interact with each other.[6,7] This results in increased solution viscosity which leads to difficulties in pumping, filling, filtering and recovering product from vessels increasing both the time and production costs. High solution viscosity also possesses problems in the delivery of the formulations through syringes leading to patient inconvenience.[4,5] The increased tendency of proteins to form higher order reversible (native) or irreversible (non-native) aggregates at high protein concentration can also compromise protein activity, physical stability of the product and cause immunogenicity concerns.[6,8,9]

Recently, opalescence and liquid-liquid phase separation have also been observed as potential problems at high concentrations for monoclonal antibody solutions.[10-16] Opalescence at high concentrations not only compromises aesthetic appeal of the formulation

but also can be a precursor to phase separation or indicator of the presence of aggregates in solution signifying reduced product stability. Protein formulations under specific solution conditions can undergo phase transition resulting in solid-liquid phase separation (crystallization or amorphous precipitation) or liquid-liquid phase separation (formation of protein-rich and protein-poor phase).[17] Phase separation of biological fluids is a reason for physiological conditions generally known as condensation diseases. Examples include cold cataract [18,19] sickle-cell diseases[20], neurodegenerative and amyloidogenic diseases[21] and cryoimmunoglobinemia.[22]

The literature provides examples of solution opalescence followed by phase separation, and also examples of opalescence without phase separation. Sukumar et al., related the increased opalescence of IgG1 antibody to Rayleigh scattering at higher concentrations. They also observed that opalescence was temperature dependent which increased with decreasing temperature.[10] In another study, Salinas and coworkers investigated the effect of ionic strength on solution opalescence and viscosity by measuring the osmotic second virial coefficient (B_2) by light scattering and sedimentation techniques. Higher opalescence at high ionic strength was attributed to attractive interactions between the molecules, indicated by negative B_2 values. The authors also pointed to the possibility of phase separation in solution on lowering the temperature, however, at the studied temperature, no such effect was observed.[11] Woods et al., tried to correlate increased opalescence to aggregation and change in protein structure, but were not able to get conclusive results. They attributed increased opalescence to reversible self-association between the molecules.[12] Wang and coworkers concluded from their studies that ionic strength rather than a specific ion influences the opalescence in solution.[15] No phase

separation was observed in any of these scientific studies. Mason and coworkers observed opalescence for an IgG2 monoclonal antibody solution, which was mainly due to liquid-liquid phase separation. They concluded that solution opalescence was maximum near the vicinity of the critical point (C_c: 87 mg/mL, T_c: 268.5K) and was due to increased concentration fluctuations.[14] Nishi et al., attributed the increased opalescence and liquid-liquid phase separation at low ionic strength to electrostatic interactions, which reversed on increasing the ionic strength of the solution.[13] In another study by the same group, authors concluded that Fc-Fc region mediated attractive electrostatic interactions resulted in phase separation in the solution. This property of undergoing liquid-liquid phase separation, depending on the solution conditions, is unique to some proteins and depends on how Fc regions of a mAb interact with other Fc and Fab region.[16] Opalescence observed in mAb solutions due to liquid-liquid phase separation is an important issue for product development. Hence, a thorough investigation of the formulation factors such as pH, ionic strength, protein concentration and temperature affecting opalescence because of phase separation in solution is needed. A detailed analysis of how these factors affect the nature of intermolecular interactions resulting in opalescence would help in developing stable formulations.

The objective of the current work was to study the factors responsible for the observed opalescence in a monoclonal antibody solution and determine the nature of the protein-protein interactions (PPI). All recent studies mentioned in the literature have attempted to correlate the nature of intermolecular interactions as measured using techniques such as light scattering,[10-13] analytical-ultracentrifuge [10,13] or membrane osmometry[11] with opalescence in solution. However, all these techniques employed measure PPI in dilute solutions, whereas opalescence is seen at relatively higher concentrations. Hence, in the

current study ultrasonic shear rheometer was employed to study the nature of intermolecular interactions at higher protein concentrations.[23-29] Zeta potentials were measured and charges on molecule were calculated in order to assess the role of electrostatic and dipole-mediated interactions between protein molecules on increased solution opalescence. Temperature studies were performed to determine T_{cloud}, temperature that marks the onset of phase separation in solution. The current study addresses the following questions related to opalescence in protein solutions

1. Is opalescence in solution due to liquid-liquid phase separation or increased Rayleigh scattering?
2. How do the extrinsic factors affect protein-protein interactions resulting in solution opalescence?
3. Can interactions determined at low concentrations predict high concentration behavior?

3. Materials and Methods

3.1. Materials

Monoclonal antibody (mAb-A, pI ~ 6.5) was supplied by Abbvie (Worcester, MA) as 65 mg/mL solution in 15 mM Histidine buffer at pH 5.5. All chemicals used were reagent grade or higher. All chemicals including acetic acid, sodium acetate, sodium chloride, histidine hydrochloride, monobasic and dibasic sodium phosphate, sodium hydroxide and hydrochloric acid were obtained from Fisher Scientific (Fair Lawn, New Jersey). Histidine base was obtained from Sigma (St. Louis, MO). All the solutions were prepared with deionized water equivalent to Milli-Q™. Solutions were dialyzed and concentrated in

Millipore (Billerica, Massachusetts) Amicon Ultra centrifugation tubes with a molecular weight cutoff of 10 kDa and were obtained from Fisher Scientific. Quartz crystal discs with gold plated electrodes on both sides and with fundamental vibrating frequencies of 10 MHz were acquired from International Crystal Manufacturing Company (Oklahoma City, Oklahoma).

Acetate, Histidine and Phosphate buffers were prepared to maintain pH of the solution at 5.1, 6.1 and 7.0, respectively. At pH 5.1, buffer concentration of 8 and 23 mM; at pH 6.1, buffer concentration of 10 and 30 mM; and at pH 7.0, buffer concentration of 3 and 8.5 mM were selected to maintain ionic strengths of 5 and 15 mM, respectively, without addition of any salt. Sodium chloride was used to adjust the ionic strength to 150 mM. Protein solutions with varying ionic strengths of 1, 2.5 and 10 mM were prepared at pH 6.1 by maintaining appropriate buffer strength. To maintain ionic strength at 0 mM, the protein was extensively dialyzed in water in dialysis cassette over a period of 24 hrs; water was changed once during this period. To ensure complete removal of ions after dialysis, sample was recovered and dialyzed with water in Amicon Ultra centrifugation tubes and concentrated further.

All antibody solutions were buffer exchanged with appropriate buffers and pH was checked for each dialyzed sample. Concentrations of the samples were determined using a UV-vis spectrophotometer with an extinction coefficient of 1.4 $mg^{-1}/mL^{-1}cm^{-1}$ for mAb-A at 280 nm for 0.1% (w/v) IgG solutions. The pH of all the solutions was within ±0.1 of the target values as measured by a Denver Instrument pH meter. All analyses were conducted at room temperature (23 ± 1°C).

3.2. Opalescence Measurements

Opalescence of the solution was measured as percent transmittance using UV-vis spectrophotometer (Varian Cary 50) at 510 nm in a quartz cuvette with a path length of 3 mm (60 μL). 10 readings averaging over 2 seconds were recorded, and duplicate measurements were made at each sample concentration. Opalescence measured as percent transmittance can be expressed in standard NTU's by using calibration standards. Opalescence was measured as function of concentration, pH and ionic strength. All measurements were made at room temperature (23 ± 1°C).

3.3. Zeta Potential Measurements

Zeta potential measurements were performed using Malvern Zetasizer Nano Series (Worcestershire, UK). Dip cell (ZEN1002) and glass cuvette assembly was used to make the measurements that required a sample volume of 800 μL. Measurements were made in duplicate at 25 ± 0.1 ˚C, and at a concentration of 4 mg/mL. Poisson–Boltzmann equation, also known as the Debye–Huckel approximation, was used to calculate the effective charge on the molecule assuming an equivalent sphere.[30,31] Equation is given as,

$$z = \frac{4\pi\varepsilon a(1+\kappa a)\xi}{e} \quad (1)$$

where, e is the electronic charge, a is the particle radius and κ is the inverse Debye length. The linearized Poisson-Boltzman equation was used to calculate effective charge on a spherical particle and hence, for estimating charge on proteins, radius a was substituted by r_H or hydrodynamic radius for equivalent sphere. Diffusion coefficient, D_s, obtained from dynamic light scattering was used to calculate r_H using Stokes-Einstein equation.

3.4. Dynamic Light Scattering (DLS)

DLS studies were performed using a Malvern Instrument's Zetasizer Nano Series equipped with a 632.8 nm Helium–Neon laser and 173˚ Noninvasive Back-Scatter technique. Malvern Instrument's DTS2145 low volume glass cuvette was used that requires a sample volume of 60 µL for analysis. For DLS analysis, the buffers and sample stock solutions were filtered through sterile 0.22 µm Millipore's Durapore membrane filters before making the dilution to required concentrations. The protein solutions were then centrifuged using an Eppendorf minispin (Hamburg, Germany) mini-centrifuge at 12,110 x g for 5 min before every measurement. All the samples were analyzed in duplicate and measurements were made at 25 ± 0.1˚C. Linear plot of mutual diffusion coefficient (D_m) obtained from software plotted against concentration was used to calculate self-diffusion coefficient (D_s) and interaction parameter (k_D) using following relation,

$$D_m = D_s(1 + k_D c) \tag{2}$$

c is the concentration of the protein (g/mL).[32] Hydrodynamic radius (r_H) was calculated from D_s using Stokes-Einstein equation

$$D_s = \frac{kT}{6\pi\eta\, r_H} \tag{3}$$

where, k is the Boltzmann constant, T is the absolute temperature, and η is the solution viscosity.

3.5. Static Light Scattering (SLS)

SLS studies were conducted at 25 ± 0.1˚C using a Malvern Instrument's Zetasizer Nano Series to determine B_2, which signifies first deviation from ideality. Sample preparation and experimental steps were similar to those used for DLS. A detailed procedure

to obtain correct average scattered intensities for measuring SLS parameters is discussed elsewhere.[33] The average scattered intensities were used to calculate B_2 by constructing the Debye plot according to the following equation,[34]

$$\frac{Kc}{R_\theta} = \frac{1}{M_w} + 2B_2c \tag{4}$$

where, K is the optical constant given by,

$$K = \frac{[2\pi\eta\left(\frac{dn}{dc}\right)]^2}{N_A\lambda_0^4} \tag{5}$$

In the above equations, R_θ is the excess Rayleigh ratio, i.e., a measure of light scattered by the solute; η is the solvent refractive index, dn/dc is the refractive index increment of the solute, N_A is the Avogadro number, and λ_0 is the wavelength of the incident light. The average *dn/dc* value reported in the literature for mAb is 0.185 ml/g and was used for calculation of optical constant K in this study.[35,36]

3.6. High Frequency Rheological Measurements

Ultrasonic shear rheometer with quartz crystals vibrating at a fundamental frequency of 10 MHz was employed to determine the rheological properties of the protein molecule.[37] In this study, 30 µL samples of mAb A solution were analyzed in duplicate. A temperature controlled water jacket was used to maintain the temperature of the liquid samples at 25 ± 0.2˚C during measurements. A brief description of the technique is presented in Appendix 1. Change in conductance (G) and the series resonance frequency (f_{max}), defined as the frequency where the conductance of the crystal is the highest, before and after loading the liquid on the crystal is used to calculate the change in the series resistance (R) and reactance (X) of the crystal, i.e., R_2 and X_2. The change in resistance and reactance is then used to

calculate storage modulus (G'), loss modulus (G'') and complex viscosity (η^*) using following equations,

$$G'(\omega) = \frac{R_2^2 - X_2^2}{A^2 \rho_{liq}} \quad (6)$$

$$G^{"}(\omega) = \frac{2R_2X_2}{A^2 \rho_{liq}} \quad (7)$$

$$\eta^* = \frac{(G'^2 + G"^2)^{\frac{1}{2}}}{\omega} \quad (8)$$

where, A is a crystal calibration constant, ρ_{liq} is liquid density, and ω is the quartz crystal frequency. A is determined by calibrating the crystal with glycerol-water mixtures of known density and viscosity.

3.7. Temperature Studies

Temperature studies were performed using temperature control peltier plate attached with UV-Vis spectrophotometer. Temperature was varied between 2-35 ºC. Samples were allowed to equilibrate at each temperature for 2 min before taking the measurements. Samples were subjected to heating-cooling cycles, by first decreasing the temperature to 5 ºC and then increasing the temperature, and percent transmittance was measured to assess the reversibility of the opalescence. Onset of the liquid-liquid phase separation is characterized by a dramatic increase in solution turbidity; this temperature is marked as T_{cloud}. All the studies were done at pH 6.1 and ionic strengths of 5 and15 mM. Three concentrations were studied: 25, 75 and 125 mg/mL.

4. Results and Discussion

Systems that exhibit liquid-liquid phase separation are characterized by a temperature-concentration phase diagram which has a critical point defined by a critical temperature (T_c) and a critical concentration (C_c). As the solution conditions are changed, intensity of concentration fluctuations in solution increases and reaches a maximum in the vicinity of the critical point. These concentration fluctuations cause a change in refractive index which in turn results in enormous increase in the scattering of light from the solution, making it appear opalescent. Increased scattering intensity in the vicinity of the critical point due to divergence of thermodynamic properties i.e, density and concentration fluctuations, is termed as 'Critical Opalescence'.[38-40] Figure 1 represents a typical temperature–concentration phase diagram. Binodal or coexistence curve is the phase boundary, above which the solution exists as stable one-phase system over the entire concentration range. In the area between the binodal and spinodal curves, the system exists in the metastable phase (formation of two phases is kinetically hindered). Inside the spinodal curve, the system is thermodynamically unstable, and there is no kinetic barrier; hence, the system spontaneously separates into two phases at all conditions of temperature and concentration.[17,39,41] On attaining thermodynamic equilibrium, chemical potential of the substance is same throughout the sample regardless of the number of phases present. Therefore, in a protein solution upon phase separation, the chemical potential of the protein would be same in both phases even though their concentrations are different.[41,42]

4.1. Opalescence Measurements

The protein solution does not absorb radiations at 510 nm. A reduction in transmitted light at this wavelength is caused by light scattering from the solution. A lower transmittance relates to higher opalescence. Figure 2 shows a plot of percent transmittance for mAb A as a function of protein concentration at pH 5.1, 6.1 and 7.0, and ionic strengths of 5 mM (♦), 15 mM (▲) and 150 mM (■). At pH 5.1, for both 5 mM and 15 mM ionic strengths, percent transmittance recorded is close to 100, indicating that there is no solution opalescence under these conditions. A slight decrease in transmittance observed at this condition is due to Rayleigh scattering. At pH 6.1 and 7.0, the opalescence increases initially and then gradually decreases with increasing concentration at 5 and 15 mM ionic strength; however, at 150 mM ionic strength (pH 6.1) the solution exhibits extremely low opalescence.

According to light scattering theory, scattering intensity is directly related to the number and size of the particles in solution.[43] Hence, the concentration and presence of aggregates in solution result in increased scattering of light from the solution and are generally the cause of increased opalescence, which shows a gradual increase with concentration. In the present study, high opalescence is observed in an intermediate concentration range (50-75 mg/mL), which decreases at higher concentrations. Critical concentration range (concentrations where opalescence is maximum) is around 50-75 mg/mL similar to values reported in the literature for mAbs.[11,14,44] This intermediate concentration dependence of opalescence in protein solutions may be critical opalescence, which increases close to the critical point. The correlations of fluctuations, which become infinitely large on approaching the critical point, are characterized by a correlation length. This correlation

length becomes comparable to the wavelength of light resulting in intense scattering from the solution resulting in critical opalescence.[39,40]

4.2. Nature of Protein-Protein Interactions

Opalescence in solution is attributed to attractive protein-protein interactions.[11,15,16] Determining the nature of these attractive interactions is important, so as to select suitable formulation conditions/excipients to reduce these PPI and develop a physically stable product. Protein-protein interactions in solution depend on the separation distance or proximity between them and the nature of these interactions are strongly influenced by molecular properties and solution conditions; and are briefly summarized in Table 1. Readers are referred to some excellent literature reviews that describe molecular crowding in solution, pair-wise interactions between protein molecules, the proximity energies of these interactions as a function of solution conditions and their implications in solutions.[6,45-47]

The short-range, non-specific attractive interactions usually associated with proteins, include van der Waals interaction, interactions arising from permanent and induced dipole moment of the molecules and hydrophobic interactions associated with hydrophobic patches on protein surface. Presence of charges results in both repulsions in dilute solutions and attractions in concentrated solutions. Dipole mediated interactions are strongly influenced by orientation of the molecule, asymmetric charge distribution on protein surface and charge/proton fluctuations between acidic and basic groups on protein surface.[26] Increasing ionic strength weakens all charge and dipole mediated interactions in solution.[29,48]

4.2.1. Zeta Potential and Charge Measurements

The effective pI of the molecule was determined by linear interpolation of the zeta potential measured between pH 5.1 and 7.0 to find the x-intercept where zeta potential is zero. This method might induce some uncertainty in the exact value of the pI but for the discussion here this approximation will suffice. Theoretical pI of the molecule calculated from the amino acid sequence is 6.5, but the presence of various ions and their binding may affect the solution pI of the protein depending on the nature of the ions. This behavior (decrease in experimental pI due to ion binding as compared to theoretical pI) has been reported previously for mAbs and other proteins.[28] Zeta potential values in millivolts for mAb A at different pH conditions in solutions with 5 mM ionic strength are plotted in Figure 3. The crossover from positive to negative values occurs around pH 6.35 (obtained from linear interpolation) and is used as the effective pI of the molecule for this work.

Values for the measured zeta potential and experimental charges calculated using Poisson-Boltzmann equation (equation 1) are compiled in Table A1.1 and elaborated in the Appendix 1. Zeta potential and charge values and the effect of changing the ionic strength from 5 mM to 15 mM follow the rank order pH 5.1 > 7.0 > 6.1. This indicates that the net charge on the molecule is high at pH 5.1, and changing the ionic strength has higher impact on charges at this pH. While, at pH 6.1, net charge on molecule is low and ionic strength has minimal effect at this pH.

4.2.2. Interactions in Dilute Solutions

The nature of the intermolecular interactions was measured in dilute solutions using Static and Dynamic light scattering to determine B_2 (osmotic second virial coefficient) and k_D

(interaction parameter), respectively. B_2 and k_D were further used to determine molecular weight, hydrodynamic diameter and self-diffusion coefficient for mAb A. A brief description of k_D and B_2 as important parameters to measure PPI in solution is provided in the Appendix 1. B_2 is the first measure of the deviation from ideality in the solution and characterizes interactions between the solute molecules. The value of B_2 reflects the magnitude of deviation from ideality, while its sign reflects the nature of this deviation. A positive value corresponds to net repulsive interactions between the solute molecules and a negative value corresponds to net attractive interactions.[49] DLS measures the diffusion coefficient of a solute molecule in solution and is used to find the interaction parameter k_D using equation 2. k_D is a measure of inter-particle interactions and has contributions from both the thermodynamic and hydrodynamic parameters. Similar to B_2, a positive k_D implies repulsive interactions, and a negative k_D implies attractive intermolecular interactions in solution only if B_2 is also negative. There is a small range of negative k_D values where interactions are repulsive in nature (where hydrodynamic contribution is larger than thermodynamic contribution), resulting in a negative k_D.

Figure A1.1, in Appendix 1 shows a plot of D_m obtained from DLS against concentration at varying solution conditions. k_D and B_2 values follow similar trend at all the pH and ionic strength conditions studied. Change in k_D with change in ionic strength follow the trend as pH 6.1> pH 7.0 > pH 5.1, i.e. on changing ionic strength attractive interactions decrease significantly at pH 6.1 while, ionic strength has minimal effect on PPI at pH 5.1.

4.2.3. *Correlation between k_D and Opalescence*

Figure 4 shows a plot of k_D values (obtained from the initial slopes of D_m versus concentration data in Figure A1) at different solution conditions. The numbers under the bars represent effective charges on the molecule calculated from the zeta potential measurements. Interactions in dilute solutions represented by k_D and charges were correlated with opalescence measurements from Figure 2. At pH 5.1, no opalescence was observed in the solution. The molecules carry a net positive charge; however, the k_D values were negative. Changing the ionic strength showed a significant effect on the calculated charges which were reduced by one-half (from +8.13 Z at 5 mM to +4.05 Z at 15 mM) but the magnitude of negative k_D values increased (-18.04 mL/g and -26.69 mL/g at 5 and 15 mM, respectively). Since dipolar interactions should be screened by higher ionic strength in the solution, an increase in k_D indicates the presence of hydrophobic interactions which become dominant at higher concentrations.

Maximum opalescence (Figure 2) is recorded at pH 6.1 and 5 mM ionic strength and can be correlated to strong attractive interactions in solution (-99.92 mL/g). Both opalescence as well as attractive interactions decrease on increasing the ionic strength to 15 mM (-35.04 mL/g). The net effective charge on the protein is low (+2.82 Z at 5 mM and +1.13 at 15 mM) at both ionic strengths compared to other pH conditions away from the pI. Low charge and strong attractive interactions at this condition indicate the possibility of the presence of mid-range dipole mediated interactions in solution, which decrease on increasing the ionic strength (Table 1). Similar trend is observed at pH 7.0 where interactions are attractive at 5 mM (-35.42 mL/g) and molecule carries a net negative charge (-5.59 Z); both attractive interactions and charge decrease as ionic strength is increased to 15 mM (-20.46 mL/g and -

3.17 Z, respectively). From Figure 2, opalescence shows a similar decrease from 5 to 15 mM. However, the change in the magnitude of attractive interactions on increasing the ionic strength from 5 mM to 15 mM at pH 6.1 is large (Δk_D ~ 65 mL/g) and it is small at pH 7.0 (Δk_D ~ 15 mL/g). While the change in the magnitude of opalescence, indicated by percent transmittance at 50 mg/mL is ~ 17 % at pH 6.1 and ~ 11 % at pH 7.0, on changing ionic strength from 5 mM to 15 mM.

From k_D and opalescence measurements, high opalescence can be attributed to strong attractive interactions in solution; however, no definite correlation could be established between magnitude of the change in interactions and opalescence, especially at pH conditions away from the pI. This discrepancy results due to the fact that attractive interactions in solution were assessed by light scattering in dilute conditions (concentration < 10 mg/mL), while high opalescence is seen at relatively higher concentrations (~ 50- 75 mg/mL). At higher concentrations, though the charge-charge repulsive interactions are present, the overall proximity energy increases and strengthens the short-range interactions, diminishing the effect of long-range repulsions.[29,46] Hence, along with dilute solution measurement, intermolecular interactions were measured at high concentrations where the solution exhibits opalescence.

4.2.4. Interactions in Concentrated Solutions

Interactions at high concentrations were assessed using ultrasonic shear rheometer. The technique was developed and applied in our lab to measure and quantify the factors that are responsible for high solution viscosity at high protein concentrations.[23-29] A brief explanation of the High frequency rheology and *G'* as a useful parameter to characterize the

nature of intermolecular protein-protein interactions at high concentrations is provided in the Appendix 1. Solution *G′*, *G″*, tan δ (*G″/G′*) and complex viscosity were measured as a function of protein concentration. Data here is shown only for G' values and other parameters (*G″*, tan δ and complex viscosity) follow similar trend.

Figure 5 shows a plot of solution *G′* as a function of protein concentration between 20 to 160 mg/mL at different pHs and ionic strengths. At pH 5.1 (Figure 5a), change in the ionic strength from 5 to 15 mM has almost no effect (within experimental error) on the magnitude of *G′*. As the ionic strength is increased to 150 mM, there is a significant decrease in the magnitude of *G′*. Light scattering measurements at pH 5.1 indicated the possibility of the presence of hydrophobic interactions in solution, which can be confirmed from rheology measurements; as interactions are highly attractive at high concentrations indicated by high *G′* values and do not change on increasing the ionic strength. However, these forces do not result in solution opalescence at pH 5.1.

From Figure 5b, at pH 6.1, *G′* values are high at 5 mM and there is a significant decrease in the magnitude of *G′* on increasing the ionic strength to 15 mM. On further increasing the ionic strength to 150 mM, *G′* reduces considerably. This trend in the change in *G′* with changing ionic strength relates well with opalescence, where high opalescence is observed at low ionic strength and decreases at higher ionic strengths. Similar trend is observed at pH 7.0 (Figure 5c), where, change in the magnitude of *G′* is small when ionic strength is increased from 5 to 15 mM, but the magnitude of *G′* decreases significantly when ionic strength is increased to 150 mM. Dipole mediated specific interactions become dominant at high concentrations as they are strongly dependent on orientation and asymmetric charge distribution on the molecule and have been previously reported by Yadav

et al., for increased viscosity close to the pI of the molecule.[26] In the current study, similar forces may be responsible for increased opalescence close to the pI of the molecule and are investigated further by studying the effect of ionic strength on the solution properties.

From the opalescence measurements, light scattering and rheology studies, it can be concluded that attractive interactions are responsible for high solution opalescence, especially at pH close to the pI of the molecule. However, there is discrepancy in attractive interactions both in dilute and concentrated solutions and opalescence measured at pH conditions away from the pI (dilute- pH 7.0 and concentrated-pH 5.1). Also, maximum opalescence is observed in the concentration range of 50-75 mg/mL, there is no abnormal/abrupt change in *G'* observed in this concentration range. More than one type of intermolecular interactions are present in solution at high concentration (concentration dependent excluded-volume effect, hydrophobic and dipole interactions) which result in increased G' of the solution, however, opalescence cannot be explained just on the basis of protein-protein interactions and detailed investigation is necessary to understand this phenomena at the molecular level.

4.3. Effect of Ionic Strength

High opalescence was observed at low ionic strength, which decreased as the ionic strength was increased. To further understand the effect of ionic strength on opalescence, all studies (opalescence measurements, DLS, Rheology and zeta potential) were performed at pH 6.1 at varying ionic strengths.

4.3.1. Effect of Ionic Strength on Opalescence

Opalescence was measured at different protein concentrations (horizontal axis) at pH 6.1 as a function of ionic strengths (depth axis) as shown in Figure 6. Percent transmittance exhibits minima as a function of both concentration and ionic strength. Critical concentration range (concentration where opalescence is maximum) is around 50-75 mg/mL (from Figure 2 and 6). Similar behavior is seen with respect to ionic strength, where solution opalescence initially increases and then decreases with increasing ionic strength, maximum being at 5 mM (Figure 6- depth axis).

4.3.2. Effect of Ionic Strength on Interaction Parameter (k_D) and Charges on the Molecule

Protein-protein interactions in dilute solutions were measured using DLS for mAb A at pH 6.1 and varying ionic strengths from 0-150 mM (Figure A1.2). A detailed explanation for the D_m plot obtained is provided in the Appendix 1. Interactions are highly repulsive at 0 mM ionic strength (in the absence of any ions in solution) and become highly attractive on increasing the ionic strength, and follow the rank order as 1 mM > 2.5>5>10>15>150 mM. Charges on the molecule were also calculated from the zeta potential measurements as a function of ionic strength at pH 6.1 (complied in Table A1.2 in the Appendix 1). Zeta potential and charges decrease with an increase in the ionic strength; as Debye length is inversely related to the square root of the ionic strength.

Figure 7 shows a plot of k_D values obtained from DLS (primary axis) at pH 6.1 as a function of ionic strength and opalescence measured as percent transmittance at 50 mg/mL (secondary axis) at the same solution conditions. Interactions are strongly repulsive in nature

at 0 mM (data not plotted) indicated by large positive values (+591.98 mL/g) and can be attributed to high positive charge (calculated) on the molecule (~ +87.29 Z). Strong repulsions correlate with the absence of solution opalescence at 50 mg/mL protein concentration. As the ionic strength is increased to 1 mM, k_D shows a large negative value (-143.89 mL/g) indicating strong attractive protein-protein interactions. However, there is only a slight increase (transmittance decreases by 3 %) in solution opalescence at 50 mg/mL compared to 0 mM. Increasing the ionic strength to 2.5 mM increases opalescence but again to a very small extent (transmittance again decreases by 3 %), however k_D values become less negative (-118.67 mL/g) indicating a decrease in attractive interactions. As the ionic strength is increased to 5 mM, k_D values become less negative (-99.92 mL/g), and opalescence reaches maximum (transmittance decreases by 20 %). As the ionic strength is further increased to 10, 15 and 150 mM, k_D values become less negative and opalescence decreases linearly. Similar to our previous observations correlating opalescence and interaction parameter k_D, from Figure 7, opalescence can be correlated to attractive intermolecular interactions (5 mM), but there is a discrepancy in interactions at low ionic strengths (1 and 2.5 mM) and opalescence in solution.

4.3.3. Effect of Ionic Strength on Viscoelasticity

Viscoelastic solutions exhibit both G' (storage modulus) and G'' (loss modulus); tan δ (the ratio of G''/G') serves as a measure of the viscoelastic nature of the liquid. Dilute and non-interacting systems exhibit higher tan δ values, while strongly interacting systems exhibit lower tan δ values. G' is expected to increase with solute concentration as the number of solute molecules in the system increases and irrespective of the interactions in solution,

excluded volume contribution is always present. Hence, tan δ is a better indicator of interactions in solutions as a function of ionic strength to relate it to the point of maximum interactions (indicated by low tan δ or high G') before protein solution undergoes change in some physical property.

Figure 8 shows a plot of tan δ and storage modulus (G') for 60 mg/mL and 160 mg/mL mAb A solutions as a function of ionic strength at pH of 6.1 versus opalescence measured as percent transmittance at similar concentrations (secondary axis). From Figure 8a, at 60 mg/mL, tan δ values decreases slightly from 0 mM to 2.5 mM ionic strength and then increases on increasing the ionic strength up to 150 mM. Trend is similar for G' at 60 mg/mL (Figure 8b), where G' increases up to 2.5 mM, indicating increased interactions in solutions, and then decrease as ionic strength is increased further to 150 mM. This indicates that rigidity of the system increases as ionic strength is increased from 0 mM up to 2.5 mM, and then as the ionic strength is increased further from 5 to 150 mM rigidity or attractive interactions decrease. While, opalescence indicated by percent transmittance for 50 mg/mL solutions, increases from 0 mM, reaches a maximum at 5 mM and then decrease with further increase in the ionic strength.

At 150 mg/mL, mAb A did not exhibit any opalescence at any ionic strengths studied, while, tan δ values (Figure 8c) and G' (Figure 8d) at 160 mg/mL show a trend similar to 60 mg/mL; initially decreases as ionic strength is increased from 0 mM, reaches a minimum at 2.5 mM and then increases as the ionic strength is increased further up to 150 mM. However at 160 mg/mL, there is a sharp increase and decrease in G' values as the ionic strength is increased compared to that observed at 60 mg/mL. This sharp change in G' values with changing solution conditions can be attributed to the excluded volume effect at higher

concentrations. This shows that tan δ and G' indicates rigidity of the system with respect to ionic strength, where interactions reaches maximum and as the ionic strength is increased beyond this maximum point i.e. from 2.5 mM to 5 mM; system will exhibit change in certain physical property, as increased opalescence in the current study.

Interactions measured in dilute solution by light scattering and at high concentration by high frequency rheology show that attractive interactions result in high solution opalescence, however; there is a discrepancy in attractive interactions and opalescence measured. As discussed above, critical opalescence show a concentration and ionic strength dependence, i.e, high opalescence occurs at intermediate concentration (~ 50-75 mg/mL) and at an intermediate ionic strength (5 mM) and decreases above and below this concentration and ionic strength. Similarly, from light scattering and rheology measurements as a function of ionic strength, it can be seen that high opalescence correlates with attractive interactions in an intermediate range with respect to k_D and tan δ (G').

This discrepancy in low opalescence and strong attractive interactions in solution especially at low ionic strength can be attributed to the Donnan effect in the solution. If a system undergoes liquid-liquid phase separation, protein separates in two phases with different concentrations, but same chemical potential.[41] Hence salts in the system will partition themselves in the two phases according to the concentration gradient of the protein. Protein-rich phase will have a low salt concentration; while protein-poor phase will have a high-salt concentration. However, at low ionic strength of 1 and 2.5 mM, the overall salt present in the solution is so low that on partitioning not enough salt is present in lower phase to stabilize the protein-rich phase; system will revert back to being homogenous. At 5 mM ionic strength, even after partitioning ionic strength of the lower phase is sufficient enough to

promote formation of a stable phase and system phase separates. Hence at extremely low ionic strengths, phase separation is in transient state and never really occurs, resulting in the discrepancy in measurements.

Another reason for discrepancy in attractive interactions and opalescence may be due to the fact that opalescence and hence liquid-liquid phase separation that follows it, show temperature dependence (influencing entropy of the system) and all interactions were measured at 25 ˚C/ room temperature. To get a better understanding of temperature dependence of opalescence, percent transmittance was measured as a function of temperature.

4.4. Effect of Temperature

The phase separation phenomenon assumes a great significance since various protein formulations are stored under refrigerated conditions (2-8 ºC), where tendency to phase separate is higher. A physically more stable product should exhibit a lower phase separation temperature (T_{cloud}). Taratuta and coworkers established the coexistence curve for lysozyme solution at various pH, ionic strengths and salt types, and found that the shift in the coexistence curve as a function of solution conditions affects only the critical temperature (T_c), while the critical concentration (C_c) remains constant (230 ± 10mg/mL).[50] In another study, authors constructed the co-existence curve for four different γ-crystallin proteins, which differed in their amino acid residues, and concluded that C_c (240 ± 10 mg/mL) remains same for different γ-crystallin but T_c changes.[51] Similar shift in coexistence curve of a monoclonal antibody solution with increasing concentration of Human serum albumin (HSA) was reported by Wang and coworkers.[44] Critical concentration is assumed to be

dependent on the size of the molecule, and hence should be constant for similar sized molecule, while T_c is a physical parameter and depends on the solution conditions.[44,50,51] Hence, a change in pH, ionic strength and nature of the salt, determines the parallel shift in T_c, which in turn determines the opalescence in solution. A better understanding of the shift in the phase separation temperature (T_{cloud}) would help in better optimization of formulation conditions.

Figure 9 shows a plot of percent transmittance against concentration as a function of temperature at pH 6.1 and ionic strengths of (a) 5 mM and (b) 15 mM. At both the ionic strengths studied, curve shifts with change in temperature. At 5 mM, the shift in curve to extremely low transmittance, indicating turbidity in solution, occurs at around 10 °C. No opalescence is observed at 125 mg/mL at any of the temperatures. At 25 mg/mL, low opalescence is observed at higher temperatures, however at 10 °C, there is sudden increase in opalescence. At 75 mg/mL solution opalescence increases consistently as temperature is decreased and then increases to a significant extent at 10 °C. Similar trend is observed at 15 mM, however, only at 75 mg/mL, opalescence shows significant increase as temperature is lowered. From Figure 9, at 5 mM ionic strength, the phase separation temperature (T_{cloud}) lies around 10 ºC, while at higher ionic strength (15 mM), T_{cloud} decreases and lies between 2-5 ºC. Percent transmittance measurements show that opalescence is reversible on increasing the temperature (data not shown).

From these studies, it is confirmed that the opalescence in solution is due to liquid-liquid phase separation. Shift in T_{cloud} to lower temperatures on increasing the ionic strength indicates better physical stability of the solution. Also, T_{cloud} marks the onset of liquid-liquid phase separation in solution indicating the presence of attractive interactions in solution.

Hence, it would serve as a better parameter to assess PPI than k_D or G' or tan δ, as it takes into account, temperature dependence of opalescence and liquid-liquid phase separation. Figure 10 shows images for liquid-liquid phase separation in 65 mg/mL, mAb A solution at pH 6.1 and ionic strength of 15 mM at different conditions. Solution exhibited opalescence at room temperature (Figure 10a). Opalescence increased when sample was stored in refrigerator for 30 min (Figure 10b) and then ultimately separated in two distinct phases on storage in refrigerator for 12 hours (Figure 10c).

On undergoing liquid-liquid phase separation, the protein-rich phase so formed will have higher interactions in solution (negative enthalpy) as compared to protein-poor phase (less negative enthalpy); while the entropic effect will be unfavorable in protein-rich phase (system will be more ordered at higher concentrations) and favorable in protein-poor phase (disordered system at low concentrations). This balance of entropic and enthalpy effect, which has strong temperature dependence, will influence the free energy of mixing of the solution. The change in miscibility or immiscibility with the change in solution conditions result in increased solution opalescence for mAb. While, protein-protein interactions measured in solution may simply represent self-association between two protein molecules, phase separation is due to formation of multimers in solution attributed to attractive interactions. Hence, though the presence of attractive interactions in solution is an important criterion for phase separation to occur, enthalpy-entropy balance is what controls the phase separation process.

5. Conclusion

The monoclonal antibody molecule studied shows a unique property of high opalescence that can be attributed to Liquid-liquid phase separation. Temperature dependence of opalescence confirms that liquid-liquid phase separation results in opalescence for mAb A. Formulation factors like pH, ionic strength and concentration have a significant effect on solution opalescence; opalescence increases close to the pI of the molecule, in an intermediate concentration range and at an intermediate ionic strength. High opalescence and liquid-liquid phase separation can be attributed to attractive interactions in solutions measured in dilute and concentrated solutions, but attractive interactions do not always imply phase separation.

6. Acknowledgments

Authors would like to thank AbbVie Bioresearch Center, Worcester, MA for material and financial support for the work; and Dr. Ravi Chari, Dr. Vineet Kumar (currently at Johnson & Johnson) and Dr. Michael Siedler for scientific discussions.

7. References

1. An Z. 2010. Monoclonal antibodies - a proven and rapidly expanding therapeutic modality for human diseases. Protein Cell 1(4):319-330.
2. Elbakri A, Nelson PN, Abu Odeh RO. 2010. The state of antibody therapy. Hum Immunol 71(12):1243-1250.
3. Shire SJ, Shahrokh Z, Liu J. 2004. Challenges in the development of high protein concentration formulations. J Pharm Sci 93(6):1390-1402.
4. Harris RJ SS, Winter C. . 2004. Commercial Manufacturing Scale Formulation and Analytical Characterization of Therapeutic Recombinant Antibodies. Drug Dev Res 61:137–154.
5. Daugherty AL, Mrsny RJ. 2006. Formulation and delivery issues for monoclonal antibody therapeutics. Adv Drug Deliv Rev 58(5-6):686-706.
6. Saluja A, Kalonia DS. 2008. Nature and consequences of protein-protein interactions in high protein concentration solutions. Int J Pharm 358(1-2):1-15.
7. Hall D, Minton AP. 2003. Macromolecular crowding: qualitative and semiquantitative successes, quantitative challenges. Biochim Biophys Acta 1649(2):127-139.
8. Wang W, Singh S, Zeng DL, King K, Nema S. 2007. Antibody structure, instability, and formulation. J Pharm Sci 96(1):1-26.
9. Wang W. 2005. Protein aggregation and its inhibition in biopharmaceutics. Int J Pharm 289(1-2):1-30.
10. Sukumar M, Doyle BL, Combs JL, Pekar AH. 2004. Opalescent appearance of an IgG1 antibody at high concentrations and its relationship to noncovalent association. Pharm Res 21(7):1087-1093.
11. Salinas BA, Sathish HA, Bishop SM, Harn N, Carpenter JF, Randolph TW. 2010. Understanding and modulating opalescence and viscosity in a monoclonal antibody formulation. J Pharm Sci 99(1):82-93.
12. 12. Woods JM, Nesta D. 2010. Formulation effects on opalescence of a high-concentration MAb. BioProcess Int 8(9):48-59.
13. Nishi H, Miyajima M, Nakagami H, Noda M, Uchiyama S, Fukui K. 2010. Phase separation of an IgG1 antibody solution under a low ionic strength condition. Pharm Res 27(7):1348-1360.
14. Mason BD, Zhang L, Remmele RL, Jr., Zhang J. 2011. Opalescence of an IgG2 monoclonal antibody solution as it relates to liquid-liquid phase separation. J Pharm Sci 100(11):4587-4596.
15. Wang N HB, Ionescu R, Mach H, Sweeney J, Hamm C, Kirchmeier MJ, Meyer BK. 2009. Opalescence of an IgG1 monoclonal antibody formulation is mediated by ionic strength and excipients. BioPharm Int 22(4):36-47.
16. Nishi H, Miyajima M, Wakiyama N, Kubota K, Hasegawa J, Uchiyama S, Fukui K. 2011. Fc domain mediated self-association of an IgG1 monoclonal antibody under a low ionic strength condition. J Biosci Bioeng 112(4):326-332.
17. Vekilov PG. 2012. Phase diagrams and kinetics of phase transitions in protein solutions. J Phys Condens Matter 24(19):193101.
18. Siezen RJ, Fisch MR, Slingsby C, Benedek GB. 1985. Opacification of gamma-crystallin solutions from calf lens in relation to cold cataract formation. Proc Natl Acad Sci U S A 82(6):1701-1705.

19. Pande A, Pande J, Asherie N, Lomakin A, Ogun O, King J, Benedek GB. 2001. Crystal cataracts: human genetic cataract caused by protein crystallization. Proc Natl Acad Sci U S A 98(11):6116-6120.
20. Eaton WA, Hofrichter J. 1990. Sickle cell hemoglobin polymerization. Adv Protein Chem 40:63-279.
21. Koo EH, Lansbury PT, Jr., Kelly JW. 1999. Amyloid diseases: abnormal protein aggregation in neurodegeneration. Proc Natl Acad Sci U S A 96(18):9989-9990.
22. Yagi H, Takahashi N, Yamaguchi Y, Kato K. 2004. Temperature-dependent isologous Fab-Fab interaction that mediates cryocrystallization of a monoclonal immunoglobulin G. Mol Immunol 41(12):1211-1215.
23. Saluja A, Kalonia DS. 2005. Application of ultrasonic shear rheometer to characterize rheological properties of high protein concentration solutions at microliter volume. J Pharm Sci 94(6):1161-1168.
24. Saluja A, Badkar AV, Zeng DL, Nema S, Kalonia DS. 2006. Application of high-frequency rheology measurements for analyzing protein-protein interactions in high protein concentration solutions using a model monoclonal antibody (IgG2). J Pharm Sci 95(9):1967-1983.
25. Saluja A, Badkar AV, Zeng DL, Nema S, Kalonia DS. 2007. Ultrasonic storage modulus as a novel parameter for analyzing protein-protein interactions in high protein concentration solutions: correlation with static and dynamic light scattering measurements. Biophys J 92(1):234-244.
26. Yadav S, Liu J, Shire SJ, Kalonia DS. 2010. Specific interactions in high concentration antibody solutions resulting in high viscosity. J Pharm Sci 99(3):1152-1168.
27. Yadav S, Shire SJ, Kalonia DS. 2010. Factors affecting the viscosity in high concentration solutions of different monoclonal antibodies. J Pharm Sci 99(12):4812-4829.
28. Yadav S, Shire SJ, Kalonia DS. 2012. Viscosity behavior of high-concentration monoclonal antibody solutions: correlation with interaction parameter and electroviscous effects. J Pharm Sci 101(3):998-1011.
29. Chari R, Jerath K, Badkar AV, Kalonia DS. 2009. Long- and short-range electrostatic interactions affect the rheology of highly concentrated antibody solutions. Pharm Res 26(12):2607-2618.
30. RJ H. 1981. The calculation of zeta potential. In: Ottewill RH, Rowell RL, editors. Zeta potential in colloid science principles and applications. New York: Academic Press. 1:59–124.
31. Chun M LI. 2008. Rigorous estimation of effect protein charge from experimental electrophoretic mobilities for proteomics analysis using microchip electrophoresis. Colloids Surf A 318:191-198.
32. Berne BJ, Pecora R. 2000. Dynamic light scattering: with applications to chemistry, biology, and physics. ed.: Courier Dover Publications, New York, NY.
33. Yadav S, Scherer TM, Shire SJ, Kalonia DS. 2011. Use of dynamic light scattering to determine second virial coefficient in a semidilute concentration regime. Anal Biochem 411(2):292-296.
34. Hunter RJ. 2001. Foundation of colloidal science, vol 1. Oxford University Press, New York, NY.

35. Lutanie E, Voegel JC, Schaaf P, Freund M, Cazenave JP, Schmitt A. 1992. Competitive adsorption of human immunoglobulin G and albumin: consequences for structure and reactivity of the adsorbed layer. Proc Natl Acad Sci U S A 89(20):9890-9894.
36. David C, M. C. Millot, E. Renard, and B. Sebille. 2002. Coupling of antibodies to b-cyclodextrin-coated gold surfaces via an intermediate adamantyl-modified carboxymethylated dextran layer. J. Inclusion Phenom. Macro. Chem. 44:369-372.
37. Saluja A, Kalonia DS. 2004. Measurement of fluid viscosity at microliter volumes using quartz impedance analysis. AAPS PharmSciTech 5(3):e47.
38. Stanley HE. 1987. Introduction to Phase Transitions and Critical Phenomena. Oxford University Press. New York, NY.
39. D. Beysens JS, and D.J. Turner,. 1987. Phase Transition and Near Critical Phenomena,. ed., Berlin: Springer,.
40. Gopal ESR. 2000. Critical opalescence. Resonance 5(4):37-45.
41. Van Dijk, M.A., Wakker, A. 1997. Concepts of Polymer Thermodynamics, Technomic Publishing Co., Lancaster, PA.
42. Atkins P, De Paula J. 2014. Atkins' physical chemistry. ed.: Oxford University Press, Oxford, UK.
43. Hiemenz, R C. and Rjagopalan, R. 1997. Principles of Colloid and Surface Chemistry, 3rd ed., Marcel Dekker, Inc., New York, NY.
44. Wang Y, Lomakin A, Latypov RF, Benedek GB. 2011. Phase separation in solutions of monoclonal antibodies and the effect of human serum albumin. Proc Natl Acad Sci U S A 108(40):16606-16611.
45. Zhou HX, Rivas G, Minton AP. 2008. Macromolecular crowding and confinement: biochemical, biophysical, and potential physiological consequences. Annu Rev Biophys 37:375-397.
46. Laue T. 2012. Proximity energies: a framework for understanding concentrated solutions. J Mol Recognit 25(3):165-173.
47. Israelachvili JN. 2011. Intermolecular and Surface Forces Third ed., San Diego: Academic Press.
48. Lockhart DJ, Kim PS. 1993. Electrostatic screening of charge and dipole interactions with the helix backbone. Science 260(5105):198-202.
49. Neal BL, D. Asthagiri, and A. M. Lenhoff. 1998. Molecular origins of osmotic second virial coefficients of proteins. Biophys. J. 75:2469-2477.
50. Taratuta VG HA, Thurston GM, Blankschtein D, Benedek GB. 1990. Liquid–liquid phase separation of aqueou lysozyme solutions: Effects of pH and salt identity. J Phys Chem 94:2140-2144.
51. Broide ML, Berland CR, Pande J, Ogun OO, Benedek GB. 1991. Binary-liquid phase separation of lens protein solutions. Proc Natl Acad Sci U S A 88(13):5660-5664.

8. Tables and Figures

Table 1: Effect of molecular properties and formulation factors on protein-protein interactions in solution. (Adapted from literature[29,46,47])

Interactions	Range on Interactions	Distance dependence[a]	Molecular properties	Formulation factors affecting PPI
Repulsive Interactions				
Charge-Charge	Long	r^{-1}	Charges	Dominant away from pI, Ionic strength decreases PPI
Excluded Volume[b] (Molecular crowding)	Short	r^{-12}		
Attractive Interactions				
Charge-Dipole (fixed)	Mid	r^{-2}	Charge, Geometry and orientation	Dominant close to pI Ionic strength decreases PPI
Charge-Dipole (freely rotating)	Mid	r^{-4}		
Charge-Induced dipole	Mid	r^{-4}		
Dipole-dipole[c]	Short	r^{-6}	Geometry and orientation	
Dipole-induced dipole[c]	Short	r^{-6}		
Induced dipole-induced dipole[c]	Short	r^{-6}		
Hydrophobic	Short		Surface amino acids (non-polar)	Low ionic strength has no effect, high ionic strength increases attractions

a: Distance dependence of mean potential W(r)between the interacting molecules

b:Distance dependence based on repulsive interactions term in the Lenard Jones potential[34,47]

c:Dipole-dipole, dipole-induced dipole, induced dipole-induced dipole together constitute van der Waals interactions

Figures

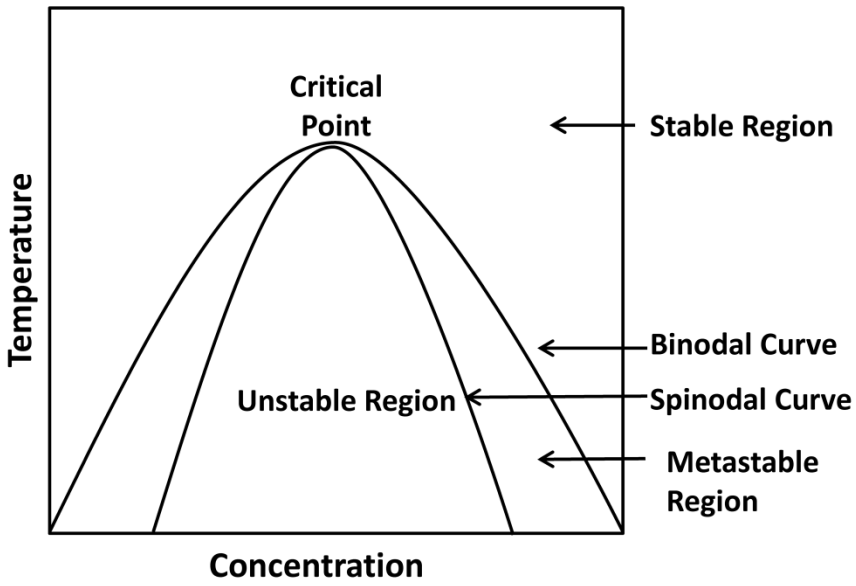

Figure 1: Temperature-concentration curve showing liquid-liquid phase separation. Adapted from general references.[38, 39, 41,42]

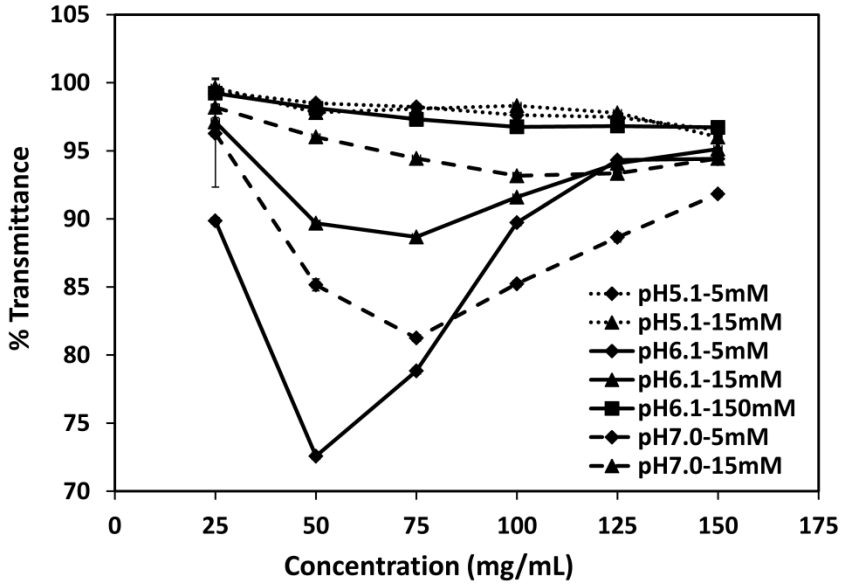

Figure 2: Percent transmittance as a function of protein concentration at various solution pH (pH 5.1- acetate, pH 6.1-histidine, pH 7.0-phosphate) and at ionic strengths of 5 mM (♦), 15 mM (▲) and 150 mM (■). All solutions were analyzed at room temperature (23 ± 1˚C) in duplicate. Error bars if not visible are smaller than the symbols used.

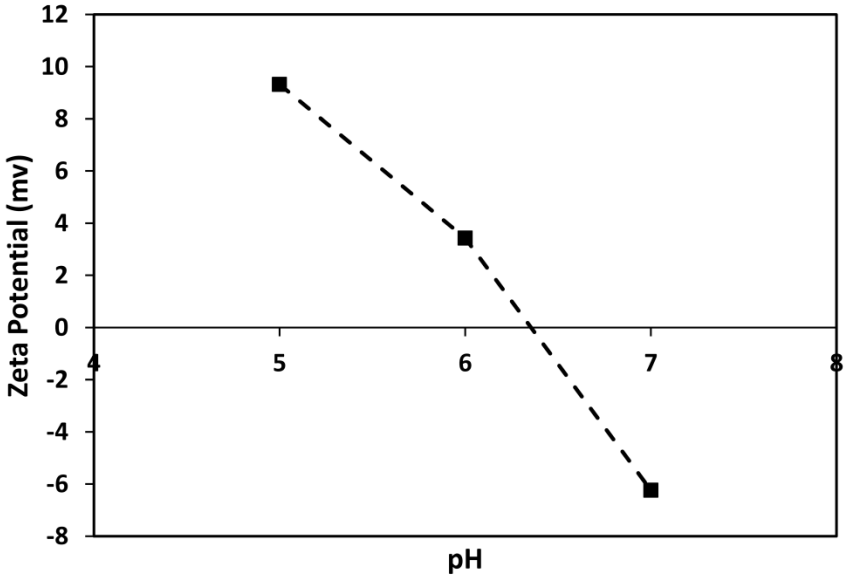

Figure 3: Zeta potential of mAb A as a function of solution pH at 5mM ionic strength. The line connecting the data points is to guide the eye and is not a result of model fitting to the data. All solutions were analyzed at 25 ± 0.1˚C in duplicate. Error bars if not visible are smaller than the symbols used.

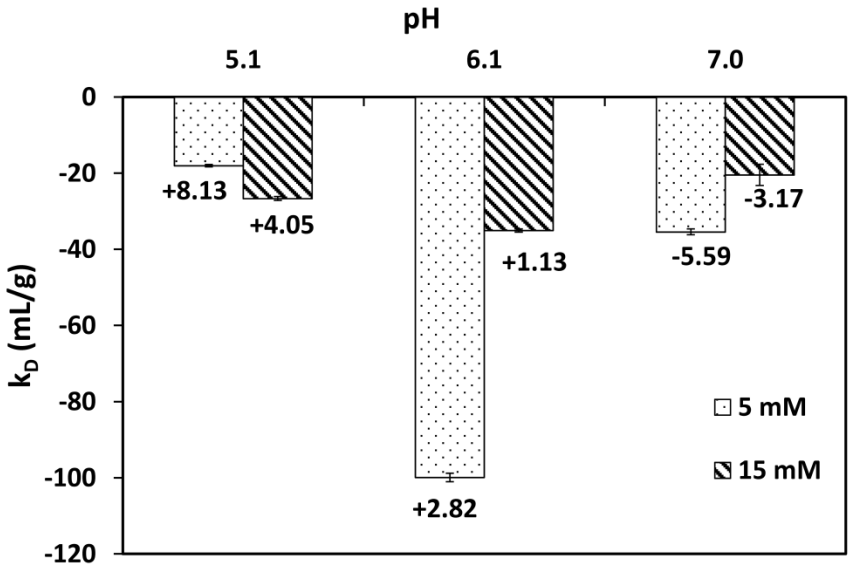

Figure 4: Plot of k_D obtained from Dynamic light scattering as a function of pH and ionic strength. The numbers under the bar represent the effective charge on the molecule, calculated from linear correlation of electrophoretic mobility and zeta potential. Zeta potential and charges calculated in duplicates have been averaged. All solutions were analyzed at 25 ± 0.1˚C.

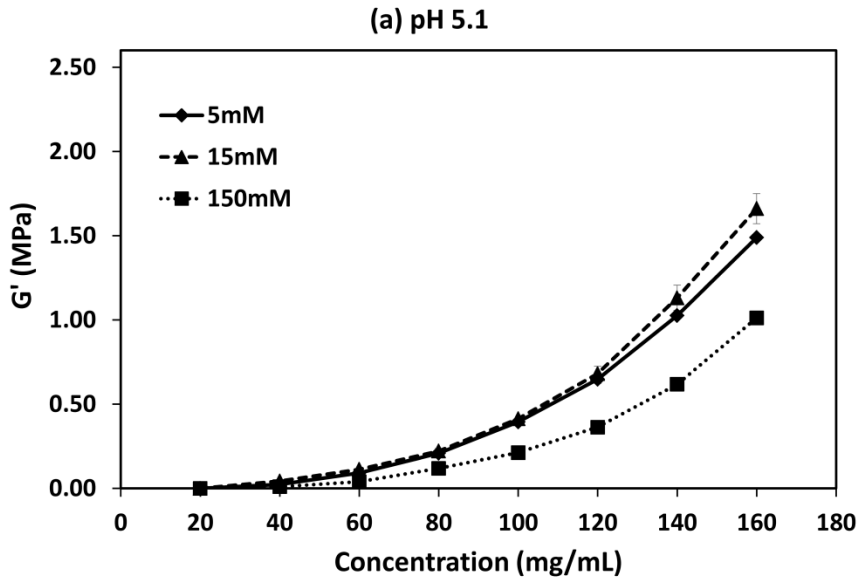
(a) pH 5.1
2.50
2.00
1.50
1.00
0.50
0.00
G' (MPa)
5mM
15mM
150mM
0
20
40
60
80
100
120
140
160
180
Concentration (mg/mL)

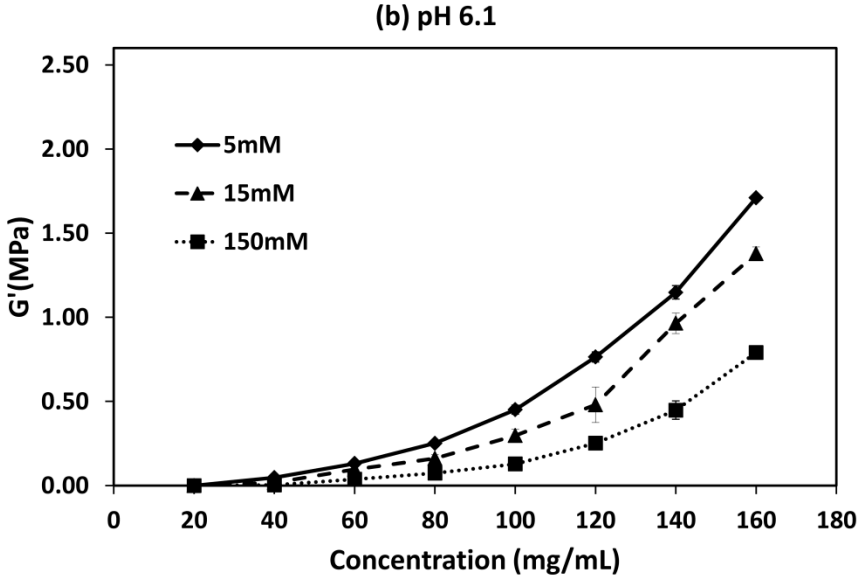
(b) pH 6.1
2.50
2.00
1.50
1.00
0.50
0.00
G'(MPa)
5mM
15mM
150mM
0
20
40
60
80
100
120
140
160
180
Concentration (mg/mL)

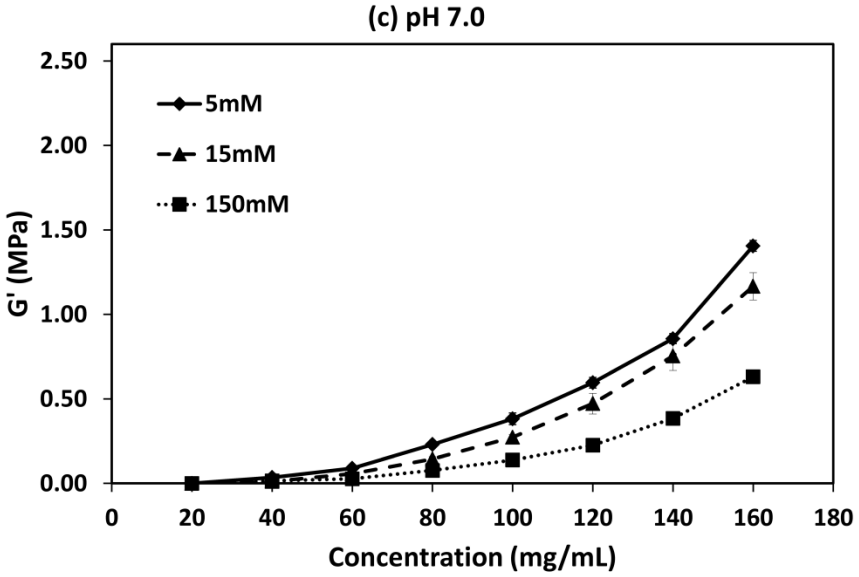

Figure 5: Solution *G'* as a function of concentration at ionic strengths of 5 mM (♦), 15 mM (▲) and 150 mM (■), at (a) pH 5.1 (acetate buffer), (b) 6.1 (histidine buffer) and (c) 7.0 (phosphate buffer). All solutions were analyzed at 25 ± 0.1˚C in duplicate. Error bars if not visible are smaller than the symbols used.

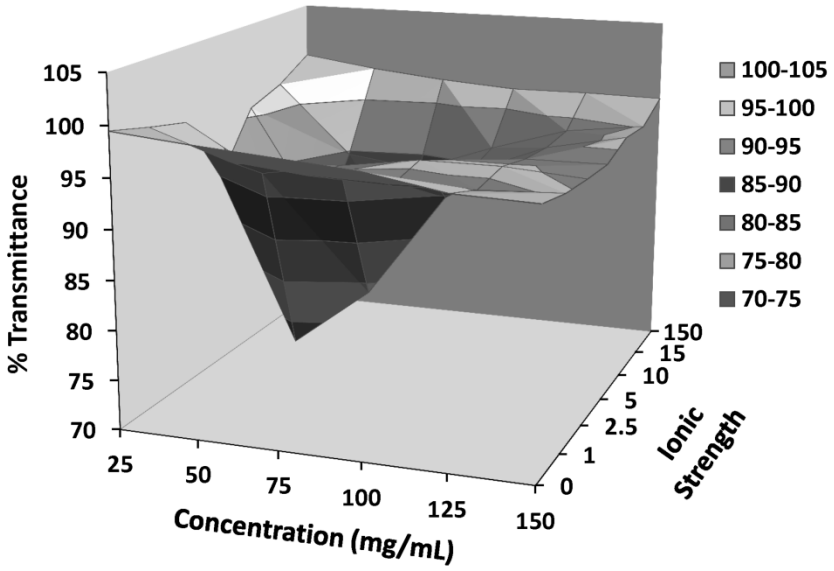

Figure 6: Percent transmittance at pH 6.1 (histidine buffer) as a function of protein concentration (horizontal axis) and ionic strengths (depth axis). Ionic strength of 1, 2.5, 5, 10 and 15 mM were maintained by preparing histidine solutions with appropriate buffer strength. Sodium chloride was added to maintain ionic strength of 150 mM. Ionic strength of 0 mM, represents protein solution extensively dialyzed in water. All solutions were analyzed at room temperature (23 ± 1˚C). Plot represents averages of percent transmittance measured at all conditions in duplicate.

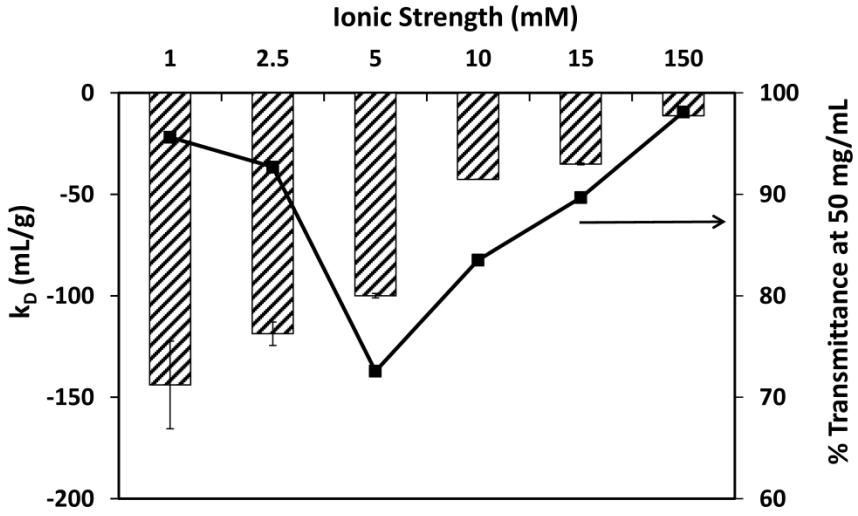

Figure 7: Plot of k_D (primary axis) and percent transmittance at 50 mg/mL (secondary axis) as a function of ionic strength at pH 6.1. All solutions were analyzed at 25 ± 0.1˚C for light scattering and at room temperature (23 ± 1˚C) for opalescence in duplicate. Error bars if not visible are smaller than the symbols used.

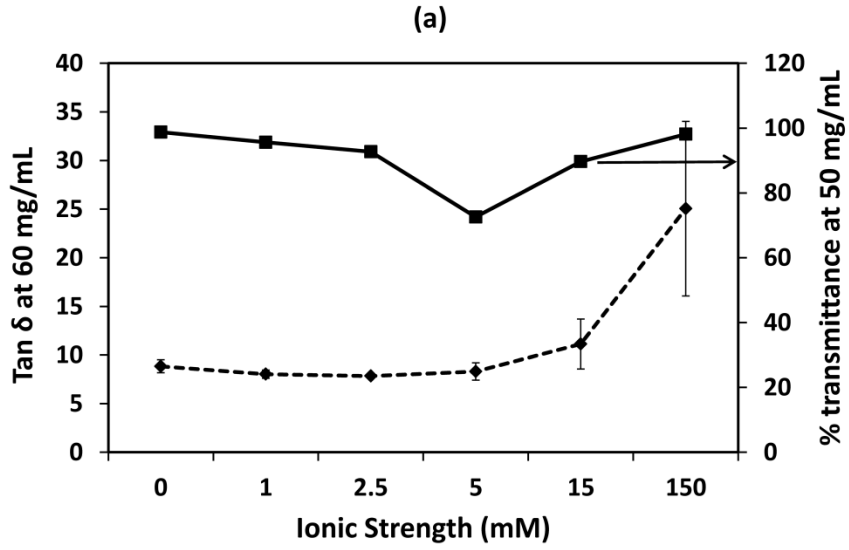
(a)
Tan δ at 60 mg/mL
% transmittance at 50 mg/mL
Ionic Strength (mM)
0
1
2.5
5
15
150

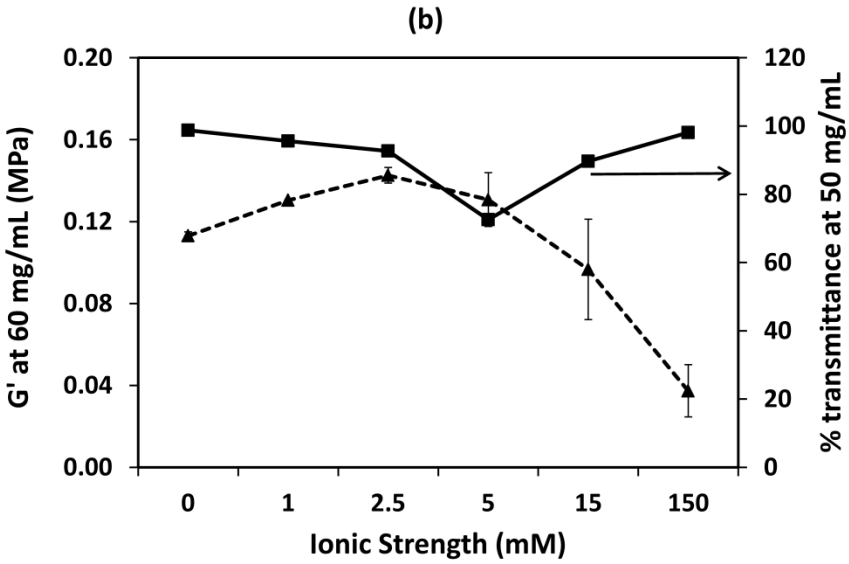
(b)
G' at 60 mg/mL (MPa)
% transmittance at 50 mg/mL
Ionic Strength (mM)
0
1
2.5
5
15
150

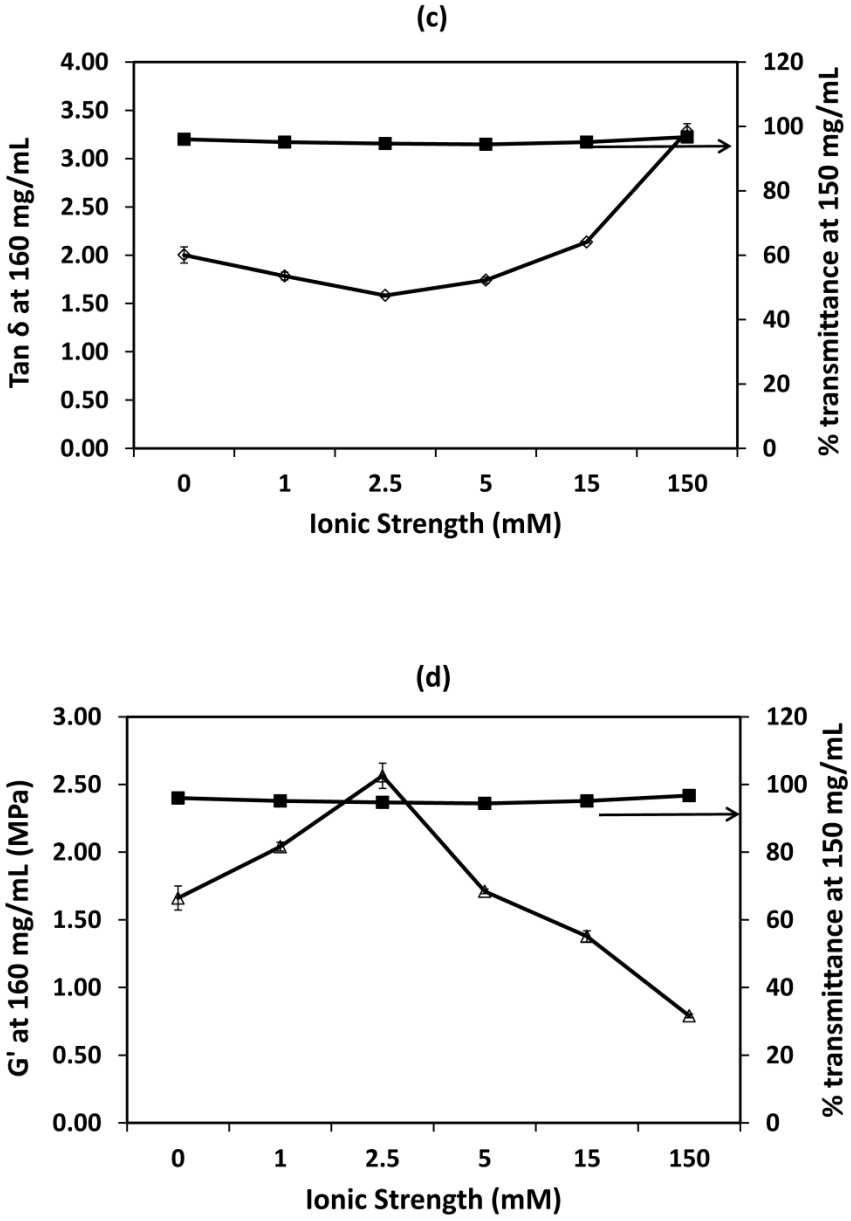

Figure 8: Plot of (a) tan δ (primary axis) at 60 mg/mL, and (b) G' (primary axis) at 60 mg/mL versus percent transmittance at 50 mg/mL (secondary axis), (c) tan δ (primary axis) at 160 mg/mL and (d) G' (primary axis) at 160 mg/mL versus percent transmittance at 150 mg/mL (secondary axis) as a function of ionic strength at pH 6.1. All solutions were analyzed at 25˚C ± 0.1˚C in duplicate. Error bars if not visible are smaller than the symbols used.

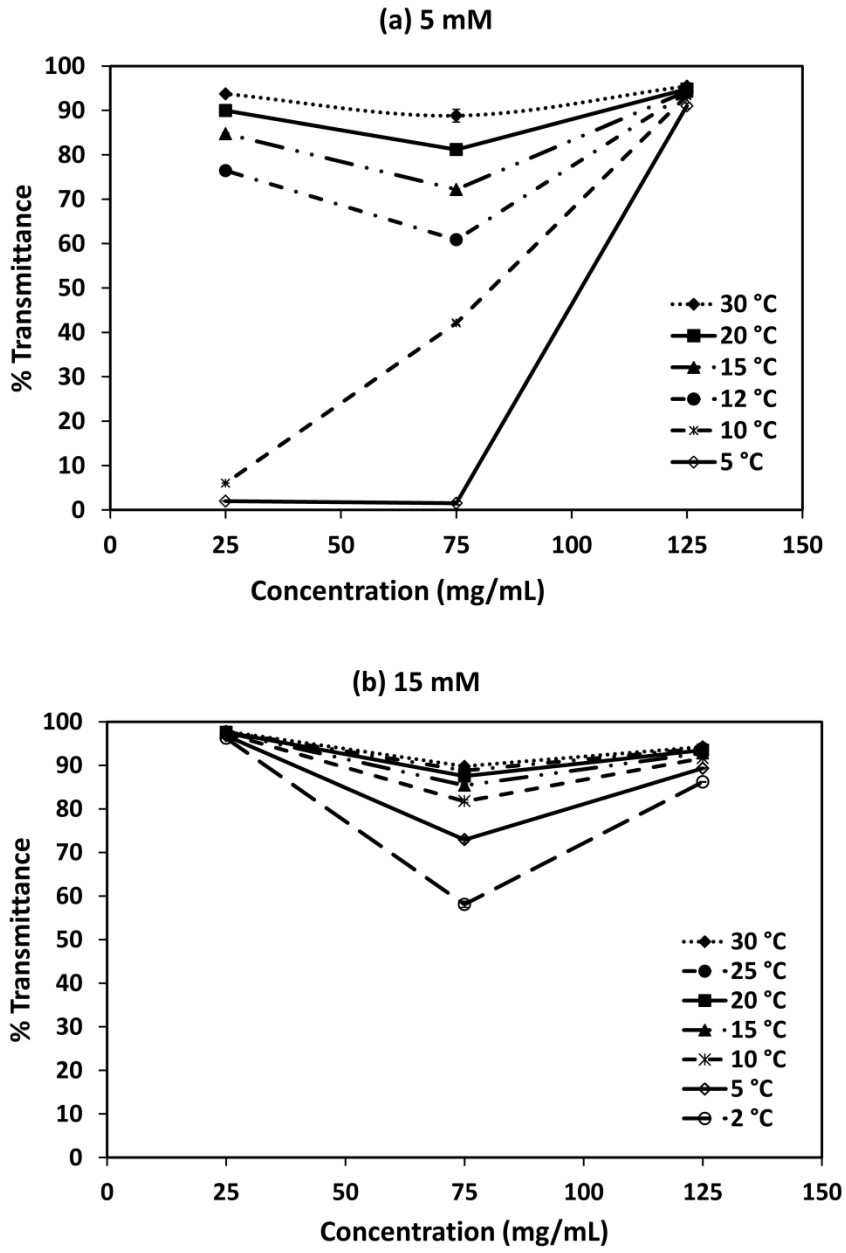

Figure 9: Plot of percent transmittance at pH 6.1 and at concentrations of 25 mg/mL, 75 mg/mL and 125 mg/mL as a function of temperature and varying ionic strengths of (a) 5 mM and (b) 15 mM. All the samples were analyzed in duplicate. Error bars if not visible are smaller than the symbols used. The lines connecting the points have been added as a guide to the eye and are not the result of any model fitting to the data.

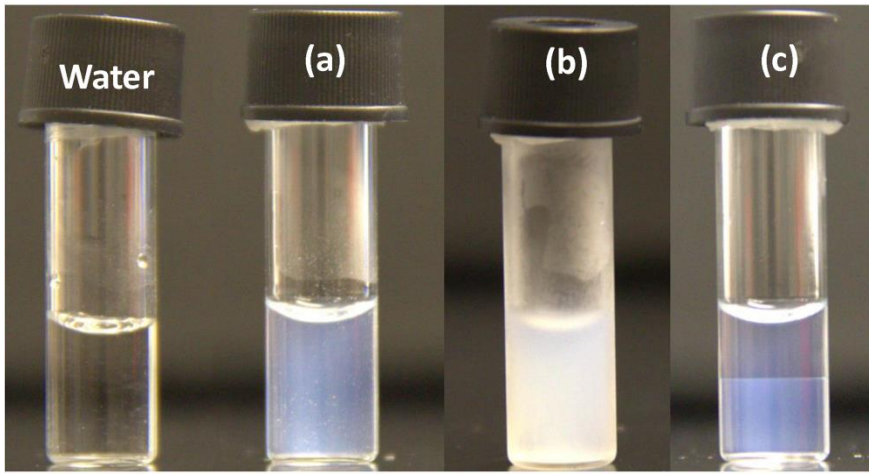

Figure 10: Images for mAb A at pH 6.1- 5 mM ionic strength and at a concentration of 65 mg/mL at (a) Room temperature (~23 ˚C), (b) 4 ˚C after 30 min, and (c) 4 ˚C after 12 hours.

Chapter 4

Liquid-Liquid Phase Separation in a Dual Variable Domain Immunoglobulin Protein Solution: Effect of Formulation Factors and Protein-Protein Interactions

Contents

Chapter 4

1. Abstract

Dual variable domain immunoglobulin proteins (DVD-Ig^{TM} proteins) are large molecules (MW~ 200 kDa) with increased asymmetry because of their extended Y-like shape, which results in increased formulation challenges. Liquid-liquid phase separation (LLPS) of protein solutions into protein-rich and protein-poor phases reduces solution stability at intermediate concentrations and lower temperatures, and is a serious concern in formulation development as therapeutic proteins are generally stored at refrigerated conditions. In the current work, LLPS was studied for a DVD-Ig^{TM} protein molecule as a function of solution conditions by measuring solution opalescence. LLPS of the protein was confirmed by equilibrium studies and by visually observing under microscope. The protein does not undergo any structural change after phase separation. Protein-protein interactions were measured by light scattering (k_D) and T_{cloud} (temperature that marks the onset of phase separation). There is a good correlation between k_D measured in dilute solution with T_{cloud} measured in critical concentration range. Results indicate that the increased asymmetry of the molecule (with respect to both size and charge distribution on the molecule) increases contribution of specific and non-specific interactions in solution, which are affected by formulation factors, resulting in LLPS for DVD-Ig^{TM} protein.

Keywords: Liquid-liquid phase separation, opalescence, formulation development, physical stability, protein-protein interactions, light scattering, T_{cloud}, histidine buffer, phase diagram

2. Introduction

Dual Variable Domain Immunoglobulin protein (DVD-Ig™ protein) is a bispecific antibody-like molecule and is engineered from two monoclonal antibodies (mAbs) by adding an additional binding domain to each variable domain; thus making it specific for dual-targeting resulting in improved therapeutic efficacy.[1, 2] Antibody based therapeutics are generally administered by parenteral route at high concentrations.[3] Protein-protein interactions at high concentrations result in several formulation challenges including high viscosity, formation of reversible and/or irreversible aggregates, reduced solubility, opalescence and phase transitions.[4-9] These challenges become more exaggerated in DVD-Ig™ protein solutions since these molecules are larger and more complex.

Liquid formulation of proteins can undergo solid-liquid phase transition resulting in the formation of crystals or amorphous precipitates, or liquid-liquid phase separation (LLPS) into protein-rich and protein-poor phases. Phase separation at physiological conditions is responsible for condensation diseases like cataract,[10] sickle-cell anemia[11] etc. From a pharmaceutical point of view, liquid-liquid phase separation is a concern for formulation development since most protein solutions are stored at refrigerated conditions (2-8˚C) where proteins show a higher tendency to phase separate. Protein-rich phase formed on phase separation can promote aggregation in solution which could compromise physical stability of the formulation. However, under controlled conditions, LLPS can be used to concentrate proteins as the formation of a protein-rich phase in the solution is spontaneous.[12, 13] High concentrations of monoclonal antibody formulation can be easily achieved on a large scale compared to other such techniques as ultrafiltration, drying, chromatography and dialysis, which are time consuming and increase production cost.[14]

Phase diagram for a binary system has a liquidus or solubility line, corresponding to solid-liquid transition in one-component system, and a liquid–liquid coexistence line (binodal curve) corresponding to the gas-liquid phase transition in one-component system. Liquid-liquid phase separation curve lies below the solid-liquid curve and is metastable with respect to crystallization and amorphous precipitate formation.[15] Liquid-liquid phase separation (LLPS) of a protein solution into a protein-rich and protein-poor phase is both a thermodynamic and kinetic process.[16] The two phases formed upon phase separation have different physical properties including concentration, density and refractive index. The phase separation is preceded by increased solution opalescence, which is due to dispersion of the protein-rich phase in protein-poor phase with different refractive indices and result in multiple scattering from the solution. Upon phase separation, the chemical potential of the protein would be same in both phases (thermodynamic equilibrium) even though their concentrations are different.[17, 18] To account for the Donnan effect, salts in the solution would also partition in two phases according to the concentration gradient and maintain the chemical potential across the solution. This can result in pH shift/ionic strength difference in two phases and may further enhance physical instability.

Coexistence curve which characterizes LLPS in solution has a critical point defined by a critical temperature (T_c) and critical concentration (C_c). Majority of the proteins that undergo phase separation exhibit an upper critical solution temperature (UCST) type of phase behavior i.e, phase separation occurs at lower temperatures and system is homogeneous at higher temperatures. Exception is hemoglobin that exhibits lower critical solution temperature (LCST) type of phase behavior, where phase separation occurs as temperature is raised and protein solubility increases at lower temperatures (also termed as retrograde

solubility).[19, 20] Liquid-liquid phase separation has been reported for globular proteins[13, 21-25] and monoclonal antibody.[26-32]

Though DVD-Ig™ proteins (MW 200 kDa) may have therapeutic properties similar to parent mAbs, their larger size results in more complex physicochemical properties, and hence, the formulation and processing at high concentrations becomes even more challenging. The objective of this work is to investigate the effect of various formulation factors on liquid-liquid phase separation in DVD-Ig™ protein solutions and understand the role of various protein-protein interactions affecting this phenomenon.

3. Materials and Methods

3.1. Materials

Dual Variable Domain Immunoglobulin protein (pI ~7.0 - 7.5) was supplied by AbbVie (Worcester, MA) as 85 mg/mL solution in 15 mM Histidine buffer at pH 5.5. All chemicals including acetic acid, sodium acetate, sodium chloride, monobasic and dibasic sodium phosphate, sodium hydroxide and hydrochloric acid were obtained from Fisher Scientific (Fair Lawn, New Jersey). Histidine base and histidine hydrochloride were obtained from Sigma (St. Louis, MO). All chemicals used were reagent grade or higher. Solutions were prepared with deionized water equivalent to Milli-Q™.

Acetate and Histidine buffers were prepared to maintain pH of the solution at 5.0 and 6.1, respectively, while Phosphate buffer was used to maintain pH at 6.5, 7.0 and 8.0. Ionic strength of 15 mM was maintained by selecting appropriate buffer concentration without the addition of any salt at all pHs. Sodium chloride was used to adjust the ionic strength to 50 mM. To study the effect of ionic strength, phosphate buffers with ionic strengths of 5 and 15

mM were prepared at pH 6.5 by maintaining appropriate buffer strength, and sodium chloride was used to adjust the ionic strength to 50 and 100 mM. Three buffers were prepared at pH 6.5 to study the effect of specific ions: (1) Phosphate buffer with ionic strength of 15 mM, (2) Histidine buffer with ionic strength of 15 mM, and (3) Histidine buffer with ionic strength of 1 mM adjusted to 15 mM using sodium chloride.

All solutions were buffer exchanged with appropriate buffers using Millipore (Billerica, Massachusetts) Amicon Ultra centrifugation tubes with a molecular weight cutoff of 10 kDa obtained from Fisher Scientific. Concentrations of the samples were determined using a UV-vis spectrophotometer with an extinction coefficient of 1.5 $mg^{-1}/mL^{-1}cm^{-1}$ for DVD-Ig™ protein at 280 nm for 0.1% (w/v) IgG solutions. The pH of all the above solutions was within ± 0.1 of the target values as measured by a Denver Instrument pH meter.

3.2. Opalescence Measurements

Opalescence of the solution was measured using UV-vis spectrophotometer (Varian Cary 50). Opalescence was measured as percent transmittance at 510 nm in a quartz cuvette with a path length of 3 mm, requiring a sample volume of 60 µL. All the studies were performed at 25 ˚C in duplicate. Opalescence of DVD-Ig™ protein was measured as a function of protein concentration, pH and ionic strength.

3.3. Sample Preparation for Equilibrium Studies

For equilibrium studies, protein solutions were extensively dialyzed in water and concentrated using Amicon Ultra centrifugation tubes. Concentration of the protein stock solution prepared in water was 96.5 mg/mL. Stock solution of sodium phosphate (110 mM

buffer strength) was prepared at pH 6.5 with ionic strength of 150 mM. Effect of initial protein concentration on phase separation was studied by preparing protein solutions at 8, 16, 30 and 60 mg/mL and ionic strength was maintained at 50 mM by appropriately diluting phosphate stock solution. Solutions were stored at 4 ˚C for 48 hours to induce phase separation. Effect of ionic strength (15 and 50 mM) and temperature (4 ˚C and 22˚C) were also studied for 16 mg/mL protein solutions. All the samples were checked for pHs. Protein concentration was measured using UV-Vis spectrophotometer after 48 hours by taking aliquots of sample from upper and lower phase and diluting appropriately. All the concentrations were measured in duplicate.

3.4. Microscopy Studies

Digital images were captured using a Polarized Light microscope (Olympus BH2) equipped with a digital camera (Q Imaging Micropublisher 3.3). 16 mg/mL of DVD-Ig^{TM} protein samples were prepared in phosphate buffer at pH 6.5 and ionic strength was maintained at 15 and 50 mM. 20 μL of sample was placed on a microscope slide and observed under microscope without any coverslip, with 100X magnification. All studies were performed at ambient temperature (23 ± 1 ˚C).

3.5. Circular Dichroism Measurements

Secondary and tertiary structural changes in DVD-Ig^{TM} protein solution before and after phase separation were studied using far-UV (190-250 nm) and near-UV (240-340 nm) circular dichroism (CD) spectroscopy, respectively. CD spectra were recorded using a Jasco 700 spectropolarimeter (Jasco, Inc., Easton, MD) for protein samples freshly dialyzed

(immediately diluted to low concentration to avoid phase separation) in phosphate buffer at pH 6.5 with ionic strength of 15 mM. Samples were allowed to phase separate for 24 hours at room temperature and CD spectra were recorded for the samples collected from the two phases (protein-rich and protein-poor phase) after phase separation. CD spectra were again recorded for previously diluted sample. Protein concentration of 0.3 mg/mL in 0.05 cm path length cells and 0.75 mg/mL in 1.0 cm path length were used for far-UV and near-UV analyses, respectively. An average of 10 scans was accumulated, at a resolution of 1.0 nm and a scan rate of 50 nm min^{-1}. Buffer scans were also accumulated under the same measurement conditions and were subtracted from the protein scans prior to analysis.

3.6. T_{cloud} Measurements

Temperature ramp studies were performed using temperature control Peltier plate attached with the UV-vis spectrophotometer. Temperature was ramped down in steps from 35 ºC to 3 ˚C and samples were allowed to equilibrate at each temperature for 2 min before recording the measurements as percent transmittance. T_{cloud} marks the onset of the liquid-liquid phase separation in the solution. For the current study, the temperature where percent transmittance reaches 70 is termed as T_{cloud}. Concentrations of 16 and 60 mg/mL were studied as a function of the pH at ionic strengths of 15 and 50 mM. Samples were also analyzed to study the effect of ionic strength at a constant pH of 6.5.

3.7. Dynamic Light Scattering (DLS)

Malvern Instruments Zetasizer Nano Series (Worcestershire, UK) was used to perform DLS studies to determine k_D. Instrument utilizes a 632.8 nm Helium–Neon laser and

analyzes scattered light at an angle of 173˚. For DLS analysis, the buffers and sample stock solutions were filtered through sterile 0.22 μm Millipore's Durapore membrane filters before making the dilution to required concentrations. The protein solutions were then centrifuged using an Eppendorf minispin (Germany, HA) mini-centrifuge at 12,110×g for 5 min before every measurement. All the samples were analyzed in duplicate and measurements were made at 25 ± 0.1˚C. A detailed procedure and relevant equations to obtain correct DLS parameters to calculate interaction parameter (k_D), and hydrodynamic radius (r_H) is discussed elsewhere.[33]

4. Results

4.1. Opalescence Measurements

Opalescence for the DVD-Ig™ protein was measured as percent transmittance using UV-vis spectrophotometer at 510 nm, a non-absorbing wavelength. Here, a lower transmittance relates to higher opalescence of the solution. Figure 1 shows a plot of opalescence of DVD-Ig™ protein as a function of concentration and pH at 15 mM ionic strength. At pH 5.0, there is no opalescence in the solution as indicated by percent transmittance close to 100. Opalescence increases slightly at pH 6.1. At pH 6.5, solution exhibits high opalescence in the concentration range of 25-90 mg/mL. Even at a lower concentration of 10 mg/mL, solution exhibits opalescence where percent transmittance is around 85. High viscosity of the solution at higher concentrations (> 100 mg/mL) limited the concentration range that could be studied for opalescence. Solutions at pH 7.0 could not be analyzed as they showed high tendency to phase separate. As pH is further increased to 8.0,

solution exhibits high opalescence in the concentration range of 20-80 mg/mL. However, above 80 mg/mL, solution opalescence decreases with increase in concentration.

The effect of ionic strength and pH on opalescence at 60 mg/mL protein concentration is plotted in Figure 2. At pH 5.0, percent transmittance is close to 100, indicating the absence of solution opalescence at the two ionic strengths studied. The transmittance decreases slightly at pH 6.1. At pH 6.5, solution exhibits high opalescence at 5 and 15 mM ionic strengths (percent transmittance is close to 0), which decreased significantly on increasing the ionic strength to 50 and 100 mM. At pH 7.0, 50 mM ionic strength solution exhibits higher opalescence compared to other pHs at 50 mM. At pH 8.0, DVD-Ig^{TM} protein exhibits high opalescence at 15 mM ionic strength which decreases as the ionic strength is increased to 50 mM.

4.2. Equilibrium Studies

Equilibrium studies were performed for DVD-Ig^{TM} protein molecule at different solution conditions to investigate the effect of concentration and temperature on liquid-liquid phase separation. The effect of the initial protein concentration before phase separation on the protein concentrations of the protein-rich phase and protein-poor phase at 4 ˚C is plotted in Figure 3. Protein concentration measured in the two phases after phase separation is nearly constant irrespective of the initial protein concentration. Average concentration in the upper phase (protein-poor) is ~ 4.5 mg/mL, while the concentration in the lower phase (protein-rich) is ~127 mg/mL. Initial volume for all the samples was 150 μL, however, on phase separation, volumes for the two phases for each initial concentration are different (not analyzed, visually assessed).

Similar studies were performed at a constant concentration (16 mg/mL) to study the effect of temperature and ionic strength on LLPS. Figure 4 shows a plot of the effect of temperature on the protein concentration in protein-rich and protein-poor phases at 15 mM (Figure 4a) and 50 mM (Figure 4b) ionic strength in phosphate buffer at pH 6.5. Protein in 15 mM ionic strength buffer phase separates at 4 ˚C and 22 ˚C. At 22 ˚C, protein concentration in the upper phase and lower phase are 4.3 mg/mL and 124.2 mg/mL, respectively. While at 4 ˚C, protein concentration in the upper and lower phase are 0.8 mg/mL and 132.6 mg/mL, respectively. Protein sample in 50 mM ionic strength buffer does not undergo phase separation at 22 ˚C. However, at 4 ˚C protein phase separates and concentrations in the upper phase and lower phase are 4.4 mg/mL and 125 mg/mL, respectively.

4.3. Microscopy

LLPS in DVD-Ig^{TM} protein solution was confirmed by observing under microscope. From equilibrium studies, solution with ionic strength of 15 mM undergoes phase separation at room temperature while 50 mM solution remains homogenous. Figure 5 (a) and (b) are digital images captured for DVD-Ig^{TM} protein using polarized light microscope equipped with camera. In the 15 mM ionic strength solution, which undergoes phase separation (Figure 5a), droplets of the protein-rich phase are dispersed in the protein poor-phase, while protein solution at 50 mM ionic strength remains homogeneous (Figure 5b).

4.4. Circular Dichroism

Circular dichroism studies were performed to detect structural changes in the protein before and after undergoing phase separation. Figure 6a shows near-UV CD spectra for

DVD-Ig^{TM} protein in pH 6.5 phosphate buffer with ionic strength of 15 mM. The near-UV CD spectra for most proteins are due to absorption by aromatic amino acid side chain chromophores between 250-300 nm. From the spectra, the characteristic peak at 293 nm can be attributed to Tryptophan residues in the molecule. Negative peak at 218 nm in the far-UV spectra (Figure 6b) indicates that DVD-Ig^{TM} protein has greater β sheet content. However, both the near and far-UV CD spectra for the protein before and after phase separation show similar intensities, suggesting that there are no major structural alterations in the secondary and tertiary structure of the protein on phase separation.

4.5. T_{cloud} Measurements

Temperature studies were performed for DVD-Ig^{TM} protein at different solution conditions by measuring percent transmittance as the solution temperature was lowered.[34] Onset of the liquid-liquid phase separation is characterized by a dramatic increase in solution turbidity; this temperature is marked as $T_{opacity}$. Temperature is then increased step wise till solution becomes clear, and this temperature is marked as T_{clear}. Average temperature between $T_{opacity}$ and T_{clear} is the T_{cloud} temperature.[35] For qualitative analysis, the temperature where percent transmittance reaches 70 is termed as T_{cloud}[36]; values for same are compiled in Table 1. Two concentrations, 16 mg/mL (below the critical concentration range) and 60 mg/mL (in the critical concentration range), were analyzed.

At pH 5.0, no phase separation was observed. At pH 6.1, T_{cloud} is around 10 ˚C at both 16 and 60 mg/mL protein concentrations at 15 mM ionic strength. On increasing the ionic strength to 50 mM, T_{cloud} shifts to higher temperatures of 12 ˚C and 16 ˚C at 16 and 60 mg/mL, respectively. At pH 6.5, for 16 mg/mL solution, a higher T_{cloud} of 33˚C was observed

at 15 mM ionic strength, which shifted to a lower temperature (19.3 ˚C) on increasing the ionic strength to 50 mM. At 15 mM ionic strength, 60 mg/mL protein solution exhibited very high opalescence even at 37 ˚C; higher temperatures were not studied to avoid protein denaturation and misinterpretation of the results. T_{cloud} decreased to 24.5 ˚C on increasing the ionic strength to 50 mM.

Protein solutions at pH 7.0 and 15 mM ionic strength were not studied as they exhibited very high opalescence even at high temperatures. At 50 mM, both 16 and 60 mg/mL solutions exhibited higher T_{cloud} of 21.0 ˚C and 25.0 ˚C, respectively, compared to other pH conditions at higher ionic strengths. Solutions at pH 8.0 showed a trend similar to that at pH 6.5, where higher T_{cloud} was observed at 15 mM ionic strength for both 16 and 60 mg/mL solutions (27.5 ˚C and 32.5 ˚C, respectively), which shifted to lower temperatures (15.5 ˚C and 19.5 ˚C, respectively) on increasing the ionic strength to 50 mM.

The effect of ionic strength on T_{cloud} at pH 6.5 was studied for 16 mg/mL (Figure 7a) and 60 mg/mL (Figure 7b) DVD-Ig^{TM} protein solutions. At 5 mM ionic strength, it was not possible to prepare the required concentrations because of a high tendency of the protein to undergo phase separation. Therefore, a lower concentration of 9.8 mg/mL (instead of 16 mg/mL in Figure 7a) and a higher concentration of 78 mg/mL (instead of 60 mg/mL in Figure 7b) were analyzed. At 5 mM ionic strength, the solution exhibited higher opalescence and higher phase separation temperature compared to other ionic strengths, both at low and high concentrations studied. The errors in the measurements were large due to rapid phase separation. At 16 mg/mL, the protein showed a high phase separation temperature at 15 mM ionic strength (33 ˚C) and the curve shifted to lower temperatures on increasing the ionic strength to 50 and 100 mM (19.5 ˚C and 10.5 ˚C, respectively). Similar trend was observed

for 60 mg/mL solution where a high phase separation temperature was recorded at 15 mM (> 37 ˚C) and shifted to lower temperatures at higher ionic strengths (24.5 ˚C at 50 mM and 14.5 ˚C at 100 mM, respectively) indicating increased physical stability on increasing the ionic strength of the solution. Phase separation occurs at higher temperatures at 60 mg/mL protein solutions (temperature curves shifted to right) compared to 16 mg/mL at all ionic strengths. On approaching phase separation temperature, plot of percent transmittance against temperature showed steep decrease at 16 mg/mL while decrease was more gradual at 60 mg/mL.

4.6. Dynamic Light Scattering

The nature of protein-protein interactions in solution is generally measured by determining interaction parameter, k_D, from dynamic light scattering. The interaction parameter includes both the thermodynamic (second virial coefficient- B_2) and hydrodynamic (frictional coefficient- ξ and partial specific volume- v_{sp}) contributions. While the sign of k_D values indicate nature of protein-protein interactions in solution, its magnitude indicates the strength of these interactions. A positive k_D implies repulsive interactions, and a negative k_D implies attractive intermolecular interactions in solution only if B_2 is also negative. There is a small range of negative k_D values where interactions are repulsive in nature (where hydrodynamic contribution is larger than thermodynamic contribution resulting in a negative k_D).[33]

Figure 8a, shows a plot of k_D for DVD-Ig™ protein at varying pH and ionic strengths of 15 mM (solid line), and 50 mM (dashed line). At pH 5.0, k_D is positive (+5.00 mL/g) at 15 mM and become negative (-8.25 mL/g, B_2= -0.49 *10^{-5} mol.ml/g^2) at 50 mM ionic strength.

At all other pHs, k_D values are negative indicating attractive interactions, with maximum attractive interactions being at pH 6.5. The interactions become less attractive when the ionic strength is increased to 50 mM except at pH 6.1 where ionic strength has no effect. The k_D values were also measured for DVD-Ig™ protein at pH 6.5 as a function of ionic strengths (Figure 8b). At 5 mM (-83.95 mL/g) and 15 mM (-76.51 mL/g), k_D values are most negative indicating strong attractive interactions in solution. On increasing the ionic strength to 50 mM and 100 mM, k_D values decrease gradually (-42.25 mL/g and -30.95 mL/g, respectively) indicating decreased attractive interactions in solution.

4.7. Effect of Histidine and Phosphate Buffer

The effect of different buffer species (phosphate and histidine) on opalescence (Figure 9) and liquid-liquid phase separation was studied by measuring percent transmittance as a function of protein concentration at constant pH (6.5 ± 0.1) and constant ionic strength (15 mM). DVD-Ig™ protein samples prepared in sodium phosphate buffer exhibited very high solution opalescence in the concentration range of 25-90 mg/mL, indicated by percent transmittance recorded close to 0. However, on changing the buffer species to histidine, opalescence decreased significantly. Maximum opalescence was observed at a concentration around 60 mg/mL (percent transmittance ~ 80) and decreased above and below this concentration. To confirm the effect of specific ions resulting in increased solution opalescence, protein samples were prepared in histidine buffer with 1 mM ionic strength adjusted to 15 mM using sodium chloride. Opalescence measurements showed similar trend as for the phosphate buffer, where solution was highly opalescent in the concentration range of 25 to 75 mg/mL, and decreased as the concentration was increased.

Protein-protein interactions were also analyzed for DVD-Ig™ protein solutions prepared in phosphate, histidine and sodium chloride at pH 6.5 and 15 mM ionic strength by measuring interaction parameter, k_D. Figure 10 shows a plot of Mutual diffusion coefficient (D_m) against concentration for three different ions. Slopes are negative for all three ions indicating attractive interactions in solution. Slopes overlap for phosphate (k_D = -76.50 mL/g) and chloride ions (k_D = -76.20 mL/g); the magnitude of the attractive interactions is similar in the two solutions. For histidine solutions, slope is slightly less negative than phosphate and chloride, and k_D value is -61.45 mL/g.

Figure 11 shows a plot of temperature studies performed for DVD-Ig™ protein in phosphate and histidine buffers at 16 and 60 mg/mL. In phosphate buffer, 60 mg/mL solution shows very high opalescence even at 37 ˚C. Phase separation occurs at around 32 ˚C for 16 mg/mL protein solutions. In the presence of histidine buffer species, phase separation temperature curve overlaps for 16 mg/mL and 60 mg/mL solutions and phase separation occurs at around 20 ˚C.

5. Discussion

Recent literature on opalescence in monoclonal antibody formulations attributes high opalescence to liquid-liquid phase separation of proteins in solution[27, 29, 37] From Figure 1, high opalescence (low percent transmittance) is observed in the concentration range of 20-100 mg/mL and opalescence decreases at concentrations above and below this range,[37] a behavior similar to the concentration dependence observed in temperature-concentration phase diagram for LLPS.[17] Literature reports for phase separation in protein solutions show that the critical concentration (C_c) is dependent on the size of the molecule (globular proteins

versus mAb), while, critical temperature (T_c) depends on the solution conditions.[22] Wang et al., plotted a scaled coexistence curve (binodal curve of phase diagram) for three different proteins and hard-spheres.[30] Globular proteins, crystallins (MW ~ 20 kDa) and lysozyme (MW ~ 14 kDa) have narrow and symmetrical coexistence curves, similar to that for a hard sphere, while monoclonal antibody (MW ~ 150 kDa) exhibits a wider and asymmetrical coexistence curve due to its non-spherical shape and increased flexibility. Critical concentration for crystallins and lysozyme are 240 ± 10 mg/mL[21] and 230 ± 10 mg/mL[22], respectively, while for the mAb the critical concentration is a range of 50- 100 mg/mL.[29, 30, 37, 38] From Figure 1, DVD-Ig™ protein with a molecular weight of around 200 kDa has a coexistence curve wider (C_c is around 20 -100 mg/mL) than that reported for mAbs. From temperature studies (Figure 7), plot of percent transmittance against temperature shows steep decrease at 16 mg/mL while decrease was more gradual at 60 mg/mL indicating asymmetry of the coexistence curve at higher concentrations. This is consistent with the hypothesis that the width and asymmetry of coexistence curve (or concentration range in which solution exhibits opalescence and LLPS) increases as the size of the molecule increases. Therefore, bispecific antibody-like molecules, in general, will have a tendency to show a larger concentration range where they can phase separate, resulting in increased challenges to formulate physically stable products.

5.1. Confirmation of Liquid-Liquid Phase Separation

As described in the introduction, upon attaining thermodynamic equilibrium, chemical potential of the protein in two phases is equal, though their concentrations are different. At a fixed temperature, these two concentrations are the binodal points of the

binodal or the coexistence curve. Equilibrium studies were performed to determine the effect of initial protein concentrations, temperature and ionic strength on phase separation. From Figure 3, protein concentration in upper and lower phases of the phase separated sample remains constant irrespective of the initial protein concentration; i.e chemical potential of the protein is same in the two phases, while their volumes are different. Similar results have been reported in the literature for mAbs, confirming that LLPS is an equilibrium process.[27] Figure 4 shows the effect of temperature and ionic strength on phase separation. At 15 mM ionic strength, protein shows a higher tendency to phase separate (phase separation occurs at both 4 ˚C and 22 ˚C) than at 50 mM ionic strength (phase separation occurs only at 4 ˚C), which is in agreement with opalescence measurements (Figure 2), where high opalescence is recorded at 15 mM compared to 50 mM. On undergoing phase separation at 4 ˚C, 15 mM sample shows a lower concentration in protein-poor phase and higher concentration in protein-rich phase (0.8 mg/mL and 132.6 mg/mL, respectively) than the phase separated sample at 50 mM ionic strength (4.3 mg/mL and 124.2 mg/mL, respectively). Coexistence curve shifts to lower temperatures as the ionic strength is increased from 15 mM to 50 mM.

Phase separation in solution was confirmed by visually observing under microscope. Liquid-liquid phase separation is preceded by opalescent appearance of the solution.[39] Inside the coexistence curve and before phase separation occurs (kinetically controlled), both protein-rich and protein-poor phases coexist in solution, where protein rich-phase is dispersed in protein-poor phase. This results in multiple scattering of light from the solution, which makes it appear opalescent. On overcoming the kinetic barrier (either by nucleation and growth mechanism by metastable system or spinodal decomposition by unstable system), due to the density difference between the two phases, protein-rich phase being denser settles

down forming the lower phase, while protein-poor phase forms the upper phase of the phase separated system. From Circular Dichroism studies (Figure 6a and 6b), it is confirmed that protein does not undergo any secondary or tertiary structural changes (structural change if any is reversible in dilute solution) on undergoing phase separation indicating that protein retains its native conformation.

5.2. Protein-Protein Interactions Resulting in LLPS

Attractive interactions in protein solution could be due to the presence of electrostatic charge, dipole moments in macromolecules (charge-dipole, charge–induced dipole, and van der Waals forces) and/or the hydrophobic patches on the surface of the protein (hydrophobic interactions).[37, 40, 41] Apart from these classical, non-covalent interactions in solutions, there may be specific interactions pertaining to surface amino acid residues including cation-π interactions.[42, 43] These specific interactions can be modulated by certain amino acid excipients and organic buffers and have been reported to affect the structural stability of the proteins in solution.[44]

Liquid-liquid coexistence curve shifts to upper or lower temperatures with changes in the pH or ionic strength of the solution, indicating increase or decrease in attractive interactions.[22, 23, 26, 36] Extensive work has been carried out for determination of colloidal stability by assessing shifts in the coexistence curve of protein solutions using PEG-induced LLPS.[45-49] Mechanism by which PEG increases attractive interactions between protein molecules is by preferential exclusion/ depletion forces; however, it is also known to bind to proteins and/or buffer and salt species in solution resulting in uncertainties in LLPS determination.[50] In our previous study, we have shown that the opalescence measured as a

function of temperature for a monoclonal antibody solution is a better measure of interactions in solution than that measured at ~25 °C using routine techniques.[37] In the current study, interactions measured in dilute solution by light scattering (Figure 8a) were correlated to shifts in T_{cloud} (Table 1) at fixed concentrations (16 and 60 mg/mL); a low T_{cloud} value indicates weak attractive interactions in solution, or a physically stable product, while high T_{cloud} values or shift to higher temperatures indicate increased attractive interactions in solution.

At pH 5.0, which is away from the pI (~7.0 – 7.5), molecules carry a high net charge resulting in repulsive interactions at low ionic strength as indicted by a positive k_D (+5.00 mL/gm). On increasing the ionic strength to 50 mM, charge shielding occurs resulting in a decrease in net repulsive interactions, therefore, the net interactions become attractive (k_D= -8.25 mL/gm, B_2=-0.49*10^{-5} mol.mL/g^2). At pH 5.0, T_{cloud} could not be determined at studied temperature at any of the conditions as phase separation may be occurring at temperature below 3 °C. The presence of repulsive or weak attractive interactions in solution correlates well with the absence of phase separation and opalescence at this pH.

From light scattering measurements, ionic strength has no effect on attractive interactions at pH 6.1. T_{cloud} is nearly constant (10˚C and 10.5 ˚C) at both 16 and 60 mg/mL at 15 mM ionic strength. At 50 mM, T_{cloud} shifts to a higher temperature; however the shift at 60 mg/mL (6 ˚C) is more significant than at 16 mg/mL (2 ˚C), indicating that increasing the ionic strength increases the attractive interactions more at higher concentrations. Hydrophobic interactions are the only short range attractive interactions that are not affected by changing the ionic strength of the solution at low salt concentrations. These interactions become relatively stronger on increasing the ionic strength due to preferential exclusion of

salts from the vicinity of the proteins. Even though these interactions are present in dilute solution, they become dominant as protein concentration increases. Both, light scattering and T_{cloud} measurements at pH 6.1 suggest the presence of attractive hydrophobic interactions in solution which results in phase separation at this condition.

Interactions measured at pH 6.5 as a function of ionic strength using light scattering (Figure 8b) and T_{cloud} measurements (Figure 7), indicate the presence of strong attractive interactions at low ionic strength, which decrease on increasing the ionic strength from 5 mM to 100 mM. Closer to the pI of the molecule, net charge on the protein decreases; high attractive interactions at low ionic strength may be due to dipole on the molecule. Similar trend is observed at pH 7.0 and 8.0, i.e. attractive interactions decrease as ionic strength is increased from 15 mM to 50 mM. Charge-dipole or charge-induced dipole and van der Waals interactions (London, Debye and Keesom) arise due to the presence of dipoles and multipoles on the protein molecule and have been previously reported to increase viscosity[51] and opalescence for mAb solutions.[37] At pI, though the net charge on the protein is minimal, a protein molecule carries large number of positive and negative charges. Asymmetric distribution of these charges on the protein surface produces a dipole which leads to increased protein-protein attractive interactions in the solution. DVD-Ig™ protein has an increased asymmetry in shape due to its additional variable domains, which would further enhance asymmetric charge distribution on the surface of the protein as compared to a mAb, which results in increased tendency to exhibit opalescence and phase separation at low ionic strength conditions. These dipoles are shielded on increasing the ionic strength resulting in a net decrease in attractive interactions. This dipole-shielding effect is more prominent at pH closer to the pI of the molecule.

Close to the pI of the molecule, the trend observed for opalescence measured at 25 °C, (Figure 2) and at 60 mg/mL correlates fairly well with Light scattering and T_{cloud} measurements; maximum opalescence is seen at an ionic strength of 15 mM and decreases on increasing the ionic strength. Similarly, interactions are strongly attractive at 15 mM and become less attractive at 50 mM ionic strength. Away from the pI, at pH 5.0 where interactions are repulsive in nature (from light scattering and absence of phase separation), there is no opalescence in solutions. However there is discrepancy at pH 6.1, where solution exhibits a low opalescence at both ionic strengths while significant attractive interactions are present in the solution. From Figure 2, high opalescence was observed at pH 6.5, 7.0 and 8.0, where phosphate buffers are used, while opalescence decreased at pH 6.1, which uses histidine buffer. Therefore, the effect of different buffer species on opalescence was investigated.

5.3. Effect of Different Buffer Species

Effect of phosphate and histidine buffer species was studied at a constant pH (6.5) and constant ionic strength (15 mM). As observed from Figure 9, solution exhibited high opalescence in phosphate buffer which decreased when buffer was changed to histidine. Opalescence measurements with sodium chloride confirmed that cationic histidine species reduces solution opalescence. The pI of the molecule is around pH 7.0. At pH 6.5, the molecule should have a slight net positive charge. Ideally, the protein properties should be more impacted by oppositely charged anions than similarly charged cations. For cationic histidine species to exert its effect, it must be specifically interacting with certain amino acids on the protein surface resulting in reduced opalescence. From light scattering measurements,

interactions are highly attractive at all three conditions (Figure 10), however, k_D values are highly negative and equal for both phosphate and sodium chloride and become less negative in the presence of histidine buffer. From temperature studies (Figure 11), T_{cloud} is high for the protein in phosphate buffer at both the concentrations and shifts to lower temperatures in histidine buffer, indicating reduced attractive protein-protein interactions and confirming specific binding of histidine with the protein in solution.

Histidine has been reported to improve physical stability of high concentration mAb formulations and also reduce its viscosity.[52] Histidine is a basic amino acid with ionizable imidazole moiety (pKa ~ 6.0) in its side chain; pKa of the amino acid varies from ~6.0-6.5 depending on the neighboring moieties. Interactions of histidine with other amino acids depend on its protonated-deprotonated state which varies with solution pH. Interactions of the positively charged imidazole group with amino acid on protein surface may be the possible mechanism by which it reduces protein-protein interactions and hence opalescence in solution. The mechanisms by which histidine interacts with other amino acids include, cation-π interaction, π-π stacking interaction, hydrogen-π interaction, coordinate bond interaction, hydrogen bond interaction.[43] Katayama and coworkers attributed reduced aggregation of Interferon-tau in histidine buffer relative to phosphate buffer to binding of histidine to the native state thereby stabilizing it.[53] Similar effect was observed by Salinas and coworkers on reduced fragmentation of mAb in histidine buffer compared to phosphate buffer due to (weak) preferential binding of histidine with mAb.[54]

Phosphate is a strong kosmotrope in the Hofmeister series and increases conformational stability of the proteins while decreasing its solubility in solutions.[55] Phosphate is strongly hydrated with high charge density and is known to stabilize proteins

(increase its precipitation tendency) by acting as water structure maker. The mechanisms by which phosphate and histidine buffers act are different and hence exert different effect on solution opalescence; phosphate increases opalescence by salting-out mechanism while histidine specifically interacts with amino groups on protein surface and reduce solution opalescence. Though, the magnitude of the change in opalescence on switching from phosphate to histidine buffer is quite significant (Figure 9); samples at both buffer conditions will undergo phase separation on storage at refrigerated conditions (4 ˚C), indicating loss of physical stability of the solution. Opalescence in solution is due to scattering of light and can be attributed to presence aggregates in solution or liquid-liquid phase separation (LLPS).[37] Opalescence measurements are usually conducted at room temperature/25 °C, however tendency to phase separate is higher as the temperature is lowered. These results strongly suggest that T_{cloud} may serve as a better indicator of possible phase separation in solutions than opalescence measurement (as results may be interpreted as false positive) and can be used as an orthogonal technique along with light scattering to screen excipients and salts to determine protein-protein interactions and develop a robust protein formulation. Both these techniques can be easily optimized for high-throughput analysis; hence is of great significance especially for preformulation candidate selection, where only small amount of material is available.

6. Conclusion

Liquid-liquid phase separation is of great significance for formulation development from both pharmaceutical and physiological point of view. LLPS is a thermodynamic process and protein does not undergo structural changes on phase separation. Mechanism by which

different buffers (or excipients) interacts with proteins and influence its physicochemical properties is different and hence determining the nature of specific and non-specific protein-protein interactions is of utmost significance. Strong attractive interactions are observed in systems exhibiting liquid-liquid phase separation; presence of hydrophobic interactions in addition to dipolar interactions results in liquid-liquid phase separation for DVD-Ig^{TM} protein solutions. The measured values of T_{cloud} and k_D are dependent on the solution conditions (pH, ionic strength and buffer species) confirming that T_{cloud} can be utilized as a predictive tool in preformulation devolvement.

7. Acknowledgments

Authors would like to thank AbbVie Bioresearch Center, Worcester, MA for material and financial support for the work and Dr. Ravi Chari and Dr. Michael Siedler for scientific discussions.

8. References

1. Gu, J.; Ghayur, T. Generation of dual-variable-domain immunoglobulin molecules for dual-specific targeting. *Methods Enzymol* **2012,** *502*, 25-41.
2. Kontermann, R. E. Dual targeting strategies with bispecific antibodies. *mAbs* **2012,** *4*, (2), 182-97.
3. Chang, B. S.; Hershenson, S. Practical approaches to protein formulation development. *Pharmaceutical biotechnology* **2002,** *13*, 1-25.
4. Harris RJ, S. S., Winter C. . Commercial Manufacturing Scale Formulation and Analytical Characterization of Therapeutic Recombinant Antibodies. *Drug Dev Res* **2004,** *61*, 137–154.
5. Daugherty, A. L.; Mrsny, R. J. Formulation and delivery issues for monoclonal antibody therapeutics. *Advanced drug delivery reviews* **2006,** *58*, (5-6), 686-706.
6. Manning, M. C.; Chou, D. K.; Murphy, B. M.; Payne, R. W.; Katayama, D. S. Stability of protein pharmaceuticals: an update. *Pharmaceutical research* **2010,** *27*, (4), 544-75.
7. Saluja, A.; Kalonia, D. S. Nature and consequences of protein-protein interactions in high protein concentration solutions. *International journal of pharmaceutics* **2008,** *358*, (1-2), 1-15.
8. Goswami, S.; Wang, W.; Arakawa, T.; Ohtake, S. Developments and Challenges for mAb-Based Therapeutics. *Antibodies* **2013,** *2*, (3), 452-500.
9. Vekilov, P. G. Phase transitions of folded proteins. *Soft matter* **2010,** *6*, (21), 5254-5272.
10. Pande, A.; Pande, J.; Asherie, N.; Lomakin, A.; Ogun, O.; King, J.; Benedek, G. B. Crystal cataracts: human genetic cataract caused by protein crystallization. *Proceedings of the National Academy of Sciences of the United States of America* **2001,** *98*, (11), 6116-20.
11. Eaton, W. A.; Hofrichter, J. Sickle cell hemoglobin polymerization. *Advances in protein chemistry* **1990,** *40*, 63-279.
12. Johnson, H. R.; Lenhoff, A. M. Characterization and suitability of therapeutic antibody dense phases for subcutaneous delivery. *Molecular pharmaceutics* **2013,** *10*, (10), 3582-91.
13. Dumetz, A. C.; Chockla, A. M.; Kaler, E. W.; Lenhoff, A. M. Protein phase behavior in aqueous solutions: crystallization, liquid-liquid phase separation, gels, and aggregates. *Biophysical journal* **2008,** *94*, (2), 570-83.
14. Shire, S. J.; Shahrokh, Z.; Liu, J. Challenges in the development of high protein concentration formulations. *Journal of pharmaceutical sciences* **2004,** *93*, (6), 1390-402.
15. Rosenbaum, D. F.; Zukoski, C. F. Protein interactions and crystallization. *Journal of Crystal Growth* **1996,** *169*, (4), 752-758.
16. D. Beysens, J. S., and D.J. Turner,, *Phase Transition and Near Critical Phenomena,*. Springer,: Berlin, 1987.
17. Van Dijk M.A, W. A., *Polymer Thermodynamics Library;*. Technomic Publishing Company: Pennyslyvania, 1997; Vol. 2, p 205.
18. P., A., *Atkin's Physical Chemistry*. 8 ed.; Oxford University Press: 2006.

19. Vekilov, P. G.; Feeling-Taylor, A. R.; Petsev, D. N.; Galkin, O.; Nagel, R. L.; Hirsch, R. E. Intermolecular interactions, nucleation, and thermodynamics of crystallization of hemoglobin C. *Biophysical journal* **2002,** *83*, (2), 1147-56.
20. Galkin, O.; Chen, K.; Nagel, R. L.; Hirsch, R. E.; Vekilov, P. G. Liquid-liquid separation in solutions of normal and sickle cell hemoglobin. *Proceedings of the National Academy of Sciences of the United States of America* **2002,** *99*, (13), 8479-83.
21. Thomson, J. A.; Schurtenberger, P.; Thurston, G. M.; Benedek, G. B. Binary liquid phase separation and critical phenomena in a protein/water solution. *Proceedings of the National Academy of Sciences of the United States of America* **1987,** *84*, (20), 7079-83.
22. Taratuta VG, H. A., Thurston GM, Blankschtein D, Benedek GB. Liquid–liquid phase separation of aqueou lysozyme solutions: Effects of pH and salt identity. *J Phys Chem* **1990,** *94*, 2140-2144.
23. Broide, M. L.; Berland, C. R.; Pande, J.; Ogun, O. O.; Benedek, G. B. Binary-liquid phase separation of lens protein solutions. *Proceedings of the National Academy of Sciences of the United States of America* **1991,** *88*, (13), 5660-4.
24. Manno, M.; Xiao, C.; Bulone, D.; Martorana, V.; San Biagio, P. L. Thermodynamic instability in supersaturated lysozyme solutions: effect of salt and role of concentration fluctuations. *Physical review. E, Statistical, nonlinear, and soft matter physics* **2003,** *68*, (1 Pt 1), 011904.
25. Wentzel, N.; Gunton, J. D. Liquid-liquid coexistence surface for lysozyme: role of salt type and salt concentration. *The journal of physical chemistry. B* **2007,** *111*, (6), 1478-81.
26. Mason, B. D.; Zhang-van Enk, J.; Zhang, L.; Remmele, R. L., Jr.; Zhang, J. Liquid-liquid phase separation of a monoclonal antibody and nonmonotonic influence of Hofmeister anions. *Biophysical journal* **2010,** *99*, (11), 3792-800.
27. Nishi, H.; Miyajima, M.; Nakagami, H.; Noda, M.; Uchiyama, S.; Fukui, K. Phase separation of an IgG1 antibody solution under a low ionic strength condition. *Pharmaceutical research* **2010,** *27*, (7), 1348-60.
28. Nishi, H.; Miyajima, M.; Wakiyama, N.; Kubota, K.; Hasegawa, J.; Uchiyama, S.; Fukui, K. Fc domain mediated self-association of an IgG1 monoclonal antibody under a low ionic strength condition. *Journal of bioscience and bioengineering* **2011,** *112*, (4), 326-32.
29. Mason, B. D.; Zhang, L.; Remmele, R. L., Jr.; Zhang, J. Opalescence of an IgG2 monoclonal antibody solution as it relates to liquid-liquid phase separation. *Journal of pharmaceutical sciences* **2011,** *100*, (11), 4587-96.
30. Wang, Y.; Lomakin, A.; Latypov, R. F.; Benedek, G. B. Phase separation in solutions of monoclonal antibodies and the effect of human serum albumin. *Proceedings of the National Academy of Sciences of the United States of America* **2011,** *108*, (40), 16606-11.
31. Trilisky, E.; Gillespie, R.; Osslund, T. D.; Vunnum, S. Crystallization and liquid-liquid phase separation of monoclonal antibodies and fc-fusion proteins: screening results. *Biotechnology progress* **2011,** *27*, (4), 1054-67.
32. Lewus, R. A.; Darcy, P. A.; Lenhoff, A. M.; Sandler, S. I. Interactions and phase behavior of a monoclonal antibody. *Biotechnology progress* **2011,** *27*, (1), 280-9.
33. Hiemenz, P. C.; Rajagopalan, R., *Principles of Colloid and Surface Chemistry, revised and expanded*. CRC Press: 1997; Vol. 14.

34. Asherie, N. Protein crystallization and phase diagrams. *Methods* **2004,** *34*, (3), 266-272.
35. Ishimoto, C.; Tanaka, T. Critical Behavior of a Binary Mixture of Protein and Salt Water. *Physical review letters* **1977,** *39*, (8), 474-477.
36. Broide, M.; Tominc, T.; Saxowsky, M. Using phase transitions to investigate the effect of salts on protein interactions. *Physical Review E* **1996,** *53*, (6), 6325-6335.
37. Raut, A. S.; Kalonia, D. S. Opalescence in Monoclonal Antibody Solutions and Its Correlation with Intermolecular Interactions in Dilute and Concentrated Solutions. *Journal of pharmaceutical sciences* **2015,** *104*, (4), 1263-1274.
38. Salinas, B. A.; Sathish, H. A.; Bishop, S. M.; Harn, N.; Carpenter, J. F.; Randolph, T. W. Understanding and modulating opalescence and viscosity in a monoclonal antibody formulation. *Journal of pharmaceutical sciences* **2010,** *99*, (1), 82-93.
39. Galkin, O.; Vekilov, P. G. Control of protein crystal nucleation around the metastable liquid–liquid phase boundary. *Proceedings of the National Academy of Sciences* **2000,** *97*, (12), 6277-6281.
40. Laue, T. Proximity energies: a framework for understanding concentrated solutions. *Journal of molecular recognition : JMR* **2012,** *25*, (3), 165-73.
41. Israelachvili, J. N., *Intermolecular and Surface Forces* Third ed.; Academic Press: San Diego, 2011.
42. Crowley, P. B.; Golovin, A. Cation–π interactions in protein–protein interfaces. *Proteins: Structure, Function, and Bioinformatics* **2005,** *59*, (2), 231-239.
43. Mahadevi, A. S.; Sastry, G. N. Cation-pi interaction: its role and relevance in chemistry, biology, and material science. *Chemical reviews* **2013,** *113*, (3), 2100-38.
44. Falconer, R. J.; Chan, C.; Hughes, K.; Munro, T. P. Stabilization of a monoclonal antibody during purification and formulation by addition of basic amino acid excipients. *Journal of Chemical Technology & Biotechnology* **2011,** *86*, (7), 942-948.
45. Annunziata, O.; Asherie, N.; Lomakin, A.; Pande, J.; Ogun, O.; Benedek, G. B. Effect of polyethylene glycol on the liquid-liquid phase transition in aqueous protein solutions. *Proceedings of the National Academy of Sciences of the United States of America* **2002,** *99*, (22), 14165-70.
46. Wang, Y.; Annunziata, O. Comparison between protein-polyethylene glycol (PEG) interactions and the effect of PEG on protein-protein interactions using the liquid-liquid phase transition. *The journal of physical chemistry. B* **2007,** *111*, (5), 1222-30.
47. Wang, Y.; Lomakin, A.; Latypov, R. F.; Laubach, J. P.; Hideshima, T.; Richardson, P. G.; Munshi, N. C.; Anderson, K. C.; Benedek, G. B. Phase transitions in human IgG solutions. *J Chem Phys* **2013,** *139*, (12), 121904.
48. Wang, Y.; Latypov, R. F.; Lomakin, A.; Meyer, J. A.; Kerwin, B. A.; Vunnum, S.; Benedek, G. B. Quantitative evaluation of colloidal stability of antibody solutions using PEG-induced liquid-liquid phase separation. *Molecular pharmaceutics* **2014,** *11*, (5), 1391-402.
49. Jion, A. I.; Goh, L. T.; Oh, S. K. Crystallization of IgG1 by mapping its liquid-liquid phase separation curves. *Biotechnology and bioengineering* **2006,** *95*, (5), 911-8.
50. Bloustine, J.; Virmani, T.; Thurston, G. M.; Fraden, S. Light Scattering and Phase Behavior of Lysozyme-Poly(Ethylene Glycol) Mixtures. *Physical review letters* **2006,** *96*, (8), 087803.

51. Yadav, S.; Liu, J.; Shire, S. J.; Kalonia, D. S. Specific interactions in high concentration antibody solutions resulting in high viscosity. *Journal of pharmaceutical sciences* **2010,** *99*, (3), 1152-68.
52. Chen, B.; Bautista, R.; Yu, K.; Zapata, G. A.; Mulkerrin, M. G.; Chamow, S. M. Influence of histidine on the stability and physical properties of a fully human antibody in aqueous and solid forms. *Pharmaceutical research* **2003,** *20*, (12), 1952-60.
53. Katayama, D. S.; Nayar, R.; Chou, D. K.; Valente, J. J.; Cooper, J.; Henry, C. S.; Vander Velde, D. G.; Villarete, L.; Liu, C. P.; Manning, M. C. Effect of buffer species on the thermally induced aggregation of interferon-tau. *Journal of pharmaceutical sciences* **2006,** *95*, (6), 1212-26.
54. Salinas, B. A.; Sathish, H. A.; Shah, A. U.; Carpenter, J. F.; Randolph, T. W. Buffer-dependent fragmentation of a humanized full-length monoclonal antibody. *Journal of pharmaceutical sciences* **2010,** *99*, (7), 2962-2974.
55. Zhang, Y.; Cremer, P. S. Interactions between macromolecules and ions: the Hofmeister series. *Current opinion in chemical biology* **2006,** *10*, (6), 658-663.

9. Tables and Figures

Table 1: T_{cloud} (determined as temperature where transmittance is 70%) for DVD-Ig™ as a function of solution conditions. (IS= Ionic strength).

	T_{cloud} (˚C)			
	IS =15 mM		**IS =50 mM**	
pH	**16 mg/mL**	**60 mg/mL**	**16 mg/mL**	**60 mg/mL**
5.0	< 3.0	< 3.0	< 3.0	< 3.0
6.1	10.0 ± 0.0	10.3 ± 0.4	12.0 ± 0.0	15.8 ± 0.4
6.5	33.0 ± 0.7	> 37.0	19.3 ± 0.00	24.5 ± 0.0
7.0	-	-	21.0 ± 0.0	25.0 ± 0.0
8.0	27.5 ± 0.0	32.5 ± 0.0	15.5 ± 0.0	19.5 ± 0.0

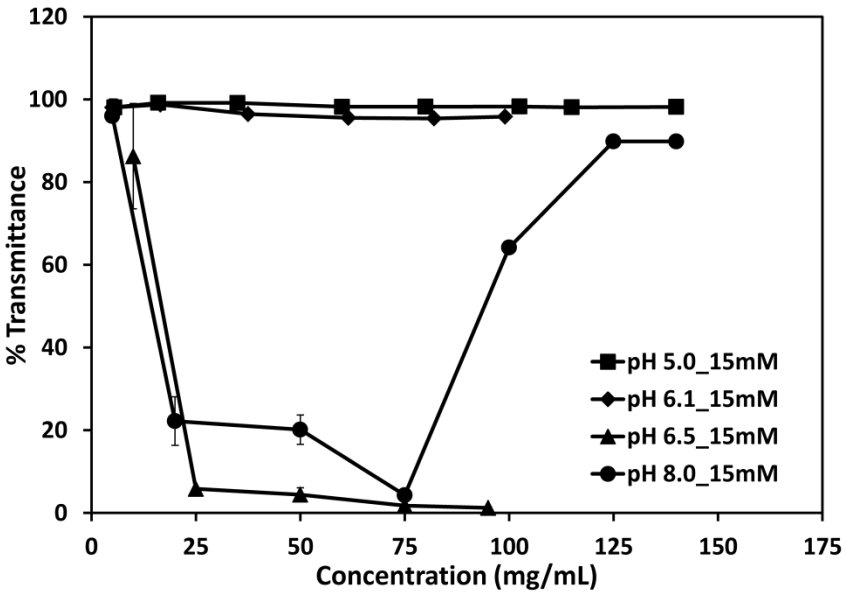

Figure 1: Percent transmittance for DVD-Ig™ protein as a function of protein concentration at various solution pH (pH 5.1- acetate, pH 6.1-histidine, pH 6.5-phosphate, pH 7.0-phosphate, pH 8.0-phosphate) and at ionic strength of 15 mM. All solutions were analyzed at 25 ± 1˚C in duplicate. Error bars if not visible are smaller than the symbols used.

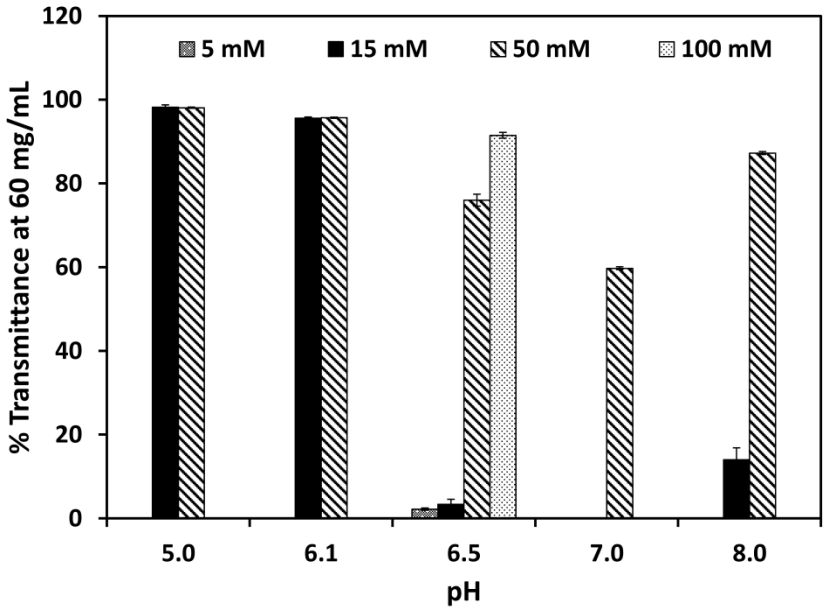

Figure 2: Percent transmittance for DVD-Ig™ protein at 60 mg/mL as a function of pH and ionic strength. Ionic strength of 15 and 50 mM were analyzed at pH 5.0, 6.1 and 8.0, while only 50 mM was analyzed at pH 7.0. Ionic strength of 5, 15, 50 and 100 mM were studied at pH 6.5. 5 and 15 mM ionic strengths were maintained by preparing solutions with appropriate buffer strength. Sodium chloride was added to adjust ionic strength to 50 and 100 mM. All solutions were analyzed at 25 ± 1˚C in duplicate.

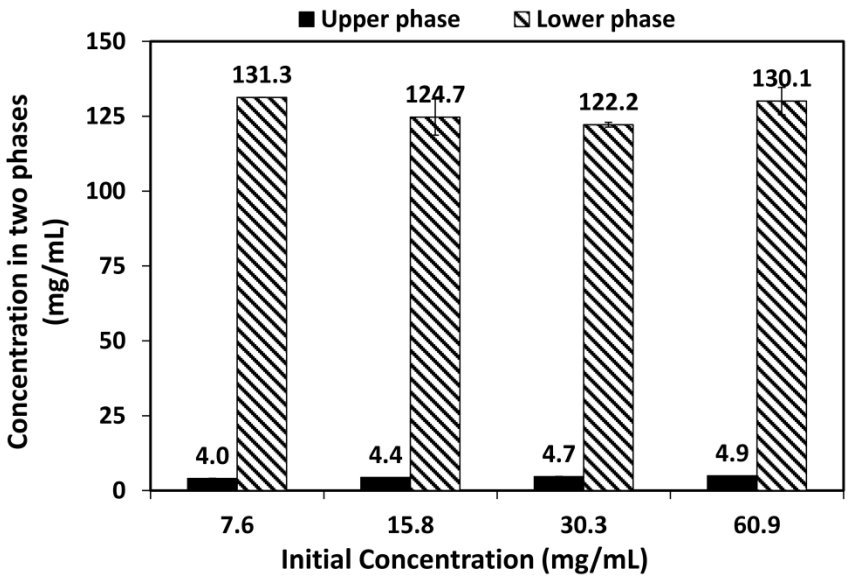

Figure 3: Effect of the initial concentration of DVD-Ig^{TM} protein before phase separation on the protein concentrations of the protein-rich phase (dashed bars) and protein-poor phase (closed bars) at 4°C in sodium phosphate solution at pH 6.5 with ionic strength of 50 mM. Numbers over the bars represent the concentration of each phase. Ionic strength was maintained by appropriately diluting sodium phosphate stock with ionic strength of 150 mM. All solutions were analyzed in duplicate.

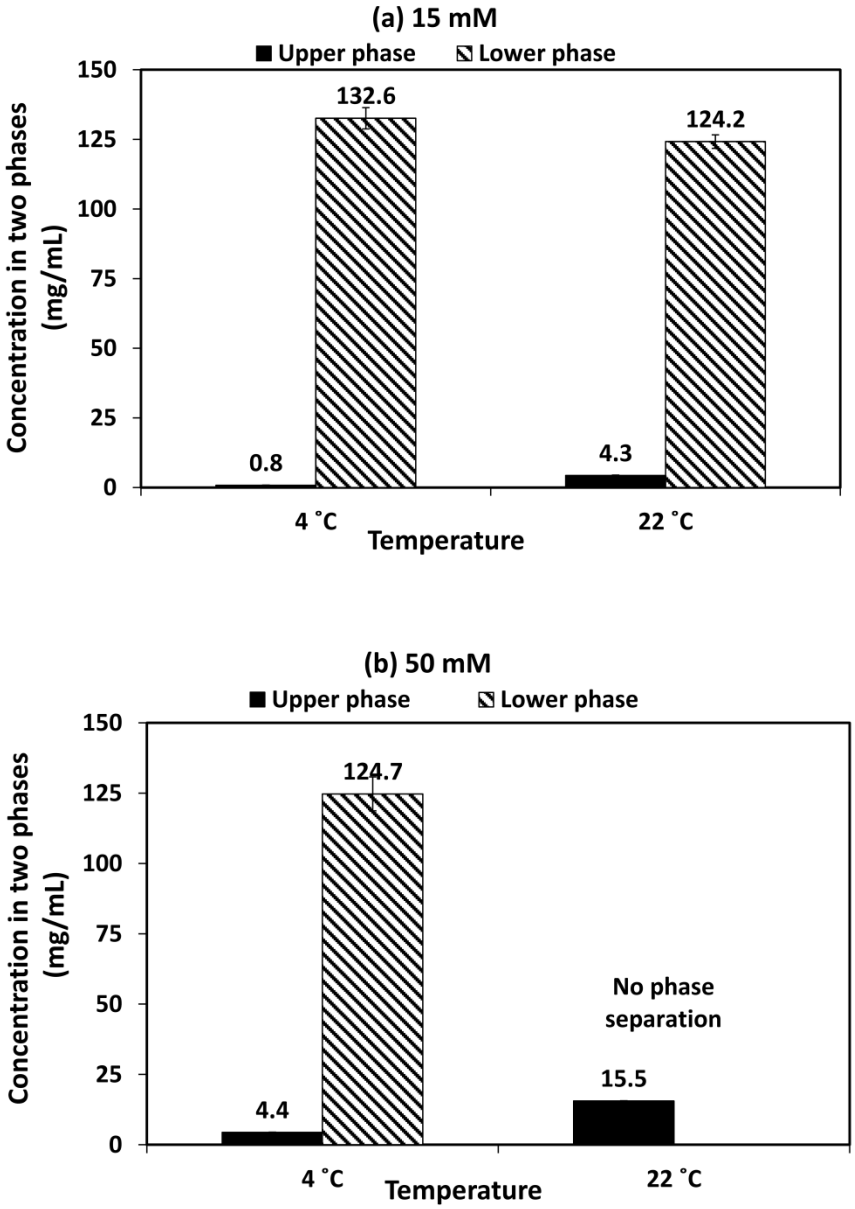

Figure 4: Effect of the temperature on initial concentration of DVD-Ig™ protein on undergoing liquid-liquid phase separation at (a) 15 mM and (b) 50 mM. Initial protein concentration was maintained at 16 mg/mL. Numbers over the bars represent the concentration of each phase. Ionic strength was maintained by appropriately diluting sodium phosphate stock with ionic strength of 150 mM. All solutions were analyzed in duplicate.

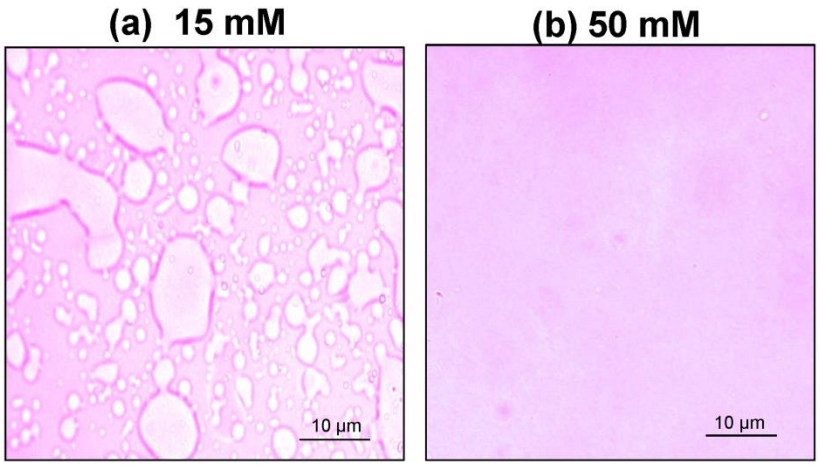

Figure 5: LLPS for DVD-Ig™ protein observed under Polarized Light Microscope (100x magnification) for 16 mg/mL solution at pH 6.5 and at room temperature (23 ± 1 ˚C). Ionic strength was maintained by appropriately diluting sodium phosphate stock solution with ionic strength of 150 mM.

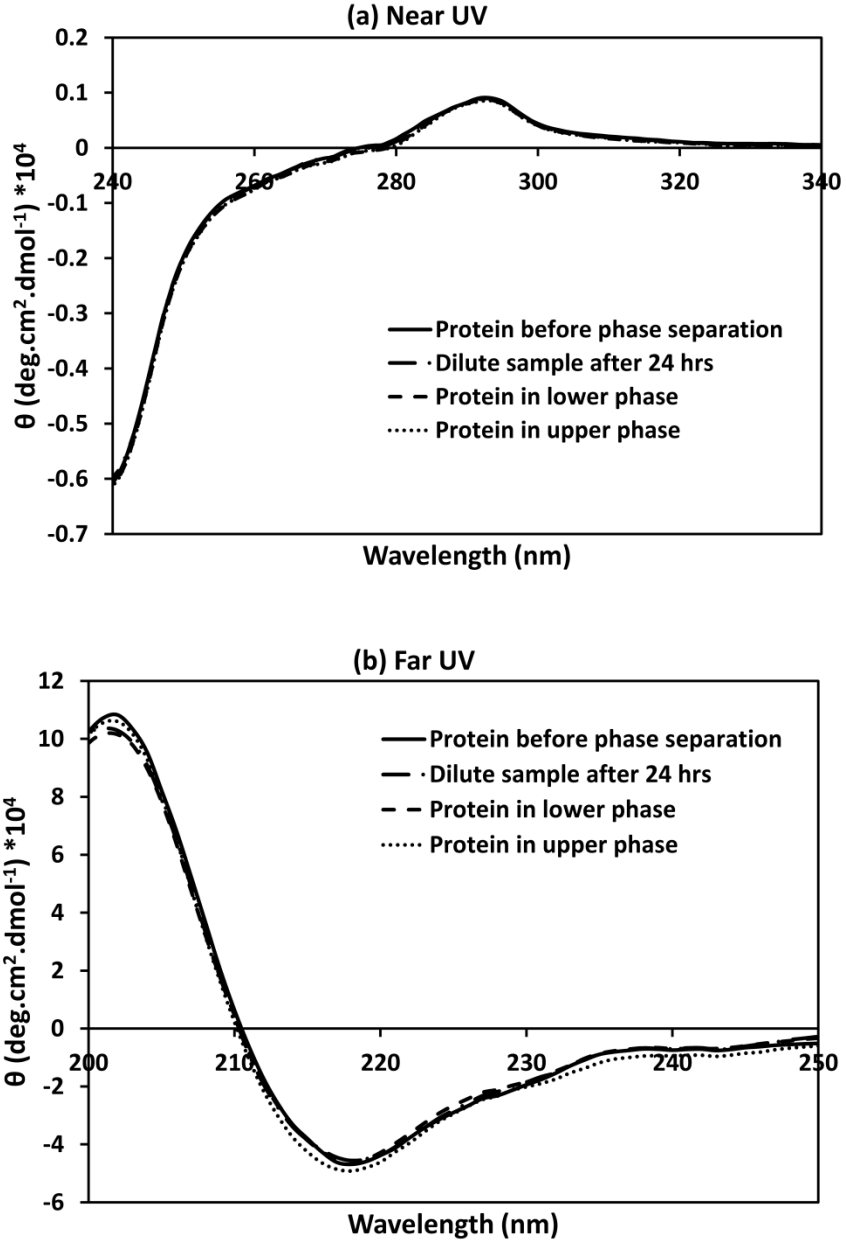

Figure 6: (a) Near-UV and (b) far-UV circular dichroism spectra of DVD-Ig^{TM} protein at pH 6.5 at 15 mM ionic strength (Phosphate buffer) before phase separation (solid line), and after phase separation in protein-rich phase (dotted line) and protein-poor phase (dashed line). The ellipticity is represented as molar ellipticity. All solutions were analyzed at room temperature (23 ± 1˚C).

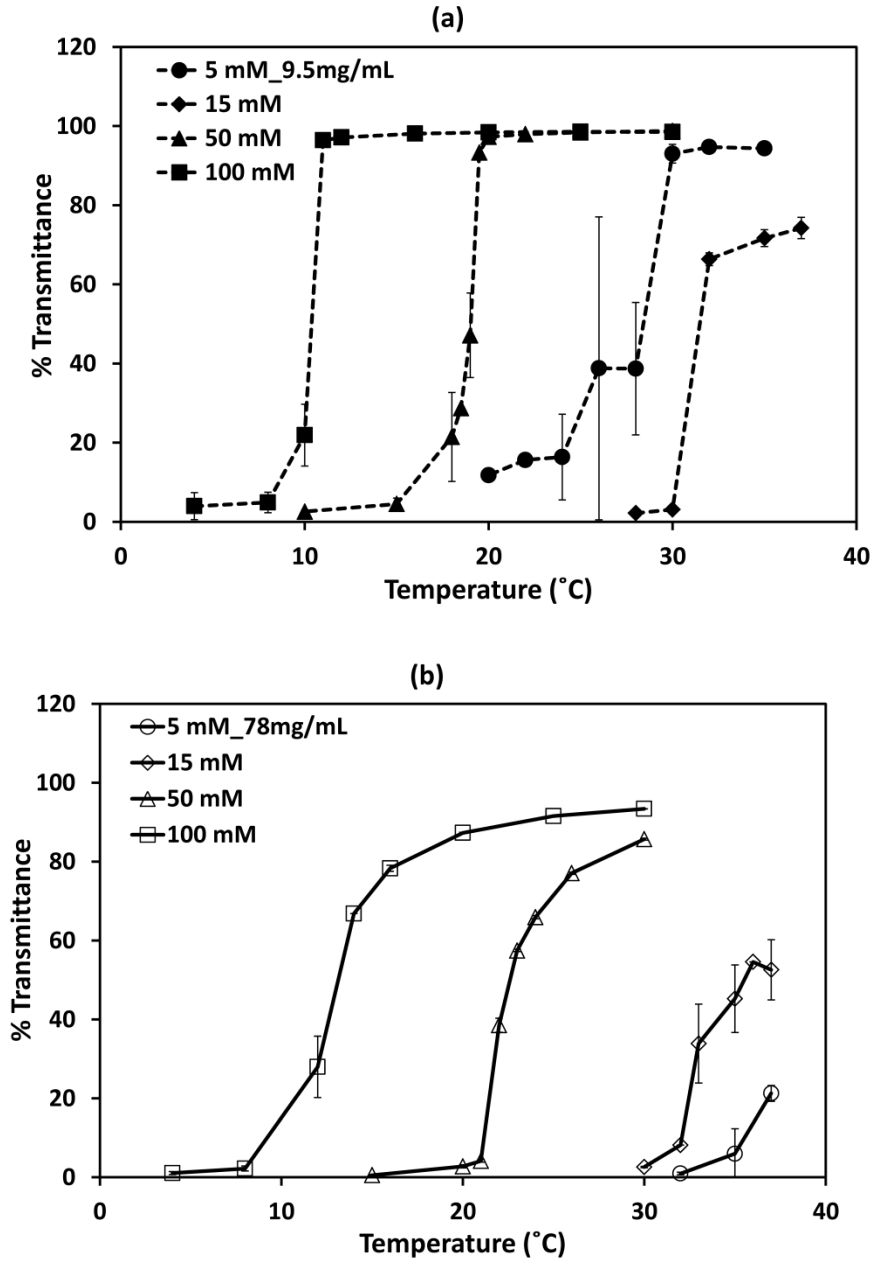

Figure 7: Temperature ramp studies for DVD-Ig^{TM} protein as a function of ionic strength at pH 6.5 at concentrations of (a) 16 mg/mL and (b) 60 mg/mL. At 5 mM ionic strength low and high concentrations are 9.8 and 78 mg/mL respectively (represented by closed and open circles). Ionic strength of 5 and 15 mM were maintained by preparing phosphate solutions with appropriate buffer strength. Sodium chloride was added to maintain ionic strength of 50 and 100 mM. All solutions were analyzed in duplicate.

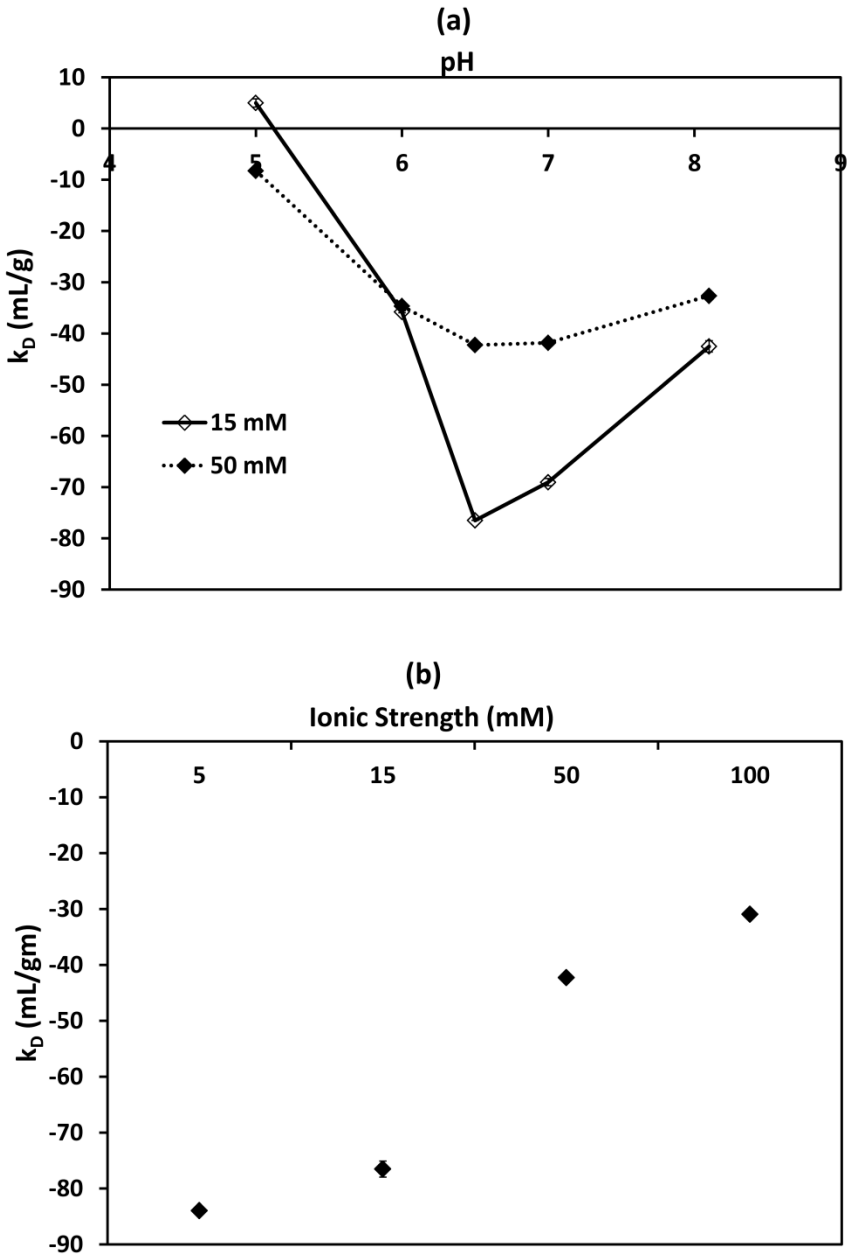

Figure 8: Plot of k_D obtained from Dynamic light scattering as a function of (a) pH (pH 5.1-acetate, pH 6.1-histidine, pH 6.5-phosphate, pH 7.0-phosphate, pH 8.0-phosphate) and at ionic strengths of 15 mM (solid line) and 50 mM (dotted line) and (b) varying ionic strengths at pH 6.5. All solutions were analyzed at 25 ± 1˚C in duplicate. Error bars if not visible are smaller than the symbols used.

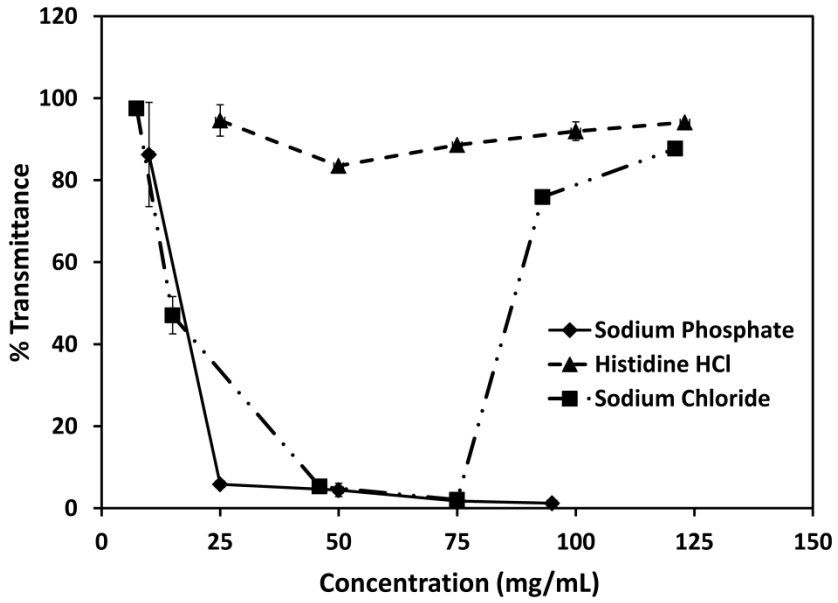

Figure 9: Percent transmittance for DVD-Ig™ protein as a function of different salt/buffer, sodium phosphate (♦), histidine hydrochloride (▲) and sodium chloride (■),at pH 6.5 and ionic strength of 15 mM. All solutions were analyzed at 25 ± 1˚C in duplicate. Error bars if not visible are smaller than the symbols used

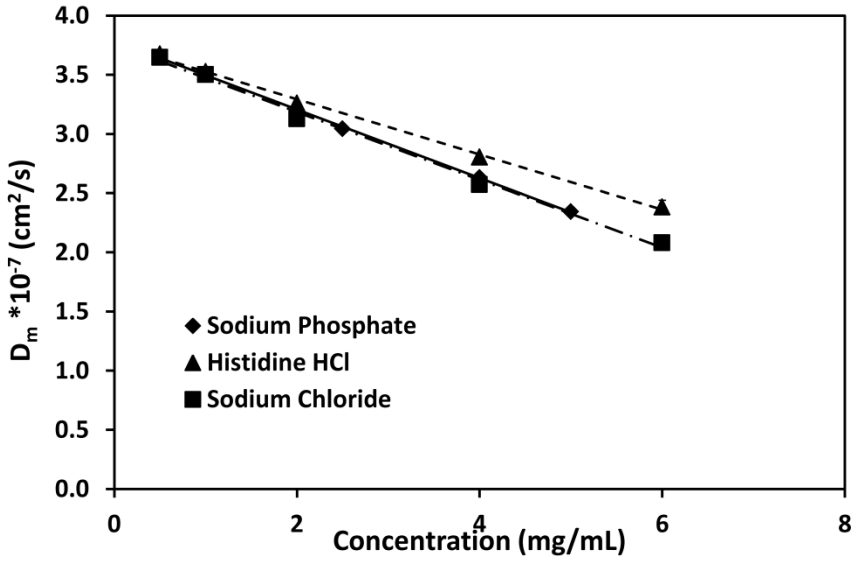

Figure 10: D_m plot for DVD-Ig^{TM} protein as a function of different salt/buffer, sodium phosphate (♦), histidine hydrochloride (▲) and sodium chloride (■), at pH 6.5 and ionic strength of 15 mM. All solutions were analyzed at 25 ± 1˚C in duplicate. Error bars if not visible are smaller than the symbols used.

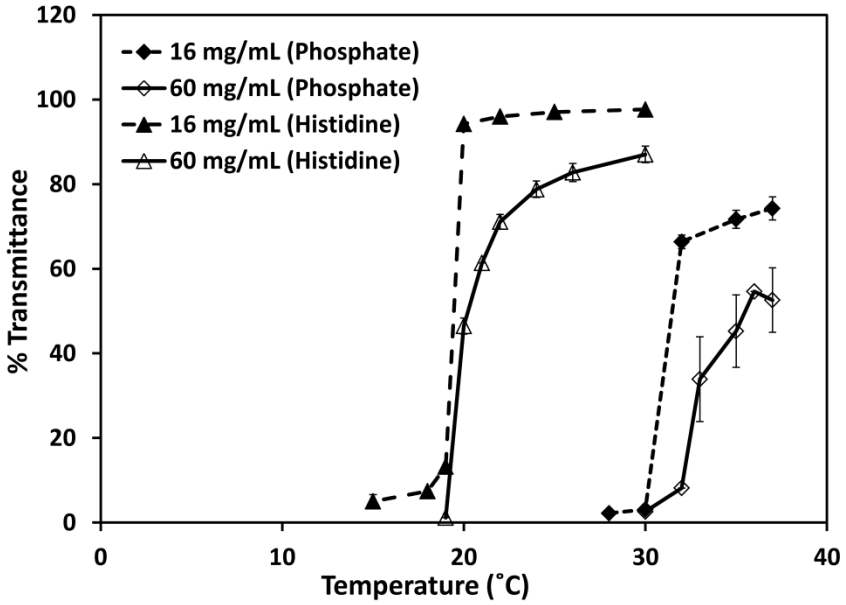

Figure 11: Temperature ramp studies for DVD-Ig™ protein at 16 mg/mL (dashed line) and 60 mg/mL (solid line) in 15 mM ionic strength Histidine (▲) and Phosphate (♦) buffers.

Chapter 5

Effect of Excipients on Liquid-Liquid Phase Separation and Aggregation in Dual Variable Domain Immunoglobulin Protein Solutions

Contents

Chapter 5

1. Abstract

Liquid-liquid phase separation (LLPS) and aggregation can reduce the physical stability of therapeutic protein formulations. On undergoing LLPS, the protein-rich phase can promote aggregation during storage due to high concentration of the protein. Effects of different excipients on aggregation in protein solution is well documented, however data on the effect of excipients on LLPS is scarce in the literature. In this study, the effect of three excipients (PEG 400, Tween 80 and Sucrose) on liquid-liquid phase separation and aggregation in a Dual variable domain immunoglobulin protein (DVD-Ig^{TM}) solution was investigated. Sucrose suppressed both LLPS and aggregation, Tween 80 had no effect on either and PEG 400 increased LLPS and aggregation. However, the mechanism by which these excipients exert positive or negative effect on LLPS and aggregation varies. Results indicate that, LLPS and aggregation are highly temperature dependent; at low temperature protein exhibits LLPS, at high temperature protein exhibits aggregation and at an intermediate temperature both phenomena occur simultaneously depending on the solution conditions.

Keywords: liquid-liquid phase separation, aggregation, excipients, protein-protein interactions, physical stability, protein formulation, sucrose, PEG, temperature effects

2. Introduction

Formulation development of protein therapeutics aims to have efficacious products wherein the protein remains in solution and maintains stability across its shelf life. Phase separation and aggregate formation in protein solutions can compromise physical stability of the formulation.[1, 2] These solutions can exhibit solid-liquid phase separation resulting in the formation of either crystals or amorphous precipitate or a metastable liquid-liquid phase separation into a protein-rich and a protein-poor phase.[3-5] In either case, protein retains its native structure in the formulation and the decreased solubility is associated with the change in the chemical potential of the protein in solution or increased intermolecular interactions between the protein molecules. Aggregation on the other hand is associated both with native and/or non-native species and can be reversible or irreversible in nature.[6] Aggregates can result in reduced efficacy of the product and can elicit immunogenic response.[7] Aggregation of the therapeutic proteins has been extensively reported in the literature and readers are referred to some excellent reviews on aggregation pathways (physical and chemical)[8, 9] and kinetics[10] in solution, general terminologies associated with classification of aggregates[11] and assessment of aggregates[12-14] in protein solutions.[15, 16]

Excipients play a significant role in maintaining the physical stability of protein formulations.[17, 18] Depending on the concentration and nature, certain excipients can exert dual effect, e.g, preferentially excluded co-solutes increase the conformational stability of proteins in solution, while they can also promote phase separation (or reduced solubility) if the increase in the chemical potential of the protein in solution phase exceeds that in the solid phase.[19] Excipients exert their stabilizing effect by modulating protein-protein interactions in solution or by changing conformational stability. Sugars, polyols, polymers, salts,

surfactants, amino acids and their derivatives are some of the excipients used in therapeutic protein formulations to improve physical stability of the protein.[17, 18]

The three commonly used excipients PEG 400, Tween 80 and Sucrose were investigated for their effect on liquid-liquid phase separation (LLPS) and aggregation in DVD-Ig™ protein solution. PEG 400 is a macromolecular crowding agent and is a commonly used protein precipitant; it enhances conformational stability of proteins in solution by the preferential exclusion mechanism.[20] Extensive studies for PEG-induced LLPS are reported in the literature for therapeutic proteins including mAbs.[21-24] Tween 80 is a surfactant which competes with the protein to adsorb at the air-water interface, thereby, reducing its tendency to denature at the interface.[25-27] Sucrose is a widely used protein stabilizing excipient against thermal denaturation, which is preferentially excluded, and exerts its effect by increasing the surface tension of water.[28-31]

Though many reports in the literature highlight the effectiveness of Sucrose and Tween in reducing aggregation of the proteins in solution, to the best of our knowledge, there are no studies on the effect of these excipients on liquid-liquid phase separation in DVD-Ig™ protein solution. Therefore, the effect of Sucrose, PEG 400 and Tween 80 on aggregation and LLPS in DVD-Ig™ protein solution was studied. The purpose of the current study was (i) to understand the effect of excipients on LLPS and aggregation in DVD-Ig™ protein and (ii) to understand the relationship between LLPS and aggregate formation in DVD-Ig™ protein solution in the presence of the excipients and as a function of temperature.

3. Materials and Methods

3.1. Materials

All buffer reagents and chemicals used were of the highest purity grade and were obtained from commercial sources. Histidine base and histidine hydrochloride were purchased from Sigma (St. Louis, MO). Monobasic and dibasic sodium phosphate, sodium sulfate, Sucrose, Tween 80 and Polyethylene Glycol 400 were purchased from Fisher Scientific (Fair Lawn, New Jersey). Dual Variable Domain protein, DVD-Ig^{TM} (pI ~7.0-7.5) as 85 mg/mL solution in 15 mM Histidine buffer at pH 5.5 was supplied by Abbvie (Worcester, MA). Solutions were prepared with deionized water equivalent to Milli-Q^{TM}.

Histidine buffer was used to maintain pH at 6.6. Ionic strength of 15 mM was maintained by selecting appropriate buffer strength without addition of any salts. All the excipient stock solutions were prepared in Histidine buffer, filtered through 0.22 μm Millipore's Durapore membrane filters and then diluted down to the required concentrations with same buffer (Stock: 50% PEG 400, 40% Sucrose, 0.1% Tween 80). All antibody solutions were buffer exchanged with Histidine buffer using Millipore (Billerica, MA) Amicon Ultra centrifugation tubes with a molecular weight cutoff of 10 kDa obtained from Fisher Scientific. Concentrations of the samples were determined using a UV-vis spectrophotometer with an extinction coefficient of 1.5 $mg^{-1}/mL^{-1}cm^{-1}$ for DVD-Ig^{TM} protein at 280 nm for 0.1% (w/v) IgG solutions. The pH of all the above solutions was within ± 0.1 of the target values as measured by a Denver Instrument pH meter.

3.2. Accelerated Stability Studies

DVD-Ig™ protein samples with a concentration of 33 mg/mL were prepared in Histidine buffer, pH 6.6- 15 mM ionic strength and appropriate concentration of excipients was maintained (10% Sucrose, 10% PEG, 0.01% Tween). All the solutions were filtered through sterile 0.22 μm Millipore's Durapore membrane filters before incubation. 150 μL samples for each condition (in duplicate) were filled in sterile Fischerbrand (Fischer Scientific) 0.5 mL microcentrifuge tubes with loop and O-ring and incubated at 4 ˚C in refrigerator and at 20 ˚C and 40 ˚C in isotemp oven (Fischer Scientific). At the set time-points (7, 21 and 45 days), samples were brought to room temperature and thoroughly mixed. Appropriate amount of aliquot was withdrawn and diluted to around 2 mg/mL and then centrifuged at 6708×g for 5 min using an Eppendorf minispin (Hamburg, Germany). Supernatant was further diluted down to 1 mg/mL and directly filtered through 0.22 μm syringe filters into HPLC vials.

At 45 day time-point samples were also analyzed for structural changes by second-derivative fluorescence spectroscopy (0.2 mg/mL concentration at all conditions was analyzed; other steps are similar to that reported for Intrinsic fluorescence). A third set of samples was stored at 4 °C, which were analyzed for concentration of protein in protein-rich and protein-poor phase (to assess phase separation after 45 days).

3.3. HPLC-Size Exclusion Chromatography

Analysis of the stability samples was conducted using SEC-HPLC system with an inline UV detector set at 280 nm. A TSK G3000 SWXL gel filtration column (Tosoh Biosciences) was used for separation. 100 mM sodium phosphate buffer at pH 7 containing

200 mM sodium sulfate was used as mobile phase for elution. Flow rate was maintained at 0.3 mL/min and 10 μL of sample volume was injected into the system. HPLC analysis was also performed for samples before subjecting to stress conditions to determine monomer and aggregate content (labeled as t_0). Samples were collected and analyzed at 7 day, 21 day and 45 day. Chromatograms obtained were analyzed for percent of monomer, soluble aggregates and fragments using ChemStation software.

3.4. Intrinsic Fluorescence

Fluorescence spectra for protein–excipient samples were acquired using a Photon Technology International (PTI) 814 spectrofluorometer, equipped with a turreted 4-position Peltier-controlled cell holder. DVD-Ig^{TM} protein samples were prepared at a concentration of 0.2 mg/mL at pH 6.6 in Histdine buffer (15 mM ionic strength) keeping the excipient concentration constant. An excitation wavelength of 295 nm was used and the emission scans were recorded from 310 to 450 nm with a step size of 2 nm and a 1-s integration time. The excitation and emission slit width was set at 2 nm and eight emission spectra were collected and averaged to obtain the final spectrum. Sample volume of 60 μL was placed in 3 mm path length quartz cuvettes and measurements were made at 25 ˚C after equilibration for 2 min. Buffer peak was subtracted from each spectra and all the emission scans were normalized to 1.0 (FeliX32™ software, PTI) before obtaining second order derivative spectra for each solution condition.

3.5. Thermal Stability Studies

Onset of aggregation temperature for DVD-Ig^{TM} protein was determined from Malvern Instrument's Zetasizer Nano Series (Worcestershire, UK) at a wavelength of 632.8 nm and at 173˚. All samples were prepared in pH 6.6 histidine buffer with ionic strength of 15 mM and protein concentration was maintained at 34 mg/mL. Sample volume of 60 µL was placed in 3 mm path length quartz cuvettes and intensity and particle size of the sample was recorded from 30-60 °C in increments of 1 °C. All samples were allowed to equilibrate at each temperature for 2 min.

3.6. T_{cloud} Measurements

Temperature studies were performed using UV-Vis spectrophotometer attached with a temperature control peltier plate, where percent transmittance was recorded as temperature was lowered in steps from 35 ºC to 3 ˚C. 60 µL of samples were studied in 3 mm quartz cuvette and samples were allowed to equilibrate at each temperature for 2 min before recording the measurements. Onset of the liquid-liquid phase separation is characterized by a dramatic increase in solution turbidity; this temperature is marked as T_{cloud}. For current study, temperature at which percent transmittance is 70 is termed as T_{cloud}. Protein concentration of 16 mg/mL was analyzed for Sucrose, PEG and Tween 80. After addition of excipients to protein solutions, all the samples were allowed to equilibrate for 2 hours and filtered directly into the cuvette before making the measurement.

3.7. Dynamic Light Scattering (DLS)

DLS studies were performed using a Malvern Instrument's Zetasizer Nano Series at a wavelength of a 632.8 nm and at 173˚. All the buffers and sample stock solutions were filtered through 0.22 μm Millipore's Durapore membrane filters before making the dilution to required concentrations. Excipient concentration was kept constant and protein concentration was varied from 0.25 – 10 mg/mL for each set of measurements in duplicate. The protein and excipient solutions were then centrifuged using an Eppendorf minispin mini-centrifuge at 12,110×g for 5 min before every measurement. Light scattering measurements were made at 25 ± 0.1˚C. Linear plot of D_m against concentration was used to calculate self-diffusion coefficient (D_s) and interaction parameter (k_D) using following relation,

$$D_m = D_s(1 + k_D c) \quad (1)$$

c is the concentration of the protein (g/mL).[32]

4. Results and Discussions

4.1. Effect of Excipients on Aggregation

Formation of aggregates in protein solution compromises physical stability of the formulation and can also reduce its efficacy and safety. Determining or quantifying the amount of aggregates in solution in the presence of different excipients can help in optimizing the solution conditions to increase the shelf-life of the product. Mechanism by which different excipients exert their stabilizing/destabilizing effects on protein aggregation is thoroughly studied and reported in the literature.[17, 18] Figures 1 through 3 represents effect of different excipients on aggregation in DVD-Ig™ protein samples incubated at different temperatures over a period of 45 days.

4.1.1. Stability Studies at 4 ºC

Figure 1 show a plot of percent aggregation (Figure 1a) and fragmentation (Figure 1b) of DVD-Ig™ protein as a function of different excipients after 7, 21, and 45 days at 4 ˚C. Before the samples were subjected to stress conditions, a small amount of aggregate was present in the solution (t_0~ 1.5 %) as analyzed with SEC-HPLC at time t=0. No change in percent aggregate or fragmentation was observed after samples were incubated for 45 days.

4.1.2. Stability Studies at 20 ºC

Percent aggregates and fragmentation for DVD-Ig™ protein after incubation at 20 ˚C is plotted in Figure 2 at different time points. From Figure 2a, after 7 days, no change in aggregate content was observed in any of the samples (within experimental error). However, after 21 days, percent aggregates increased for DVD-Ig™ protein in the presence of PEG 400, which further increased for samples analyzed after 45 days. There was no change in aggregate content in the presence of other excipients. From Figure 2b, no fragmentation was observed at any of the conditions after incubation for 45 days.

4.1.3. Stability Studies at 40 ºC

Figure 3a and 3b shows a plot of percent aggregates and fragmentation, respectively, for DVD-Ig™ protein incubated with different excipients at 40 ˚C. From Figure 3a, percent aggregate shows an increase after 7 days compared to that analyzed at t=0, and increased significantly after 21 and 45 days at all the conditions. In the presence of PEG 400, percent aggregates increased significantly (by ~12%) after 7 days compared to protein samples in the presence of other excipients. However, the rate of aggregate formation decreased from day

21 to day 45. Amount of aggregates in the presence of Tween are almost similar to buffer (absence of excipients). Sucrose showed increased thermal stability as percent aggregate content was low than in buffer. Percent fragmentation (Figure 3b) for DVD-Ig^{TM} protein showed a significant increase at all the conditions after 45 days. For Tween and Sucrose, percent fragmentation is almost equal to that observed in the buffer at all the time points. However, for PEG, percent fragmentation increased significantly after 21 days and 45 days while aggregate formation remained nearly constant from 21 to 45 days.

4.1.4. Structural Changes

Intrinsic fluorescence and second derivative fluorescence spectroscopy[33, 34] studies were performed for DVD-Ig^{TM} protein in the presence and absence of excipients to determine tertiary structural changes after samples were incubated at 40 ºC for 45 days (Appendix 2). Fluorescence spectra were also recorded for freshly prepared DVD-Ig^{TM} protein samples at similar solution conditions. No shift in intensity or wavelength (blue shift or red shift) in the presence or absence of excipients was observed. Similarly, second derivative spectra did not show any change in the tertiary structure for samples at any of the conditions studied. Hydrophobic amino acids usually reside in the core of the protein (both in native and aggregated form) to reduce the free energy of the system and very few amino acids are present on protein surface. Small change in signal intensity due to minor structural perturbations (which may be reversible on diluting the sample) may not be sufficient to be detected by fluorescence spectroscopy for the samples that exhibited aggregation at high temperatures.

4.1.5. Thermal Stability

Figure 4 shows a plot for intensity of DVD-Ig^{TM} protein as a function of temperature to assess thermal stability in the presence and absence of excipients. Onset of aggregation in protein solution is marked by dramatic increase in intensity and size of the protein in solution.[35] The arrows in the Figure 5, indicate the onset of aggregation temperature for DVD-Ig^{TM} protein in the current study. T_{onset} in presence of buffer is 51.8°C and is in agreement with onset of aggregation value for DVD-Ig^{TM} protein in buffer reported in the literature.[36] In presence of PEG 400, T_{onset} decreases to 49.6°C indicating reduced thermal stability, while in presence of Sucrose, thermal stability increases as T_{onset} increases to 54 °C. There is no change in T_{onset} (51.6°C) in presence of Tween 80.

Sucrose is known to stabilize protein against thermal degradation by preferential exclusion mechanism.[31] Though, the overall amount of aggregates in DVD-Ig^{TM} protein solution increased at 40 °C (Figure 3b), aggregation and T_{onset} (Figure 4) decreased in the presence of sucrose compared to buffer which is consistent with literature reports.[28, 29] PEG increases conformational stability of proteins by preferential exclusion mechanism (steric effect),[20, 30] which can also increase attractive protein-protein interactions in solution, resulting in increased aggregates in DVD-Ig^{TM} protein solution. Similarly, from Figure 4 reduced thermal stability was observed in presence of PEG. Though no structural changes were observed in solution, increased amount of fragments at 40 °C indicate the possibility of covalent interactions (disulfide linkage) between the molecules, resulting in monomer loss at high temperature over a period of time. Formation of peroxides and other chemical moieties (aldehydes and esters) in PEG solutions due to air exposure/aging and increased temperatures has been reported in literature and may promote covalent interactions in protein solutions.[37-

[39] Tween 80 has no effect on aggregation, fragmentation and thermal stability in solution compared to buffer. Surfactants are amphiphilic molecules and adsorb/concentrate at air-water interface, reducing the concentration in bulk and hence no effect on aggregation was observed. Though, Tween 80 stabilizes protein against surface-induced aggregation, it has been reported to destabilize proteins against thermal degradation[25, 40] and is also known to induce chemical degradation in proteins via oxidation due to formation of peroxides.[27, 41]

4.2. Effect of Excipients on Liquid-liquid Phase Separation

Liquid-liquid phase separation (LLPS) is a concern in protein formulation development as the protein solutions are generally stored at refrigerated conditions (4-8 ˚C) where they show a higher tendency to phase separate. LLPS in solution can be attributed to attractive protein-protein interactions (PPI).[42-44] Excipients that decrease the interactions between the protein molecules will reduce their tendency to undergo LLPS in solution.[45] T_{cloud} was determined by measuring percent transmittance as solution temperature was lowered to determine the effect of excipients on LLPS in DVD-Ig™ protein solution. PPI in the presence of different excipients was further confirmed by well-established light scattering studies, where k_D or interaction parameter was determined from diffusion coefficient measured using Dynamic light scattering. A positive k_D value indicates repulsive PPI, while a negative k_D value indicates attractions between the protein molecules. All the negative k_D values in the current study are outside the hydrodynamic range (small range where interactions are repulsive in nature, indicated by positive B_2 values, but k_D values are negative due to larger hydrodynamic contributions) and hence indicate attractions between the molecules.

Figure 5 shows a plot of T_{cloud} on the primary axis and k_D on the secondary axis against different excipients (10 % PEG 400, 10 % Sucrose and 0.01 % Tween 80) for 16 mg/mL protein solution. The ionic strength and pH of the solutions were maintained constant at pH 6.6 (Histidine buffer) and 15 mM, respectively. In the absence of any excipients, T_{cloud} for DVD-Ig^{TM} protein is around 20 ºC and k_D shows a large negative value (-60 mL/g) indicating strong attractive interactions in the solution. In the presence of 10 % PEG, T_{cloud} increases to ~25.5 ºC and k_D becomes more negative (~ -68 mL/g), both indicating increased attractive interactions in the solution and reduced solution stability. As described in the previous section, PEG is a crowding agent; hence in the presence of PEG less volume is available for the protein molecules, which results in enhanced protein-protein interactions (non-covalent). The results are consistent with those reported in the literature, where PEG has been shown to shift the coexistence curve for proteins to higher temperatures.[22, 24]

Tween (0.01%) has no effect on T_{cloud} (~19.5 ºC) and k_D (~-61.5 mL/g) measured for DVD-Ig^{TM} protein compared to buffer. The concentration of Tween studied was extremely low; and at such low concentrations it may be affecting the surface properties, there are no effects on the bulk solution property. Therefore, the effect of a higher concentration of Tween (0.05%) on T_{cloud} and k_D was also studied; no change in T_{cloud} or k_D was observed.

Sucrose (10 % w/v) shows a significant decrease in T_{cloud} (~ 11 ºC) of the solution as compared to DVD-Ig^{TM} protein in buffer. Attractive interactions in solution also decrease as indicated by a less negative k_D value (~-35 mL/g). While both PEG and Sucrose increase thermodynamic stability of the protein in solution by preferential exclusion mechanism, they affect the LLPS in solution differently. Although, sugars are polar molecules they have some hydrophobicity associated with it, therefore have variable effects on solubility of proteins due

to weak binding.[46, 47] Based on the measurements of transfer free energies (Δg_{tr}), previous studies in our lab reported increased solubility for aromatic amino acids[47] and its derivative (negative Δg_{tr}) and decreased solubility for aliphatic amino acid derivative (positive Δg_{tr}) in the presence of sucrose.[48] Hydrophobic interactions chromatography studies were performed for DVD-Ig™ protein molecule; sharp peaks were observed using phenyl column as opposed to broad peaks with butyl column indicating specific binding of the aromatic groups with phenyl (Zecca E. et al., unpublished data). Site specific binding of sucrose with the aromatic amino acids on protein surface may be responsible for reduced T_{cloud} and k_D for DVD-Ig™ protein.

4.3. Relationship between Aggregation and LLPS

Liquid-Liquid phase separation of a solution into a protein-rich and protein-poor phase is more likely to promote protein self-association and/or irreversible aggregation since these phenomena are concentration dependent. However, LLPS and aggregation respond to the temperature in opposite ways; aggregate formation increases with increasing temperatures while tendency to phase separate decreases. Earlier sections discussed the effect of excipients on aggregation and LLPS; this section discusses the relationship between aggregation and LLPS as a function of different excipients and temperature.

4.3.1. Effect of Temperature

At 4 ˚C, all the samples exhibited liquid-liquid phase separation in the presence of excipients studied (Figure 5). On undergoing LLPS, two phases of different protein concentrations are formed and due to the Donnan effect excipients will also partition in two

phases; concentration of the excipient in the upper phase or protein-poor phase will be much higher than in protein-rich phase. Ideally, both, high concentration of the protein and lower concentration of the excipient in protein-rich phase should accelerate the aggregation of proteins. However, no change in aggregate or fragment content was observed after sample was incubated at 4 °C for 45 days (Figure 1). This indicates that LLPS does not result in aggregate formation at this temperature during this period (45 days stability studies).

At 20 °C, increase in aggregate formation was observed for DVD-Ig™ protein solution in presence of PEG 400, while at all other conditions monomer content remained same after 45 days. From Figure 5, T_{cloud} for DVD-Ig™ protein in buffer and in the presence of Tween 80 is around 20 ˚C. T_{cloud} marks the onset of phase separation in solution, and in the current study, for qualitative analysis temperature where percent transmittance is 70 is termed as T_{cloud}. However, actual separation in two phases may be occurring at temperatures slightly away from reported T_{cloud} and strongly depends on the kinetics of phase separation and viscosity of the solution (which may impede phase separation process). At 20 °C, though the solution exhibits significant opalescence in buffer and in presence of Tween 80, phase separation may be in transient state due to kinetic hindrance. On the other hand, T_{cloud} for PEG is around 25.5 ºC and hence on lowering the temperature, solution phase separates (visually confirmed at room temperature, 23 ºC). This indicates that though LLPS can accelerate aggregation in solution, temperature is the dominant factor in aggregation kinetics. This was further confirmed from SEC analysis of samples incubated at 40 ºC, where, significant increase in aggregate and fragment content was observed for DVD-Ig™ protein solutions at all conditions. However, all the samples were homogenous and no liquid-liquid phase separation was observed at any of the conditions. Hence, at 4 ºC, even though all the

samples are phase separated, they do not aggregate as temperature acts as a kinetic barrier for aggregate formation; while at 20 ºC, both LLPS and increased temperature promote formation of irreversible, soluble aggregates in the solution.

It is well-known that the rate of protein degradation pathways is accelerated at higher temperatures and forms the basis of accelerated stability studies. However prediction of degradation rates from higher temperatures may not be representative of the actual storage conditions, which is refrigerated conditions for most proteins. Though, many models are routinely used to extrapolate accelerated stability conditions to storage conditions and predict shelf-life, several literature reports have cited the inefficiency of these models.[49] In a recent paper, Saluja et al., have reemphasized the inadequacy of these models and have also highlighted the fact that these models do not take into consideration structure of multi-domain proteins which do not follow simple two-step transition; hence, predicting aggregation rate for such molecules is even more challenging.[50] Though, we do not attempt to determine or correlate the aggregation kinetic behavior at different temperature conditions, current study highlights the facts that at low temperatures, possible liquid-liquid phase separation may alter the protein aggregation kinetics (especially for DVD-Ig™ protein as observed at 20 ºC) over long period of time. At 4 ºC, aggregation kinetics are slow; hence sample analysis after 45 days may not be representative of long-term stability at this condition. For better prediction of protein shelf-life either real time stability studies needs to be performed or better predictive models, which take into account other physical instabilities at low temperatures, needs to be developed.

4.3.2. Effect of Excipients and Interactions in Solution

Figure 6 represents LLPS (Figure 6a) and aggregation (Figure 6b) measured in 33 mg/mL DVD-Ig^{TM} protein solutions in the presence of different excipients, after sample was incubated for 45 days at 4 °C and 40 °C, respectively. Concentration of the protein in protein-poor phase at 4° C indicating LLPS (Figure 6a) and percent monomer loss at 40 °C (Figure 6b) are correlated to the k_D values (first secondary axis) measured in dilute solutions (<10 mg/mL) and T_{cloud} (second secondary axis) measured at 16 mg/mL. From the earlier sections it was established that at 4 °C, DVD-Ig^{TM} protein exhibited only LLPS and no aggregation, while at 40 °C all the solutions were homogenous (no LLPS was observed) and percent monomer loss/aggregation is significant over 45 days.

From Figure 6a, LLPS for PEG 400 at 4 °C shows a good correlation with T_{cloud}; higher the T_{cloud} value lower is the concentration in the protein-poor phase. Percent monomer loss (Figure 6b) in the presence of PEG is also significantly higher than in presence of buffer. Similarly, DVD-Ig^{TM} protein solution has most negative k_D value in the presence of PEG, indicating strong attractive protein-protein interactions which increases both aggregation and phase separation in solution. PEG increases LLPS by preferential exclusion mechanism; however, it also increases the formation of irreversible aggregates in solution possibly due to covalent interactions at high temperatures. Tween 80 has no effect on either LLPS (Figure 6a) or aggregation (Figure 6b) in solution. The concentration of the protein in the upper-phase in the presence of Tween is almost similar to that in buffer. Also, the T_{cloud} and k_D values are similar to values in buffer. Low concentration of Tween in monomeric form is the possible reason that it has no effect on either phenomena. In the presence of sucrose, concentration of the protein in the upper-phase after phase separation increases compared to

that in buffer which is in agreement with lower T_{cloud} value. Attractive interactions between the protein molecules also reduce significantly as measured using DLS. Sucrose is a thermal stabilizer and reduces the percent monomer loss by preferential exclusion effect, while it reduces LLPS in solution by increasing solubility of the aromatic amino groups on the protein surface. Although used as a stabilizer, sucrose shows a high tendency to degrade and form glucose and fructose which may degrade protein by glycation (Maillard reaction) of Lysine residues.[51, 52] Hence, it is more frequently used in freeze-dried protein formulation, where degradation is suppressed in the absence of water, than in liquid formulations.

After incubation for 45 days, the phase separated samples exhibited stability of the individual phases indicated by a good correlation with T_{cloud} values (measured at t=0) at all the conditions. Our studies indicate that the mechanism for LLPS and aggregation in protein solution is different and shows strong temperature dependence. Similarly, any excipient used in a formulation may interact with the protein by more than one mechanism depending on the protein itself (specific amino acids on protein surface) and other extrinsic factors, including but not limited to pH, ionic strength, protein concentration, excipient concentration and temperature. Hence the selection of a suitable excipient for a formulation may not be straightforward and has to be investigated on a case by case basis.

5. Conclusion

Tween has no effect on phase separation temperature, attractive interactions or aggregate formation in solution. PEG adversely affects both phase separation and aggregate formation in solution, while, Sucrose has positive effect and reduces both phase separation temperature for DVD-Ig™ protein as well as percent aggregates in solution. However, the

mechanism by which these different excipients exert their effect (positive or negative) on aggregation and LLPS is different. Though, no aggregate formation was observed at 4 ºC, where solution exhibited phase separation, 20 ºC data suggests that aggregate formation is accelerated on phase separation. Temperature plays a dominant role in both, liquid-liquid phase separation and formation of soluble, irreversible aggregates in solution.

6. Acknowledgments

Authors would like to thank AbbVie Bioresearch Center, Worcester, MA for material and financial support for the work.

7. References

1. Manning, M.; Chou, D.; Murphy, B.; Payne, R.; Katayama, D. Stability of Protein Pharmaceuticals: An Update. *Pharmaceutical research* **2010,** *27*, (4), 544-575.
2. Bye, J.; Platts, L.; Falconer, R. Biopharmaceutical liquid formulation: a review of the science of protein stability and solubility in aqueous environments. *Biotechnology letters* **2014,** *36*, (5), 869-875.
3. Vekilov, P. G. Phase transitions of folded proteins. *Soft matter* **2010,** *6*, (21), 5254-5272.
4. Vekilov, P. G. Phase diagrams and kinetics of phase transitions in protein solutions. *Journal of physics. Condensed matter : an Institute of Physics journal* **2012,** *24*, (19), 193101.
5. Dumetz, A. C.; Chockla, A. M.; Kaler, E. W.; Lenhoff, A. M. Protein phase behavior in aqueous solutions: crystallization, liquid-liquid phase separation, gels, and aggregates. *Biophysical journal* **2008,** *94*, (2), 570-83.
6. Roberts, C. J. Protein aggregation and its impact on product quality. *Current opinion in biotechnology* **2014,** *30*, (0), 211-217.
7. Jiskoot, W.; Randolph, T. W.; Volkin, D. B.; Middaugh, C. R.; Schöneich, C.; Winter, G.; Friess, W.; Crommelin, D. J. A.; Carpenter, J. F. Protein instability and immunogenicity: Roadblocks to clinical application of injectable protein delivery systems for sustained release. *Journal of pharmaceutical sciences* **2012,** *101*, (3), 946-954.
8. Mahler, H. C.; Friess, W.; Grauschopf, U.; Kiese, S. Protein aggregation: pathways, induction factors and analysis. *Journal of pharmaceutical sciences* **2009,** *98*, (9), 2909-34.
9. Li, Y.; Roberts, C. J., Protein Aggregation Pathways, Kinetics, and Thermodynamics. In *Aggregation of Therapeutic Proteins*, John Wiley & Sons, Inc.: 2010; pp 63-102.
10. Sanchez-Ruiz, J. M. Protein kinetic stability. *Biophysical chemistry* **2010,** *148*, (1-3), 1-15.
11. Ahamed, T.; Esteban, B. N.; Ottens, M.; van Dedem, G. W.; van der Wielen, L. A.; Bisschops, M. A.; Lee, A.; Pham, C.; Thommes, J. Phase behavior of an intact monoclonal antibody. *Biophysical journal* **2007,** *93*, (2), 610-9.
12. den Engelsman, J.; Garidel, P.; Smulders, R.; Koll, H.; Smith, B.; Bassarab, S.; Seidl, A.; Hainzl, O.; Jiskoot, W. Strategies for the assessment of protein aggregates in pharmaceutical biotech product development. *Pharmaceutical research* **2011,** *28*, (4), 920-33.
13. Sharma, V. K.; Kalonia, D. S., Experimental Detection and Characterization of Protein Aggregates. In *Aggregation of Therapeutic Proteins*, John Wiley & Sons, Inc.: 2010; pp 205-256.
14. Zölls, S.; Tantipolphan, R.; Wiggenhorn, M.; Winter, G.; Jiskoot, W.; Friess, W.; Hawe, A. Particles in therapeutic protein formulations, Part 1: Overview of analytical methods. *Journal of pharmaceutical sciences* **2012,** *101*, (3), 914-935.
15. Weiss, W. F.; Young, T. M.; Roberts, C. J. Principles, approaches, and challenges for predicting protein aggregation rates and shelf life. *Journal of pharmaceutical sciences* **2009,** *98*, (4), 1246-1277.

16. Wang, W.; Roberts, C. J., *Aggregation of therapeutic proteins*. Wiley Online Library: 2010.
17. Ohtake, S.; Kita, Y.; Arakawa, T. Interactions of formulation excipients with proteins in solution and in the dried state. *Advanced drug delivery reviews* **2011,** *63*, (13), 1053-1073.
18. Kamerzell, T. J.; Esfandiary, R.; Joshi, S. B.; Middaugh, C. R.; Volkin, D. B. Protein–excipient interactions: Mechanisms and biophysical characterization applied to protein formulation development. *Advanced drug delivery reviews* **2011,** *63*, (13), 1118-1159.
19. Timasheff, S. N. Protein Hydration, Thermodynamic Binding, and Preferential Hydration. *Biochemistry* **2002,** *41*, (46), 13473-13482.
20. Bhat, R.; Timasheff, S. N. Steric exclusion is the principal source of the preferential hydration of proteins in the presence of polyethylene glycols. *Protein Science* **1992,** *1*, (9), 1133-1143.
21. Annunziata, O.; Asherie, N.; Lomakin, A.; Pande, J.; Ogun, O.; Benedek, G. B. Effect of polyethylene glycol on the liquid-liquid phase transition in aqueous protein solutions. *Proceedings of the National Academy of Sciences of the United States of America* **2002,** *99*, (22), 14165-70.
22. Wang, Y.; Annunziata, O. Comparison between protein-polyethylene glycol (PEG) interactions and the effect of PEG on protein-protein interactions using the liquid-liquid phase transition. *The journal of physical chemistry. B* **2007,** *111*, (5), 1222-30.
23. Wang, Y.; Lomakin, A.; Latypov, R. F.; Laubach, J. P.; Hideshima, T.; Richardson, P. G.; Munshi, N. C.; Anderson, K. C.; Benedek, G. B. Phase transitions in human IgG solutions. *J Chem Phys* **2013,** *139*, (12), 121904.
24. Wang, Y.; Latypov, R. F.; Lomakin, A.; Meyer, J. A.; Kerwin, B. A.; Vunnum, S.; Benedek, G. B. Quantitative evaluation of colloidal stability of antibody solutions using PEG-induced liquid-liquid phase separation. *Molecular pharmaceutics* **2014,** *11*, (5), 1391-402.
25. Katakam, M.; Bell, L. N.; Banga, A. K. Effect of surfactants on the physical stability of recombinant human growth hormone. *Journal of pharmaceutical sciences* **1995,** *84*, (6), 713-716.
26. Kerwin, B. A. Polysorbates 20 and 80 used in the formulation of protein biotherapeutics: Structure and degradation pathways. *Journal of pharmaceutical sciences* **2008,** *97*, (8), 2924-2935.
27. Wang, W.; Wang, Y. J.; Wang, D. Q. Dual effects of Tween 80 on protein stability. *International journal of pharmaceutics* **2008,** *347*, (1–2), 31-38.
28. Back, J. F.; Oakenfull, D.; Smith, M. B. Increased thermal stability of proteins in the presence of sugars and polyols. *Biochemistry* **1979,** *18*, (23), 5191-6.
29. Oshima, H.; Kinoshita, M. Effects of sugars on the thermal stability of a protein. *J Chem Phys* **2013,** *138*, (24), 245101.
30. Gregory, R., *Protein-solvent interactions*. CRC Press: 1995.
31. Lee, J. C.; Timasheff, S. N. The stabilization of proteins by sucrose. *Journal of Biological Chemistry* **1981,** *256*, (14), 7193-7201.
32. Berne, B. J.; Pecora, R., *Dynamic light scattering: with applications to chemistry, biology, and physics*. Courier Dover Publications: 2000.

33. Kumar, V.; Sharma, V. K.; Kalonia, D. S. Second derivative tryptophan fluorescence spectroscopy as a tool to characterize partially unfolded intermediates of proteins. *International journal of pharmaceutics* **2005,** *294*, (1–2), 193-199.
34. Abbas, S. A.; Gaspar, G.; Sharma, V. K.; Patapoff, T. W.; Kalonia, D. S. Application of second-derivative fluorescence spectroscopy to monitor subtle changes in a monoclonal antibody structure. *Journal of pharmaceutical sciences* **2013,** *102*, (1), 52-61.
35. Arzenšek, D., Dynamic light scattering and application to proteins in solutions.
36. Kumar, V.; Dixit, N.; Zhou, L. L.; Fraunhofer, W. Impact of short range hydrophobic interactions and long range electrostatic forces on the aggregation kinetics of a monoclonal antibody and a dual-variable domain immunoglobulin at low and high concentrations. *International journal of pharmaceutics* **2011,** *421*, (1), 82-93.
37. Han, S.; Kim, C.; Kwon, D. Thermal/oxidative degradation and stabilization of polyethylene glycol. *Polymer* **1997,** *38*, (2), 317-323.
38. Bergh, M.; Magnusson, K.; Nilsson, J. L.; Karlberg, A. T. Formation of formaldehyde and peroxides by air oxidation of high purity polyoxyethylene surfactants. *Contact dermatitis* **1998,** *39*, (1), 14-20.
39. Knop, K.; Hoogenboom, R.; Fischer, D.; Schubert, U. S. Poly (ethylene glycol) in drug delivery: pros and cons as well as potential alternatives. *Angewandte Chemie International Edition* **2010,** *49*, (36), 6288-6308.
40. Liu, L.; Qi, W.; Schwartz, D. K.; Randolph, T. W.; Carpenter, J. F. The effects of excipients on protein aggregation during agitation: an interfacial shear rheology study. *Journal of pharmaceutical sciences* **2013,** *102*, (8), 2460-70.
41. Ha, E.; Wang, W.; Wang, Y. J. Peroxide formation in polysorbate 80 and protein stability. *Journal of pharmaceutical sciences* **2002,** *91*, (10), 2252-2264.
42. Nishi, H.; Miyajima, M.; Wakiyama, N.; Kubota, K.; Hasegawa, J.; Uchiyama, S.; Fukui, K. Fc domain mediated self-association of an IgG1 monoclonal antibody under a low ionic strength condition. *Journal of bioscience and bioengineering* **2011,** *112*, (4), 326-32.
43. Mason, B. D.; Zhang-van Enk, J.; Zhang, L.; Remmele, R. L., Jr.; Zhang, J. Liquid-liquid phase separation of a monoclonal antibody and nonmonotonic influence of Hofmeister anions. *Biophysical journal* **2010,** *99*, (11), 3792-800.
44. Raut, A. S.; Kalonia, D. S. Opalescence in Monoclonal Antibody Solutions and Its Correlation with Intermolecular Interactions in Dilute and Concentrated Solutions. *Journal of pharmaceutical sciences* **2015,** *104*, (4), 1263-1274.
45. Broide, M.; Tominc, T.; Saxowsky, M. Using phase transitions to investigate the effect of salts on protein interactions. *Physical Review E* **1996,** *53*, (6), 6325-6335.
46. Janado, M.; Yano, Y. Hydrophobic nature of sugars as evidenced by their differential affinity for polystyrene gel in aqueous media. *Journal of solution chemistry* **1985,** *14*, (12), 891-902.
47. Kumar, V.; Chari, R.; Sharma, V. K.; Kalonia, D. S. Modulation of the thermodynamic stability of proteins by polyols: Significance of polyol hydrophobicity and impact on the chemical potential of water. *International journal of pharmaceutics* **2011,** *413*, (1–2), 19-28.
48. Abbas, S. A.; Sharma, V. K.; Patapoff, T. W.; Kalonia, D. S. Solubilities and transfer free energies of hydrophobic amino acids in polyol solutions: Importance of the

hydrophobicity of polyols. *Journal of pharmaceutical sciences* **2011,** *100*, (8), 3096-3104.
49. Roberts, C. J.; Das, T. K.; Sahin, E. Predicting solution aggregation rates for therapeutic proteins: Approaches and challenges. *International journal of pharmaceutics* **2011,** *418*, (2), 318-333.
50. Saluja, A.; Sadineni, V.; Mungikar, A.; Nashine, V.; Kroetsch, A.; Dahlheim, C.; Rao, V. M. Significance of unfolding thermodynamics for predicting aggregation kinetics: a case study on high concentration solutions of a multi-domain protein. *Pharmaceutical research* **2014,** *31*, (6), 1575-87.
51. Gadgil, H. S.; Bondarenko, P. V.; Pipes, G.; Rehder, D.; McAuley, A.; Perico, N.; Dillon, T.; Ricci, M.; Treuheit, M. The LC/MS analysis of glycation of IgG molecules in sucrose containing formulations. *Journal of pharmaceutical sciences* **2007,** *96*, (10), 2607-2621.
52. Banks, D. D.; Hambly, D. M.; Scavezze, J. L.; Siska, C. C.; Stackhouse, N. L.; Gadgil, H. S. The effect of sucrose hydrolysis on the stability of protein therapeutics during accelerated formulation studies. *Journal of pharmaceutical sciences* **2009,** *98*, (12), 4501-10.

8. Figures

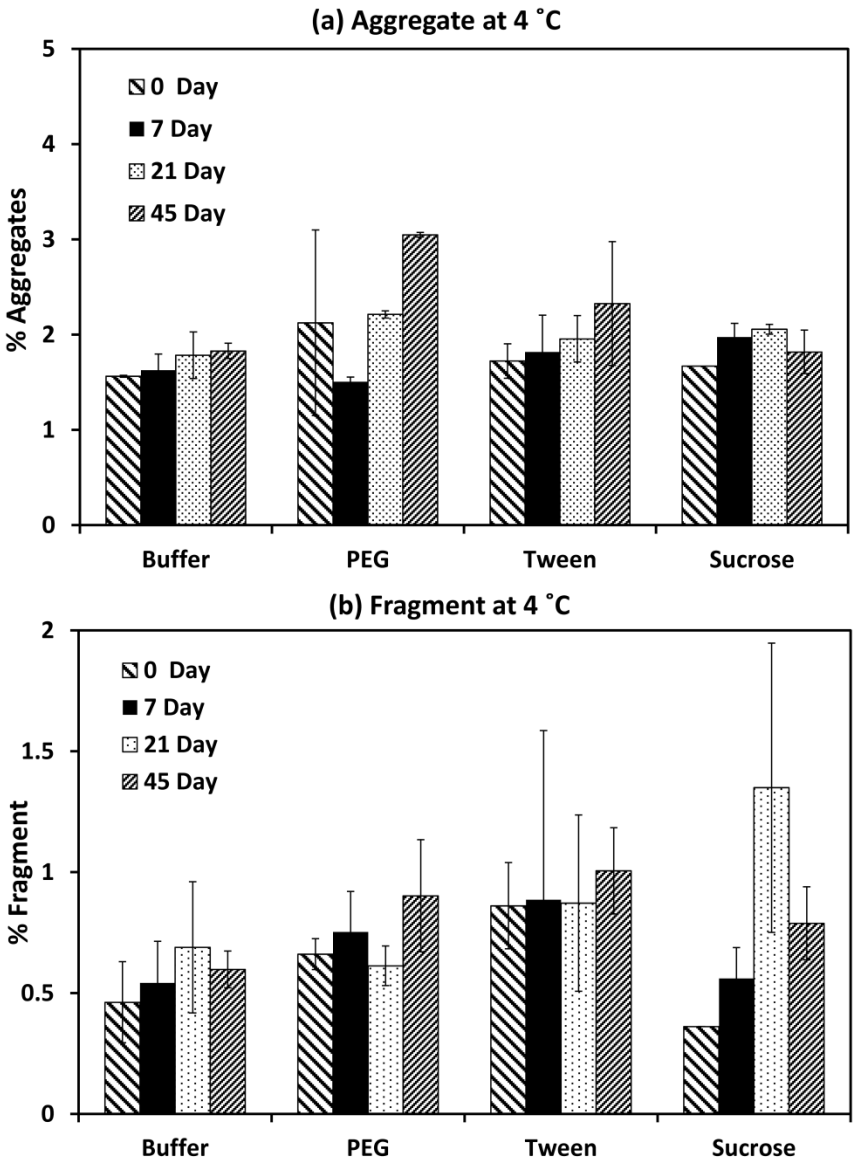

Figure 1: (a) Percent soluble aggregates and (b) fragmentation observed for DVD-Ig™ protein stored at **4 ºC** in the presence and absence of excipients, at t=0, 7, 21 and 45 days. Samples were analyzed at a concentration of 1 mg/mL. Percent aggregates were calculated by SE-HPLC using Chemstation software. All solutions were prepared in pH 6.6 Histidine buffer with ionic strength of 15 mM. All samples were analyzed at 25 ± 1 ºC in duplicate. Mobile Phase: 100 mM sodium phosphate buffer at pH 7 containing 200 mM sodium sulfate.

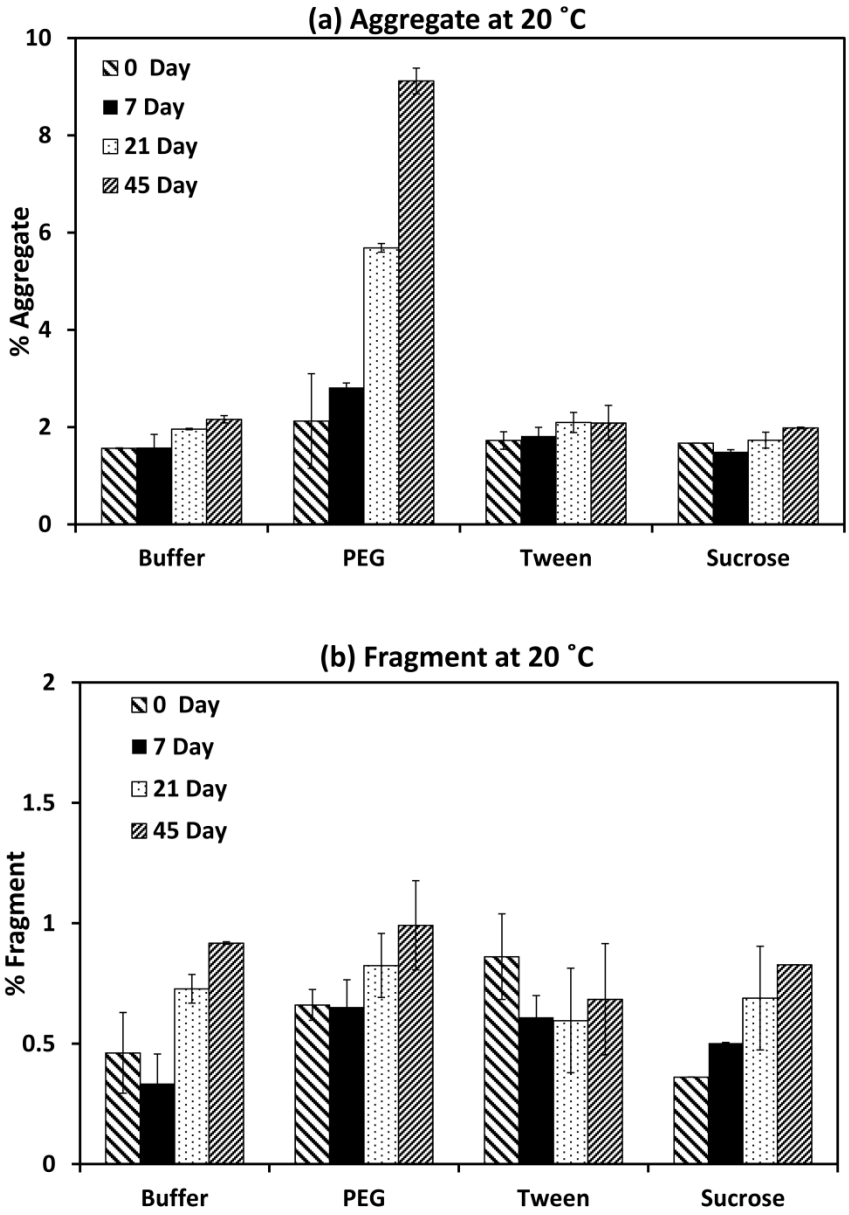

Figure 2: (a) Percent soluble aggregates and (b) fragmentation observed for DVD-Ig™ protein stored at **20 ºC** in presence and absence of excipients, at t=0, 7, 21 and 45 days Samples were analyzed at a concentration of 1 mg/mL. Percent aggregates were calculated by SE-HPLC using Chemstation software. All solutions were prepared in pH 6.6 Histidine buffer with ionic strength of 15 mM. All samples were analyzed at 25 ± 1 ºC in duplicate. Mobile Phase: 100 mM sodium phosphate buffer at pH 7 containing 200 mM sodium sulfate.

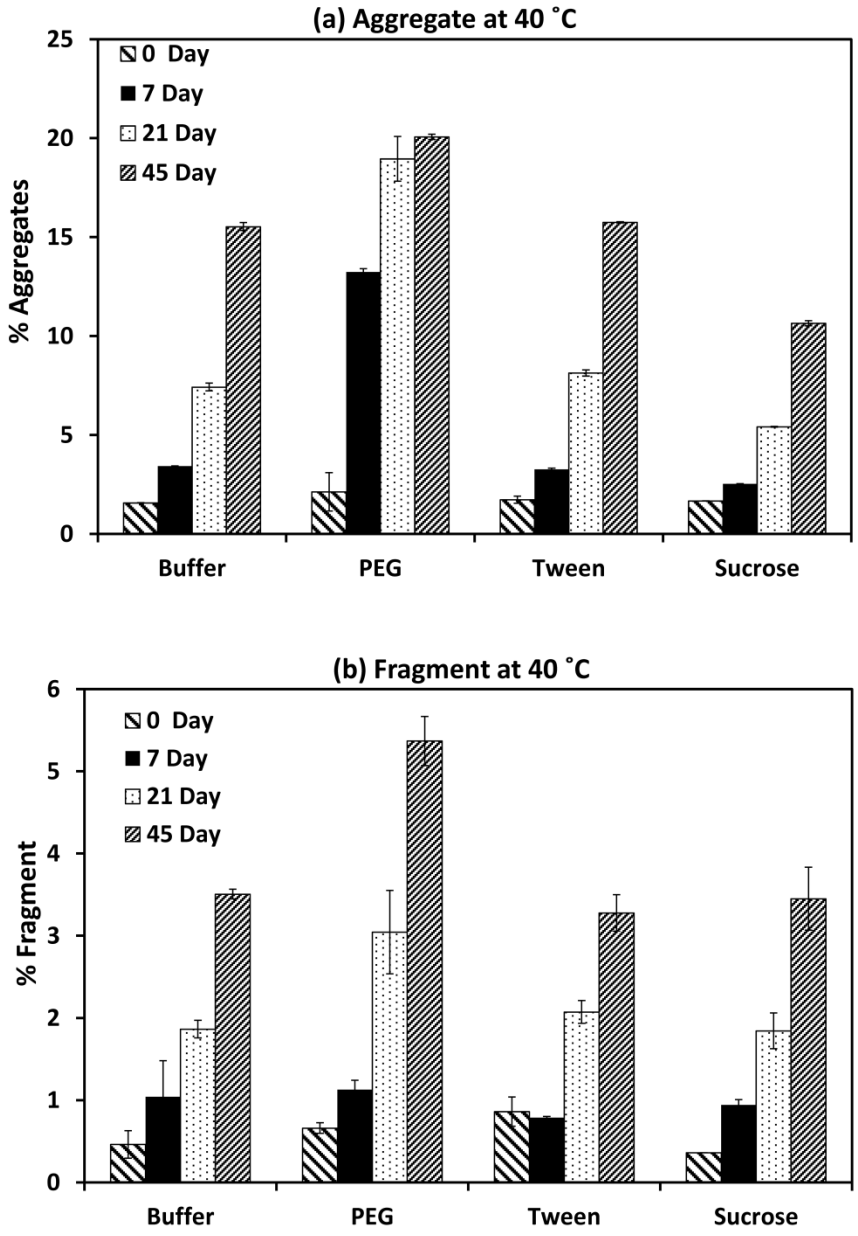

Figure 3: (a) Percent soluble aggregates and (b) fragmentation observed for DVD-Ig™ protein incubated at **40 ºC** in presence and absence of excipients, at t=0, 7, 21 and 45 days. Samples were analyzed at a concentration of 1 mg/mL. Percent aggregates were calculated by SE-HPLC using Chemstation software. All solutions were prepared in pH 6.6 Histidine buffer with ionic strength of 15 mM. All samples were analyzed at 25 ± 1 ºC in duplicate. Mobile Phase: 100 mM sodium phosphate buffer at pH 7 containing 200 mM sodium sulfate.

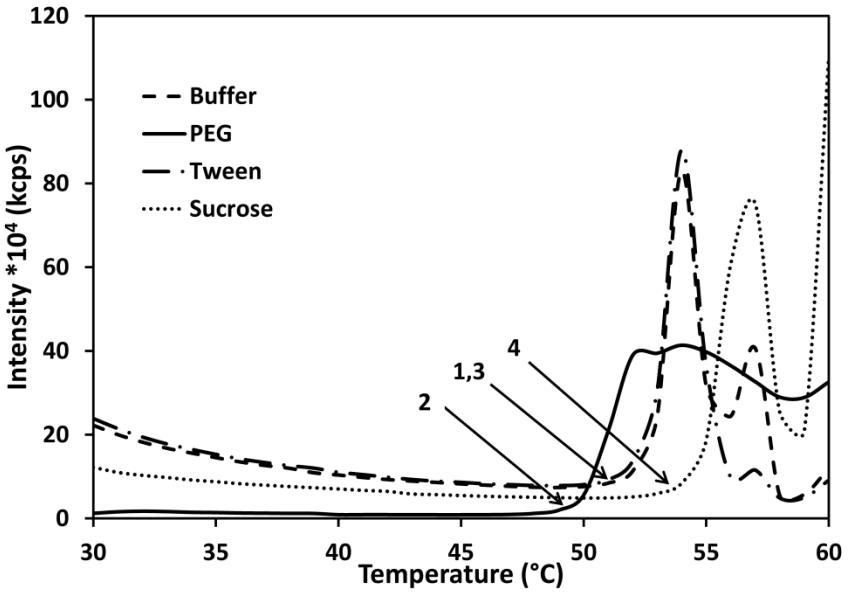

Figure 4: Plot of Intensity as a function of temperature for DVD-Ig^{TM} protein at a concentration of 34 mg/mL determined from Light scattering in presence and absence of excipients. Stock solutions of PEG 400, Sucrose and Tween 80 were prepared in histidine buffer at pH 6.6 with ionic strength of 15 mM and then diluted appropriately to obtain final concentrations of 10 % PEG, 10% Sucrose and 0.01% Tween. T_{onset} (temperature marking onset of aggregation) is indicated by arrows (1-Buffer, 2-PEG, 3-Tween and 4- Sucrose). Plot represents averages of intensity measured at all conditions in duplicate.

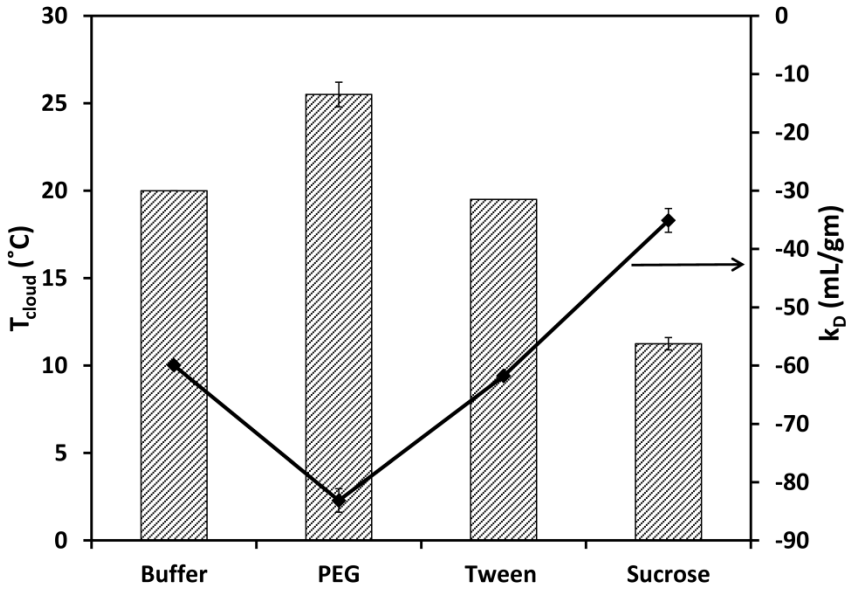

Figure 5: Plot of T_{cloud} (primary axis) for DVD-Ig^{TM} protein at a concentration of 16 mg/mL determined from Temperature studies and k_D (secondary axis) determined from Dynamic light scattering in presence and absence of excipients. Stock solutions of PEG, Sucrose and Tween were prepared in histidine buffer at pH 6.6 with ionic strength of 15 mM and then diluted appropriately to obtain final concentrations of 10 % PEG, 10% Sucrose and 0.01% Tween. T_{cloud} is termed as the temperature where percent transmittance is 70. k_D is obtained from slope/intercept of the linear plot of mutual diffusion coefficient (D_m) against protein concentration. Light scattering measurements were made at 25 ± 0.1˚C. All solutions were analyzed in duplicate. Error bars if not visible are smaller than the symbols used.

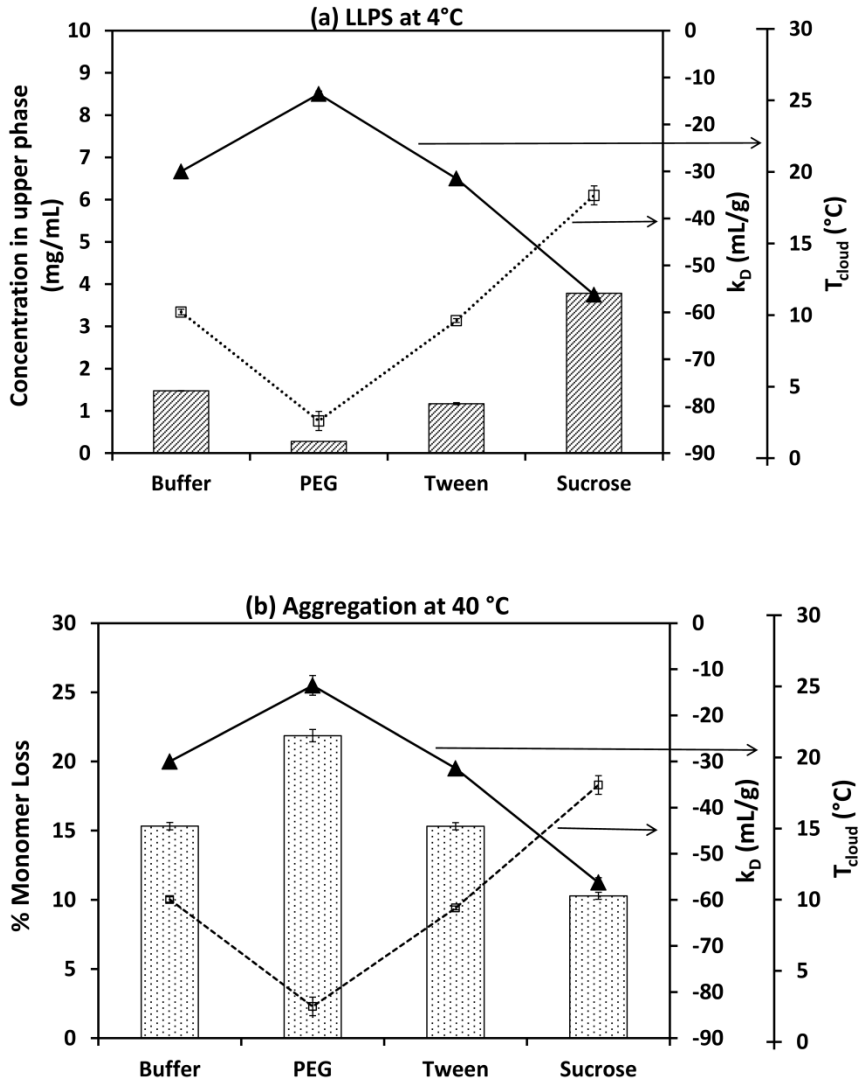

Figure 6: (a) Concentration of protein in protein-poor phase for DVD-Ig^{TM} protein sample stored at 4°C for 45 days and (b) Percent monomer loss for DVD-Ig^{TM} protein after sample was incubated at 40 °C for 45 days, as a function of different excipients. Initial protein concentration was maintained at 33 mg/mL in pH 6.6 Histidine buffer with ionic strength of 15 mM. Interaction parameter, k_D, (dashed line) obtained from Dynamic light scattering at 25 °C is plotted on first secondary axis and T_{cloud} (solid line) measured at similar solution conditions at a concentration of 16 mg/mL is plotted on second secondary axis. All solutions were analyzed in duplicate. Error bars if not visible are smaller than the symbols used.

Chapter 6

Viscosity Analysis of Dual Variable Domain Immunoglobulin Protein Solutions: Role of Size, Electroviscous Effect and Protein-Protein Interactions

Contents

Chapter 6

1. Abstract

Purpose: Increased solution viscosity results in difficulties in manufacturing and delivery of therapeutic protein formulations, increasing both the time and production costs, and leading to patient inconvenience. The solution viscosity is affected by the molecular properties of both the solute and the solvent. The purpose of this work was to investigate the effect of the size, charge and protein-protein interactions on the viscosity of Dual Variable Domain Immunoglobulin (DVD-Ig^{TM}) protein solutions.

Method: The effect of size of the protein molecule on solution viscosity was investigated by measuring intrinsic viscosity and excluded volume calculations for monoclonal antibody (mAb) and DVD-Ig^{TM} protein solutions. The role of the electrostatic charge resulting in electroviscous effects for DVD-Ig^{TM} protein was assessed by measuring zeta potential. Light scattering measurements were performed to detect protein-protein interactions affecting solution viscosity as a function of formulation factors.

Results: DVD-Ig^{TM} protein exhibited significantly higher viscosity compared to mAb. Intrinsic viscosity values and excluded volume calculations indicated that the size of the molecule affects solution viscosity significantly at higher concentrations, while the effect was minimal at intermediate concentrations. Electroviscous contribution to the viscosity of DVD-Ig^{TM} protein varied depending on the presence or absence of ions in the solution. In buffered solutions, negative k_D and B_2 values indicated the presence of attractive interactions which resulted in high viscosity for DVD-Ig^{TM} protein at certain pH and ionic strength conditions.

Conclusion: Results show that more than one factor contributes to the increased viscosity of DVD-Ig™ protein and interplay of these factors modulates the overall viscosity behavior of the solution, especially at higher concentrations.

Keywords: monoclonal antibody, bispecific antibody, excluded volume, charge, hydration, protein formulation

2. Introduction

Monoclonal antibodies (first-generation) and their derivatives (second-generation) are ever growing class of bio-therapeutics and have been successfully implemented in the treatment of several terminal diseases.[1,2] For better patient compliance, these proteins are generally administered by the subcutaneous route, preferably in pre-filled syringes; however, SC administration has a low volume restriction of <1.5 mL. This combined with the lower potency and high dose requirements make it necessary for the therapeutic proteins to be formulated at higher concentrations. High viscosity is often observed for high concentration formulations. Viscous protein formulations result in difficulties in manufacturing processes such as pumping, filtration, recovery of the product from the vessels, leading to the increased time and production costs. In preformulation development process, high viscosity hinders the biophysical characterization of proteins in solution.[3-5] Viscous solutions also require higher injection forces to deliver the formulation through pre-filled syringe resulting in patient inconvenience.[6,7]

Viscosity of a macromolecular solution can be expressed as a virial expansion,[8]

$$\frac{\eta_{sp}}{c} = ([\eta] + k_1[\eta]^2 c + k_2[\eta]^3 c^2 + k_3[\eta]^4 c^3 + \cdots \quad (1)$$

where, η_{sp} is the specific viscosity (η_{sp}=1-η/η_0, η is the solution viscosity and η_0 is the solvent viscosity), $[\eta]$ is the intrinsic viscosity, c is the solute concentration, k_1 k_2, k_3 are higher order virial coefficients. In dilute solution, higher order terms are neglected and intrinsic viscosity is the only contributor to the solution viscosity. Excluded volume effect (crowding in solution)[9,10] also includes contribution from the intrinsic viscosity, which is mainly due to the size of the molecule,[11,12] and results in a significant increase in solution viscosity at high concentrations.

Charge on the protein molecule is another major factor contributing to the viscosity due to the electroviscous effect. Protein carries a net positive or negative charge at pH conditions below or above its pI. Electroviscous effect is the overall contribution of three effects; primary, secondary and tertiary effect. Primary effect is due to the presence of diffuse double layer around the protein molecule. Secondary effect is essentially due to the intermolecular repulsions between the two double layers. Tertiary effect is the change in the effective shape of the macromolecule due to the repulsive forces. These three effects result in increased drag on the molecule in solution causing increased viscosity.[13-15]

Viscosity shows an exponential increase with concentration due to the contribution of higher order terms in equation 1 and can be attributed to increased tendency of the molecules to interact with each other (self-associate), due to specific and/or non-specific interactions in solution.[16-21] Asymmetric charge distribution/anisotropy on the molecule significantly affects its dipole-multipole and has been reported to increase viscosity for mAbs due to increased self-association between the molecules.[20,22,23] Viscous behavior of the solution due to non-specific protein-protein interactions (electrostatic, charges, dipole-mediated) can be modulated by changing the pH and ionic strength of the solution and has been extensively reported in the literature.[16-18,22,24-26] Hydrophobic salts[27,28] and certain solvents (DMSO, DMA)[29] that disrupt the transient network between protein molecules, which is due to hydrophobic interactions, have also been shown to significantly diminish solution viscosity. Similarly, amino acids and their derivatives have been reported to effectively reduce viscosity of monoclonal antibody solutions at high concentrations by specifically interacting with protein molecules.[16,30-32]

Investigating factors resulting in increased viscosity for protein solutions (especially mAbs) has been a subject of interest for over a decade, and several models have been proposed to predict the viscosity behavior or underline the cause for increased viscosity at higher concentrations. However, the assumptions made for these models do not fit to all molecules, which are becoming a challenge especially with the advent of newer molecules which show increased asymmetry in shape, charge distribution, surface hydrophobic patches and larger size.[23,33,34] DVD-Ig™ protein is a bispecific antibody-like molecule, where variable domains of a mAb are linked to the variable domain of a second mAb making it specific for dual targeting. Increased size of the molecule in comparison to mAb is hypothesized to increase the formulation related difficulties for DVD-Ig™ protein including increased viscosity. The purpose of the current study was to investigate and rank-order the effect of, the size of the molecule with respect to the excluded volume effect, charges on the molecule resulting in the electroviscous effects and contribution of attractive protein-protein interactions on viscosity of DVD-Ig™ protein solutions.

3. Material and Methods

3.1. Materials

Dual Variable Domain Immunoglobulin, DVD-Ig™ protein (pI ~7.5) as 85 mg/mL solution and monoclonal antibody, mAb (pI ~6.5) as 65 mg/mL solution in 15 mM Histidine buffer at pH 5.5 was supplied by Abbvie (Worcester, MA). Histidine base and histidine hydrochloride were obtained from Sigma (St. Louis, MO). Sodium chloride was obtained from Fisher Scientific (Fair Lawn, NJ). All chemicals used were reagent grade or higher. Solutions were prepared with deionized water equivalent to Milli-Q™.

Histidine buffer was prepared to maintain pH of the solution at 5.1, 6.1, 6.6 and 7.1, and appropriate buffer strength was selected so as to maintain ionic strength at 15 mM without addition of any salt. Sodium chloride was added to adjust the ionic strength to 50 mM. To prepare salt-free solutions (0 mM), proteins were extensively dialyzed in water in dialysis cassette over a period of 24 hrs. All antibody solutions were buffer exchanged with appropriate buffers using Millipore (Billerica, MA) Amicon Ultra centrifugation tubes with a molecular weight cutoff of 10 kDa obtained from Fisher Scientific. Concentrations of the samples were determined using a UV-vis spectrophotometer with an extinction coefficient of 1.4 $mg^{-1}/mL^{-1}cm^{-1}$ for mAb and 1.5 mg-1/$mL^{-1}cm^{-1}$ for DVD-Ig™ protein at 280 nm for 0.1% (w/v) IgG solutions. The pH of all the above solutions was within ± 0.1 of the target values as measured by a Denver Instrument pH meter.

3.2. Viscosity Measurements

Viscosity measurements were performed using VISCOlab 500 viscometer system (Cambridge Viscometer, Medford, MA) in which a piston is propelled repeatedly through the sample chamber by a controlled magnetic field. Average time travelled by the piston then measures the viscosity of the sample. Pistons measuring viscosity in the range of 0.5–5.0, 2.5–50 and 5–100 cP were calibrated using appropriate standards. A sample volume of 70 μL was used and the temperature was precisely controlled at 25 ± 0.1˚C by a peltier plate. All the samples were analyzed in duplicate and the sample chamber was thoroughly cleaned with double distilled water and dried with nitrogen before each measurement.

3.3. Intrinsic/Reduced Viscosity

Intrinsic viscosity (or reduced viscosity) of the sample was measured using Malvern's Viscotek GPCmax assembly (Worcestershire, UK) connected to model 305 Triple Detector Array (TDA) with a 7˚ angle light scattering detector (LALS), a 90˚angle light scattering detector (RALS), a refractive index detector (RI, concentration detector set at 670 nm), and a four-capillary differential viscometer (DP). A stainless steel tubing coil of ~25ft was used between auto-injector and detector for viscosity measurements. Buffer in which intrinsic viscosity was to be determined was used as the mobile phase; flow rate was maintained at 0.8 mL/min and runtime at 15 min. All the injections were made in duplicate and temperature was controlled at 25 ± 1˚C. OmniSEC software program was used for the acquisition and analysis of the Viscotek data.

3.4. Zeta Potential Measurements

Zeta potential measurements were performed using Malvern Zetasizer Nano Series (Worcestershire, UK). Dip cell (ZEN1002) and a glass cuvette assembly was used to make the measurements that required a sample volume of 800 µL. Measurements were made in duplicate at 25 ± 0.1 ˚C, and at concentrations of 4 mg/mL and 2 mg/mL for mAb and DVD-Ig™ protein, respectively. Zeta potential is calculated from electrophoretic mobility using Henry's equation,

$$\mu_E = \frac{2\varepsilon\xi f1(\kappa a)}{3\eta} \qquad (2)$$

where, μ_E is the electrophoretic mobility under the applied voltage, ε is the dielectric constant or the permittivity of the medium, η is the viscosity of the dispersant, ξ is the zeta potential in Volts and $f1(\kappa a)$ is the Henry's function. Value of $f1(\kappa a)$ depends upon the

ratio of the radius of curvature (a) to the thickness of the electrical double layer around the particle (κ). For zeta potential measurements in this study Smoluchowski approximation of 1.5 was used.[35]

3.5. Dynamic Light Scattering (DLS)

DLS studies were performed using a Malvern Instrument's Zetasizer Nano Series. A detailed procedure and experimental set-up is similar to our previous studies.[36] Malvern's DTS software was used to analyze the acquired correlogram (correlation function vs. time) and obtain the mutual diffusion coefficient (D_m). Self-diffusion coefficient (D_s) and interaction parameter (k_D) were then calculated from the measured D_m using following relation,

$$D_m = D_s(1 + k_D c + k_{2D} c^2 + k_{3D} c^3 + \cdots) \quad (3)$$

c is the concentration of the protein (g/mL).[37] In dilute solution higher order terms are neglected and linear plot of D_m as a function of concentration can be used to determine D_s and k_D from intercept and slope respectively.[38]

3.6. Static Light Scattering (SLS)

SLS studies were conducted at 25 ± 0.1˚C using a Malvern Instrument's Zetasizer NanoS to determine B_2, which signifies first deviation from ideality.[39] Sample preparation and experimental steps were similar to those used for DLS. A detailed procedure to obtain correct SLS parameters using a Malvern Zetasizer is discussed elsewhere.[40] The average scattered intensities were used to calculate B_2 by constructing the Debye plot according to the following equation,[41]

$$\frac{Kc}{R_\theta} = \frac{1}{M_w} + 2B_2c + 3B_3c^{\,2} + 4B_4c^{\,3} + \cdots \quad (4)$$

where, K is the optical constant given by

$$K = \frac{[2\pi\eta\left(\frac{d\eta}{dc}\right)]^2}{N_A\lambda_0^4} \quad (5)$$

In the above equation, R_θ is the excess Rayleigh ratio, i.e., a measure of light scattered by the solute, η is the solvent refractive index, $d\eta/dc$ is the refractive index increment of the solute, N_A is the Avogadro number, and λ_0 is the wavelength of the incident light.

4. Results and Discussion

Several factors contribute to the increased viscosity of a therapeutic protein formulation, and understanding the effect of these factors is necessary to develop a solution with minimal viscosity. The effect of the size of the protein molecule taking into account the excluded volume effect, protein-protein interactions and charges on the proteins as a function of solution conditions on the increased viscosity of DVD-Ig™ protein was investigated in this study. All these factors are inter-related, and changing certain conditions can positively impact one factor, while negatively affecting the other. For example, increasing charges on the protein molecule can increase the repulsive interactions or decrease the attractions between the molecules; however, they can still result in increased viscosity because of the electroviscous effect. Hence, rank-ordering these factors can provide valuable information on how to approach the high viscosity problem for protein formulations.

Viscosity Measurements

Viscosity for mAb and DVD-Ig™ protein solutions was analyzed for samples prepared in water and buffer. Samples dialyzed in water are also referred to as 0 mM ionic strength solution or salt-free solutions; pH of the solution was measured to be pH 6.1 ± 0.1. Figure 1 show viscosity profiles of mAb and DVD-Ig™ protein as a function of concentration at pH 6.1 at 0 mM (water) and at 15 mM ionic strength (30 mM histidine buffer). Compared to mAb, DVD-Ig™ protein exhibited significantly higher viscosity which increased sharply with increasing concentration. For both the molecules higher viscosity was observed at 0 mM (solid line), which decreases as the ionic strength was increased to 15 mM (dashed line).

4.1. Size of the Protein Molecule

DVD-Ig™ protein is a bispecific antibody-like molecule with an additional variable domain resulting in increased size and asymmetry with respect to mAb. This increase in the size of the molecule can result in an inherent increase in the viscosity as observed in Figure 1 and was investigated further by measuring intrinsic viscosity and hydrodynamic size of the molecule.

4.1.1. Reduced/ Apparent Intrinsic Viscosity

Intrinsic viscosity $[\eta]$ is the intrinsic volume contribution of the dissolved or dispersed solute to viscosity of the solution. It is the property of the shape and size/hydration of the protein molecule and can be represented as;[42]

$$[\eta] = \nu . V_s \tag{6}$$

where, ν is the Simha shape parameter[43] and V_s indicates the size or hydrated or swollen volume. Intrinsic viscosity is usually determined by linear extrapolation of reduced viscosity (η_{red}) or inherent viscosity (η_{inh}) to zero concentration. It can also be directly determined using single point determination methods (Viscotek) at extremely dilute conditions.[44,45] From Figure 2a, reduced viscosity for DVD-Ig™ protein determined from Viscotek increases with increasing concentrations (up to 1.0 mg/mL) and is significantly higher for 1.0 mg/mL; hence is not the true intrinsic viscosity for the solution. Further lower concentrations could not be analyzed due to low signal to noise ratio.

For comparative analysis, reduced viscosity at 1.0 mg/mL is considered as the apparent intrinsic viscosity $[\eta]_{app,}$ and is plotted in Figure 2b at 0 and 15 mM ionic strength for mAb and DVD-Ig™ protein. Viscosity obtained from extrapolation to c→0 for mAb and DVD-Ig™ protein (from Figure 2a) at 0 mM ionic strength is also plotted in Figure 2b as extrapolated intrinsic viscosity ($[\eta]_{exp}$). At 0 mM ionic strength, $[\eta]_{exp}$ for DVD-Ig™ protein is higher (9.97 mL/g) than for mAb (6.2 mL/g), indicating that the size and shape of the molecule is larger for DVD-Ig™ protein. Similar trend is observed at 15 mM ionic strength, where $[\eta]_{app}$ for DVD-Ig™ protein and mAb is 8.65 mL/g and 5.9 mL/g, respectively. The intrinsic viscosity value obtained for mAb is around 6.0 mL/g and is similar to the values reported in the literature.[19,22] There are no reports for viscosity or intrinsic viscosity values for DVD-Ig™ protein in the literature. At 0 mM ionic strength, non-ideality of the DVD-Ig™ protein solution even at low protein concentration of ~1.0 mg/mL was observed from both reduced viscosity measurements (Figure 2a) as well as light scattering measurements (Figure 4), while 15 mM ionic strength solutions are fairly linear over a higher concentration range. For intrinsic viscosity measurements (by linear extrapolation or single point method),

ideality of the solution is a required condition and none of the available techniques are sensitive enough to measure the true intrinsic viscosity of the protein in water due to its non-ideal behavior even at extremely dilute conditions. The intrinsic viscosity values obtained at 15 mM, for both mAb and DVD-Ig™ protein, are used for further analysis.

Shape parameter presented in equation 6 is 2.5 for spherical particles[11] and values larger than 2.5, indicate increased asymmetric shape of the macromolecule. mAb is an asymmetric molecule due to its Y-like shape and has larger intrinsic viscosity (~6 mL/g)[19,22] than globular proteins which are spherical in shape. DVD-Ig™ protein, exhibits further increased asymmetry compared to mAb due to the additional variable domain, and can further result in increased intrinsic viscosity of the molecule, which is around ~8.7 mL/g (Figure 2b). Intrinsic viscosity measurements ($[\eta]_{app}$ and $[\eta]_{exp}$) at both the conditions (0 mM and 15 mM ionic strength) indicate that the inherent contribution of DVD-Ig™ protein to the overall solution viscosity is higher than mAb due to both its increased size (hydration) as well as increased asymmetry.

4.1.2. Hydrodynamic Radius

Hydrodynamic diameter (d_H) for mAb and DVD-Ig™ protein solutions was calculated from self-diffusion coefficient (D_s), using the Stokes–Einstein equation;

$$D_s = \frac{kT}{3\pi\eta\, d_H} \tag{7}$$

where, k is the Boltzmann constant, T is the absolute temperature, and η is the solution viscosity.

D_s is obtained from the intercept of a linear plot of mutual diffusion coefficient (measured using Dynamic light scattering) against concentration. Values for D_s and hydrodynamic

diameter (d_H) at different solution conditions are compiled in Table 1. Hydrodynamic diameter (d_H) in the salt-free solutions are lower than in buffered solutions due to non-linearity at low concentrations (linear and polynomial fit will be discussed in the next section). At 15 mM ionic strength, d_H for DVD-Ig™ protein is ~14 nm and is larger than that for mAb, which is ~11 nm, indicating that as the size of the molecule increases, protein diffuses slowly resulting in the increased drag in the solution, increasing its viscosity.

4.1.3. Excluded Volume Effect

Excluded volume or crowding in protein solutions results in a significant contribution to the increased viscosity at higher concentrations. Excluded volume (volume of the solution not available to another molecule) is roughly calculated as 6.7 times the molecular volume of an equivalent sphere (taking into account surface roughness).[46] Assuming, mAb (r_{mAb} ~ 5.5 nm) and DVD-Ig™ protein (r_{DVD} ~ 7 nm) represent equivalent spheres, ratio of the excluded volume contribution can be represented as,

$$\frac{V_{ex,mAb}}{V_{ex,DVD}} = \frac{r_{mAb}^3}{r_{DVD}^3} = 0.54 \quad (8)$$

Assuming only hard-sphere interactions are present in protein solutions at higher concentrations, from equation 8, excluded volume by itself results in roughly twice the contribution to the viscosity for DVD-Ig™ protein than mAb.

The contribution of excluded volume to viscosity of the protein solutions was further evaluated using the modified Ross and Minton equation, which includes the concentration effect on molecular crowding and intrinsic viscosity;[19]

$$\eta_{inh} = \frac{k}{\nu}[\eta] ln(\eta_{rel}) + [\eta] \quad (9)$$

where, η_{inh} (η_{inh} =η_{rel}/c)is the inherent viscosity, k is the crowding factor, ν is the shape parameter, [η] is the intrinsic viscosity and η_{rel} (η_{rel}=η/η_0) is the relative viscosity of the solution. A linear plot of η_{inh} against $ln(\eta_{rel})$ indicates only excluded volume contribution to the viscosity and deviation from linearity indicates that interactions other than excluded volume are present in the solution resulting in increased viscosity. A curvature with increasing concentration indicates that the slope is changing either due to change in shape factor (due to increased asymmetry or self-association) or increased crowding in the solution.[19,47]

The intrinsic viscosity value of 8.7 mL/g, determined from Viscotek measurements (Figure 2b), was used for calculations of inherent viscosity for DVD-Ig™ protein. Simha shape parameter (ν) for sphere is 2.5; as the asymmetry of the molecule increases, ν deviates from 2.5.[42,43] Crowding factor (k) varies from 1.35 to 1.91 and represents the inverse of maximum packing density (Φ) which is usually between 0.52-0.74 (0.74 being maximum for spherical particles).[48] The k/ν ratio are varied from 0.2 to 0.5 to take into account change in shape and/or crowding in the solution. Figure 3a shows calculated relative viscosity for DVD-Ig™ protein only due to excluded volume contribution using Equation 9. An exponential increase in the relative viscosity was observed at higher k/ν ratio (0.5) at higher concentrations. Relative viscosity was also calculated for mAb ([η] = 5.9 mL/g) at highest k/ν value (0.5) and compared with relative viscosity of DVD-Ig™ protein (Figure 3b). Excluded volume contribution to relative viscosity for DVD-Ig™ protein is higher than that for mAb, however, this significant difference in viscosity is observed at concentration >100 mg/mL. Relative viscosities are less than 5 cP (Figure 3b inset) in the lower concentration range (< 100 mg/mL) where measured viscosities of the two proteins are compared in Figure

1. This indicates that though the size of the molecule is an important factor contributing to the solution viscosity, its effect is significant only at higher concentrations, and increased viscosity of DVD-Ig™ protein is due to the contribution from additional factors/forces in the solution.

4.2. Electroviscous Effect

Charges regulate the electroviscous effect, which are repulsive interactions in solution, and influence the viscosity behavior especially at pH conditions away from the pI of the molecule. High viscosity at 0 mM was observed for both mAb and DVD-Ig™ protein, which decreased on increasing the ionic strength. This can be attributed to the electroviscous effects in solution and was investigated further by measuring zeta potential of the molecule and interactions in the solution.

4.2.1. Lights Scattering

Second virial coefficient (B_2) and interaction parameter (k_D) determined from Static and Dynamic Light scattering, respectively, are routinely used to characterize the nature of intermolecular interactions in dilute solutions. Correlation between viscosity and protein-protein interactions measured by light scattering is well documented in the literature.[18,21,24,25,49-51] A positive B_2 indicates repulsive interactions in solution, while a negative B_2 indicates attractive interactions. The interaction parameter, k_D is represented as,

$$k_D = 2B_2M_w - (\zeta_1 + 2v_{sp}) \quad (10)$$

where, ζ_1 is the coefficient of the linear term in the virial expansion of the frictional coefficient as a function of solute concentration and v_{sp} is the partial specific volume of the

solute. k_D has contributions from both the thermodynamic (B_2) and hydrodynamic ($\zeta_1 + 2\nu_{sp}$) parameters. Similar to B_2, a positive k_D implies repulsive interactions and a negative k_D implies attractive intermolecular interactions in solution. There is a small range of negative k_D values where interactions are repulsive in nature, i.e., hydrodynamic contribution is larger than the thermodynamic contribution.

Figure 4a shows a plot of scattering intensity measured as Kc/R_θ against concentration (Static light scattering) and Figure 4b shows a plot of D_m or mutual diffusion coefficient against concentration (Dynamic light scattering) for mAb and DVD-Ig™ protein at 0 and 15 mM ionic strengths. Both, mAb and DVD-Ig™ protein molecules show positive slopes at 0 mM indicating repulsive interactions, while 15 mM ionic strength solutions show negative slopes indicating attractive interactions.

At 0 mM, DVD-Ig™ protein has a larger positive slope compared to mAb, indicating stronger repulsive interactions. Slopes for both mAb and DVD-Ig™ protein show non-linearity with increasing concentration (in the range of 2-10 mg/mL). At this condition, higher order terms dominate as represented in equations 3 and 4 (for DLS and SLS, respectively) and cannot be neglected. A linear plot of intensity (SLS) or mutual diffusion coefficient (DLS) is a required condition for the calculation of protein-protein interactions (k_D and B_2) and other parameters (Mw, D_s, r_H) from light scattering. Therefore, all the parameters measured from Static and Dynamic light scattering studies, considering both linear part (in low concentration range) and polynomial fit (over the entire concentration range) were calculated and are summarized in Table 1. For both the molecules, values obtained from linear fit and polynomial fit are in close agreement. Both k_D and B_2 values for DVD-Ig™ protein are roughly three times larger than for mAb at 0 mM ionic strength. At 15

mM ionic strength, the slopes are negative for both the molecules, but the difference in the attractive interactions is not as significant as that observed at 0 mM ionic strength.

4.2.2. Zeta Potential Measurements and Charge Calculations

Effective charge on the molecule is calculated from the measured zeta potential values (ξ) using linearized Poisson–Boltzmann equation, also known as the Debye–Huckel approximation, assuming an equivalent sphere,[35]

$$z = \frac{4\pi\varepsilon a(1+\kappa a)\xi}{e} \tag{11}$$

where, e is the electronic charge, a is the particle radius and κ is the inverse Debye length. Radius "a" is substituted by r_H or hydrodynamic radius for equivalent sphere calculated from D_s (self-diffusion coefficient), using Stokes-Einstein equation (eq 7). The inverse Debye length, κ, is related to the square-root of the ionic strength of the solution; on increasing ionic strength, κ decreases, thereby reducing the effective charge on the molecule. For calculation purposes, 0 mM solution is considered to have an ionic strength of 0.1 mM.

Figure 5 shows a plot of measured zeta potential values for mAb and DVD-Ig™ protein at 0 mM and 15 mM ionic strength at pH 6.1. The isoelectric point (pI) for the mAb molecule is 6.5 and for DVD-Ig™ protein is around 7.0-7.5. The zeta potential values for mAb and DVD-Ig™ protein are similar at 0 mM (~16.5 mV). However, the effective charge values are significantly higher for DVD-Ig™ protein (116 Z) than mAb (87 Z), as the Poisson Boltzman equation (eq 11) takes into account the size (hydrodynamic radius) of the protein molecule which is larger for DVD-Ig™ protein (~7 nm) compared to mAb (~5.5 nm). Higher the charge associated with the molecule, larger will be the hydration and hence strong repulsive interactions as indicated by large positive k_D and B_2 values (Figure 4) at 0 mM. At

15 mM ionic strength, zeta potentials are positive for both the molecules, and DVD-Ig^{TM} protein has higher value than mAb, 4.9 mV and 2.2 mV, respectively. On increasing the ionic strength to 15 mM, charges on the molecule decrease significantly and interactions become attractive in nature, thereby, reducing the electroviscous effects and viscosity of the solution.

High viscosity at 0 mM is due to the electroviscous effect, for both mAb and DVD-Ig^{TM} protein solutions. Both, intrinsic viscosity values and hydrodynamic radius indicate increased size of DVD-Ig^{TM} protein compared to mAb. However, the excluded volume calculations show that the effect of the size of the molecule on viscosity is dominant only at higher concentrations (>100 mg/mL). At concentrations below 100 mg/mL, there may be additional contributions to the increased viscosity of DVD-Ig^{TM} protein compared to mAb and therefore the effect of pH and ionic strength was further studied.

4.3. Protein-Protein Interactions- Formulation factors

Formulation factors (pH, ionic strength, salt-type, excipients) significantly affect protein properties such as charges, dipoles, hydrophobic patches, etc., resulting in changes in physicochemical properties. The effect of pH and ionic strength was investigated on the solution viscosity (Figure 6) for DVD-Ig^{TM} protein and was correlated to zeta potential (Figure 7) at different pHs, intermolecular protein-protein interactions as measured by light scattering (Figure 8) and T_{cloud} (Figure 9). Detailed experimental procedure to determine T_{cloud} of a solution is described in Chapter 4. Briefly, percent transmittance for a sample is measured at 510 nm using UV-vis spectrophotometer as the temperature of the solution is lowered. In the current study, for comparative evaluation, temperature where percent transmittance reaches 70 is termed as T_{cloud}.

4.3.1. Viscosity Measurements

Figure 6 shows a plot of viscosity for DVD-Ig^{TM} protein as a function of concentration at different pHs and at ionic strength of 15 mM (solid line) and 50 mM (dotted line). At pH 5.1, viscosity values for DVD-Ig^{TM} protein are lower compared to the other pHs. Ionic strength has no effect on the viscosity at pH 5.1. At a lower ionic strength of 15 mM, viscosity values are significantly higher at pH conditions close to the pI of the molecule (pH 6.1, 6.6 and 7.1). Viscosities of the protein do not change with change in the pH (within experimental error). On increasing the ionic strength to 50 mM, viscosity decreases compared to 15 mM at all pH conditions.

4.3.2. Interactions in DVD-Ig^{TM} Solutions

Figure 7 shows a plot of zeta potential for DVD-Ig^{TM} protein as a function of pH at 15 mM ionic strength. Molecules carry a net positive charge at all pH conditions studied. At pH 5.1, molecules have a higher zeta potential value (+8.76 mV) which decreases gradually as the pH is adjusted close to the pI of the molecule (~7.0-7.5). At pH 7.1, though the molecules have low zeta potential value (+1.30 mV), there is no crossover to negative values; pI of the molecule is above pH 7.1.

Figures 8a and 8b shows plots of interactions measured as B_2 and k_D in dilute solution for DVD-Ig^{TM} protein as a function of pH at ionic strength of 15 mM (solid line) and 50 mM (dashed line). B_2 and k_D show similar trends with changing solution conditions. Interactions in solutions were also assessed by measuring T_{cloud} of the solution as a function of pH and ionic strength and are plotted in Figure 9a and 9b for 16 and 60 mg/mL protein concentrations, respectively. In our previous studies, we have established a good correlation

between shifts in T_{cloud} (temperature that marks the onset of liquid-liquid phase separation in solution) and change in attractive interactions with change in solution conditions; low T_{cloud} values indicate weak attractive interactions in solution, while high T_{cloud} values indicate strong attractions in solution (Chapter 4). The change in T_{cloud} with change in pH and ionic strength is consistent at both 16 and 60 mg/mL protein concentration; T_{cloud} values at 60 mg/mL are slightly higher than at 16 mg/mL.

At pH 5.1, which is away from the pI of the molecule, viscosity is minimal compared to other pH conditions and is not affected by the ionic strength. Zeta potential measurement indicate presence of significant effective charge on the molecule at 15 mM ionic strength, which results in repulsion as indicated by positive k_D and B_2 values (B_2= +1.28*10^{-4} mol.mL/g^2, k_D= +6.38 mL/g). On increasing the ionic strength to 50 mM, negative B_2 and k_D values indicate weak attractive interactions in solution (B_2= -0.27*10^{-4} mol.mL/g^2, k_D=-11.08 mL/g) and can be attributed to charge shielding at high ionic strength. However, these attractive interactions are not strong enough to have any significant effect on solution viscosity. At low ionic strength, high charge and repulsive interactions indicate electroviscous effect in solution, which decreases on increasing the ionic strength. However, contribution from electroviscous effect to the overall solution viscosity is not as significant (compared to other pHs) and is opposite to our previous observation of high viscosity in salt-free solutions/0 mM ionic strength at pH 6.1 (Figure 1). This contradiction in the electroviscous contribution to the viscosity of DVD-Ig^{TM} protein in presence and absence of ions will be discussed later.

At pH 6.1, 6.6 and 7.1, there is no change in viscosity with change in pH of the solution at both 15 mM and 50 mM ionic strength (Figure 6); however, DVD-Ig^{TM} protein

has significant attractive interactions as seen from light scattering measurements (Figure 8). At pH 6.1, attractive interactions are present, which do not change with ionic strength (B_2= ~-1.1*10^{-4} mol.mL/g^2, k_D=~-35 mL/g). At pH 6.6 and 15 mM ionic strength, interactions are strongly attractive compared to the other pH conditions as indicated by larger negative B_2 and k_D values (B_2= -2.3*10^{-4} mol.mL/g^2, k_D=-61.46 mL/g) and decreases at 50 mM ionic strength. Similar trend is observed at pH 7.1, where attractive interactions decrease on increasing the ionic strength. At 50 mM ionic strength, significant attractive interactions are present in the solution and are almost similar in magnitude at pH 6.1, 6.6 and 7.1 (B_2 ~ -1.0*10^{-4} mol.mL/g^2). From Figure 9a and 9b, at pH 6.1, T_{cloud} shifts to higher temperatures on increasing the ionic strength indicating increased attractive interactions in solution. Hydrophobic interactions are the only short-range attractive interactions that become dominant as the ionic strength of the solution is increased, thereby increasing the T_{cloud} at pH 6.1. T_{cloud} values and hence attractive interactions decrease at pH 6.6 and 7.1, on increasing the ionic strength from 15 to 50 mM. The decrease is more significant at pH 7.1 than at pH 6.6, possibly due to the presence of significant dipoles on the molecule close to its pI (> pH 7.1). In Chapter 4, we have discussed that both hydrophobic interactions and dipole-mediated interactions results in increased tendency of DVD-Ig^{TM} protein to undergo phase separation (hence indicating shifts in T_{cloud}). These attractive interactions also result in increased viscosity of DVD-Ig^{TM} protein solution and contribution of each type of interaction was investigated further.

4.3.3. Contribution of Dipole and Hydrophobic Interactions

Charge-dipole interactions are mid-range (show r^{-4} distance dependence)[36,52,53] and hence result in strong attractions even in dilute solutions as observed from light scattering. Increasing ionic strength decreases charge and dipolar interactions in solutions, while ionic strength has no effect on hydrophobic interactions. For further understanding the contribution of dipole and hydrophobic interactions, k_D obtained from DLS is plotted against B_2 obtained from SLS at different pH conditions and as a function of ionic strength (Figure 10). All samples prepared for viscosity measurements are in histidine buffer while, the DVD-Ig™ protein samples prepared at pHs where k_D and B_2 from DLS and SLS was determined (for Figure 10) are in different buffer systems (pH 5.1-acetate, pH 6.1-histidine, pH 6.6, 7.0 and 8.1-phosphate buffer). Plots are linear at all three ionic strengths studied; 15 mM (♦), 50 mM (Δ) and 150 mM (○). Slopes are fairly constant; however, the intercept for all the three conditions vary. From equation 10, a linear plot of k_D vs. B_2 gives $2M_w$ as the slope while the intercept represents the hydration parameter ($\zeta_1+2\ v_{sp}$). As the ionic strength is increased the hydration on the protein molecules decreases and the effect is significant from 15 mM (12.97 units) to 50 mM (6.87 units), while on increasing the ionic strength further to 150 mM (5.22 units), hydration decreases to lesser extent. At 150 mM, hydrodynamic contribution to k_D decreases significantly compared to 15 mM, however the thermodynamic contribution results in overall attractive interactions in solution, which are hydrophobic in nature.

Depending on the solution conditions, i.e., pH and ionic strength, contribution of these interactions changes; at pH 6.1 hydrophobic interactions are dominant, while at pH 7.1 dipole interactions contribute significantly to the solution viscosity. At pH 6.6, both hydrophobic and dipole-charge mediated interactions are present in the solution. At low ionic

strength, more than one intermolecular protein interactions contribute to attractions and hence increased solution viscosity, while at high ionic strengths, where dipole and charge mediated interactions are shielded, hydrophobic interactions dominate solution viscosity.

4.4. Electroviscous Effect in Presence and Absence of Ions

Electroviscous effect contribution to the overall solution viscosity is opposite for DVD-Ig^{TM} protein at two different conditions; pH 6.1-0 mM ionic strength, where viscosity is significantly higher (Figure 1), and at pH 5.1- 15 mM ionic strength, where viscosity is minimal (Figure 6). Electroviscous effect at pH 6.1 (0 mM ionic strength) resulting in significantly high viscosity is also contradictory to the majority of the studies in the literature, where, the electroviscous effect contribution to the viscosity are significant only in relatively dilute solutions and contribution of attractive interactions to viscosity increases as protein concentration increases.[24,54]

From light scattering studies, interactions are repulsive at both the conditions; however, k_D and B_2 in the buffered solutions at pH 5.1- 15 mM ionic strength (k_D = + 5.90 mL/g, B_2= +0.64*10^{-4} mol.mL/g^2) are lower than at pH 6.1- 0 mM ionic strength (k_D = + 1890 mL/g, B_2= +63.5*10^{-4} mol.mL/g^2). The measured zeta potential values at pH 5.1- 15 mM ionic strength and at pH 6.1- 0 mM ionic strength are +8.76 mV and +16.7 mV, respectively. The pI of the molecule is in the range of pH 7.0-7.5; therefore, DVD-Ig^{TM} protein should carry a higher positive charge (surface potential) at pH 5.1 than at pH 6.1. However, according to the double layer theory, the measured zeta potential (potential at the boundary of the slipping plane), which is influenced by the concentration and charge of ions in solution, is higher at low ionic strength than at high ionic strength (irrespective of the pH

of the solution).[41] As previously described (Figure 10), hydrodynamic contribution in protein solution decreases on increasing the ionic strength. At pH 5.1 and 15 mM ionic strength, the presence of oppositely charged ions from buffer species results in the formation of a double layer associated with the molecule which gives rise to the primary electroviscous effect. The thickness of this double layer (also known as inverse Debye length) is inversely related to the square-root of the ionic strength of the solution and is ~2.5 nm at 15 mM ionic strength. While at 0 mM ionic strength, there is no double layer associated with the molecule. Hence, for salt-free solutions only OH^- and H^+ species are associated with proteins which results in an extended field that is affected by the charge on the molecule, as compared to the double layer at 15 mM ionic strength which has a finite thickness. This in turn, results in structuring of the water molecules around the protein which significantly increases viscosity in the absence of ions. Results indicate that, though pH of the solution is an important factor that determines the presence of charges on the molecule, ionic strength has a more significant impact on hydration and hence the viscosity of the protein solution.

4.5. Contributions of Individual Factors

Viscosity is influenced by many factors, and the net effect involves interplay of these factors. Figure 11 provides an overview of the contribution of the dominant individual forces to the solution viscosity. For positive k_D values, the electroviscous contribution is minimal in the presence of ions and it is maximum in the absence of ions. At pH 7.1, close to the pI of DVD-Ig™ protein where k_D values are negative, both the dipole-mediated interactions and hydrophobic interactions contribute to the attractive interactions, but as the ionic strength is increased from 15 to 50 mM the dipole contribution is significantly reduced and hydrophobic

contribution becomes dominant. The excluded volume contribution is always present in the solution; however, its effect on viscosity is minimal at lower concentrations (approximately 100 mg/mL or less) compared to other forces. At higher concentrations, excluded volume contribution shows an exponential increase as seen in Figure 3a. Based on these studies, contribution from various factors to increased viscosity of DVD-Ig^{TM} protein can be rank ordered for solutions with protein concentrations of less than 100 mg/mL as: electroviscous effects in absence of ions > dipole-mediated attractive interactions>hydrophobic interactions> electroviscous effects in presence of ions>size of the molecule ~excluded volume effects.

5. Conclusion

DVD-Ig^{TM} protein shows higher viscosity compared to a monoclonal antibody molecule at similar solution conditions. Large size of the molecule inherently contributes to the increased viscosity due to larger intrinsic viscosity (also considering increased asymmetry of the molecule); however the size effects are significant only at higher concentrations. Protein molecules exhibit a unique behavior in absence of any ions or in water, where significantly high solution viscosity is due to high charge on the molecule and hydration. Ionic strength plays a dominant role in modulating solution viscosity for DVD-Ig^{TM} protein than pH of the solution. Attractive protein-protein interactions also contribute significantly to increased viscosity of DVD-Ig^{TM} protein; contribution of dipole-mediated interactions is greater than hydrophobic interactions. However, interplay of more than one type of interactions at high concentrations contributes to the overall solution viscosity.

6. Acknowledgments

Authors would like to thank AbbVie Bioresearch Center, Worcester, MA for material and financial support for the work.

7. References

1. Evans JB, Syed BA 2014. From the analyst's couch: Next-generation antibodies. Nature reviews Drug discovery 13(6):413-414.
2. Reichert JM, Beck A, Lugovskoy AA, Wurch T, Coats S, Brezski RJ 2014. 9th annual European Antibody Congress, November 11-13, 2013, Geneva, Switzerland. mAbs 6(2):309-326.
3. Harris RJ SS, Winter C. 2004. Commercial Manufacturing Scale Formulation and Analytical Characterization of Therapeutic Recombinant Antibodies. Drug Dev Res 61:137–154.
4. Shire SJ, Shahrokh Z, Liu J 2004. Challenges in the development of high protein concentration formulations. Journal of pharmaceutical sciences 93(6):1390-1402.
5. Daugherty AL, Mrsny RJ 2006. Formulation and delivery issues for monoclonal antibody therapeutics. Advanced drug delivery reviews 58(5-6):686-706.
6. Burckbuchler V, Mekhloufi G, Giteau AP, Grossiord JL, Huille S, Agnely F 2010. Rheological and syringeability properties of highly concentrated human polyclonal immunoglobulin solutions. European journal of pharmaceutics and biopharmaceutics : official journal of Arbeitsgemeinschaft fur Pharmazeutische Verfahrenstechnik eV 76(3):351-356.
7. Allmendinger A, Fischer S, Huwyler J, Mahler H-C, Schwarb E, Zarraga IE, Mueller R 2014. Rheological characterization and injection forces of concentrated protein formulations: An alternative predictive model for non-Newtonian solutions. European Journal of Pharmaceutics and Biopharmaceutics 87(2):318-328.
8. Simha R 1949. Effect of concentration on the viscosity of dilute solutions. Journal of research of the National Bureau of Standards 42:409-417.
9. Hall D, Minton AP 2003. Macromolecular crowding: qualitative and semiquantitative successes, quantitative challenges. Biochimica et biophysica acta 1649(2):127-139.
10. Zhou HX, Rivas G, Minton AP 2008. Macromolecular crowding and confinement: biochemical, biophysical, and potential physiological consequences. Annual review of biophysics 37:375-397.
11. Mooney M 1951. The viscosity of a concentrated suspension of spherical particles. Journal of Colloid Science 6(2):162-170.
12. Ross PD, Minton AP 1977. Hard quasispherical model for the viscosity of hemoglobin solutions. Biochemical and biophysical research communications 76(4):971-976.
13. Bull HB 1940. The electroviscous effect in egg albumin solutions. Transactions of the Faraday Society 35(0):80-84.
14. Buzzell JG, Tanford C 1956. The Effect of Charge and Ionic Strength on the Viscosity of Ribonuclease. The Journal of Physical Chemistry 60(9):1204-1207.
15. Tanford C, Buzzell JG 1956. The Viscosity of Aqueous Solutions of Bovine Serum Albumin between pH 4.3 and 10.5. The Journal of Physical Chemistry 60(2):225-231.
16. Liu J, Nguyen MD, Andya JD, Shire SJ 2005. Reversible self-association increases the viscosity of a concentrated monoclonal antibody in aqueous solution. Journal of pharmaceutical sciences 94(9):1928-1940.
17. Kanai S, Liu J, Patapoff TW, Shire SJ 2008. Reversible self-association of a concentrated monoclonal antibody solution mediated by Fab-Fab interaction that impacts solution viscosity. Journal of pharmaceutical sciences 97(10):4219-4227.

18. Yadav S, Liu J, Shire SJ, Kalonia DS 2010. Specific interactions in high concentration antibody solutions resulting in high viscosity. Journal of pharmaceutical sciences 99(3):1152-1168.
19. Yadav S, Shire SJ, Kalonia DS 2010. Factors affecting the viscosity in high concentration solutions of different monoclonal antibodies. Journal of pharmaceutical sciences 99(12):4812-4829.
20. Yadav S, Laue TM, Kalonia DS, Singh SN, Shire SJ 2012. The Influence of Charge Distribution on Self-Association and Viscosity Behavior of Monoclonal Antibody Solutions. Molecular pharmaceutics 9(4):791-802.
21. Connolly BD, Petry C, Yadav S, Demeule B, Ciaccio N, Moore JM, Shire SJ, Gokarn YR 2012. Weak interactions govern the viscosity of concentrated antibody solutions: high-throughput analysis using the diffusion interaction parameter. Biophysical journal 103(1):69-78.
22. Zarraga IE, Taing R, Zarzar J, Luoma J, Hsiung J, Patel A, Lim FJ 2013. High shear rheology and anisotropy in concentrated solutions of monoclonal antibodies. Journal of pharmaceutical sciences 102(8):2538-2549.
23. Yearley Eric J, Zarraga Isidro E, Shire Steven J, Scherer Thomas M, Gokarn Y, Wagner Norman J, Liu Y 2013. Small-Angle Neutron Scattering Characterization of Monoclonal Antibody Conformations and Interactions at High Concentrations. Biophysical journal 105(3):720-731.
24. Yadav S, Shire SJ, Kalonia DS 2012. Viscosity behavior of high-concentration monoclonal antibody solutions: correlation with interaction parameter and electroviscous effects. Journal of pharmaceutical sciences 101(3):998-1011.
25. Salinas BA, Sathish HA, Bishop SM, Harn N, Carpenter JF, Randolph TW 2010. Understanding and modulating opalescence and viscosity in a monoclonal antibody formulation. Journal of pharmaceutical sciences 99(1):82-93.
26. Yearley EJ, Godfrin PD, Perevozchikova T, Zhang H, Falus P, Porcar L, Nagao M, Curtis JE, Gawande P, Taing R, Zarraga IE, Wagner NJ, Liu Y 2014. Observation of small cluster formation in concentrated monoclonal antibody solutions and its implications to solution viscosity. Biophysical journal 106(8):1763-1770.
27. Du W, Klibanov AM 2011. Hydrophobic salts markedly diminish viscosity of concentrated protein solutions. Biotechnology and bioengineering 108(3):632-636.
28. Guo Z, Chen A, Nassar RA, Helk B, Mueller C, Tang Y, Gupta K, Klibanov AM 2012. Structure-activity relationship for hydrophobic salts as viscosity-lowering excipients for concentrated solutions of monoclonal antibodies. Pharmaceutical research 29(11):3102-3109.
29. Kamerzell TJ, Pace AL, Li M, Danilenko DM, McDowell M, Gokarn YR, Wang YJ 2013. Polar solvents decrease the viscosity of high concentration IgG1 solutions through hydrophobic solvation and interaction: Formulation and biocompatibility considerations. Journal of pharmaceutical sciences 102(4):1182-1193.
30. He F, Woods CE, Trilisky E, Bower KM, Litowski JR, Kerwin BA, Becker GW, Narhi LO, Razinkov VI 2011. Screening of monoclonal antibody formulations based on high-throughput thermostability and viscosity measurements: Design of experiment and statistical analysis. Journal of pharmaceutical sciences 100(4):1330-1340.

31. Inoue N, Takai E, Arakawa T, Shiraki K 2014. Specific Decrease in Solution Viscosity of Antibodies by Arginine for Therapeutic Formulations. Molecular pharmaceutics 11(6):1889-1896.
32. Chen B, Bautista R, Yu K, Zapata G, Mulkerrin M, Chamow S 2003. Influence of Histidine on the Stability and Physical Properties of a Fully Human Antibody in Aqueous and Solid Forms. Pharmaceutical research 20(12):1952-1960.
33. Schmit JD, He F, Mishra S, Ketchem RR, Woods CE, Kerwin BA 2014. Entanglement Model of Antibody Viscosity. The Journal of Physical Chemistry B 118(19):5044-5049.
34. Sarangapani Prasad S, Hudson Steven D, Migler Kalman B, Pathak Jai A 2013. The Limitations of an Exclusively Colloidal View of Protein Solution Hydrodynamics and Rheology. Biophysical journal 105(10):2418-2426.
35. Hunter RJ. 1981. Zeta potential in colloid science : principles and applications. ed., London; New York: Academic Press.
36. Raut AS, Kalonia DS 2015. Opalescence in Monoclonal Antibody Solutions and Its Correlation with Intermolecular Interactions in Dilute and Concentrated Solutions. Journal of pharmaceutical sciences 104(4):1263-1274.
37. I. T. 2002. Polymer solutions: An introduction to physical properties. ed., New York: Wiley.
38. Berne BJ, Pecora R. 2000. Dynamic light scattering: with applications to chemistry, biology, and physics. ed.: Courier Dover Publications.
39. George A, Wilson WW 1994. Predicting protein crystallization from a dilute solution property. Acta crystallographica Section D, Biological crystallography 50(Pt 4):361-365.
40. Yadav S, Scherer TM, Shire SJ, Kalonia DS 2011. Use of dynamic light scattering to determine second virial coefficient in a semidilute concentration regime. Analytical biochemistry 411(2):292-296.
41. Hiemenz PC, Rajagopalan R. 1997. Principles of Colloid and Surface Chemistry, revised and expanded. ed.: CRC Press.
42. Harding SE 1997. The intrinsic viscosity of biological macromolecules. Progress in measurement, interpretation and application to structure in dilute solution. Progress in Biophysics and Molecular Biology 68(2–3):207-262.
43. MEHL JW, ONCLEY JL, SIMHA R 1940. VISCOSITY AND THE SHAPE OF PROTEIN MOLECULES. Science 92(2380):132-133.
44. Solomon OF, Ciută IZ 1962. Détermination de la viscosité intrinsèque de solutions de polymères par une simple détermination de la viscosité. Journal of Applied Polymer Science 6(24):683-686.
45. Saluja A, Kalonia DS 2005. Application of ultrasonic shear rheometer to characterize rheological properties of high protein concentration solutions at microliter volume. Journal of pharmaceutical sciences 94(6):1161-1168.
46. Neal BL, Lenhoff AM 1995. Excluded volume contribution to the osmotic second virial coefficient for proteins. AIChE Journal 41(4):1010-1014.
47. Lilyestrom WG, Yadav S, Shire SJ, Scherer TM 2013. Monoclonal Antibody Self-Association, Cluster Formation, and Rheology at High Concentrations. The Journal of Physical Chemistry B 117(21):6373-6384.

48. Zholkovskiy EK, Adeyinka OB, Masliyah JH 2006. Spherical Cell Approach for the Effective Viscosity of Suspensions. The Journal of Physical Chemistry B 110(39):19726-19734.
49. Saito S, Hasegawa J, Kobayashi N, Kishi N, Uchiyama S, Fukui K 2012. Behavior of monoclonal antibodies: relation between the second virial coefficient (B (2)) at low concentrations and aggregation propensity and viscosity at high concentrations. Pharmaceutical research 29(2):397-410.
50. Chari R, Jerath K, Badkar AV, Kalonia DS 2009. Long- and short-range electrostatic interactions affect the rheology of highly concentrated antibody solutions. Pharmaceutical research 26(12):2607-2618.
51. Saluja A, Badkar AV, Zeng DL, Nema S, Kalonia DS 2007. Ultrasonic storage modulus as a novel parameter for analyzing protein-protein interactions in high protein concentration solutions: correlation with static and dynamic light scattering measurements. Biophysical journal 92(1):234-244.
52. Laue T 2012. Proximity energies: a framework for understanding concentrated solutions. Journal of molecular recognition : JMR 25(3):165-173.
53. Israelachvili JN. 2011. Intermolecular and Surface Forces Third ed., San Diego: Academic Press.
54. Yadav S, Shire SJ, Kalonia DS 2011. Viscosity analysis of high concentration bovine serum albumin aqueous solutions. Pharmaceutical research 28(8):1973-1983.

8. Table and Figure

Table 1: Parameters measured from Dynamic and Static Light scattering using equation 3 and 4, respectively, for mAb and DVD-Ig^{TM} protein.

Parameter	**mAb**			**DVD-Ig^{TM}**		
	0 mM (linear fit)	0 mM (polynomial fit)	15 mM	0 mM (linear fit)	0 mM (polynomial fit)	15 mM
k_D **(mL/g)**	592	650	-35	1890	2017	-35.8
B_2 ***10^{-4} (mol.mL/g^2)**	19.5	21.72	-1.92	63.5	70.3	-1.15
D_s **(cm^2/s)**	4.65	4.68	4.39	3.84	3.93	3.58
d_H **(nm)**	10.56	10.51	11.2	12.77	12.5	13.73
M_w **(KDa)**	118	118	135	151	150	192

k_D :Interaction parameter, B_2: second virial coefficient, D_s: self-diffusion coefficient, d_H: Hydrodynamic diameter, M_w: Molecular weight

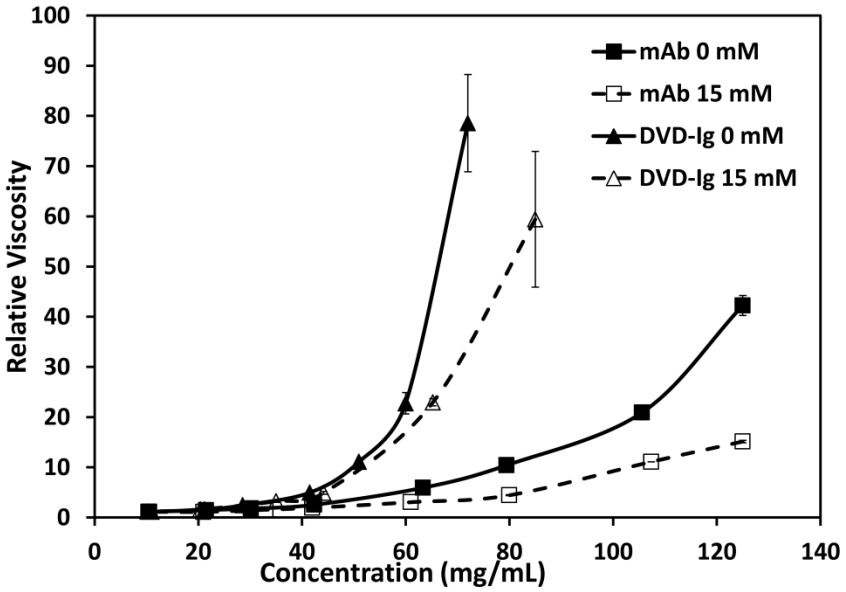

Figure 1: Relative viscosity of mAb (■) and DVD-Ig™ protein (▲) as a function of protein concentration at 0 mM (solid line) and at 15 mM (dashed line) ionic strength at pH 6.1. All solutions were analyzed at 25 ± 1˚C in duplicate. Error bars if not visible are smaller than the symbols used.

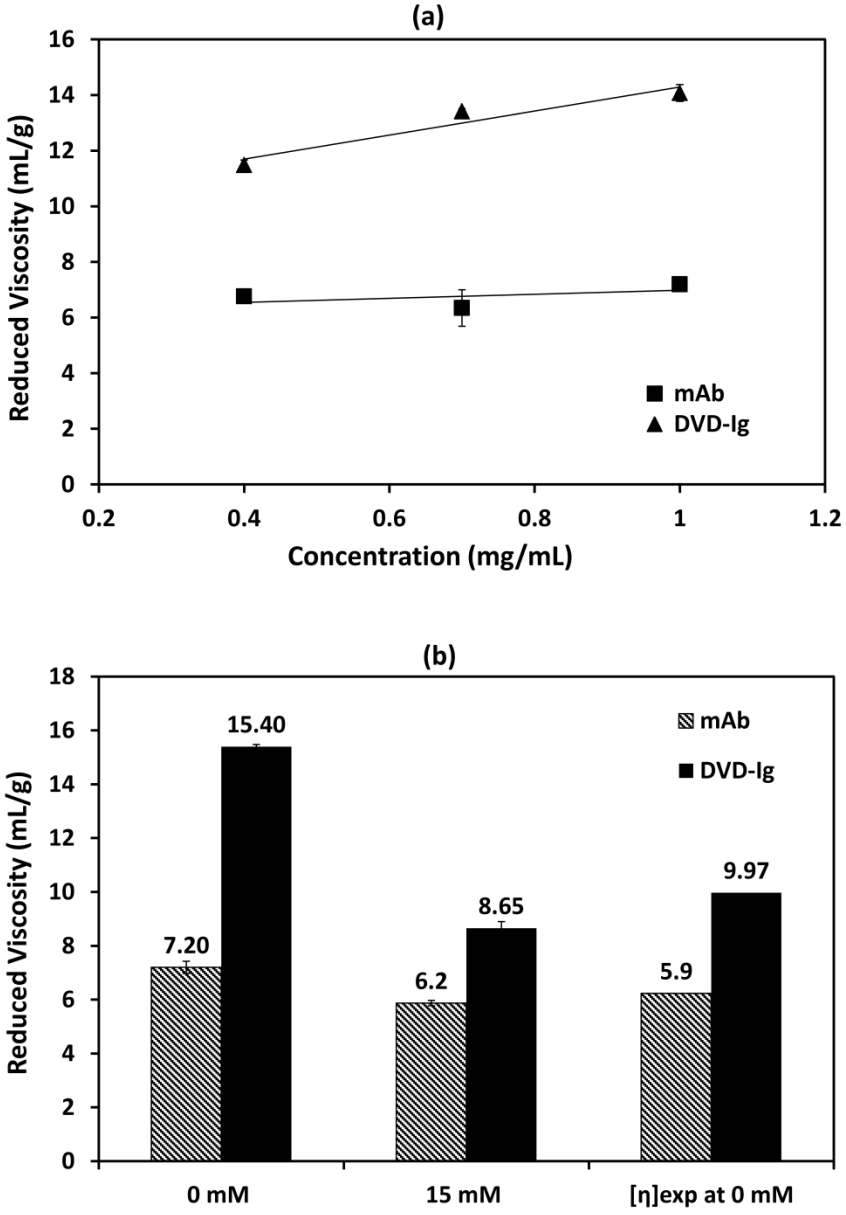

Figure 2: (a) Reduced viscosity of mAb and DVD-Ig^{TM} protein as a function of protein concentration at 0 mM ionic strength. (b) Reduced viscosity at a concentration of 1.0 mg/mL for mAb (dashed bars) and DVD-Ig^{TM} protein (closed bars) at 0 mM and 15 mM ionic strengths. The numbers on the bar represent the reduced viscosity values. $[\eta]_{exp}$ is the reduced viscosity extrapolated to c=0 (from Figure 2a) at 0 mM ionic strength. All solutions were analyzed at 25 ± 1˚C in duplicate. Error bars if not visible are smaller than the symbols used.

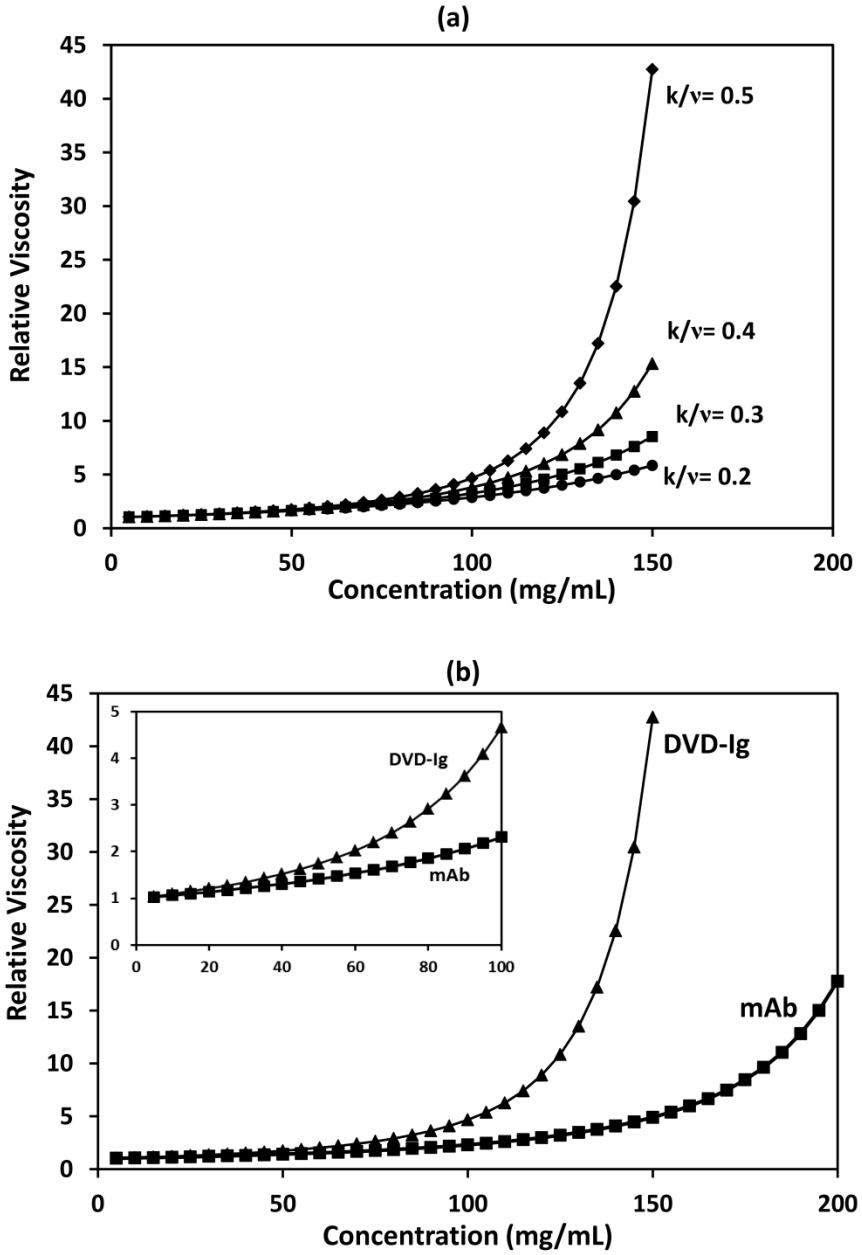

Figure 3: (a) Relative viscosity against concentration calculated from equation 9 for DVD-Ig™ protein. *k/v* ratio was varied to account for change in shape and crowding parameter. (b) Calculated relative viscosity for mAb and DVD-Ig™ protein plotted against concentration at a constant *k/v* ratio of 0.5. Intrinsic viscosity values of 8.7 mL/g and 5.9 mL/g were used for mAb and DVD-Ig™ protein, respectively. Inset shows relative viscosity up to concentrations of 100 mg/mL.

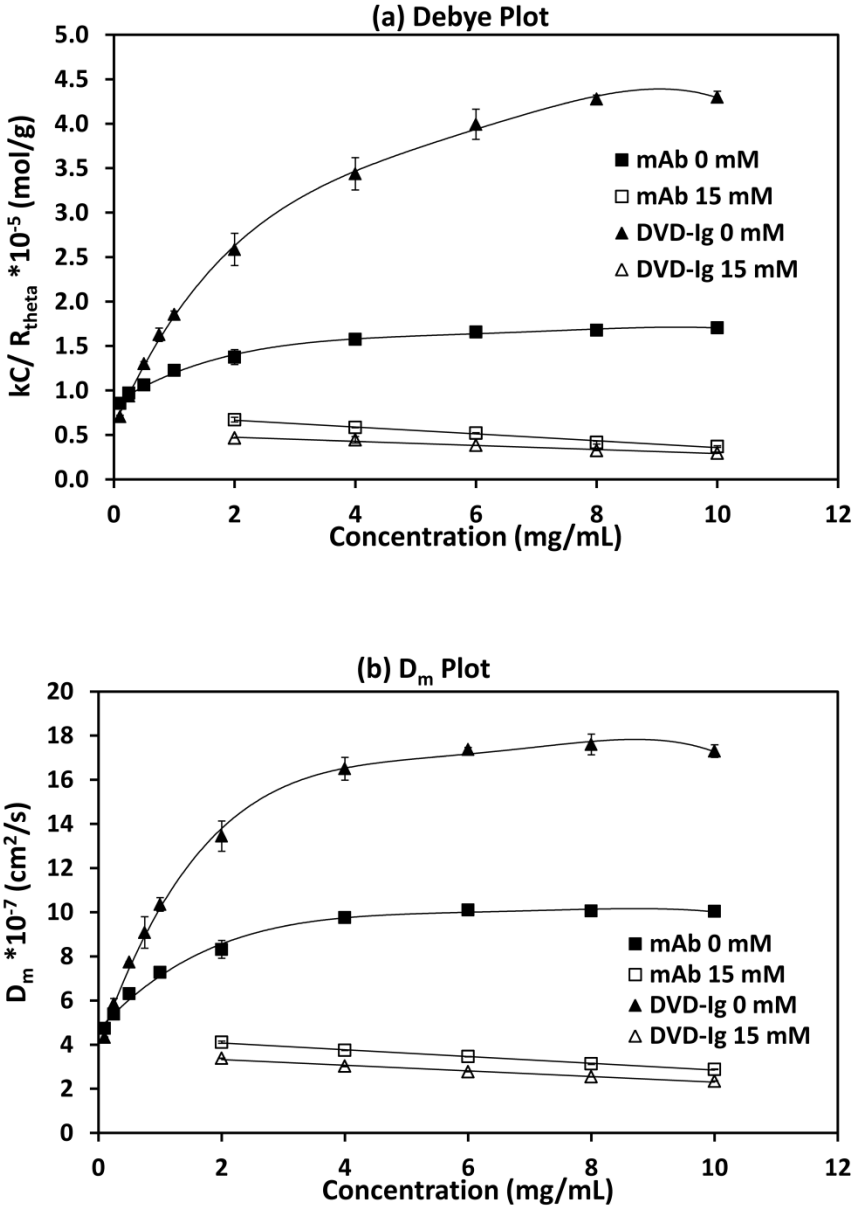

Figure 4: (a) Debye Plot and (b) D_m Plot for mAb (■) and DVD-Ig™ protein (▲) as a function of protein concentration at 0 mM (solid symbol) and at 15 mM (open symbols) ionic strengths at pH 6.1. The lines are the polynomial fit to the data points at 0 mM and linear fits to 15 mM ionic strength solutions. All solutions were analyzed at 25 ± 1˚C in duplicate. Error bars if not visible are smaller than the symbols used.

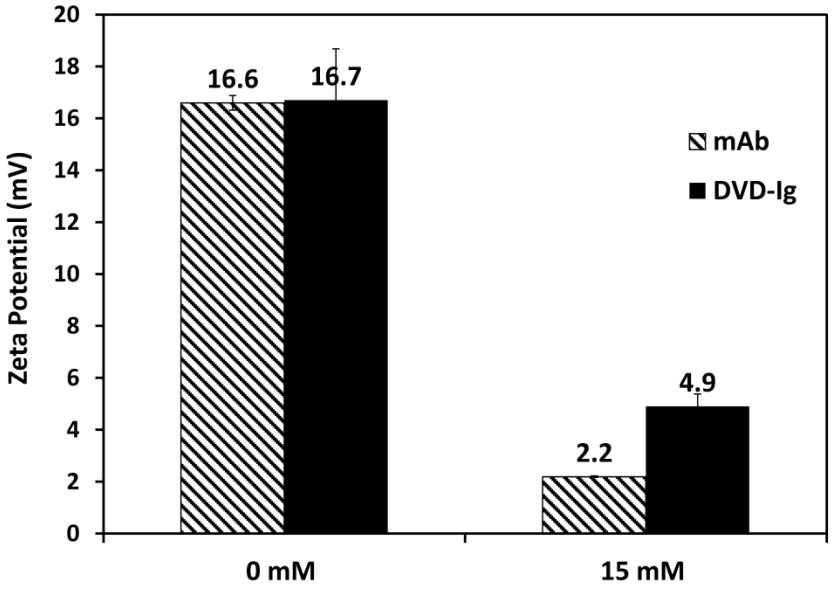

Figure 5: Zeta potential in mV for mAb (dashed bars) and DVD-Ig™ protein (closed bars) at 0 mM and 15 mM ionic strength at pH 6.1. The numbers on the bars represents the zeta potential values measured at that condition. Concentrations of 4 mg/mL and 2 mg/mL were analyzed for mAb and DVD-Ig™ protein, respectively. All solutions were analyzed at 25 ± 1˚C in duplicate. Error bars if not visible are smaller than the symbols used.

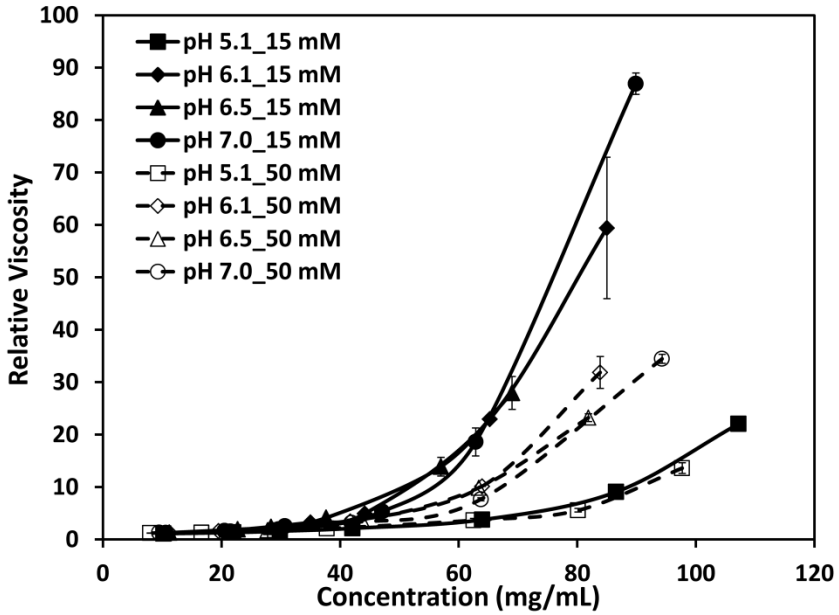

Figure 6: Relative viscosity of DVD-Ig™ protein plotted as a function of protein concentration at 15 mM (solid line) and 50 mM (dotted line) ionic strengths and varying pH conditions. Histidine buffers with appropriate concentrations were prepared to maintain the ionic strength of 15 mM. Sodium chloride was added to adjust ionic strength to 50 mM. All solutions were analyzed at 25 ± 1˚C in duplicate. Error bars if not visible are smaller than the symbols used.

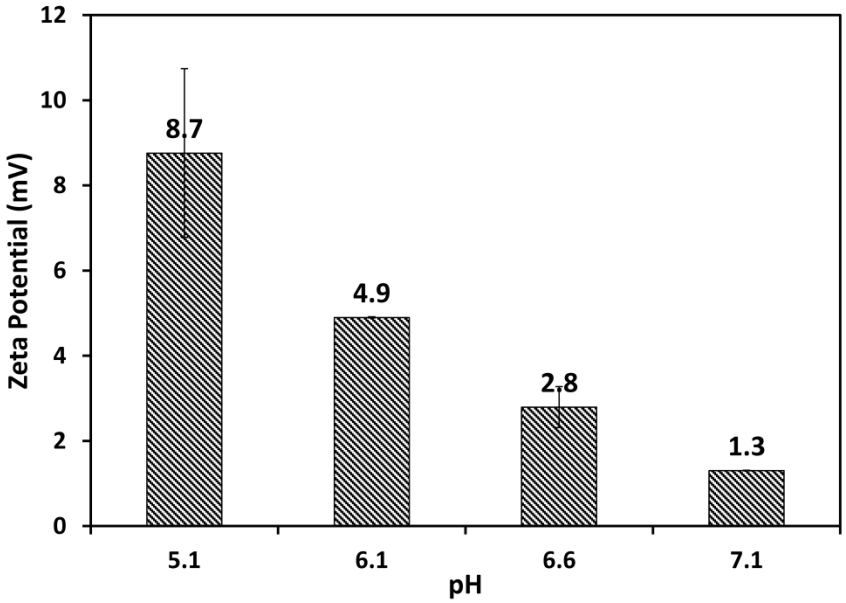

Figure 7: Zeta potential in mV for DVD-Ig^{TM} protein as a function of pH at 15 mM ionic strength. The numbers on the bars represents the zeta potential values in mV. Concentrations of 2 mg/mL were analyzed at 25 ± 1˚C in duplicate. Error bars if not visible are smaller than the symbols used.

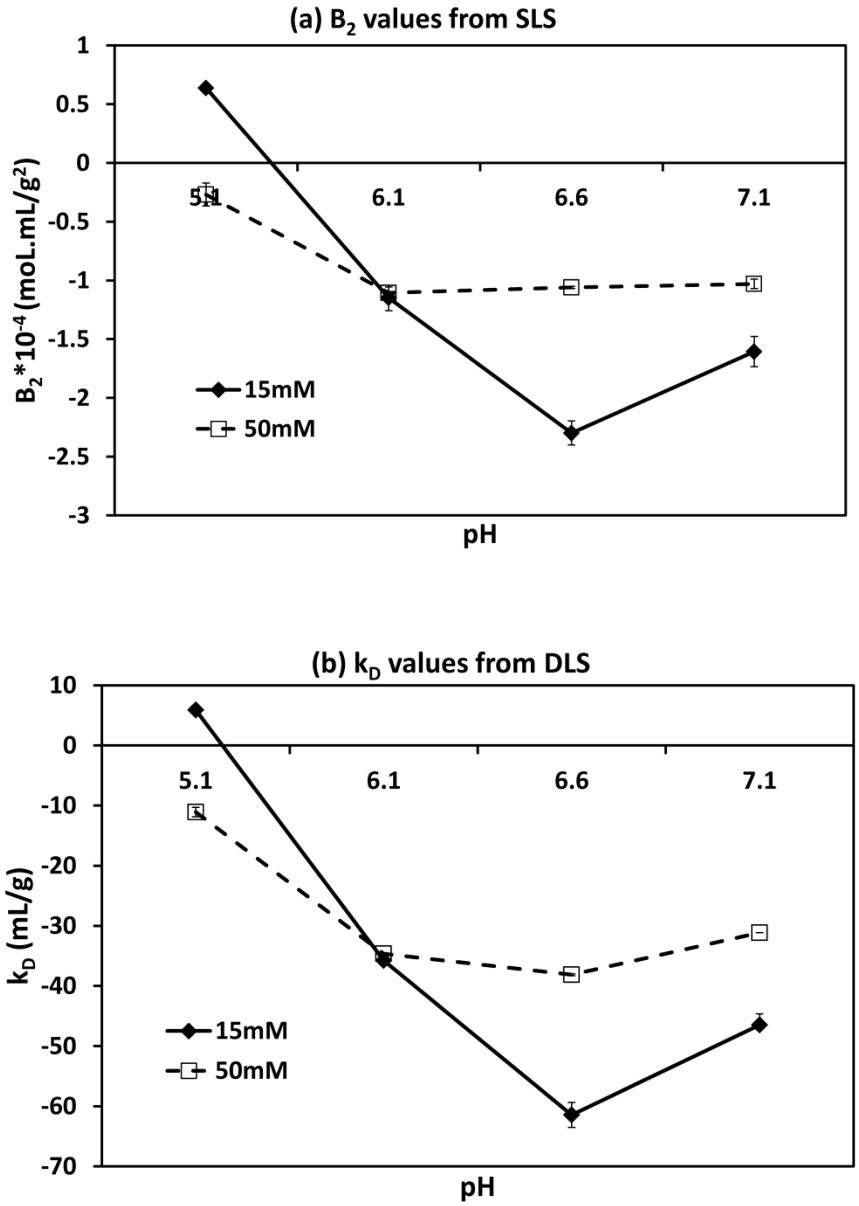

Figure 8: Plot of (a) B_2 from Static Light scattering and (b) k_D from Dynamic light scattering for DVD-Ig^{TM} protein as a function of pH and ionic strengths of 15 mM (solid line) and 50 mM (dashed line). All solutions were analyzed at 25 ± 1˚C in duplicate. Error bars if not visible are smaller than the symbols used.

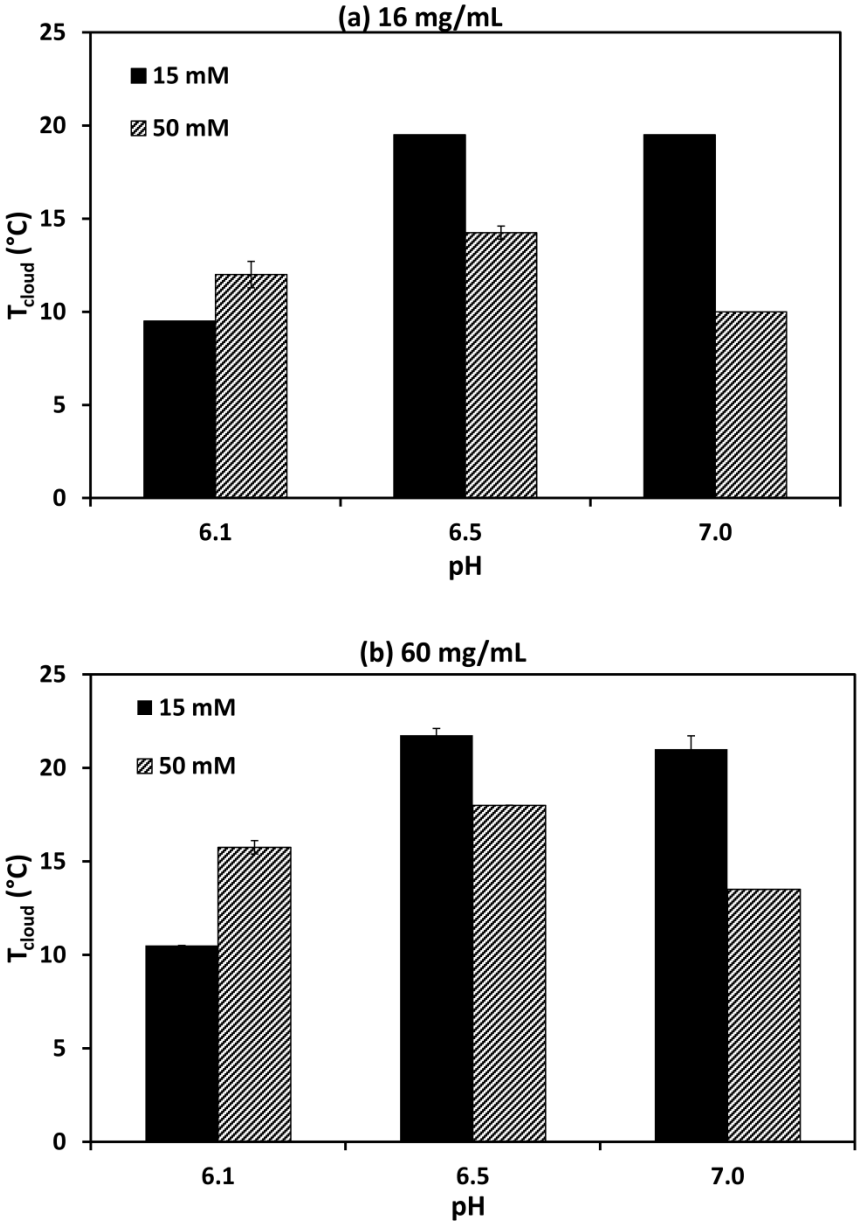

Figure 9: T_{cloud} (determined as temperature where percent transmittance is 70) for DVD-Ig™ protein at concentration of (a) 16 mg/mL and (b) 60 mg/mL, as a function of pH and at ionic strengths of 15 mM (solid bar) and 50 mM (dashed bar). All solutions were analyzed in duplicate. Error bars if not visible are smaller than the symbols used.

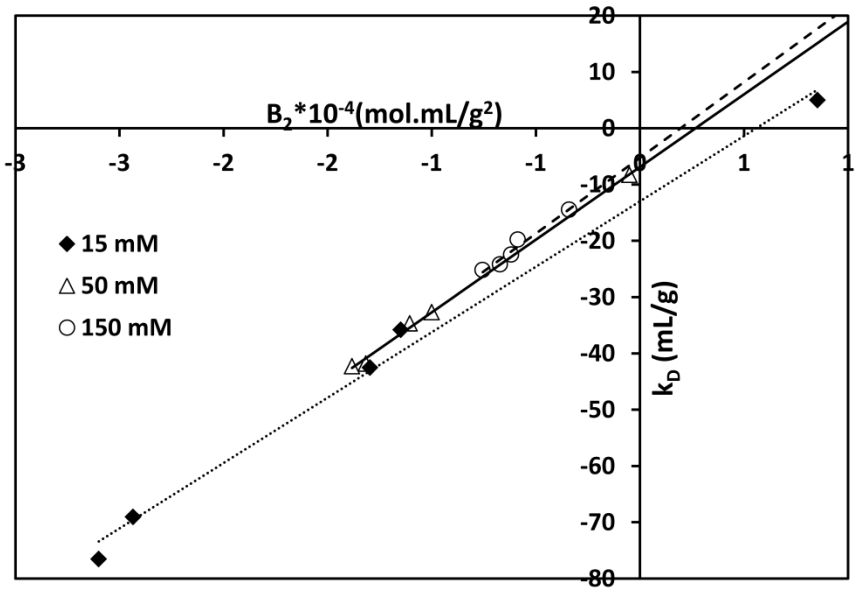

Figure 10: Plot of k_D measured from DLS against B_2 obtained from SLS at different pHs and ionic strengths of 15 mM (♦), 50 mM (Δ) and 150 mM (○) for DVD-Ig™ protein. The lines are linear fits to the data and extrapolated to x-axis to obtain hydration parameter from intercept (equation 10). The values are average of the measurements performed at 25 ± 1˚C in duplicate.

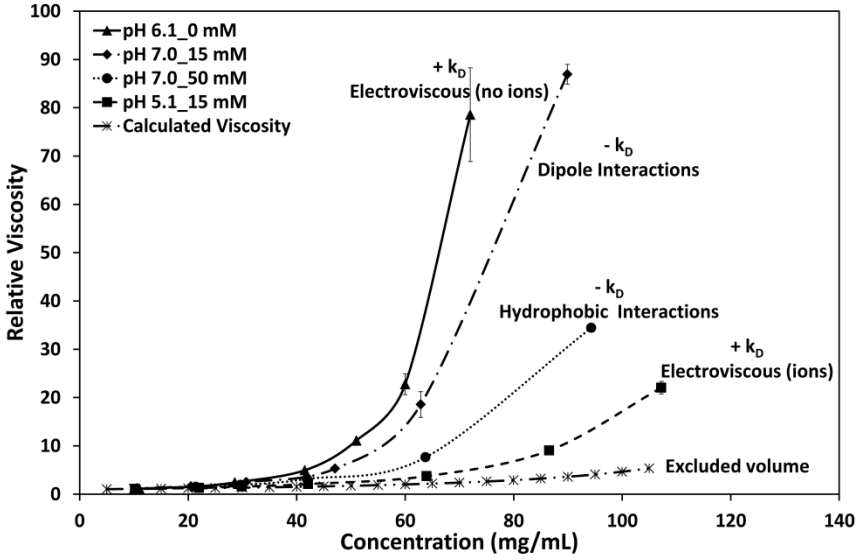

Figure 11: Plot of relative viscosity against concentration for DVD-Ig^{TM} protein at different solution conditions indicating contribution of dominant protein-protein interactions in solution at those conditions.

Chapter 7

Summary

Physical instabilities associated with therapeutic protein solutions presents challenges in the formulation development and reduce shelf-life of the product. Opalescence, phase separation, aggregation and high viscosity are a concern for high concentration protein solutions and are affected by the formulation factors; pH, ionic strength, buffer species and excipients. These formulation factors exert their effect by modulating physical interactions (non-covalent/specific) between the protein molecules. Recently, opalescence due to liquid-liquid phase separation has been reported for mAb solutions, and is a concern in formulation development as it can promote formation of irreversible aggregates in solution compromising its physical stability. However, the data for understanding the underlying factors and protein-protein interactions resulting in opalescence and liquid-liquid phase separation is scarce in the literature. These formulation challenges are further exaggerated in newer molecules like Dual variable domain immunoglobulins (DVD-Ig^{TM}) protein, which are relatively large molecules (MW~ 200 kDa) with increased asymmetry because of their extended Y-like shape. Thus, the objective of the current work was to investigate the effect of formulation factors and nature of intermolecular interactions resulting in opalescence and liquid-liquid phase separation (LLPS) for mAb and DVD-Ig^{TM} protein, and to understand their relation with increased aggregation and high viscosity of the solution.

The project is summarized in few key points as:

1. Opalescence due to LLPS in Solution

The theoretical basis for opalescence due to liquid-liquid phase separation (fluctuations in solution) and due to aggregation (presence of particles in solution) is presented in Chapter 2. Percent transmittance for mAb (Chapter 3) and DVD-Ig^{TM} protein

(Chapter 4) was measured as a function of solution conditions to determine if aggregation or LLPS results in opalescence in the solution. Strong temperature dependence for both the molecules confirmed that LLPS resulted in solution opalescence. LLPS and opalescence was also visually confirmed for both the molecules by changing solution conditions. The theoretical concepts for thermodynamic and kinetics of liquid-liquid phase separation were provided in Chapter 2. Equilibrium studies for DVD-Ig^{TM} protein in Chapter 4, confirmed the thermodynamic basis of phase separation in protein solutions.

2. Effect of Formulation Factors on Physical Instabilities

Literature examples related to formulation factors affecting opalescence and phase separation were briefly reviewed in Chapter 2. Formulation factors like pH, ionic strength and concentration have a significant effect on solution opalescence for mAb as presented in Chapter 3; opalescence increases close to the pI of the molecule, in an intermediate concentration range and at an intermediate ionic strength. In Chapter 4, similar studies were performed for DVD-Ig^{TM} protein, where pH, ionic strength and buffer species increased or decreased the tendency of protein to phase separate by modulating specific and/ or non-specific interactions in solution. Effect of commonly used excipients (PEG, Sucrose and Tween) on LLPS and aggregation for DVD-Ig^{TM} protein solutions were investigated and presented in Chapter 5. Sucrose suppressed both LLPS and aggregation, Tween 80 had no effect on either and PEG 400 increased LLPS and aggregation. In Chapter 6, effect of formulation factors on viscosity of DVD-Ig^{TM} protein solution was investigated. Ionic strength plays a dominant role in modulating viscosity for DVD-Ig^{TM} protein compared to the pH of the solution. Protein molecules exhibit a unique behavior in absence of any ions or

in water, where significantly high viscosity is due to high charge on the molecule (electroviscous effect) and hydration, while, the electroviscous effects in the presence of buffered solution exhibits minimal viscosity.

3. Molecular Properties of Protein

In Chapter 4, opalescence measurements for DVD-Ig^{TM} protein as a function of concentration confirm the hypothesis that the width and asymmetry of coexistence curve (or concentration range in which solution exhibits opalescence and LLPS) increases as the size of the molecule increases; DVD-Ig^{TM} protein shows increased tendency to phase separate at lower concentrations. In Chapter 6, the effect of the size of the molecule, on the viscosity of DVD-Ig^{TM} protein solutions were investigated. DVD-Ig^{TM} protein with a larger intrinsic viscosity (8.7 mL/g) and hydrodynamic diameter (~14 nm) exhibited significantly high viscosity compared to mAb ([η] ~5.9 mL/g and d_H ~11 nm). However, the excluded volume calculations show that the effect of size of the molecule on solution viscosity is significant only at higher concentrations (> 100 mg/mL).

4. Relation between Aggregation and LLPS in Solution

While protein retains its native structure on phase separation, aggregation is associated with formation of native and/or non-native species in solution. From Circular Dichroism studies in Chapter 4, there were no structural changes observed for DVD-Ig^{TM} protein, before and after phase separation. In Chapter 5, relationship between LLPS and formation of aggregates in protein-rich phase was investigated by performing stability studies at different temperatures (4, 20 and 40 °C) over a period of 45 days. Though, no aggregate

formation was observed at 4 ºC, where solution exhibited phase separation, 20 ºC data suggests that aggregate formation is accelerated on phase separation. Temperature plays a dominant role in both, liquid-liquid phase separation and formation of soluble, irreversible aggregates in solution; at low temperature protein exhibits LLPS, at high temperature protein exhibits aggregation and at an intermediate temperature both phenomena occur simultaneously depending on the solution conditions.

5. Protein-Protein Interactions Affecting Physical Stability

A brief overview on the nature of the intermolecular forces present in protein solutions was discussed in Chapter 2. In Chapter 3, opalescence in mAb solution was correlated to intermolecular interactions measured in dilute solution and at high concentrations; however, there was discrepancy in attractive interactions and solution opalescence. Temperature dependence of opalescence, suggested that thermodynamic contribution is significant and hence, T_{cloud} is a better parameter to assess attractive interactions resulting in phase separation. Results indicate that though, the presence of attractive interactions in solution is an important criterion for phase separation to occur, enthalpy-entropy balance is what controls the phase separation process. In Chapter 4, interactions in DVD-Ig^{TM} solution were investigated by measuring k_D and T_{cloud} as a function of solution conditions. Results implies that a protein can show a higher tendency to undergo phase separation in presence of additional forces (hydrophobic interactions for DVD-Ig^{TM} in this study), than for protein molecules which show only dipole-mediated attractive interactions in solution. Investigation of effect of histidine and phosphate buffers at constant pH and ionic strength indicated presence of specific interactions in solution. From this study

we also established the utility of T_{cloud} (temperature that marks onset of phase separation) as a predictive tool/ orthogonal technique along with light scattering, for preliminary screening of solution conditions for biologic candidates in preformulation development. Effect of excipients on protein-protein interactions in DVD-Ig™ protein solutions are presented in Chapter 5. Results indicate that, Sucrose decreased attractive PPI by specific binding to aromatic amino acids on protein surface. PEG increased attractive PPI, while Tween 80 had no effect on interactions in solution. Attractive protein-protein interactions resulting in phase separation also contribute significantly to increased viscosity of DVD-Ig™ protein and are presented in Chapter 6. Contribution of dipole-mediated interactions to the overall solution viscosity was observed to be greater than hydrophobic interactions. In addition to attractive interactions, presence of repulsive excluded volume effect and electroviscous effect (due to charge on the molecule) also contributed to the increased viscosity of DVD-Ig™ solutions.

Overall, this project highlights the importance and/or concerns related to liquid-liquid phase separation in protein solution, which is related to both, solubility of the proteins and formation of aggregates, resulting in physical instability in the formulation.

Appendix

Appendix 1

A.1. High Frequency Rheology

Ultrasonic shear rheometer with quartz crystals vibrating at a fundamental frequency of 10 MHz was employed to determine the rheological properties of the protein molecule. The rheometer is based on piezoelectric effect and employs a quartz crystal, which is sensitive to the mechanical properties of the liquid placed on top of it. The change in mechanical properties of a liquid including its viscosity and moduli can be determined by measuring the change in the electrical properties of the crystal in presence and absence of liquid.

Any interactions between the molecules are associated with a temperature-dependent relaxation process characterized by a relaxation time (τ). PPI affect conformational rearrangements and segmental motions in protein solutions and thus alter their characteristic τ. PPI occurs at the timescales of 10^{-7}-10^{-9} s, and to study such processes measurements at MHz frequencies need to be conducted, since τ is inversely related to frequency (ω). Storage (G') and loss (G'') modulus are related to τ by following relationship,

$$G' \propto \frac{\omega^2\tau^2}{1+\omega^2\tau^2} \qquad (A1)$$

$$G'' \propto \frac{\omega\tau}{1+\omega^2\tau^2} \qquad (A2)$$

For low shear viscosity measurements, ie, lower frequency strain is applied, molecules have enough time to reorient and relax within a single strain cycle, resulting in complete dissipation or loss of the applied energy. Consequently, G'' (viscous component) has a finite value but G' (elastic component) is nonexistent. As ω increases (MHz range) and approaches τ, molecules cannot relax completely and the system begins to store a part of the applied energy resulting in a finite value of G'. Strongly interacting systems, which are more

viscoelastic in nature, take more time to relax on removal of strain than dilute and non-interacting solute systems. Hence, at high measurement frequencies, strongly interacting solutions are not able to relax completely and would store a larger fraction of applied energy and exhibit a higher value of G'.[1,2]

A.2. Zeta Potential and Charge Measurements

Values for the measured zeta potential and calculated charges are compiled in Table A1. At pH 5.1, zeta potential is positive and the values are higher than those measured at other pHs at 5 mM (+9.32 mV) and 15 mM (+7.62 mV) ionic strengths. The magnitude of the change in zeta potential as ionic strength is increased from 5 to 15 mM is small; however, the experimental charge reduces almost to half from +8.13 Z at 5 mM to +4.02 Z at 15 mM ionic strength. This can be attributed to the change in Debye length on addition of salts. Debye length is inversely related to the square root of ionic strength and reduces as the ionic strength increases. At pH 6.1, which is closer to the pI of the molecule, zeta potential of +3.43 mV was observed at 5 mM ionic strength. The increase in ionic strength to 15 mM showed minimal decrease in zeta potential values (+2.19 mV). Similarly, net charge on the molecule is positive, but the values are smaller compared to other pH conditions (+2.83 Z at 5 mM and +1.13 Z at 15 mM). At pH 7.0, protein is negatively charged; a zeta potential value at 5 mM is -6.23 mV and at 15 mM is -5.85 mV. Net negative charges are present on the molecule at pH 7.0 (-5.59 Z at 5 mM and -3.17 Z at 15 mM).

A.3. Light Scattering: k_D Measurements

Light scattering techniques are routinely used to characterize the nature of intermolecular interactions in dilute solution. SLS is used for the determination of the second virial coefficient (B_2), which characterizes solute-solute interactions and indirectly solute-solvent interactions. Good correlation has been established between B_2 and protein solubility,[3,4] crystallization,[5-7] and protein precipitation,[8] which characterize phase separation in protein solutions. Virial expansion for the osmotic pressure is given by the following equation,

$$\pi = RTc\left(\frac{1}{M_w} + B_2 c + \cdots\right) \qquad (A3)$$

where, π is osmotic pressure, R is the universal gas constant, T is absolute temperature, c is solute concentration, and M_w is the weight average molecular weight. At infinite dilutions, higher order terms vanish and the equation reduces to the van't Hoff equation for ideal solution. B_2 is the first measure of the deviation from ideality in the solution and characterizes interactions between solute molecules. The value of B_2 reflects the magnitude of deviation from ideality, while its sign reflects the nature of this deviation. A positive value corresponds to net repulsive interactions between the solute molecules wherein the osmotic pressure increases above that for an ideal solution whereas a negative value corresponds to net attractive interactions between the solute molecules with a consequent decrease in solution osmotic pressure below that for an ideal solution.[9]

DLS measures the diffusion coefficient of a solute molecule in solution and is used to find the interaction parameter k_D using equation 2 (from Chapter 1). k_D is a measure of inter-particle interaction and is represented by,[10]

$$k_D = 2B_2 M_w - \zeta_1 - 2\nu_{sp} \qquad (A4)$$

where, ζ_1 is the coefficient of the linear term in the virial expansion of the frictional coefficient as a function of solute concentration and v_{sp} is the partial specific volume of the solute. k_D has contributions from both the thermodynamic and hydrodynamic parameter, and therefore, equation (A4) can be rewritten as,[11,12]

$$k_D = k_T - k_H \qquad (A5)$$

The contribution of B_2 to k_D arises from the role of chemical potential in driving the diffusion process, whereas the last two terms represent the hydrodynamic drag. Similar to B_2, a positive k_D implies repulsive interactions and a negative k_D implies attractive intermolecular interactions in solution.

Figure A1a, shows a plot of D_m as a function of concentration at varying ionic strengths at pH 5.1. At 5 mM ionic strength, the slope is negative indicating attractive protein-protein interactions (k_D = -18.04 mL/g). Slope becomes slightly more negative as the ionic strength is increased from 5 to 15 mM (k_D = -26.69 mL/g) and then becomes less negative as the ionic strength is further increased to 150 mM (k_D = -17.95 mL/g). D_m versus concentration curves for 5 and 150 mM ionic strength are almost overlapping. Figure S1b is a D_m plot for mAb A at pH 6.1. D_s or self-diffusion coefficient is determined by linear extrapolation to zero concentration. At low ionic strength of 5 mM, plot from 2-10 mg/mL protein concentration shows a curvature and it's not possible to determine the D_s by linear extrapolation, higher order virial coefficients need to be considered in this concentration range. Therefore, D_m was measured at low concentrations (below 2 mg/mL) to make a linear extrapolation. The k_D values measured from slope is most negative at this condition (-99.92 mL/g) indicating strong attractive PPI. As the ionic strength is further increased from 5 to 15 mM (k_D = -35.04 mL/g) and 150 mM (k_D = -11.24 mL/g), slope becomes less negative.

Similar trend is observed at pH 7.0. (Figure A1c) where slope is negative at an ionic strength of 5 mM (k_D = -35.42 mL/g) indicating strong attractive interactions which decrease on increasing the ionic strength to 15 (k_D = -20.46 mL/g) and 150 mM (k_D = -7.20 mL/g). B_2 was measured from SLS as a function of pH and ionic strengths of 5, 15 and 150 mM.

A.4. Effect of Ionic Strength on Interaction Parameter (k_D) and Charges on Molecule

Interactions in dilute solutions were measured using DLS for mAb A at pH 6.1 and varying ionic strengths from 0-150 mM (Figure A2a). As discussed previously, D_s or self-diffusion coefficient is determined by linear extrapolation to zero concentration, hence, D_m was measured at low concentrations (below 2 mg/mL) at 0-5 mM ionic strengths to make a linear extrapolation (Figure A2b). From Figure A2b, at pH 6.1 and ionic strength of 0 mM, slope is highly positive indicating strong repulsive interactions in the absence of any ions (k_D = +591.98 mL/g). On addition of salt and increasing the ionic strength to 1 mM, slope becomes highly negative indicating the presence of strong attractive interactions (k_D = -143.89 mL/g). At ionic strength of 2.5 mM, attractive interactions decrease as indicated by a less negative slope (k_D = -118.67 mL/g) as compared to 1 mM. As the ionic strength is further increased from 5 mM (k_D = -99.92 mL/g) to 10 mM (k_D = -42.53 mL/g) and 15 mM (k_D =-35.04 mL/g), slope becomes less negative i.e., either attractive interactions decrease or repulsive interactions increases with increase in ionic strength. At the ionic strength of 150 mM, the slope is least negative and close to zero, indicating weak attractive protein-protein interactions at this solution condition (k_D =-11.24 mL/g).

Charges on the molecule were also calculated from the zeta potential measurements as a function of ionic strength at pH 6.1 and complied in Table A2. At pH 6.1, zeta potential

is positive at all ionic strengths and the values of zeta potential and charges calculated decreases with increase in ionic strength. Zeta potential has large positive value at 0 mM ionic strength (+16.60 mV). This zeta potential value relates to the surface potential of the molecule in the absence of any counter-ions in solution. When ions are added to the solution and ionic strength is increased to 1 mM (+7.51 mV), zeta potential becomes approximately half of that at 0 mM. This is caused by the extensive ion binding to the protein surface and charge shielding because of the ionic cloud. When ionic strength is further increased to 5 mM, zeta potential value decreases in magnitude by almost half (+3.43 mV). As ionic strength is increased to 10 (+2.69 mV) and 15 mM (+2.19 mV), change in zeta potential is not as significant. At 0 mM ionic strength, for the calculation of charges, ionic strength is assumed to be 0.1 mM. In the absence of any ions, the calculated true charges on the molecule will be much larger as the Debye length is much lower than that assumed with 0.1 mM (+87.39 Z). The calculated charge reduces by nearly 5 fold when ionic strength is increased to 1 mM (+14.54 Z). Decrease in the calculated charge form zeta potential is again significant as ionic strength is increased from 1 to 5 mM (+2.83 Z). Above 5 mM, decrease in charges with increase in ionic strength to 10 mM (+1.82 Z) and 15 mM (+1.13 Z) is not as significant.

References

1. Macosko C. Rheology: Principles, measurements, and applications. 1994. VCH, New York.
2. Larson RG. 1999. The Structure and Rheology of Complex Fluids. ed., New York: Oxford University Press.
3. Demoruelle K, B. Guo, S. Kao, M. McDonald Heather, B. Nikic Dragan, C. Holman Steven, and W. W. Wilson. 2002. Correlation between the osmotic second virial coefficient and solubility for equine serum albumin and ovalbumin. . Acta Crystallogr. D Biol. Crystallogr. 58:1544-1548.
4. Valente JJ, R. W. Payne, M. C. Manning, W. W. Wilson, and C. S. Henry. 2005. Colloidal behavior of proteins: Effects of the second virial coefficient on solubility, crystallization and aggregation of proteins in aqueous solution. Curr. Pharm. Biotechnol. 6:427-436.
5. Rosenbaum DF, and C. F. Zukoski. 1996. Protein interaction and crystallization. J. Cryst. Growth. 169:752-758.
6. George A, Y. Chiang, B. Guo, A. Arabshahi, Z. Cai, and W. W. Wilson. 1997. Second virial coefficient as predictor in protein crystal growth. Methods Enzymol 276:100-110.
7. Neal BL, D. Asthagiri, O. D. Velev, A. M. Lenhoff, and E. W. Kaler. 1999. Why is the osmotic second virial coefficient related to protein crystallization? J. Cryst. Growth. 196:377-387.
8. Curtis RA, Prausnitz JM, Blanch HW. 1998. Protein-protein and protein-salt interactions in aqueous protein solutions containing concentrated electrolytes. Biotechnol Bioeng 57(1):11-21.
9. Neal BL, D. Asthagiri, and A. M. Lenhoff. 1998. Molecular origins of osmotic second virial coefficients of proteins. Biophys. J. 75:2469-2477.
10. Narayanan J, and X. Y. Liu. . 2003. Protein interactions in undersaturated and supersaturated solutions: a study using light and x-ray scattering. Biophys. J. 84:523-532.
11. JA. B. 1976. Correlations for interacting Brownian particles. J Chem Phys 64:242-246.
12. Placidi M CS. 1998. A dynamic light scattering study on mutual diffusion coefficient of BSA in concentrated aqueous solutions. Europhys Lett 43(4):476.

Figures and Tables

Table A1.1: Measured zeta potential (millivolts) and calculated experimental charges (coulombs) for mAb A at various pHs and ionic strengths

pH	Ionic strength (mM)	Zeta Potential(mV)	Experimental charge
5.1	5	+9.32 ± 0.48	+8.13 ± 0.42
5.1	15	+7.6 2± 0.16	+4.02 ± 0.09
6.1	5	+3.43 ± 0.12	+2.83 ± 0.09
6.1	15	+2.19 ± 0.03	+1.13 ± 0.02
7.0	5	-6.23 ± 0.12	-5.59 ± 0.10
7.0	15	-5.85 ± 0.13	-3.17 ± 0.01

Table A1.2: Measured Zeta potential and calculated experimental charges for MAb A at pH 6.1 and ionic strengths

pH	Ionic strength(mM)	Zeta Potential(mV)	Experimental charge
6.1	0	16.60 ± 0.28	87.39 ± 1.49
6.1	1	7.51 ± 0.70	14.54 ± 1.34
6.1	5	3.43 ± 0.12	2.83 ± 0.09
6.1	10	2.69 ± 0.23	1.82 ± 0.16
6.1	15	2.19 ± 0.03	1.13 ± 0.02

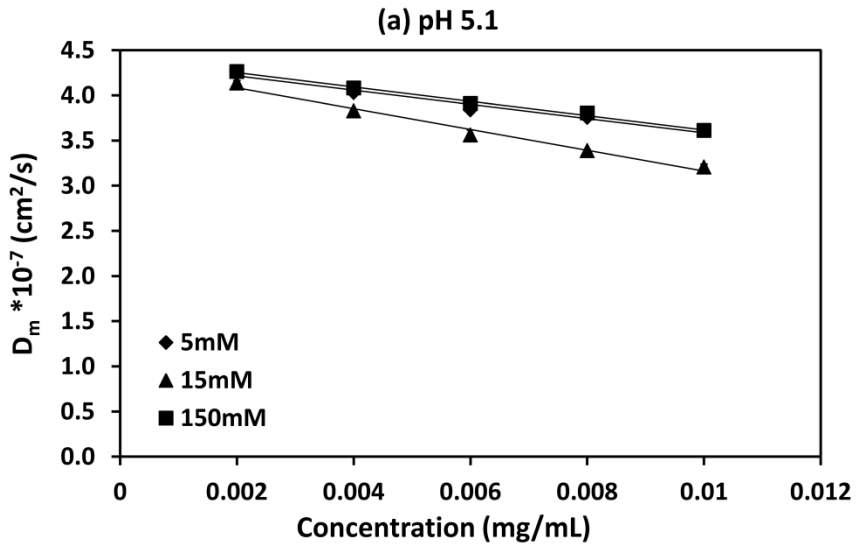
(a) pH 5.1
4.5
4.0
3.5
3.0
2.5
2.0
1.5
1.0
0.5
0.0
D_m *10^{-7} (cm^2/s)
5mM
15mM
150mM
0
0.002
0.004
0.006
0.008
0.01
0.012
Concentration (mg/mL)

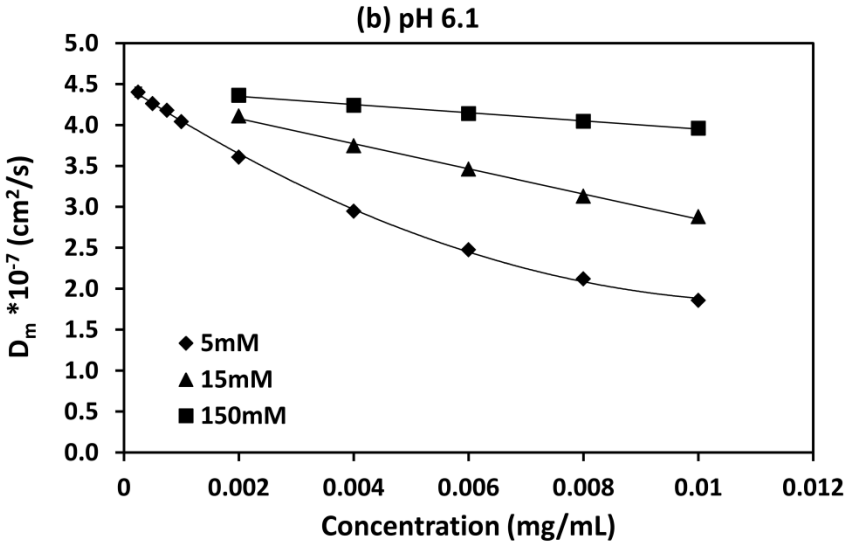
(b) pH 6.1
5.0
4.5
4.0
3.5
3.0
2.5
2.0
1.5
1.0
0.5
0.0
D_m *10^{-7} (cm^2/s)
5mM
15mM
150mM
0
0.002
0.004
0.006
0.008
0.01
0.012
Concentration (mg/mL)

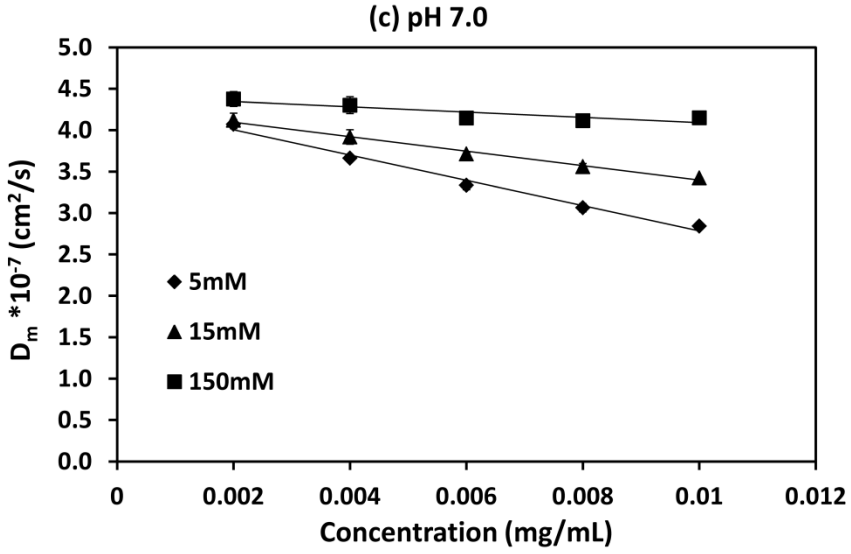

Figure A1.1: Mutual diffusion coefficient (D_m) for mAb A as a function of concentration, at (a) pH 5.1, (b) pH 6.1 and (c) pH 7.0 and ionic strengths of 5 mM (♦), 15 mM (▲) and 150 mM (■). All the solutions were analyzed at 25 ± 0.1 ˚C in duplicate. Error bars if not visible are smaller than the symbols used.

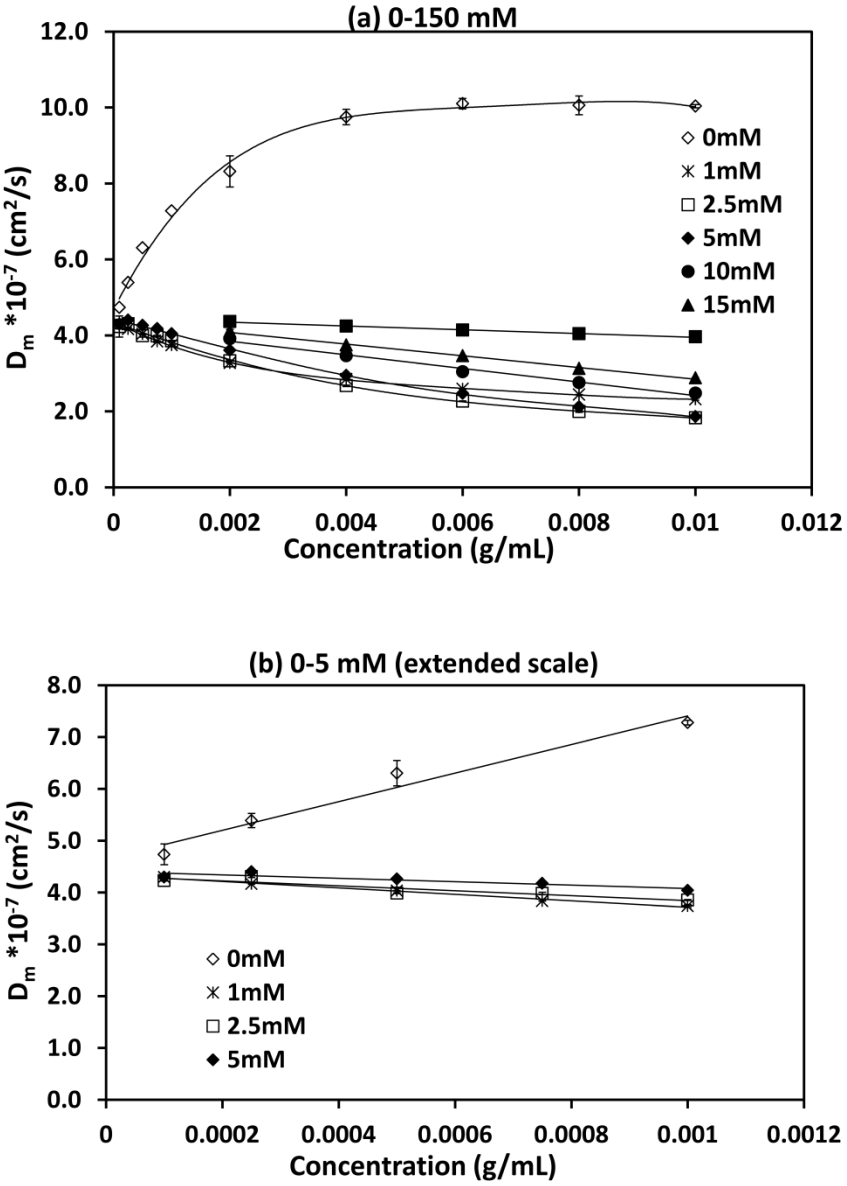

Figure A1.2: (a) Mutual diffusion coefficient (D_m) for mAb A as a function of concentration (0.1-10 mg/mL), at pH6.1 and various ionic strengths. The lines are linear best fits with slope and intercept representing $D_s k_D$ and D_s (self-diffusion coefficient), respectively. (b) D_m plots at low concentrations (0.0001-0.001 g/mL) at pH 6.1 and 0-5 mM ionic strength. All the solutions were analyzed at 25 ± 0.1 ˚C in duplicate. Error bars if not visible are smaller than the symbols used.

Appendix 2

Intrinsic Fluorescence

Intrinsic fluorescence and second derivative fluorescence spectroscopy study were performed for DVD-Ig^{TM} in presence and absence of excipients to determine tertiary structural changes after samples were incubated at 40 ºC for 45 days. Figure A2a and A2b are plots of emission scans normalized to fluorescence intensity of 1.0 at λ_{max} and second derivative spectra of the normalized emission scans for protein, respectively Spectra are presented only for samples incubated in buffer and PEG, other excipients show overlapping spectrums and are not plotted. Fluorescence spectra were also recorded for freshly prepared DVD-Ig^{TM} samples at similar solution conditions. No shift in intensity or wavelength (blue shift or red shift) in presence or absence of excipients was observed. Similarly, no change in tertiary structure was observed for samples at any of the conditions studied.

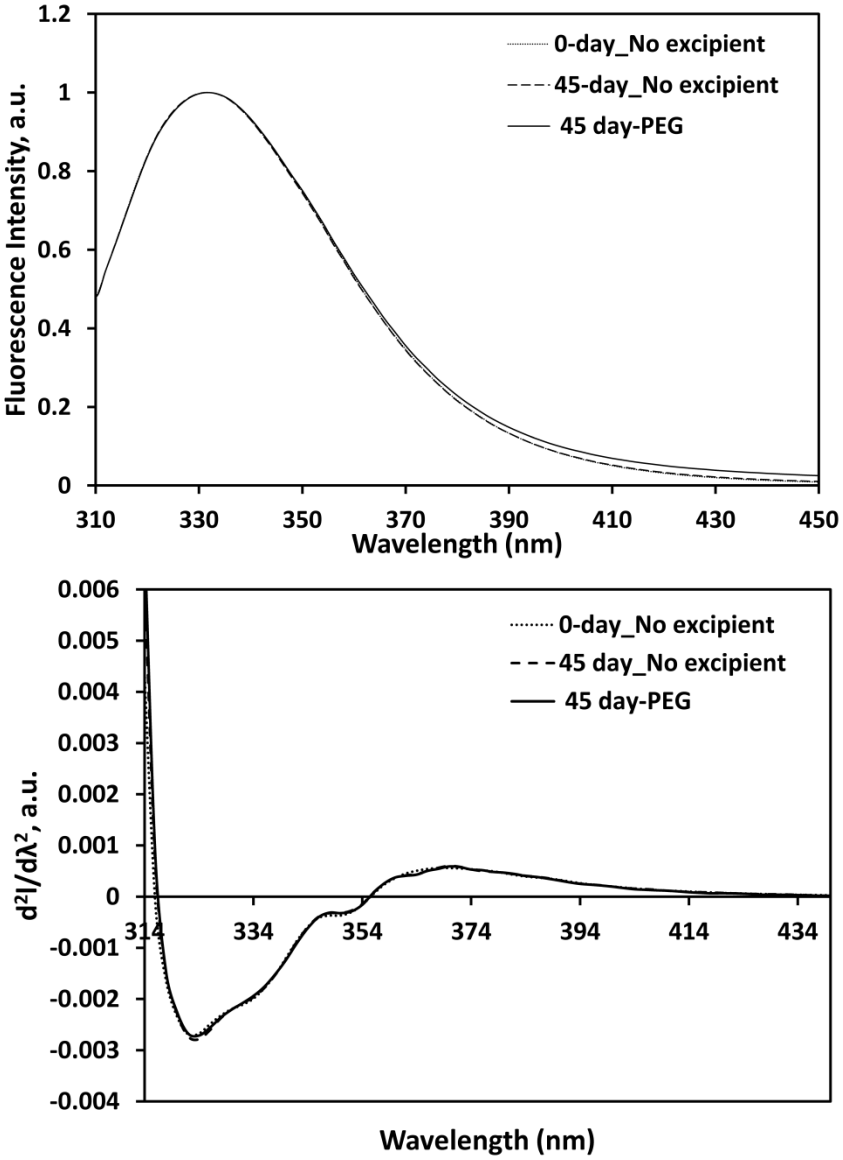

Figure A2: (a) Emission scans normalized to fluorescence intensity of 1.0 at λ_{max} and (b) second derivative spectra of the normalized emission scans of DVD-Ig™ in buffer and for samples incubated at 40 ºC in buffer and 10% PEG. Excitation wavelength was set to 295 nm to determine Trp fluorescence. 0.2 mg/mL samples were prepared in histidine buffer at pH 6.6 with ionic strength of 15 mM. Excipient stocks were prepared in same buffer and diluted to required final concentration in solution. Plot represents averages of emission scans obtained at all conditions in triplicate at 25 ± 0.1 ˚C.